



IntechOpen

Quantum Entanglement in High Energy Physics

Edited by Oliver K. Baker



Quantum Entanglement in High Energy Physics

Edited by Oliver K. Baker

Published in London, United Kingdom

Quantum Entanglement in High Energy Physics
<http://dx.doi.org/10.5772/intechopen.111219>
Edited by Oliver K. Baker

Contributors

A. Pedro Aguiar, Alexander Machavariani, Ali Saif M. Hassan, Christopher G. Timpson, Felix A. Buot, Ismail Zahed, Karin Marie Fierke, Kisalaya Chakrabarti, Maciej A. Nowak, Mohamed A. Shukri, Mohammed Boukidi, Mohammed Nadir, Nahid Binandeh Dehaghani, Nancy Lynn Bowen, Oliver K. Baker, Rachid Benbrik, Rafal Wisniewski, Shrobona Bagchi, Waleed S. A. Hasan, Yizhuang Liu, Yoram Kirsh

© The Editor(s) and the Author(s) 2024

The rights of the editor(s) and the author(s) have been asserted in accordance with the Copyright, Designs and Patents Act 1988. All rights to the book as a whole are reserved by INTECHOPEN LIMITED. The book as a whole (compilation) cannot be reproduced, distributed or used for commercial or non-commercial purposes without INTECHOPEN LIMITED's written permission. Enquiries concerning the use of the book should be directed to INTECHOPEN LIMITED rights and permissions department (permissions@intechopen.com).

Violations are liable to prosecution under the governing Copyright Law.



Individual chapters of this publication are distributed under the terms of the Creative Commons Attribution 3.0 Unported License which permits commercial use, distribution and reproduction of the individual chapters, provided the original author(s) and source publication are appropriately acknowledged. If so indicated, certain images may not be included under the Creative Commons license. In such cases users will need to obtain permission from the license holder to reproduce the material. More details and guidelines concerning content reuse and adaptation can be found at <http://www.intechopen.com/copyright-policy.html>.

Notice

Statements and opinions expressed in the chapters are those of the individual contributors and not necessarily those of the editors or publisher. No responsibility is accepted for the accuracy of information contained in the published chapters. The publisher assumes no responsibility for any damage or injury to persons or property arising out of the use of any materials, instructions, methods or ideas contained in the book.

First published in London, United Kingdom, 2024 by IntechOpen
IntechOpen is the global imprint of INTECHOPEN LIMITED, registered in England and Wales,
registration number: 11086078, 167-169 Great Portland Street, London, W1W 5PF, United Kingdom

British Library Cataloguing-in-Publication Data
A catalogue record for this book is available from the British Library

Additional hard and PDF copies can be obtained from orders@intechopen.com

Quantum Entanglement in High Energy Physics
Edited by Oliver K. Baker
p. cm.
Print ISBN 978-0-85466-083-4
Online ISBN 978-0-85466-082-7
eBook (PDF) ISBN 978-0-85466-084-1

We are IntechOpen, the world's leading publisher of Open Access books Built by scientists, for scientists

6,900+

Open access books available

186,000+

International authors and editors

200M+

Downloads

156

Countries delivered to

Our authors are among the
Top 1%

most cited scientists

12.2%

Contributors from top 500 universities



WEB OF SCIENCE™

Selection of our books indexed in the Book Citation Index
in Web of Science™ Core Collection (BKCI)

Interested in publishing with us?
Contact book.department@intechopen.com

Numbers displayed above are based on latest data collected.
For more information visit www.intechopen.com



Meet the editor



Oliver K. Baker, the D. Allan Bromley Physics Professor at Yale University, conducts research in experimental particle physics. His leadership role in the construction of the ATLAS Transition Radiation Tracker (TRT), and use of machine learning were essential in the Higgs boson discovery. His current research in quantum entanglement, quantum computing, entanglement entropy, and searches for phenomena that are beyond the

Standard Model of Particle Physics uses Higgs production and decay. Baker earned a Ph.D. in Physics, an MS in Physics and Mathematics at Stanford University, and a BS in Physics from the Massachusetts Institute of Technology. He is a member of the American Academy of Arts and Sciences and the American Physical Society. He was the 2006 US Presidential appointee to the board of the National Medal of Science.

Click the button to access an insightful interview with the editor.

Access Interview

Contents

Preface	XI
Section 1	
Introduction	1
Chapter 1	3
Introductory Chapter: Quantum Entanglement at High Energies – Experiment, Theory, and Interdisciplinarity <i>by Oliver K. Baker</i>	
Section 2	
Theory	11
Chapter 2	13
On the Questions of Spin and Spin Quantum Correlations in Relativistic Quantum Mechanics and Relativistic Quantum Information <i>by Shrobona Bagchi</i>	
Chapter 3	29
Perspective Chapter: On Entanglement Measures – Discrete Phase Space and Inverter-Chain Link Viewpoint <i>by Felix A. Buot</i>	
Chapter 4	51
Perspective Chapter: On the Contradiction between Special Relativity and Quantum Entanglement <i>by Yoram Kirsh</i>	
Chapter 5	63
Phenomenology of Heavy Quark at the LHC <i>by Rachid Benbrik and Mohammed Boukidi</i>	
Chapter 6	85
The Electromagnetic Inter-Nucleon Quark-to-Quark Bond and Its Effect on the Nuclear Force <i>by Nancy Lynn Bowen</i>	

Chapter 7	107
Exploring Strange Entanglement: Experimental and Theoretical Perspectives on Neutral Kaon Systems <i>by Nahid Binandeh Dehaghani, A. Pedro Aguiar and Rafal Wisniewski</i>	
Section 3	133
Interdisciplinarity	
Chapter 8	135
Perspective Chapter: Why Do We Care about Violating Bell Inequalities? <i>by Christopher G. Timpson</i>	
Chapter 9	161
Perspective Chapter: Experiments in Entangled Time <i>by Karin Marie Fierke</i>	
Chapter 10	187
Entanglement in High-Energy Physics: An Overview <i>by Mohammed Nadir</i>	
Section 4	207
Experiments	
Chapter 11	209
Translational Symmetry of Intermediate Nodes and Antinodes of Entangled Particles <i>by Kisalaya Chakrabarti</i>	
Chapter 12	223
Perspective Chapter: EPR Paradox – Experimental and Quantum Field Theoretical Status of Light Meson Resonances <i>by Alexander Machavariani</i>	
Chapter 13	239
Perspective Chapter: Squeezing and Entanglement of Two-Modes Quantum X Waves <i>by Ali Saif M. Hassan, Waleed S.A. Hasan and Mohamed A. Shukri</i>	
Chapter 14	257
Universality of Koba-Nielsen-Olesen Scaling in QCD at High Energy and Entanglement <i>by Yizhuang Liu, Maciej A. Nowak and Ismail Zahed</i>	

Preface

Research in the field of quantum information science can include several subfields in High Energy Physics (HEP), including quantum entanglement, entanglement entropy, Bell's inequality violation studies, and quantum computing along with quantum algorithm performance, quantum communications and quantum information and processing, quantum cryptography, and quantum sensors. There may be, overall, additional subfields that exist currently, or that may surface in the near future as the field grows in person-power and technology. Given that the research topics will now include quantum information science at high energies – elementary particle masses of order tens of GeV/c² and kinetic energies or momenta that may be measured in units of sub-TeV/c – a supplementary challenge that includes determination of relativistic effects in experimental measurements and theoretical definitions of these somewhat new concepts may ensue. It is also clear from the accentuation given in the Introductory Chapter, “Quantum Entanglement at High Energies – Experiment, Theory, and Interdisciplinarity”, that this study of physical phenomena in this way, at this level, requires that the theoretical descriptions, calculations, and results must be correct and complete, and the physical reality that is acquired and measured experimentally at high energies and masses must have a match in the theoretical culmination. Interdisciplinarity between theorists and experimentalists in physics, as well as with colleagues in other fields (mathematics, computing, social sciences, etc.) may very likely be essential to success.

The book commences with an introductory chapter that provides readers with an overview of the subject matter.

In Chapter 2, Prof. Shrobona Bagchi of the Korea Institute of Science and Technology develops and then summarizes how fundamentals in the understanding of natural phenomena with robust mathematical construct and subsequent reproducible experimental verifications have been some of the strongest pillars of physics to date.

In Chapter 3, Prof. Felix A. Buot of the University of San Carlos, explains the inverter-chain link viewpoint, the entanglement of two bare qubits, entangled qubits versus emergent qubits, the difference between mixed and pure states showing calculations, and much more.

In Chapter 4, Prof. Yoram Kirsh of the Open University of Israel describes an analysis that gives rise to an additional possibility concerning the tension between quantum entanglement in Quantum Mechanics and information transfer in Special Relativity with regards to cause and effect, are very deserving of such a test.

In Chapter 5, Prof. Rachid Benbrik and Prof. Mohammed Boukidi of Cadi Ayyad University, Marrakech, Morocco, present an intriguing argument supporting experimental vector-like quark searches that if discovered (at the Large Hadron Collider) would be a major breakthrough in particle physics.

In Chapter 6, Prof. Nancy Lynn Bowen of Colorado Mountain College explains that previous nuclear theories have ignored or lessened the electromagnetic force, considering only Coulomb forces between protons, whereas such assumptions are not valid. This leads to potential new rules in quantum mechanics inside the nucleus and nucleon.

In Chapter 7, Professors Nahid Binandeh Dehaghani, A. Pedro Aguiar from the University of Porto, and Rafal Wisniewski from Aalborg University provide an in-depth analysis of properties and phenomena associated with neutral K-mesons, and decoherence effects on entangled kaons.

In Chapter 8, Prof. Christopher G. Timpson of the University of Oxford provides an intriguing review with new insights into the meaning and significance of Bell inequalities violation as tests of whether the world is not locally causal, or the extent to which the criteria for providing these tests would be satisfied in high-energy experiments, employing a range of different philosophical approaches.

In Chapter 9, Prof. Karin Marie Fierke of the University of St. Andrews, educates readers about implications related to quantum social theory for the social sciences, many of which ask how particular socio-political phenomena look different when lifted from the assumptions of classical physics and placed in an uncertain quantum world.

In Chapter 10, Prof. Mohammed Nadir of Tampere University provides an overview (with references) of quantum entanglement, showing that if intertwined with quantum field theory and the AdS/CFT correspondence, quantum gravity, and much more at the high-energy physics frontier, may lead to an incredible, deeper understanding of the universe.

In Chapter 11, Prof. Kosalaya Chakrabarti of the Haldia Institute of Technology considers the case where a particle with spin zero splits into two separate particles, showing the spin magnitudes and direction of these two decay particles before and after the spins are measured. The author also explains why this happens.

In Chapter 12, Prof. Alexander Machavariani of the High Energy Physics Institute of Tbilisi State University uses experimental and relativistic field-theoretical amplitudes of vector meson resonance decays to check the consistency of the approach with a formulation based on Einstein-Podolsky-Rosen concepts. The author also studies the entanglement that can occur in high-energy collisions.

In Chapter 13, Professors Ali Saif M. Hassan of the University of Amran, Waleed S.A. Hasan, and Mohamed A. Shukri of the University of Sana'a and the University of Amran show that using velocity phase matching to produce X waves having orbital angular momentum can be used to determine the length of a dispersive media and more.

In Chapter 14, Professors Yizhuang Liu and Maciej A. Nowak from the Institute of Theoretical Physics at Jagiellonian University, and Ismail Zahed from the Center for Nuclear Theory at Stony Brook University show that in the context of high-energy

particle physics, the Koba-Nielsen-Olesen scaling (KNO scaling), formulated many years ago, is of tremendous importance in analysis of many high-energy hadronic multiplicities, and yet usually challenging to derive from first principles in Quantum Chromodynamics (QCD). Results are interpreted from the point of view of quantum entanglement between slow and fast degrees of freedom in QCD.

Oliver K. Baker
Wright Laboratory,
Department of Physics,
Yale University,
New Haven, CT, USA

Section 1

Introduction

Introductory Chapter: Quantum Entanglement at High Energies – Experiment, Theory, and Interdisciplinarity

Oliver K. Baker

1. Introduction

One of the most recent publications that includes descriptions of quantum entanglement in the context of quantum mechanics is found in the textbook [1]. The book contains passages that describe the development of quantum mechanics, in general, and quantum entanglement. The authors of [1] point out that the divergence of opinions about the theory is trying to inform us about our possible lack of understanding of the nature of reality and that physicists' attention is turned to the frenetic development of different technologies that make use of an understanding of the question, "... what is the interpretation of quantum mechanics?" which in this author's opinion can be expanded to the inquiry "... why are there so many interpretations of quantum entanglement, especially in high energy physics?"

More specifically, proposed interpretations appear to be more concerned with the original form of the theory, seemingly ignoring its most advanced form. The purpose of the interpretations in [1] is to encourage taking a step back and then attempting to retrace the development of the theory by investigating original sources for the original published papers and letters of the participants.

In a publication on the subject of physical reality, correctness, and completeness [2], questions are asked by the authors and explained concerning physical reality being considered complete when using a quantum mechanical description of that physical reality. As pointed out in that publication, the first question to ask is if the theoretical completion is correct and complete, that is, in this particular case, do the quantum mechanical results line up correctly with the experimental results (the data) that are acquired and measured, and to what degree is there agreement?

The second question asked by the authors is whether the theoretical description is complete in explaining the theory, again the quantum mechanical description in this particular case. The second question was given the priority in [2], that each element of the physical reality acquired and measured experimentally must have a match, a companion in the theoretical completion.

This is especially true and important when questions, especially the second question concerning high energy research results, are at the measurement frontier: (i) The Energy Frontier that makes use of the world's largest high energy facility which is in

Geneva, Switzerland, the Large Hadron Collider (LHC) at CERN [3]; (ii) The Precision Frontier of High Energy Physics where the facilities at Fermi National Accelerator Laboratory (FNAL) in Evanston, Illinois, near Chicago, comprise its epicenter; and (iii) The Cosmic Frontier where space-based and ground-based sensors and detectors, along with their data acquisition systems, are being constructed and tested currently, in several countries worldwide.

2. Quantum entanglement, Higgs bosons, and physical reality

An example of this importance can be understood in the experimental discovery of the theoretically proposed, and now confirmed, Higgs boson. Evidence of this particle's observation was made by both the ATLAS [4] and CMS [5] experimental collaborations at CERN's LHC in 2012. The Nobel Prize for the discovery of this, the first and only Standard Model fundamental boson with zero intrinsic spin angular momentum, was awarded in 2013 for theory contributions that showed how fundamental Standard Model particles acquire mass from the Higgs boson. The Higgs boson's existence (via Spontaneous Symmetry Breaking in the early universe) was considered by many theorists to be the most likely of several other, different, proposals.

Figure 1 shows the Feynman Diagram of a Higgs boson decay to two vector bosons (Z-bosons) and the vector boson decays to leptons in the "Golden Channel" (fewer background events) $H \rightarrow Z^0 Z^{0*} \rightarrow 4\text{leptons}$. The Z^0 particle shown in the figure is one of those vector bosons that have a mass of $91.19 \text{ GeV}/c^2$ at the middle of its resonance peak in the data's spectrum, corresponding to the listing in the Particle Data Group booklet, while the Z^{0*} particle shown is the vector boson that has a mass smaller than the Particle Data Group booklet value. The latter boson that has a mass of between $15 \text{ GeV}/c^2$ and $60 \text{ GeV}/c^2$ is given the label "off-mass-shell" Z^{0*} -boson, while the former bosons are simply Z^0 -boson, which is "on-mass-shell". The [g] particle lettering in **Figure 1** corresponds to two gluons that collide and couple to form particles as shown by the lines that are in the shape of a triangle in the figure, so this is a gluon-gluon fusion collision process. Gluons mediate the strong interaction in high energy physics. The Higgs boson couples to mass, so the closed triangle in **Figure 1** represents what are mainly the most massive particles of the Standard Model of Particle Physics - top plus anti-top quarks for example. Since the vector bosons shown here are neutral, they each decay into two same flavor, opposite-charge leptons, as shown in this particular type of decay. An electron-positron pair and a positively charged muon along with a negatively charged muon make up the four leptons.

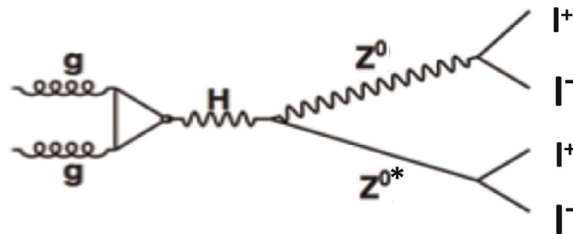


Figure 1.
Higgs boson decay Feynman diagram: $H \rightarrow Z^0 Z^{0*} \rightarrow 4\text{leptons}$ the symbols shown here are defined and explained in the main text.

Discovery of the Higgs via this process required the coincident measurement of each of these four leptons' position and energy, or momentum, relative to the decayed vector boson linear momentum direction prior to its decay. This **Figure 1** process occurs about one out of every 10^{n-th} proton-proton collisions, where $n \approx 10$ for a 7 TeV proton-proton collision energy, while n is smaller for higher proton-proton collision energies.

The Introduction section of this Introductory Chapter makes use of the Higgs boson production and decay [6] discussion in order to help clarify, in an overview, both quantum entanglement in High Energy Physics as well as the process that leads to the chosen final result. It is based upon research measurements and analysis, followed in order, to correctly search for signals of quantum entanglement, entanglement entropy, Bell's Inequality studies, and quantum computing at collider energies in both particle and nuclear physics. The Higgs decay process discussed and shown above is one of the two decay channel processes that existed in the Higgs boson discovery. The quantum entanglement overview analysis discussed in this chapter makes use of both theoretical and experimental descriptions.

When two or more particles (qubits) are produced and interact with each other so that the final quantum state under analysis will have contributions from both (in a bipartite (qubit A, qubit B) system) or the group (in the system of multiple qubits) of particles, they are both (bipartite) or all (multipartite) entangled with each other. Every particle involved must be described by a quantum state that depends upon the quantum state of the other particle, or particles, involved in the bipartite or multipartite system, respectively. And, there is no dependence on the distance between the states.

The quantum entanglement definition is shown in **Figure 2**. When there is quantum entanglement, there is a sum of terms used in describing the quantum state. It is labeled as superposition in this context.

New discoveries in high energy nuclear and particle physics can give rise to new phenomena that require new interpretations of, or additions to, quantum entanglement [7–9], that is, further experimental and theoretical research may need to be carried out and completed prior to complete physical reality success in discoveries at the energy frontier in order to make fully proper statements about quantum

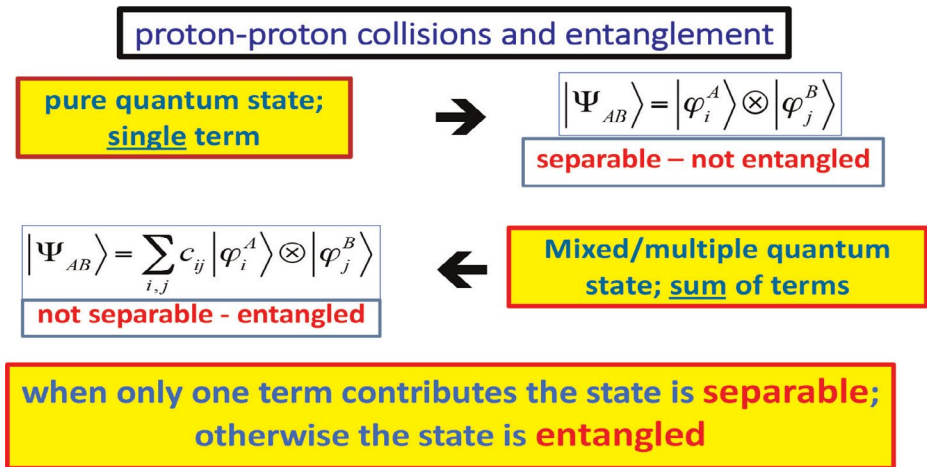


Figure 2.
Quantum entanglement definition. See details in main text.

entanglement in those cases. Quantum entanglement, while shown to exist experimentally and theoretically in quantum mechanics, is so far not observed in classical mechanics.

In production and then decay of the Higgs boson, further measurements and analyses, along with theoretical research, have been carried out [10–15] for CP-violation and further measurements, respectively, as a few examples even after the Higgs boson discovery, in order for them to be considered correct and complete when using a quantum mechanical description, as indicated in the Introduction section of this Introductory chapter.

Experimental searches are currently underway for evidence of quantum entanglement, entropy of entanglement, and Bell's Inequality violation signatures using Higgs bosons' decays to vector bosons, in the ATLAS and CMS experiments at CERN's Large Hadron Collider [16]. Additionally, theory calculations and data analyses are being studied in collaboration with the experimentalists [17–21]. In both cases, Monte Carlo-simulated events are used for analysis at this stage of ongoing research.

3. Conclusions

As underscored in the Introduction of this Introductory chapter [2], each element of physical reality acquired and measured experimentally must have a match, a companion in theoretical completion, that is, both must be correct and complete. And, the elements of each physical reality and theoretical completion sets must match.

We may gain in understanding by reinforcing very similar statements from another giant in science [22] whose quote “The proper method for inquiring after the properties of things is to deduce them from experiments” points to the importance of proper physics experiments at high energies. In addition, a follow-up quote from the same scientist [22], “It is the weight, not numbers of experiments that is to be regarded,” emphasizes that there is essentialness and significance in follow-up experiments to a major discovery such as the Standard Model Higgs boson [4, 5, 10–15] as described in the previous section of this Introductory Chapter. Significance is important since it is, in this particular case, the Higgs boson observation along with its production and decay to vector bosons that is used in quantum entanglement measurement significance at these high energies. And finally, the quote [22] “If the experiments I urge be defective, it cannot be difficult to show the defects; but if valid, then by proving the theory, they must render all objections invalid” points to the essence of correct and complete theoretical research (again, in this case, involving the Higgs boson and its decays to vector bosons) for successful measurement and reliability.

The concept, as well as the interdisciplinarity, of quantum entanglement has grown, especially in Condensed Matter Physics, Atomic, Molecular, and Optical Physics (the Nobel Prize in Physics was awarded to Alain Aspect, John Clauser, and Anton Zeilinger in 2022 for research results that tested the purity of quantum mechanics as we know it and use it by detecting evidence for Bell's Inequality violation [23]), quantum communications [24], and most recently, more, new quantum entanglement applications and results in nuclear and particle physics as highlighted in the preceding section (Section 2) of this Introductory Chapter and referenced in [7–9].

It will be interesting to compare the current research topics, their methods, means, and results, listed in this book with those that will show themselves in the next several generations!

Acknowledgements

The author (OKB) gratefully acknowledges helpful scientific discussions with Professor Steven Lamoreaux for our collaboration in completing this Introductory Chapter of the current book. And sincere thanks to Yale University for providing financial support.

Conflict of interest


The author has no conflict of interest.

Author details

Oliver K. Baker
Wright Laboratory, Department of Physics, Yale University, USA

*Address all correspondence to: oliver.baker@yale.edu

IntechOpen

© 2024 The Author(s). Licensee IntechOpen. This chapter is distributed under the terms of the Creative Commons Attribution License (<http://creativecommons.org/licenses/by/3.0>), which permits unrestricted use, distribution, and reproduction in any medium, provided the original work is properly cited. 

References

- [1] Golub R, Lamoreaux S. The Historical and Physical Foundations of Quantum Mechanics. Oxford, United Kingdom: Oxford University Press; 2023
- [2] Einstein A, Podolsky B, Rosen N, Institute for Advanced Study, Princeton, New Jersey. Can quantum-mechanical description of physical reality be considered complete? *Physical Review*. 1935;**47**:777
- [3] Peters T, Peterson C. The Higgs boson: An adventure in critical realism. *Theology and Science*. 2013;**24**: 185-207. DOI: 10.1080/14746700.2013.809948
- [4] ATLAS Collaboration. A particle consistent with the Higgs boson observed with the ATLAS detector at the large hadron collider. *Science*. 2012;**338**(6114):1576-1582. DOI: 10.1126/science.1232005
- [5] CMS Collaboration. A new boson with a mass of 125 GeV observed with the CMS experiment at the large hadron collider. *Science*. 2012;**338**(6114): 1569-1575. DOI: 10.1126/science.1230816
- [6] Internet, Constraints on Higgs boson properties.pdf. Available from: https://pure.uva.nl/ws/files/110885883/Constraints_on_Higgs_boson_properties.pdf
- [7] Michael Irving. Physicists discover completely new type of quantum entanglement. Available from: <https://newatlas.com/physics/new-type-quantum-entanglement-particles/>
- [8] Department of Energy, Office of Science. New Form of Quantum Entanglement Gives Insight into Nuclei. Washington, DC: Department of Energy, Office of Science; 2023. Available from: <https://www.energy.gov/science/article/s/new-form-quantum-entanglement-gives-insight-nuclei>
- [9] Star Collaboration. Tomography of ultrarelativistic nuclei with polarized photon-gluon collisions. *Science Advances*. 4 Jan 2023;**9**(1):eabq3903
- [10] ATLAS Collaboration. Measurement of the CP properties of Higgs boson interactions with tau-leptons with the ATLAS detector. *European Physical Journal*. 2023;**C83**:563
- [11] ATLAS Collaboration. Search for a CP-odd Higgs boson decaying to Zh in pp collisions at $\sqrt{s} = 8\text{ TeV}$ with the ATLAS detector. *PLB*. 2015;**744**: 163-183
- [12] ATLAS Collaboration. CP properties of Higgs boson interactions with top quarks in the $t\bar{t}H$ and tH processes using $H \rightarrow \gamma\gamma$ with the ATLAS detector. *PRL*. 2020;**125**:061802
- [13] ATLAS Collaboration. Measurement of the Higgs boson mass with $H \rightarrow \gamma\gamma$ decays in 140 fb^{-1} of $\sqrt{s} = 13\text{ TeV}$ pp collisions with the ATLAS detector. *PLB*. 2023;**847**:138315
- [14] ATLAS Collaboration. Combined measurement of the Higgs boson mass from the $H \rightarrow \gamma\gamma$ and $H \rightarrow ZZ^* \rightarrow 4\text{leptons}$ decay channels with the ATLAS detector using $\sqrt{s} = 7, 8$, and 13 TeV pp collision data. *Physical Review Letters*. 2023;**131**:251802(1-21)
- [15] ATLAS Collaboration. Combination of searches for invisible decays of the Higgs boson using 139 fb^{-1} of proton-proton collision data at $\sqrt{s} = 13\text{ TeV}$

collected with the ATLAS experiment.
 PLB. 2023;**842**:137963

[16] CERN, LHC Experiments; Diverse Experiments at CERN: ATLAS; CMS. Available from: <https://home.cern/science/experiments>

[17] Fabbrichesi M, Floreanini R, Gabrielli E, Marzola L. Stringent bounds on HWW and HZZ anomalous couplings with quantum tomography at the LHC. *Journal of High Energy Physics*. 2023; **2023**:1-5. Article number 195. arXiv: 2304.02403 [hep-ph]

[18] Fabbrichesi M, Floreanini R, Gabrielli E, Marzola L. Bell inequality is violated in $\mathbf{B}^0 \rightarrow J/\psi K^* (892)^0$ decays. 8 May 2023:1-5. e-Print: 2305.04982 [hep-ph]

[19] Aguilar-Saavedra JA, Bernal A, Casas JA, Moreno JM. Testing entanglement and bell inequalities in $\mathbf{H} \rightarrow \mathbf{ZZ}$. *Physical Review D*. 20 Jan 2023;**107**:016012-1-016012-12

[20] Barr A. Testing bell inequalities in Higgs boson decays. *PLB*. 2022;**825**: 136866

[21] Ashby-Pickering R, Barr AJ, Wierchucka A. Quantum state tomography, entanglement detection and bell violation prospects in weak decays of massive particles. *JHEP*. 2023; 5:20

[22] Isaac Newton Quotes. Brainy Quote Publication; 25 Dec 1642-20 Mar 1727. Available from: https://www.brainyquote.com/authors/isaac-newton-quotes?__cf_chl=tk=ekGfN5xPIEQhhLtPOzFuKns_WJunCP4E1mYVXS8TxJc-1703267060-0-gaNycGzNFDs

[23] Eva Nevelius, MLA style: The Nobel Prize in Physics 2022. Nobel Prize.org. Nobel Prize Outreach AB 2023. Available

from: <https://www.nobelprize.org/prizes/physics/2022/summary/> [Accessed: December 28, 2023]

[24] Zou N. Quantum entanglement and its application in quantum communication. *Journal of Physics: Conference Series*. 2021;**1827**:012120. DOI: 10.1088/1742-6596/1827/1/012120

Section 2

Theory

On the Questions of Spin and Spin Quantum Correlations in Relativistic Quantum Mechanics and Relativistic Quantum Information

Shrobona Bagchi

Abstract

The majority of current understanding of the quantum correlations is in the field of non-relativistic quantum mechanics. To develop quantum information and computation tasks fully, one must inevitably take into account the relativistic effects. In this regard, the spin is one of the central tools. For this purpose, it is of paramount importance to understand and characterize fully the theory of spin in relativistic quantum information theory where the spin states act as qubit. This area is still far from being resolved. As a result, this article will explore the recent studies of the concepts of the spin and spin quantum correlations in inertial frames and some apparent paradoxes regarding this concept. We will mainly focus on the problem of characterizing the spin, reduced spin density matrices and spin quantum correlations in inertial reference frames and the apparent paradoxes involved therein. Another important aspect is the use of tools of quantum field theory to extend several concepts in non-relativistic domain to relativistic one. In this regard, we analyze the development of the theory of relativistic secret sharing and a correlation measure namely the entanglement of purification.

Keywords: relativistic spin quantum correlations, relativistic spin-momentum correlation, relativistic quantum information, spin reduced density matrix in relativistic scenario, entanglement of purification

1. Introduction

Quantum correlations are an important part of modern quantum information theory [1–3]. This area is very well studied, developed, and understood in nonrelativistic quantum information using nonrelativistic quantum mechanics [4]. The study of these correlations has helped in the development and implementation of various quantum information processing protocols such as quantum teleportation, quantum cryptography, and quantum secret sharing. However, this theory is not well understood and developed in relativistic quantum information theory, which uses relativistic quantum mechanics or

quantum field theory [5–9]. There are several less-understood areas that require careful analysis and resolution. We handpick a few such areas and explore in detail the fundamental and underlying issues, explore some fundamental quantum information tasks in relativistic quantum information, and end with conclusions and potential future directions. This discussion inevitably falls in the section of quantum information in high-energy physics, since the effect of relativistic velocity or acceleration becomes relevant in high-energy physics. At the end, we also discuss how an important concept of entanglement of purification has been generalized in the area of holography, reflect on the conjecture, and raise a few important issues regarding its operational significance in this area. This analysis shall also be helpful in future space satellite-based quantum communication.

As per our knowledge of quantum mechanics and relativistic quantum mechanics, the ‘spin’ is usually thought of as an intrinsic ‘angular momentum’ associated with elementary particles like electrons, protons, or other particles as such. It is understood to be purely a quantum-mechanical property without any counterpart in classical physics. Spin in quantum mechanics is considered an existing ‘intrinsic’ angular momentum of the particle, and it is not due to the classical rotation of any internal component of the particle. Spin as a relativistic concept is still undergoing revisions to be understood to be in full glory and entirety. It is an essential part in majority of quantum information tasks in modern day quantum information and computation theory and applications. The important details start to emerge as one goes to inertial and noninertial frames and several paradoxes and inconsistencies start to show in this arena in terms of its definitions, conceptualization, and further generalizations such as the reduced spin density matrices in inertial frames. These observations point to the fact this is a partially developed concept, and its development will lead to robust implementation of various quantum information processing tasks in relativistic regimes such as in future satellite-based quantum communication. In the upcoming paragraphs, we visit some of these areas in short, which are explained in detail in the main sections later.

Spin qubit is a well-understood concept in nonrelativistic quantum mechanics, It is understood very well through the implementation of the Stern-Gerlach experiment in the nonrelativistic (low velocity, which is much smaller than the speed of light in vacuum) limit. However, the definition and understanding of the spin in the relativistic regime are still underdeveloped. This has been analyzed in various works spread out around the last decade, and research on this is still ongoing today [10–17]. One of the origins of this difficulty lies in the entangling of the spin degree of freedom with the momentum degree of freedom in the Lorentz-boosted reference frames. The second difficulty arises from the fact that for a quantum particle moving in a superposition of velocities as a quantum-mechanical possibility, it is impossible for it to suddenly transition to its rest frame, wherein its spin is defined and understood properly. Possible remedies for these problems have been proposed by various authors. They eventually propose a solution to this problem and ways of experimentally observing the relativistic features of the spin, which then in turn promises to open up the possibilities of devising quantum information protocols using spin as a qubit in the special-relativistic regime.

Another very important and recurring problem in relativistic quantum information or quantum information in high energy physics is the robust formulation of the reduced spin density matrix in the relativistic regime. Though the reduced density matrix for the spin degree of freedom is well-defined in nonrelativistic quantum mechanics, its definition and formulation run into problems when trying to simply extend this to a relativistic regime. An apparent paradox involving the definition and formalism of spin density matrix in a relativistic regime is given in [11]. It was shown that a model for particle detection wherein a linear application of the Wigner rotations was applied to the state of a massive

relativistic particle in a superposition of two counter-propagating momentum states, leads to a paradox. The paradoxical behavior is that the probability of finding the relativistic quantum particle at different positions depends on the reference frame, which is unwanted feature in the theory. A solution to the paradox was given there. According to the proposed solution, the authors argue that we cannot in general linearly apply the Wigner rotations to a quantum state without considering the appropriate physical interpretation.

Again in similar vein, there is another problem similar in nature to the above. An open problem in the field of relativistic quantum information is whether entanglement and the quantitative degree of violation of Bell's inequalities for massive relativistic particles are dependent on the frames of reference or not. At the heart of this question lies the effect that the spin degree of freedom gets entangled with the momentum degree of freedom a relativistic regime. In a more advanced work, the authors here show that the Bell's inequalities for a pair of quantum particles can be maximally violated in a 'special-relativistic regime', even without any postselection of the momentum of the particles, shown via the use of the novel methodology of quantum reference frames. The authors claim that the use of the quantum reference frames allows them to transform the problem to the rest frame of a particle, whose state can be in a superposition of relativistic momenta from the viewpoint of the laboratory frame of reference. In this work, the authors work with several problems of defining the spin density matrix in the relativistic regime and show that when the relative motion of two particles is noncollinear, the appropriate measurements for violating Bell's inequalities in the laboratory frame involve the "coherent Wigner rotations". In this work, the authors also show that the degree of violation of Bell's inequalities is independent of the choice of the newly introduced and defined quantum reference frames, which is a desired feature in theory.

After the full description of the existing line of work spin density matrices in relativistic reference frames, we turn our attention to the use of tools of quantum field theory in implementing quantum information protocols in the high energy regime [18–20]. In this respect, we review a relativistic quantum secret-sharing protocol in a relativistic regime. Here, the authors develop a quantum secret-sharing protocol that relaxes usual assumptions and considers the effects due to the accelerating motion.

Another research area is the extensions and further development of various quantum information correlation measures via quantum field theory and conformal field theory [21, 22]. One such definition is the entanglement of purification, which defines the total correlation measure for a quantum particle in an operational way [23]. Entanglement wedge cross-section has been developed to account for the counterpart of entanglement of purification in quantum field theoretic and conformal field theoretic terms. It has been termed the Holographic Entanglement of Purification by Tadashi Takayanagi and Koji Umemoto [23–25]. They suggest that it is a holographic counterpart of the entanglement of purification, which measures a bipartite correlation in a given mixed-state quantum state defined on an operational basis. We point out in our coming sections that a similar operational footing in the quantum field theoretic terms will be a promising area of research in the future.

2. On the questions of spin and spin quantum correlations in relativistic quantum mechanics and relativistic quantum information

In this section, we briefly review a few key concepts needed to understand the basic analysis of spin in quantum mechanics and the problems associated with it for its

formulation in the relativistic regime. These concepts include those of reference frames as defined in the theory of special relativity. Any physical system is defined using a set of coordinates that completely specifies its reference frame. From the principles of special relativity, we know that all physical laws hold the same way in all reference frames. The laws of physics transform covariantly in between the different reference frames. However, there is typically a reference frame that is the most convenient to use, where the system rests. This reference frame is called the rest frame of the physical system. These concepts of the classically defined reference frames, as in classical physics, are very well understood in the absence of intricacies of certain quantum-mechanical phenomena. However, when we start to analyze some quantum properties in detail using the traditionally defined reference frames, we face some problems. In this respect, it was shown that when the external degrees of freedom for example the momentum of the physical system, are in a quantum superposition with respect to the laboratory frame of reference, no classical reference frame transformation, as prescribed by the special theory of relativity, can map the description of physics from the laboratory to the rest frame [12]. This area of physics is not understood well enough. Subsequently, the concept of a quantum reference frame was introduced and leveraged to give an operational footing to the concept of spin in relativistic quantum mechanics [12]. It was claimed in [12] that such a formulation is able to solve some of the paradoxical features related to the transformation of spin in relativistic quantum mechanics. There are several claims in this direction by various authors. As a result, proper experimental verifications are needed to settle the correct theory for spin in relativistic quantum mechanics and relativistic quantum information theory. These concepts are explained later in the later paragraphs.

One of the most important concepts is spin in non-relativistic quantum mechanics, defined operationally via the Stern-Gerlach experiment. The spin of a Dirac spin-1/2 particle is defined by the 2×2 Pauli matrices $\sigma_i (i = 1, 2, 3)$. The Pauli matrices and the unit matrix generate an irreducible representation of the $SU(2)$ group. It is well known that the spin operator of a nonrelativistic spin-1/2 particle in quantum mechanics is very well understood. Also, we know that there is a clear correspondence between quantum-mechanical operators and classical variables in nonrelativistic quantum mechanics. This correspondence exists for all operators such as the position, momentum, and angular momentum etc. However, in contrast to this observation, the connection between the quantum-mechanical operators and classical variables in relativistic quantum mechanics is much more subtle and complex.

In this respect, we review the concept of spin in relativistic quantum mechanics from different perspectives provided by various authors until now. They involve the analysis of an apparent paradox caused by linear Wigner rotation and the quantum reference frames. These are presented below.

2.1 Apparent paradox of Wigner rotations for relativistic effects of spin of quantum particle

The intricacies of the conceptual and analytical foundation of spin of relativistic quantum particles were presented in [11]. In their analysis, the authors presented an apparent paradox involving the definition and formalism of spin density matrix in a super-relativistic regime. It was shown there that a method of particle detection in combination with linear Wigner rotations, which then corresponds to momentum-dependent changes of the particle spin owing to the fact that spin and momentum degrees of freedom get entangled in the relativistic scenario under Lorentz

transformations, applied to the state of a massive relativistic quantum particle in a superposition of two different momentum states leads to a paradox. The paradoxical feature is that the probability of finding the relativistic quantum particle at different positions depends on the reference frame, which should not be the case. As a solution to the paradox, which is also simple, the authors suggested that one cannot in general linearly apply the linear Wigner rotations to a quantum state without considering the appropriate physical interpretation of it. We sketch out the main steps of their analysis here. The initial state taken in this case is of the following form

$$|\Psi\rangle = \frac{1}{\sqrt{2}}[|p\hat{y}, Z\rangle - |p\hat{y}, -Z\rangle], \quad (1)$$

in the frame S_0 . Here, $|p, \pm Z\rangle$ represents a state for the particle with 4-momentum (p^0, \vec{p}) , and spin state pointing in the $\pm z$ direction, being the eigenvector of the Pauli matrix σ_z with eigenvalue ± 1 with reference to S_0 . Here, the authors have used Wigner's definition of spin, and they have taken $c = 1$. Therefore, from the perspective of the rest frame, the quantum particle is in a superposition of momentum in opposite directions. Using proper algebra, it was found out by the authors that the probability density of finding the relativistic quantum particle around position y obeys the following expression

$$p_0(y) \propto \sin^2\left(\frac{py}{\hbar}\right) \quad (2)$$

If one then makes a change of reference frame to a frame that moves with velocity βz in relation to $S(0)$, each momentum component of the state $|\Psi\rangle$ undergoes a different spin transformation. The spin and the momentum degrees of freedom get entangled when linear Wigner rotations are applied in a nontrivial way. See [11] for details. In the reference frame S_1 , the momentum state of the particle changes from before, though the y component remains the same. In this work, the authors then analyze the expressions about the y dependence of the particle wavefunction and do not analyze for z, x direction for simplification without any loss of generality. With some reasonable approximation, the probability expressions found with respect to the reference frame S_1 is given by the following

$$p_1(y) \propto \cos^2\left(\frac{\phi}{2}\right) \sin^2\left(\frac{py}{\hbar}\right) + \sin^2\left(\frac{\phi}{2}\right) \cos^2\left(\frac{py}{\hbar}\right), \quad (3)$$

where the angle ϕ is related to the boost parameter for the reference frame S_1 [11]. Therefore, this new expression for probability points to a paradox that has crept into the calculation in between, done traditionally. The authors in [11] argue that this is a paradox since the probability of finding the particle around some position should depend on the reference frame. As a result, this paradox points toward a deficiency in the current state of the art of the theory of spin in quantum mechanics. Thereafter, the authors in [11] test this observation differently via the use of quantum measurements using detectors. They consider measurements of the particle position using a detector that, by construction, responds only to the charge or the mass of the particle but does not in any case depend on its spin. Using this formalism and again placing a small number of reasonable approximations that are relevant in the experimental setup,

they again show the discrepancy in the expressions for probability expressions as calculated concerning different reference frames.

To summarize, they have shown that the application of the momentum-dependent linear Wigner rotations to the quantum state of a massive relativistic particle in a superposition of counter-propagating momentum states along with a model for particle detection leads to a paradox, since the probability of finding the particle at different positions would depend on the reference frame. Considering the physical implementation of the quantum state, they have discussed that the Wigner rotation depends on the preparation method, such that, with a change of the reference frame, the spin transformation of a quantum state in a superposition of different momenta is not exactly equivalent to the linear application of the momentum-dependent Wigner rotation to each momentum component of the state. This, they say, solves the apparent paradox. Their work and a few previous works on the subject show that relativistic quantum transformations cannot generally be computed only by following a mathematical procedure as in the traditional literature of relativistic quantum mechanics. The authors argue that the physical meaning of the transformations must always take precedence before their application in that physical scenario.

Though they have proposed the above solution to the apparent paradox, they also stress that their solution may not be the only viable solution to this apparent paradox. It may be possible that the paradox could be solved by modeling the particle detection by some more complicated scheme, keeping the linearity property of the Wigner rotations. Consequently, different solutions were proposed by different authors to this problem. The next sections discuss one of the main contenders in the name of quantum reference frames [12]. However, it is important to note that settling and reaching a proper solution to this apparent paradox needs experimental verifications under different conditions and approximations.

2.2 Relativistic Stern-Gerlach experiment and quantum reference frames

To provide a consistent description of the relativistic effects on the spin of a quantum particle, more theories were proposed, one of which is based on the relatively recent proposals of quantum reference frames. Along this line, the relativistic treatment of the Stern-Gerlach experiment was proposed and was termed as the relativistic Stern-Gerlach experiment [12]. The theory of the quantum reference frames was evoked there to give an operational interpretation to the spin in relativistic quantum mechanics. It was noted in [12] that when the particle has relativistic velocities, the spin degree of freedom transforms in a momentum-dependent way, as was noted by previous authors. Then, suppose a standard Stern-Gerlach measurement is performed on a particle in a pure quantum state moving in a superposition of relativistic velocities. In that case, the operational identification of the spin fails because it was shown in [12] that no orientation of the Stern-Gerlach apparatus returns an outcome with unit probability. The question that then arises is whether it is possible to find ‘covariant measurements’ of the spin and possibly momentum, which predict invariant probabilities in different Lorentzian reference frames for the case of a quantum relativistic particle moving in a superposition of velocities [12]. This is therefore an alternate solution to the solution proposed in [11] as described in the previous section. If such measurements are possible to construct, then it would be possible to map the description of spin in the rest frame of the particle to the frame of the laboratory in an unambiguous way. This would enable one to derive the

corresponding observables to be measured in the laboratory frame to verify the correct theory of the spin of a relativistic quantum particle.

The trial for finding such covariant measurements that preserve probability values in different reference frames is motivated by the potential applications in which the spin degree of freedom is used as a qubit to encode and transmit quantum information in the relativistic regime. As such, earlier protocols are no longer valid in a relativistic context. These severely constraints and undervalue the wide range of applicability of techniques involving spin as a quantum information carrier in the relativistic regime. It is then important to explore possible methods which can overcome this limitation. In the context of relativistic quantum information, this question has been extensively discussed in relation to Wigner rotations. It has been related to the problem of identifying a covariant spin operator [11–15]. A variety of relativistic spin operators have been proposed to date. Some of them are called the Frenkel, the Pauli-Lubanski, the Pryce, the Foldy-Wouthuysen, the Czachor, the Fleming, the Chakrabarti, and the Fradkin-Good spin operators.

To remedy the above problems, the authors in [13], use the concept of “superposition of Lorentz boosts” which allows them to make the relativistic quantum particle “jump” into the rest frame even if the particle is not in a momentum eigenstate but in a quantum state with a superposition of momentum in general. It is well known that in the rest frame, the spin observables satisfy the $SU(2)$ algebra and are operationally defined through the famous Stern-Gerlach experiment. The authors in [13] aim to make this same concept work in inertial reference frames. In the work [13], the authors transform the set of spin observables in the rest frame to an isomorphic set of observables in the laboratory frame. The transformed observables are generally entangled in the spin and momentum degrees of freedom as expected. The new set fulfills the $SU(2)$ algebra again and is operationally defined through an experiment that the authors label as the “relativistic Stern-Gerlach experiment.” In this experiment, the authors construct the interaction term and the measurement term between the spin-momentum degrees of freedom and the electromagnetic field in the laboratory frame, which gives the same probabilities as the Stern-Gerlach experiment in the rest frame, as desired, and stated earlier in the paragraph. This set of observables in the laboratory frame allows the authors to partition the total Hilbert space into two subspaces corresponding to the two outcomes, which can be termed as “spin up” and “spin down.” Hence, with techniques of the quantum reference frames, the relativistic spin states can effectively be used to construct a qubit state in an operationally well-defined way, as claimed by the authors in [13]. Thus, the quantum reference frames and the relativistic Stern-Gerlach experiment promise to be robust candidates representing the theory of intrinsic spin of relativistic quantum particles and its transformations between different reference frames. However, the correctness of the corners of this theory is still open to experimental demonstrations to be established fruitfully.

With the above background in mind, we now describe the relativistic Stern-Gerlach experiment, as discussed in [12]. One considers an experiment performed in the laboratory reference frame referred to as C. One allows the particle to have any quantum state and, in particular, to move in a superposition of momenta. This condition implies a nonclassical relationship between the two reference frames. This means that a standard boost transformation does not relate to the rest of frame A and the laboratory frame C as in classical special relativity. The authors in this work [12] implement a method to generalize the boost transformation to this case of the relativistic quantum particle. The coordinates for the mathematical analysis z are used to

describe the external degrees of freedom of particle A and the intrinsic spin degrees of freedom as \tilde{A} of the relativistic quantum particle. The state of the particle time $t = 0$ is taken to be the following

$$|\Psi\rangle = \cos\theta|\psi^+\rangle + \sin\theta|\psi^-\rangle, \quad (4)$$

where again we have the following definitions

$$|\psi^\pm\rangle = |\psi_z\rangle_A |\phi_x^\pm\rangle_{A\tilde{A}}, \quad (5)$$

is a division of the total wave function into components in x and z directions in rest frame and lab frames as per the notation. It is assumed that the motion along z direction is nonrelativistic, without any loss of generality. Writing these wave functions in terms of the superposition of momentum states, we have the following expressions

$$|\psi_z\rangle_A = \int dp_z \psi_z |p_z\rangle_A, \quad (6)$$

with ψ_z denoting Gaussian wave functions in the momentum variable p_z centered around $p_z = 0$ and standard deviation s_z . The other component is denoted as the following

$$|\phi_x^\pm\rangle_{A\tilde{A}} = \int d\mu(p_x) \phi_x |p_x, \Sigma_{p_x}^\pm\rangle_{A\tilde{A}}, \quad (7)$$

where ϕ_x^\pm is a general wavepacket expression and $|\Sigma_{p_x}^\pm\rangle_{A\tilde{A}}$ are the eigenvectors of the operator obtained via Lorentz boost and Pauli–Lubanski operator as defined in [12], with eigenvalues ± 1 . In the laboratory frame, it is possible to define the observables corresponding to the spin operators in the rest frame by transforming the spin, as defined in the rest frame, with a quantum reference frame which then correspond to the transformation. They are called the manifestly covariant Pauli–Lubanski spin operator. Now, after this, the authors engineer a Hamiltonian with the following interaction term Hamiltonian in the laboratory frame as follows

$$H_{int} = \mu B_z \xi, \quad (8)$$

where $B_z = B_z^0 - \alpha z$. ξ is the term containing the components that are obtained using the components of the manifestly covariant Pauli–Lubanski spin operator modified with parameters dependent on the boost parameters, as defined in [12]. Let us now see how the operators ξ came into the picture. The authors in [12] note that in laboratory frame C , when the particle A is in a superposition of momentum states, no spin measurement in a standard Stern–Gerlach experiment gives a result with probability one because of the following two reasons: the spin and momentum are entangled, and the relation between the laboratory and the rest frame is not a classical special-relativistic reference frame transformation. To devise such measurement that will give consistent probability values in all reference frames as in the rest frame, the authors in [12] note that in the laboratory frame, it is possible to define the observables corresponding to the spin operators in the rest frame by transforming the spin, as defined in the rest frame, with a quantum reference frame transformation, the expression of which is then derived as ξ , the details of which can be found in [12].

Now, let us look at the dynamics of the relativistic quantum particle due to the Hamiltonian as described above. The Hamiltonian term is an appropriate interaction Hamiltonian containing a magnetic field in the z direction of the laboratory frame. The state is then evolved with the action of this Hamiltonian, and its form is written down appropriately in the interaction picture as a function of time. It was shown that under the interaction with the magnetic field, the Gaussian wavepacket z gets split into two wavepackets, moving in opposite directions according to the state of the spin. After this, appropriate projection operators are applied to the wave packet, and probabilities of obtaining spin “up” or spin “down” as value is obtained denoted by p^\pm . It was shown via this calculation in [12] that for a time when the two wavepackets become distinguishable, the probabilities for obtaining up and down spins are found out to be $\cos^2\theta$ and $\sin^2\theta$, when irrelevant terms are neglected under the appropriate limit and subsequent approximation. The authors claim that in this way, one can solve the problem of ambiguity of finding the correct expressions for probabilities in rest frames in the relativistic Stern-Gerlach experiment.

In this work, the authors claimed to have provided a correct operational description of the spin of a special-relativistic quantum particle, which has been elusive for a while. Such operational description was initially difficult to obtain with standard traditional treatments due to the combined effect of special relativity and quantum-mechanical properties, which makes the spin and momentum entangled and an impossibility of jumping to the rest frame with traditional tools. To remedy this problem, the authors have introduced the concept and mathematical characterization of the “superposition of Lorentz boosts” transformation to the rest frame of a quantum particle, moving in a superposition of relativistic velocities from the point of view of the laboratory reference frame. As a result of their analysis based on the quantum reference frames, probabilities obtained in the relativistic Stern–Gerlach experiment are shown to remain the same in the rest frame and in the laboratory frame, which was a challenging task to accomplish before. This approach is relatively new to some earlier approaches and proposed theoretical remedies. However, it should be emphasized that the theoretical treatment offered in this work has yet to undergo several experimental checks in different limits, experimental conditions, and relevant approximations to be accepted and established as a correct theory for relativistic effects in spin of a quantum particle.

2.3 Other effects related to relativistic treatment of spin of a quantum particle

Several other effects are associated with the correct description of spin in relativistic quantum mechanics. An open question in relativistic quantum information is the invariance of a measure of entanglement and/or the quantitative degree of violation of Bell’s inequalities for massive relativistic particles in different frames of reference. Such questions can be extended similarly to other quantum information theoretic correlation measures. Likewise, as before, at the core of this dilemma is the effect that spin gets entangled with the momentum degree of freedom at relativistic velocities. In [13], the authors claim to show that Bell’s inequalities for a pair of particles can be maximally violated in a special-relativistic regime, even without any postselection of the momentum of the particles, again via the use of the concept of quantum reference frames. They specifically show that when the relative motion of two particles is noncollinear, the optimal measurements for violating Bell’s inequalities in the laboratory frame involve “coherent Wigner rotations” [13]. Thus, they also touch upon a

debated concept of the appropriate application of Wigner rotations in this physical setup. In this formalism, the authors also show that the degree of violation of Bell's inequalities is independent of the choice of the quantum reference frame, which is a desired effect. As a result, this work attempts to settle some important open questions involving the fundamental concepts of spin and relativity. However, for it to be established to be a correct theory or otherwise, several experimental checks must be performed consistently and in a reproducible way. As a result, experimental proposals to test out these theories in the laboratory under different conditions pose the next important steps in the full development of this area of research and enquiry.

2.4 Experimental efforts to test relativistic theory of spin of quantum particle

Experimentally, many efforts have recently been made to measure the quantum spin correlations of elementary particles. One of those proposed experiments involves studying relativistic electron pairs' quantum spin correlations to test the nonlocality of relativistic quantum mechanics. Finding the right expression and formalism for spin and spin quantum correlations in relativistic quantum mechanics is an important direction of research both from the perspective of space communications and testing the fundamentals of quantum physics and quantum gravity. Here, we report on two attempts at experiments to measure the spin quantum correlations in relativistic scenarios.

An experiment investigating the quantum spin correlations of relativistic electrons is reported here [16]. The project presented in [16] tries to make the first measurement of the quantum spin correlation function for a pair of massive relativistic particles. This measurement is claimed to be the first attempt to verify the predictions of relativistic quantum mechanics in the domain of spin correlations. This is an interesting research direction since it can settle competing theories of spin quantum correlations experimentally or even point out unknown deficiencies in the foundations of relativistic quantum mechanics. Per their description of the proposed experiment, the measurement is carried out on a pair of electrons in the final state of Moller scattering. The measurement attempts to measure correlations of spin projections on chosen directions for the final state pair after the complete evolution via the chosen dynamics. The detector consists of two Mott polarimeters, in which the spins of both Moller electrons are measured simultaneously. However, the results have not yet been linked to the theoretical predictions of the quantum reference frames or other competing theories of spin in relativistic quantum mechanics. This remains a promising future direction of research.

Another research direction has been the study of quantum spin correlations of relativistic electron pairs to test the nonlocality of relativistic quantum mechanics. The theory developed in this direction has been discussed in the previous sections. Therefore, an experiment that tests the predictions offered by the theory, for example, as offered by the quantum reference frames, will be extremely helpful in settling the correct theory of relativistic effects of quantum spin among many competing theories. This will help advance the understanding of fundamental theory in nature. This project is supposed to be a Polish–German project QUEST that will study relativistic quantum spin correlations of the Einstein–Podolsky–Rosen–Bohm type through appropriate measurements and the corresponding probabilities for relativistic electron pairs. This experiment will also use the Moller scattering method and Mott polarimetry technique.

3. Quantum information with quantum field theory: relativistic quantum secret sharing

In the previous section, we discussed the fundamental question of spin in relativistic quantum mechanics. We discussed how spin is an interesting topic and how its understanding and unraveling of exact nature and experimental verification will help develop intricate quantum technologies that use the spin as a qubit in quantum information processing tasks. However, though it is important to understand the concept of spin in relativistic quantum mechanics, one can also use the concept of quantum information processing tasks in relativistic quantum information using tools from quantum field theory. One of these approaches has been to use cavity dynamics for the case of noninertial motion in general. In this section, we report on the quantum secret-sharing protocol in the relativistic setting. Here, we focus more on the theory of a specific quantum information task called relativistic quantum secret sharing using tools from quantum field theory.

In (2,3)-threshold quantum secret sharing, the “dealer,” one of the parties taking part in the protocol, encodes the quantum secret in three quantum shares in a localized manner. The authors in [12] use the framework of accelerating cavities for this purpose, as it is a suitable choice to study the effect of nonuniform motion on localized quantum fields. Accelerating cavities are popular to study the relativistic effects on quantum information protocols. However, the authors in [12] develop a different approach from the approach of accelerating cavities. They formulate the evolution of the quantum field inside an accelerating cavity as a bosonic quantum Gaussian channel, which they then use to include the effects of the nonuniform motion of the quantum shares.

The authors in [20] focus on a relativistic variant of a (2,3)-threshold quantum secret sharing protocol. In the relativistic protocol presented in [20], similar to the nonrelativistic case, a dealer encodes the quantum secret into several quantum shares and distributes them to all the players. In this setup, the players are all located at different regions in the Minkowski spacetime, and the dealer and the players are all stationary. Under such circumstances, during the dealer’s distribution, the quantum shares experience nonuniform motion (noninertial) as they are transmitted to spacetime points in the future light cone of the dealer. Then, a subset of players within the access structure collaborate to retrieve the quantum secret by sharing their individual shares. However, to reach the same spacetime point, the shares go through phases of accelerating and decelerating motion while being transmitted, rendering the dynamics noninertial in general, in contrast to the special-relativistic regime described in the previous sections. The authors investigate how the noninertial motion of the shares affects the fidelity of the quantum secret-sharing protocol. The authors in this work claim to have solved continuous-variable quantum secret sharing wherein the quantum shares move nonuniformly in Minkowski spacetime. The tools used in this approach mainly comprise the tools developed in continuous-variable quantum information such as the formalism of the Gaussian quantum channels, dynamics of quantum field inside the cavity [20]. The authors do not use spin as the qubit in this relativistic scenario and yet are able to implement the relativistic quantum secret sharing protocol mainly via using the formalism of quantum field inside cavity, which may themselves be in noninertial motion [20]. The authors in [12] specify that they use the framework of Gaussian quantum information to write the evolution and dynamics of the quantum field inside the cavity central to their implementation of the protocol of quantum secret sharing, as a Gaussian quantum channel, in the noninertial

regime. They use this channel to study the effect of noninertial motion of the shares on the fidelity of the quantum secret sharing. As a result, this work shows that various methods can be utilized to study the effects of noninertial motion without directly referring to the transformation of spin in a super-relativistic regime.

4. Entanglement of purification and entanglement wedge cross-section

In this section, we discuss the relativistic quantum information from another angle. We discuss the quantification and characterization of correlation measures used in nonrelativistic quantum information theory using quantum field theory in relativistic regime. The quantity that is usually used is the entanglement entropy. The entanglement entropy is used to quantify the entanglement of the pure quantum states. Using the AdS/CFT correspondence, the entanglement entropy has a holographic counterpart given by the area of minimal surface [25]. This characterization, therefore, provides a relationship between spacetime geometry and quantum entanglement.

The entanglement is a pure quantum correlation. However, the mixed quantum states contain both the classical and quantum correlation together contained in the total correlation of the quantum state. Now, mutual information is a usual measure of the total correlation of a mixed quantum state. However, the justification of the mutual information as a measure of total correlation is sometimes questioned. Also, there were attempts at separating the quantum correlation from the classical correlation in the quantum mutual information via the introduction of the measure of quantum correlation called quantum discord. Another approach was proposed to quantify the total correlation in a quantum state via the transformation of the entanglement of Bell pairs via local operation and classical communication. This measure is called the entanglement of purification. Its many properties were studied in [24]. Later, a holographic quantity was proposed as a counterpart of this entanglement of purification using the concept of entanglement wedge cross-section as a conjecture. This quantity is called the holographic entanglement of purification. The definition of entanglement of purification in nonrelativistic quantum mechanics is as follows. If we have a given mixed quantum state ρ_{AB} , then at first, we purify the mixed quantum state ρ_{AB} to $|\Psi\rangle_{AA'BB'}$, and then, the entanglement of purification of the mixed quantum state ρ_{AB} is given as the follows

$$E_P(\rho_{AB}) = \min_{A'B'} E_f(AA' : BB') \quad (9)$$

In the holographic entanglement of purification, the authors have considered the quantity E_W defined as the minimal cross-section of the entanglement wedge in AdS/CFT. The authors have shown there that they have observed that their properties coincide with those of the quantity called entanglement of purification, which measures the total correlation between two subsystems for a mixed quantum state comprising both classical and quantum correlations. Based on their observations and calculations on the entanglement wedge cross-section, the authors have conjectured that the entanglement wedge coincides with the entanglement of purification in holographic conformal field theories. The authors also have given a heuristic argument for this identification. The open question remains whether this conjecture is true or not. Several works are ongoing to check this conjecture in mathematical terms.

Another very important and promising open direction along this line of research is finding an operational interpretation of the definition of entanglement

wedge cross-section; similarly, the entanglement of purification was motivated and operationally found in nonrelativistic quantum mechanics. The entanglement of purification was motivated operationally in terms of the conversion of the purely quantum correlation called entanglement in the maximally entangled state called the Bell pairs into the total correlation measure in the arbitrary quantum state using local operation and classical communication. Therefore, to settle the conjecture, another direction could be to try to find an operational footing of the entanglement wedge cross-section as well.

5. Conclusions

In this section, we summarize what we have discussed in the previous sections and open questions. Developing the fundamentals of understanding nature and natural phenomena with a robust mathematical construct and subsequent reproducible experimental verifications has been one of the strongest pillars of physics as we know it today. Many technological applications have stemmed from the robust structure of physical phenomena developed in theories in physics. Thus, we can imagine that such further developments will open up immense possibilities in future technologies that have a high potential for finding solutions for persistent problems in lives of people and such. Thus, it is clear that from the point of view of understanding nature, technological developments, and even resource allocation, the development of fundamental theories of nature is an area of research with immense potential.

Given the above motivation, we have covered a few aspects of physics that are important for developing quantum information theory in relativistic regimes; that is, in high-energy physics, it is paramount to use the relativistic effects via relativistic quantum mechanics and quantum field theory. It is well known that spin is an ill-understood concept in relativistic quantum physics. Prior approaches to spin in quantum physics have been discussed, and some recent promising approaches have been presented. It has also been discussed how a robust formulation of the concept of spin is crucial for developing quantum information in high-energy physics. We also reviewed the problem of spin quantum correlations and have presented the resources in the scientific literature that are trying to verify this experimentally in recent years. This issue is still unresolved, and a consistent resolution can open doors for the applications of relativistic quantum information and its extension of in space-based quantum technologies.

With the above open problem in mind, we also note that quantum field theory tools can be leveraged to develop quantum information protocols in relativistic quantum information in a high-energy arena, especially in the regime of noninertial motion. Such a protocol of relativistic quantum secret sharing has been discussed in detail. Similar techniques can be leveraged to develop such protocols further in high-energy physics.

In the last section of this chapter, we have covered a section on developing the definition of a total correlation measure in the language of quantum field theory and conformal field theory. The entanglement of purification, an active and open area of research, has been discussed here. Another open area of research has been pointed out in this arena, which has a high potential for development in the future. This area is the operational characterization of the quantum correlation measures defined in terms of tools as in quantum field theory and conformal theory. This area of enquiry is based on experimental verification in tabletop setups. This can be an active area of research in the future that might be challenging yet highly promising and with potential for rich dividends.

Acknowledgements


SB acknowledges funding from the Korea Institute of Science and Technology. S. B. acknowledges support from the National Research Foundation of Korea (2020M3E4A1079939 and 2022M3K4A1094774) and the KIST institutional program (2E31531).

Author details

Shrobona Bagchi
Korea Institute of Science and Technology, Seoul, South Korea

*Address all correspondence to: mailshrobona@gmail.com

IntechOpen

© 2023 The Author(s). Licensee IntechOpen. This chapter is distributed under the terms of the Creative Commons Attribution License (<http://creativecommons.org/licenses/by/3.0>), which permits unrestricted use, distribution, and reproduction in any medium, provided the original work is properly cited. 

References

- [1] Adesso G, Bromley TR, Cianciaruso M. Measures and applications of quantum correlations. *Journal of Physics A: Mathematical and Theoretical*. 2016;**49**:473001
- [2] Horodecki R, Horodecki P, Horodecki M, Horodecki K. Quantum entanglement. *Reviews of Modern Physics*. 2009;**81**:865
- [3] Modi K, Brodutch A, Cable H, Paterek T, Vedral V. The classical-quantum boundary for correlations: Discord and related measures. *Reviews of Modern Physics*. 2012;**84**:1655
- [4] Horodecki R. Quantum information. *Acta Physica Polonica A*. 2021;**139**:197
- [5] Mann RB, Ralph TC. Relativistic quantum information. *Classical and Quantum Gravity*. 2012;**29**:22
- [6] Fuentes I. Diversities in quantum computation and quantum information. In: *Lecture Series in Quantum Information*. World Scientific. 2012. pp. 107-147
- [7] Tamburini F, Licata I, editors. *Relativistic Quantum Information*. Entropy, MDPI books; 2020
- [8] Tjoa E, Gallock-Yoshimura K. Channel capacity of relativistic quantum communication with rapid interaction. *Physical Review D*. 2022;**105**:085011
- [9] Tjoa E. Quantum teleportation with relativistic communication from first principles. *Physical Review A*. 2022;**106**:032432
- [10] Saldanha PL, Vedral V. Spin quantum correlations of relativistic particles. *Physical Review A*. 2012;**85**:062101
- [11] Streiter LF, Giacomini F, Brukner Č. Relativistic bell test within quantum reference frames. *Physical Review Letters*. 2021;**126**:230403
- [12] Mikusch M, Barbado LC, Brukner Č. Transformation of spin in quantum reference frames. *Physical Review Research*. 2021;**3**:043138
- [13] Giacomini F, Castro-Ruiz E, Brukner Č. Relativistic quantum reference frames: The operational meaning of spin. *Physical Review Letters*. 2019;**123**:090404
- [14] Terno DR. Two roles of relativistic spin operators. *Physical Review A*. 2003;**67**:014102
- [15] Zou L, Zhang P, Silenko AJ. Position and spin in relativistic quantum mechanics. *Physical Review A*. 2020;**101**:032117
- [16] Włodarczyk M, Caban P, Ciborowski J, Dragowski M, Rembielinski J. Quantum spin correlations in Moller scattering of relativistic electron beams. *Physical Review A*. 2017;**95**:022103
- [17] Ciborowski J, Caban P, Dragowski M, Enders J, Fritzsche Y, Poliszczuk A, et al. A project to measure quantum spin correlations of relativistic electron pairs in Moller scattering. In: *EPJ Web of Conferences*. EDP Sciences. Vol. 164. 2017. p. 01004
- [18] Rick Perche T, Martín-Martínez E. Role of quantum degrees of freedom of relativistic fields in quantum information protocols. *Physical Review A*. 2023;**107**:042612
- [19] Benincasa DMT, Borsten L, Buck M, Dowker F. Quantum information processing and relativistic quantum

fields. Classical and Quantum Gravity.
2014;**31**:075007

[20] Bruschi DE, Lee AR, Fuentes I. Time evolution techniques for detectors in relativistic quantum information. Journal of Physics A: Mathematical and Theoretical. 2013;**46**:165303

[21] Calabrese P, Cardy J. Entanglement entropy and quantum field theory. Journal of Statistical Mechanics: Theory and Experiment. 2004;**2004**:P06002

[22] Takayanagi T. Entanglement entropy from a holographic viewpoint. Classical and Quantum Gravity. 2012;**29**:153001

[23] Ahmadi M, Ya-Dong W, Sanders BC. Relativistic (2,3)-threshold quantum secret sharing. Physical Review D. 2017;
96:065018

[24] Bagchi S, Pati AK. Monogamy, polygamy, and other properties of entanglement of purification. Physical Review A. 2015;**91**:042323

[25] Umemoto K, Takayanagi T. Entanglement of purification through holographic duality. Nature Physics. 2018;**14**:573-577

Perspective Chapter: On Entanglement Measures – Discrete Phase Space and Inverter-Chain Link Viewpoint

Felix A. Buot

Abstract

In contrast to abstract statistical analyses in the literature, we present a concrete physical diagrammatic model of entanglement characterization and measure with its underlying discrete phase-space physics. This paper serves as a pedagogical treatment of this complex subject of entanglement measures. We review the important inherent concurrence property of entangled qubits, as well as underscore its emergent qubit behavior. From the discrete phase space point of view, concurrence translates to translation symmetry of entangled binary systems in some quantitative measure of entanglement. Although the focus is on bipartite system, the technique is readily extendable to multi-partite system of qubits, as can easily be deduced from the physical inverter-chain link model. A diagrammatic analysis of the entanglement of formation for any multi-partite qubit system is given. We show that quantum mechanical joint distribution are entanglements.

Keywords: discrete phase space, inverter-chain link model, Hadamard transform, entanglement of formation, concurrence, ergodic distance

1. Introduction

Quantum entanglement has developed from a mere intellectual curiosity [1] of the fundamental structure of quantum mechanics¹ to become an important and practical resource for quantum information processing in the evolving theory of quantum information and ultra-fast computing. Thus, the quantitative measure of entanglement has developed into one of the most active fields of theoretical and experimental research. Here we will try to shed more light on some of the important concepts in the quantification of quantum entanglement by using a concrete simple mechanical model

¹ Note that although Bell's theorem asserts the nonlocality of quantum mechanics, the EPR inquiry is still not resolved, i.e., what is still left unanswered is the mysterious 'link' between qubits corresponding to our "see-saw" or mechanical inverter-chain link. (Note: Bell's inequality theorem is widely discussed in the literature and websites, we prefer not to cite specific reference).

of a bipartite system of qubits or chain of qubits. This treatment will be in contrast with mostly abstract and statistical treatment of entanglement measure in the literature.

We will focus on the so-called entanglement of formation and concurrence, two of the most important concepts to characterize entanglement resource. Here we consider a qubit as a two-state system. Moreover, we also consider an entangled qubit as effectively a two-state system, an *emergent qubit* as depicted in our physical inverter-chain link model. A two-state system has a unity entropy. Thus, a maximally entangled state has entropy equal to 1. From the discrete phase space point of view, any two-state system can be considered to possess two lattice-site states. Discrete Fourier transform or Hadamard transform implements unitary superposition of the two *lattice-site states* (also referred to as ‘*Wannier functions*’) to yield a sort of *crystal-momentum states* (also referred to as ‘*Bloch functions*’). For example, take the $|00\rangle$ and $|11\rangle$ ‘*lattice-site states*’, then the Hadamard bijective discrete transformation gives the ‘*crystal-momentum states*’, Φ^+ and Φ^- , which are two of the Bell basis states (or ‘*Bloch function*’ states).

2. Bell basis deduced from inverter-chain link model

We sketch here the derivation of the Bell basis states from our physical model, as depicted in **Figure 1**. Clearly, the entanglement of two *bare* qubits is divided into two orthogonal spaces of triplet² and singlet entanglement states.

Since the Hadamard transform is unitary, the inverse transform is well-defined, i.e., the transformation is bijective. We refer to $\{|00\rangle, |11\rangle\}$ as the “*Wannier functions*”

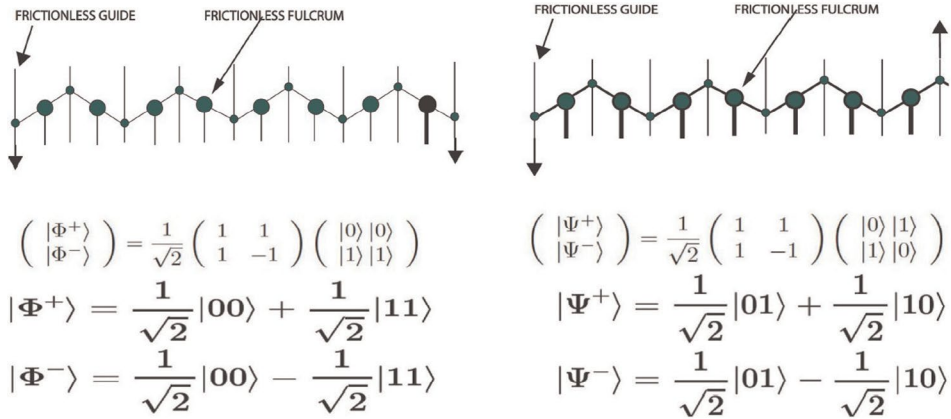


Figure 1. Physical diagrammatic model of “triplet” (left) and singlet (right) entanglement. By construction, each diagram is viewed as a two-state system, respectively. The Bell basis are readily derived below each diagram, using the Hadamard transformation. The actual physical implementation of the chain of inverters may need frictionless male/female sliding tube coupling for large-angle swing, but this is beside the point. We assume a rigid coupling model for simultaneity of events at both ends.

² The use of the term “triplet” is actually a misnomer here since the entangled system is not free to assume a singlet or zero spin state. Thus, this term is used here only as a label.

space and the $\{|\Phi^+\rangle, |\Phi^-\rangle\}$ as the corresponding “Bloch functions” space of a two-state triplet entanglement system. Likewise, $\{|01\rangle, |10\rangle\}$ as the “Wannier functions” space and the $\{|\Psi^+\rangle, |\Psi^-\rangle\}$ as the corresponding “Bloch functions” space of a two-state singlet entanglement system.

By virtue of this bijective relationship, any function of Wannier functions will have a corresponding function of Bloch functions. For example, a maximally *mixed* Wannier function states will generate a maximally mixed Bloch function states or the so-called maximally *mixed* entanglement states. Mixed and pure states will be further discussed below.

3. Entangled qubits as an emergent qubit

The virtue of our inverter-chain link model is that the emergent two-state property of entangled qubits is very transparent, since changing the state of one of the qubits also *immediately* change the states of the rest of the entangled partner(s)³. Here, we will rigorously justify our claim that entangled qubits behave, as a whole, as an *emergent* qubit.

Here, we employ the matrix representation of states and operators. We now represent $|\Phi^+\rangle$ and $|\Phi^-\rangle$ as,

$$|\Phi^+\rangle = \frac{1}{\sqrt{2}} \begin{pmatrix} 1 \\ 1 \end{pmatrix}, \quad (1)$$

$$|\Phi^-\rangle = \frac{1}{\sqrt{2}} \begin{pmatrix} 1 \\ -1 \end{pmatrix}. \quad (2)$$

Then we have

$$\langle \Phi^+ | \sigma_x | \Phi^+ \rangle = \frac{1}{2} (1 \ 1) \begin{pmatrix} 0 & 1 \\ 1 & 0 \end{pmatrix} \begin{pmatrix} 1 \\ 1 \end{pmatrix} = 1, \quad (3)$$

$$\langle \Phi^- | \sigma_x | \Phi^- \rangle = \frac{1}{2} (1 \ -1) \begin{pmatrix} 0 & 1 \\ 1 & 0 \end{pmatrix} \begin{pmatrix} 1 \\ -1 \end{pmatrix} = -1, \quad (4)$$

proving the two eigenvalues, like a qubit property of the triplet system.

For the singlet the most straightforward manipulation is to recognize that the singlet system is an independent system with its own two states which is orthogonal to the triplet states. In this sense we can also represent the singlet states just like that of the triplet states, namely,

³ The idea that entanglement is due to conservation of momentum does not hold for triplet entanglement since its two states give opposing spin-angular momentum. However, one may interpret that quantum superposition of the two-opposing angular momentum states conserves the overall zero net spin-angular momentum, as supported by their eigenvalues similar to a single qubit. On the other hand, for singlet entanglement, the zero angular momentum is conserve in both two states. This seemingly apparent physical difference of the triplet and singlet entanglements underscores the importance of resolving the “mysterious link” in the EPR inquiry, [1] in order to further advance theoretical physics.

$$|\Psi^+\rangle = \frac{1}{\sqrt{2}} \begin{pmatrix} 1 \\ 1 \end{pmatrix}, \quad (5)$$

$$|\Psi^-\rangle = \frac{1}{\sqrt{2}} \begin{pmatrix} 1 \\ -1 \end{pmatrix}. \quad (6)$$

Note that in the ‘Bloch-state’ space, σ_z in the “Wannier-state” space is transform to σ_x in entangled states,

$$\sigma_x = H\sigma_zH = \begin{pmatrix} 0 & 1 \\ 1 & 0 \end{pmatrix}. \quad (7)$$

Thus, we also have for the singlet states

$$\langle \Psi^+ | \sigma_x | \Psi^+ \rangle = \frac{1}{2} \begin{pmatrix} 1 & 1 \end{pmatrix} \begin{pmatrix} 0 & 1 \\ 1 & 0 \end{pmatrix} \begin{pmatrix} 1 \\ 1 \end{pmatrix} = 1, \quad (8)$$

$$\langle \Psi^- | \sigma_x | \Psi^- \rangle = \frac{1}{2} \begin{pmatrix} 1 & -1 \end{pmatrix} \begin{pmatrix} 0 & 1 \\ 1 & 0 \end{pmatrix} \begin{pmatrix} 1 \\ -1 \end{pmatrix} = -1. \quad (9)$$

Following this notion, Eqs. (8) and (9) can easily be extended to all entangled qubits, bipartite or multi-partite qubit systems to yield an emergent qubit. It is far more simpler to analyze the inverter-chain link diagrams, i.e., employ diagrammatic analyses.

4. Translational/shift invariance of Bell basis

The translational invariance of maximally entangled Bell basis states demonstrates a unique characteristic of entangled qubits. This unique property has been used to detect or measure how much entanglement is present in arbitrary pure and mixed states. This is implemented in terms of the notion of concurrence, to be elaborated below.

The translational or shift operation (also referred to as the *flip* operation in the literature) is demonstrated here for the Bell Basis states and their superpositions. First, let us consider all the Bell basis states. We have,

$$\Phi^+ = \frac{1}{\sqrt{2}}(|0\rangle|0\rangle + |1\rangle|1\rangle). \quad (10)$$

Upon applying the translation (shift by $+1(mod 2)$) operator, $T(+1)$, we obtain

$$\begin{aligned} T(+1)\Phi^+ &= \frac{1}{\sqrt{2}}(|0+1\rangle|0+1\rangle + |1+1\rangle|1+1\rangle), \\ &= \frac{1}{\sqrt{2}}(|1\rangle|1\rangle + |0\rangle|0\rangle) = \Phi^+, \end{aligned} \quad (11)$$

where addition obeys modular arithmetic ($mod 2$). The ‘plus’ entangled basis states are even upon the operation of $T(+1)$, whereas the ‘minus’ entangled basis states are odd when operated by $T(+1)$. We still consider the shifted, $-\Phi^-$ and $-\Psi^-$, as invariant

since it differs from the unshifted Bell states by a global phase factor. In the literature this translation operation is the so-called flipping operation first used by Wootters, et al., [2, 3].

4.1 Translational property of maximal superposition of Bell basis

Now let us consider the superposition of maximally entangled Bell basis states. We can easily see that a superposition of ‘plus’ entangled basis states with ‘minus’ entangled basis states yield *unentangled* basis states. For example, we have,

$$\frac{1}{\sqrt{2}}(\Phi^+ + \Phi^-) = |0\rangle|0\rangle, \quad (12)$$

$$\frac{1}{\sqrt{2}}(\Phi^+ - \Phi^-) = |1\rangle|1\rangle. \quad (13)$$

The thing to notice is that although the superposition is made up of two maximally entangled Bell basis, the results are not shift invariant (i.e., generation of another *Wannier* state yields *Wannier* state located at another *site*, which is orthogonal to the unshifted one). This means that the superposition given above yields unentangled states (product states) in Eq. (13). In what follows, we will see that only the following combination of entangled basis states yields another entangled basis states as long as they both belong to either ‘even’ or ‘odd’ spaces. We have, by diagrammatic construction,

$$triplet^\pm \otimes triplet^\pm = triplet^\pm \text{ or } singlet^\pm, \quad (14)$$

$$triplet^\pm \otimes singlet^\pm = singlet^\pm \text{ or } triplet^\pm, \quad (15)$$

$$singlet^\pm \otimes singlet^\pm = triplet^\pm \text{ or } singlet^\pm. \quad (16)$$

Equation (15) is quite interesting because it holds on a complete expansion of a direct product of two qubit states. These relations can easily be deduced from the physical diagrammatic model, see **Figure 1**. For example, if we define the operation as a superposition such as,

$$\frac{1}{\sqrt{2}}(\Phi^+ + \Psi^+) = \left[\frac{1}{\sqrt{2}}(|1\rangle + |0\rangle) \otimes \frac{1}{\sqrt{2}}(|1\rangle + |0\rangle) \right]. \quad (17)$$

We see that Eq. (17) is a direct product state of two qubits. We will see in what follows that this is an entangled state and corresponds to Eq. (15) of the *singlet*⁺ or *triplet*⁺ of the model diagrams depending on the actual linkage. Similarly, we have,

$$\frac{1}{\sqrt{2}}(\Phi^- + \Psi^-) = \left[\frac{1}{\sqrt{2}}(|1\rangle + |0\rangle) \otimes \frac{1}{\sqrt{2}}(|1\rangle - |0\rangle) \right], \quad (18)$$

corresponds to Eq. (15) of the *singlet* or *triplet* of the model diagrams, depending on the actual linking.

However, the following combinations of ‘even’ and ‘odd’ entangled states result in *unentangled* states, namely,

$$\frac{1}{\sqrt{2}}(\Phi^+ + \Psi^-) = \frac{1}{2}[(|1\rangle|1\rangle + |0\rangle|0\rangle) + (|0\rangle|1\rangle - |1\rangle|0\rangle)], \quad (19)$$

and

$$\frac{1}{\sqrt{2}}(\Phi^- + \Psi^+) = \frac{1}{2}[(|1\rangle|1\rangle - |0\rangle|0\rangle) + (|0\rangle|1\rangle + |1\rangle|0\rangle)], \quad (20)$$

by virtue of the failure to have global sign factors. All these claims are justified through the concept of concurrence, an inherent property of entangled qubits, to be discussed in what follows. Moreover, this feature of failing to have global sign factor is also reflected in the failure to represent by our inverter-chain link diagrams.

5. Bipartite system

Let the Hilbert spaces of a bipartite system consisting of A and B be denoted by \mathcal{H}_A and \mathcal{H}_B , respectively. A bipartite system is a system with Hilbert space equal to the direct product of \mathcal{H}_A and \mathcal{H}_B , i.e.,

$$\mathcal{H}_{AB} = \mathcal{H}_A \otimes \mathcal{H}_B \quad (21)$$

Let the density matrix for the whole system be denoted by ρ . Then the reduced density matrix of a subsystem A is given by the partial trace,

$$\rho_A = \text{Tr}_B \rho. \quad (22)$$

The entanglement entropy, S_A , is the *von Neumann entropy* of the reduced density matrix, ρ_A ,

$$S_A = -\text{Tr} \rho_A \log \rho_A. \quad (23)$$

Example 1 Let Ω be the number of distinct states in subsystem A . assume a uniform distribution among states, hence ρ_A has eigenvalues $\frac{1}{\Omega}$, i.e., ρ_A can be represented by a diagonal $\Omega \times \Omega$ matrix with identical matrix elements given by $\frac{1}{\Omega}$. Thus, in taking the trace we can use the eigenvalues of the reduced density matrix operator, ρ_A . Therefore, we have

$$\begin{aligned} S_A &= -\text{Tr} \frac{1}{\Omega} \log \frac{1}{\Omega}, \\ &= \log \Omega. \end{aligned} \quad (24)$$

Upon multiplying by the Boltzmann constant, k_B , we obtain

$$k_B S_A = k_B \log \Omega, \quad (25)$$

which is the Boltzmann thermodynamic entropy, based on ergodic theorem.

Example 2. Two qubit system.

A qubit is simply a quantum bit whose number of distinct eigenstates is 2. We denote these eigenstates as $|0\rangle$ and $|1\rangle$, i.e., a two-state system. If each subsystem A or

B is a single qubit, then the Hilbert space of the whole system is span by the following 4 direct product states, namely,

$$|00\rangle, |01\rangle, |10\rangle, |11\rangle. \quad (26)$$

Here, the first bit refers to subsystem A and the second bit refers to subsystem B . Now, the density matrix of a pure state is,

$$\rho = |\psi\rangle\langle\psi|, \quad (27)$$

then

$$\begin{aligned} \rho^2 &= |\psi\rangle\langle\psi||\psi\rangle\langle\psi| \\ &= \rho. \end{aligned} \quad (28)$$

An operator whose square is equal to itself must have an eigenvalue equal to unity. Let us write for pure state of the two qubits as,

$$|\psi\rangle = \frac{1}{\sqrt{2}}(|00\rangle + |11\rangle), \quad (29)$$

$$\langle\psi| = \frac{1}{\sqrt{2}}(\langle 00| + \langle 11|). \quad (30)$$

We have,

$$\langle\psi||\psi\rangle = 1. \quad (31)$$

Thus, indeed,

$$\begin{aligned} \rho^2 &= |\psi\rangle\langle\psi||\psi\rangle\langle\psi| \\ &= |\psi\rangle\langle\psi| = \rho. \end{aligned} \quad (32)$$

We refer to $|\psi\rangle$ as a maximally entangled state in the sense that the first qubit is exactly “link” to the second qubit. The reduced density matrix for subsystem A is

$$\rho_A = \text{Tr}_B \rho = \frac{1}{2}(|0_A\rangle\langle 0_A| + |1_A\rangle\langle 1_A|). \quad (33)$$

Now clearly

$$\begin{aligned} \rho_A^2 &= \frac{1}{4}(|0_A\rangle\langle 0_A| + |1_A\rangle\langle 1_A|)(|0_A\rangle\langle 0_A| + |1_A\rangle\langle 1_A|), \\ &= \frac{1}{4}(|0_A\rangle\langle 0_A| + |1_A\rangle\langle 1_A|) = \frac{1}{2}\rho_A, \end{aligned} \quad (34)$$

so that ρ_A is not a pure state but mixed, i.e., a mixture of two pure states, $|0_A\rangle$ and $|1_A\rangle$. Note that the mixed states density matrix do not possess *off-diagonal elements*. From the last identity, the eigenvalues of ρ_A is $\frac{1}{2}$ and since the subsystem A is a single qubit with two distinct states, then eigenvalues of ρ_A corresponds to $\frac{1}{2}$ of our first example above. Thus we refer to ρ_A as “uniformly” mixed often referred to as “*maximally mixed*” with the initial state $|\psi\rangle$ as “*maximally entangled*”.

6. Entanglement of formation of multi-partite qubit systems

The entanglement entropy of subsystem A can be calculated using the eigenvalues of the 2×2 matrix of ρ_A , which is $\lambda_A = \frac{1}{2}$. Therefore, we have for the entanglement entropy or entanglement of formation given by,

$$\begin{aligned} S_A &= -\text{Tr} \rho_A \log \rho_A, \\ &= -\text{Tr} \frac{1}{2} \log \frac{1}{2} = \log 2^1, \end{aligned} \quad (35)$$

where exponent base 2, here 1, is the number of qubits that is entangled with system B . This will be made clear in the next example.

Example 3 A four qubit system:

If each subsystem A or B has two qubits, then the Hilbert space of the whole system is span by the following 16 direct product states, i.e., $2^4 = 16$ states. The maximally entangled pure state is determined by the following eight diagrams [4], see **Figure 2**, and their flipped or translated states,

Any combination or superposition of both ‘even’ triplet and singlet states comprised a maximally entangled state, i.e.,

$$\begin{pmatrix} \Phi_1^+ \\ \Phi_1^- \end{pmatrix} = \frac{1}{\sqrt{2}} \begin{pmatrix} 1 & 1 \\ 1 & -1 \end{pmatrix} \begin{pmatrix} |0\rangle|0\rangle|0\rangle|0\rangle \\ |1\rangle|1\rangle|1\rangle|1\rangle \end{pmatrix}, \quad (36)$$

$$\begin{pmatrix} \Phi_8^+ \\ \Phi_8^- \end{pmatrix} = \frac{1}{\sqrt{2}} \begin{pmatrix} 1 & 1 \\ 1 & -1 \end{pmatrix} \begin{pmatrix} |0\rangle|1\rangle|0\rangle|1\rangle \\ |1\rangle|0\rangle|1\rangle|0\rangle \end{pmatrix}. \quad (37)$$

Thus, from the states given above, we have for example the maximally entangled state,

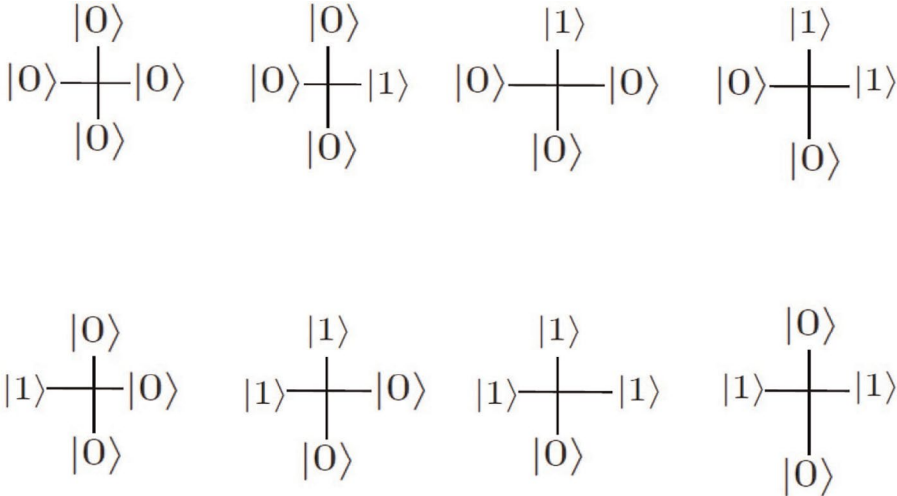


Figure 2.

Two-state eight diagrams for entangled four qubits. The so-called flip operation yields the second state for each of the above diagrams. The entangled basis is constructed by the superposition, via the Hadamard transformation, of each diagram and its corresponding flipped diagram. [Reproduced from Ref. [4]].

$$|\psi\rangle = \frac{1}{\sqrt{2}}(\Phi_1^+ + \Phi_8^+), \quad (38)$$

and similarly, we can also form another entangled state,

$$|\psi\rangle = \frac{1}{\sqrt{2}}(\Phi_1^- + \Phi_8^-), \quad (39)$$

where the first two bits belongs to subsystem A and the second two bits belong to subsystem B . We note that

$$\langle\psi||\psi\rangle = 1. \quad (40)$$

Therefore

$$\begin{aligned} \rho^2 &= (|\psi\rangle\langle\psi|)^2, \\ &= |\psi\rangle\langle\psi| = \rho. \end{aligned} \quad (41)$$

So $|\psi\rangle$ is a pure state.

In general, the following maximally entangled state corresponds to a chain of entangled basis states, namely,

$$|\psi^+\rangle = \frac{1}{\sqrt{8}}(\Phi_1^+ + \Phi_2^+ + \Phi_3^+ + \Phi_4^+ + \Phi_5^+ + \Phi_6^+ + \Phi_7^+ + \Phi_8^+), \quad (42)$$

$$|\psi^-\rangle = \frac{1}{\sqrt{8}}(\Phi_1^- + \Phi_2^- + \Phi_3^- + \Phi_4^- + \Phi_5^- + \Phi_6^- + \Phi_7^- + \Phi_8^-), \quad (43)$$

of a four qubit system.

The density matrix operator for the whole 4-qubit system can be written as,

$$\rho = \frac{1}{\sqrt{2}}(|\Phi_1^- + \Phi_8^- \rangle) \frac{1}{\sqrt{2}}(\langle\Phi_1^- + \Phi_8^-|), \quad (44)$$

$$\rho = \frac{1}{4}[|00, 00\rangle + |01, 01\rangle + |10, 10\rangle + |11, 11\rangle][\langle 00, 00| + \langle 01, 01| + \langle 10, 10| + \langle 11, 11|]. \quad (45)$$

The reduced density matrix operator for subsystem A is again obtained by taking partial trace with respect to subsystem B .

$$\begin{aligned} \rho_A &= Tr_B \rho, \\ &= \langle 00_B|\rho|00_B\rangle + \langle 01_B|\rho|01_B\rangle + \langle 10_B|\rho|10_B\rangle + \langle 11_B|\rho|11_B\rangle, \\ &= \frac{1}{4}|00_A\rangle\langle 00_A| + |01_A\rangle\langle 01_A| + |10_A\rangle\langle 10_A| + |11_A\rangle\langle 11_A|. \end{aligned} \quad (46)$$

To determine the eigenvalues for ρ_A , we take its square,

$$\begin{aligned} \rho_A^2 &= \frac{1}{16}(|00_A\rangle\langle 00_A| + |01_A\rangle\langle 01_A| + |10_A\rangle\langle 10_A| + |11_A\rangle\langle 11_A|), \\ &\quad \times (|00_A\rangle\langle 00_A| + |01_A\rangle\langle 01_A| + |10_A\rangle\langle 10_A| + |11_A\rangle\langle 11_A|), \\ &= \frac{1}{16}(|00_A\rangle\langle 00_A| + |01_A\rangle\langle 01_A| + |10_A\rangle\langle 10_A| + |11_A\rangle\langle 11_A|), \\ &= \frac{1}{4}\rho_A. \end{aligned} \quad (47)$$

So we have

$$\rho_A^2 = \frac{1}{4}\rho_A \quad (48)$$

and the eigenvalues of ρ_A is $\frac{1}{4}$. We can now calculate the entanglement entropy of subsystem A . We have

$$\begin{aligned} S_A &= -\text{Tr} \rho_A \log \rho_A, \\ &= \log 2^2. \end{aligned} \quad (49)$$

The exponent 2 correspond to the number of qubits that is entangled with subsystem B . In general, for maximally entangled bipartite system A and B , each having k number of qubits S_A is given by,

$$S_A = \log 2^k. \quad (50)$$

Now of course, for this bipartite system,

$$S_A = S_B, \quad (51)$$

which simply means a complete matching of configurations of each system A and B , respectively, otherwise some degrees of freedom will be hanging, not matched or cannot be entangled.

Example 4. Tripartite system of three qubits:

The following diagrams represent the entangled tripartite system of qubits (**Figure 3**). The entangled basis states are as follows,

$$\begin{pmatrix} \Xi^+ \\ \Xi^- \end{pmatrix} = \frac{1}{\sqrt{2}} \begin{pmatrix} 1 & 1 \\ 1 & -1 \end{pmatrix} \begin{pmatrix} |0\rangle|1\rangle|1\rangle \\ |1\rangle|0\rangle|0\rangle \end{pmatrix}, \quad (52)$$

$$\begin{pmatrix} \Theta_3^+ \\ \Theta_3^- \end{pmatrix} = \frac{1}{\sqrt{2}} \begin{pmatrix} 1 & 1 \\ 1 & -1 \end{pmatrix} \begin{pmatrix} |0\rangle|0\rangle|0\rangle \\ |1\rangle|1\rangle|1\rangle \end{pmatrix}, \quad (53)$$

$$\begin{pmatrix} \Omega^+ \\ \Omega^- \end{pmatrix} = \frac{1}{\sqrt{2}} \begin{pmatrix} 1 & 1 \\ 1 & -1 \end{pmatrix} \begin{pmatrix} |0\rangle|1\rangle|0\rangle \\ |1\rangle|0\rangle|1\rangle \end{pmatrix}, \quad (54)$$

$$\begin{pmatrix} \Gamma^+ \\ \Gamma^- \end{pmatrix} = \frac{1}{\sqrt{2}} \begin{pmatrix} 1 & 1 \\ 1 & -1 \end{pmatrix} \begin{pmatrix} |0\rangle|0\rangle|1\rangle \\ |1\rangle|1\rangle|0\rangle \end{pmatrix}. \quad (55)$$

A chain or superposition of any choice of entangled *even* basis states also form a maximally entangled state, e.g.,

$$|\Psi^4\rangle = \frac{1}{\sqrt{4}} [\Xi^+ + \Theta_3^+ + \Omega^+ + \Gamma^+], \quad (56)$$

$$|\Psi^3\rangle = \frac{1}{\sqrt{3}} [\Xi^+ + \Theta_3^+ + \Omega^+], \quad (57)$$

$$|\Psi^2\rangle = \frac{1}{\sqrt{2}} [\Xi^+ + \Theta_3^+], \quad (58)$$

$$|\Psi^1\rangle = \Xi^+, \quad (59)$$

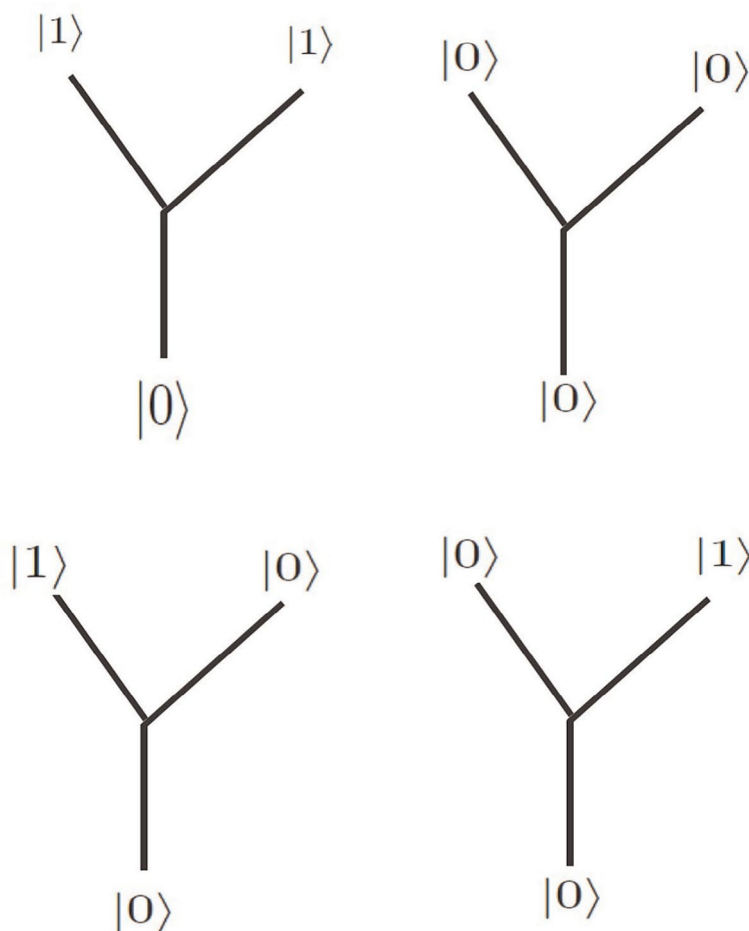


Figure 3.
 Two-state four diagrams for entangled three qubits of a tripartite system. Flip operations yield the respective second states. [Reproduced from Ref. [4]].

are all, respectively, maximally entangled states with emergent two-state or qubit properties.

Example 5 Multi-partite systems:

It is important to point out that any entangled qubits, irrespective of their number, identically behave like a single qubit, i.e., behaving exactly like a two-state system. Thus, the natural order of disentangling is as follows: First, one entangles one qubit from the remaining two entangled qubits. The entanglement of formation is equivalent to one qubit. Next, one disentangled the remaining entangled two qubits. This further give an entanglement of formation of one qubit. Thus, the total entanglement of formation is $1 + 1 = 2$ qubits

6.1 Monogamy inequality of entanglement of formation

The reasoning we have given above yields exact equality of the monogamy, usually given as *inequality* in the literature as deduced from statistical analysis, e.g., one given

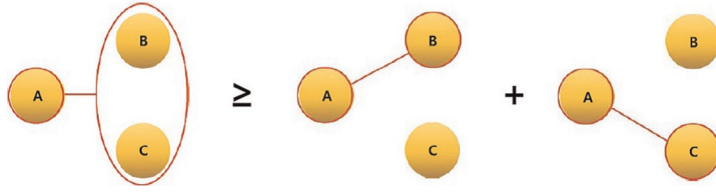


Figure 4. Figure reproduced from Ref. [5]. In our diagrammatic analysis the right-hand side of the figure yields $1 + 1 = 2$ as the entanglement of formation, being the sum of two 2-qubit entanglements. Thus, in our diagrammatic analysis, we obtained exact monogamy equality not inequality.

by Kim [5], The exact equality relation for the entanglement of formation is diagrammatically shown in **Figure 4**.

The exact equality comes about by construction, since on both sides of **Figure 4**, two 2-qubit entangled states are being unentangled to obtain the entanglement of formation of this multi-partite system. This comes about through the knowledge that any multi-partite entangled qubits behave as an emergent qubit.

Similarly, for an entangled 4-partite system, the entanglement of formation is determined schematically by the diagrams of **Figure 5**, where the unentangling operations to be done on the left side are itemized on the unentangling operations of *three* entangled 2-qubits on the right side of the equality sign,

This sort of diagrammatic analysis of the entropy of entanglement of formation can straightforwardly be employed to all multi-partite qubit systems by a simple counting argument as is done here. For example, for 18 multi-partite entangled qubits in **Figure 6**, we have the entanglement of formation schematically depicted by the equality where there is 17 number of monogamy in the right-hand side yielding 17 qubits of entropy of entanglement of formation.

7. Joint distributions as entanglements

In this section, we will explicitly show the discrete phase-space physics of qubit entanglements. We will demonstrate that a *joint* “Bloch-function” distributions in “momentum space” transforms into entangled qubits (“Wannier states”) in “lattice-site space”⁴. To the author’s knowledge, this demonstrates for the first time the entanglement properties of joint distributions in quantum mechanics, which is ubiquitous in quantum transport theory of topological insulators discussed in Ref. [6].

Consider the generalized Fourier transformation between two Hilbert spaces,

$$|p\rangle = \sum_q \langle q|p\rangle |q\rangle, \quad (60)$$

where the $\langle q|p\rangle$ is the transformation function. This is particularly given by the discrete Fourier transform function,

$$\langle q|p\rangle = \frac{1}{\sqrt{N}} \exp\left(-\frac{i}{\hbar} p \cdot q\right). \quad (61)$$

⁴ We maintained the *Bloch function/Wannier function* analogy for convenience, and to stress the wide-ranging impact of the discrete phase-space physics.

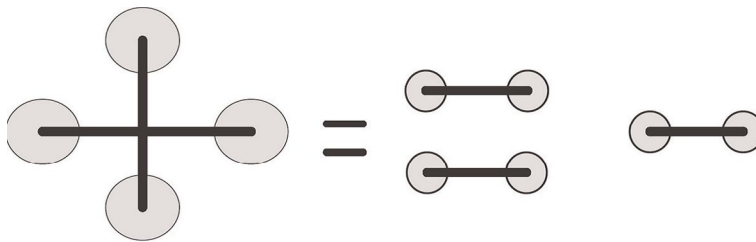


Figure 5.
 In our diagrammatic analysis the right-hand side of the figure yields $1 + 1 + 1 = 3$ as the entanglement of formation, being the sum of three 2-qubit entanglements. Thus, in our diagrammatic analysis, we obtained exact equality not inequality.

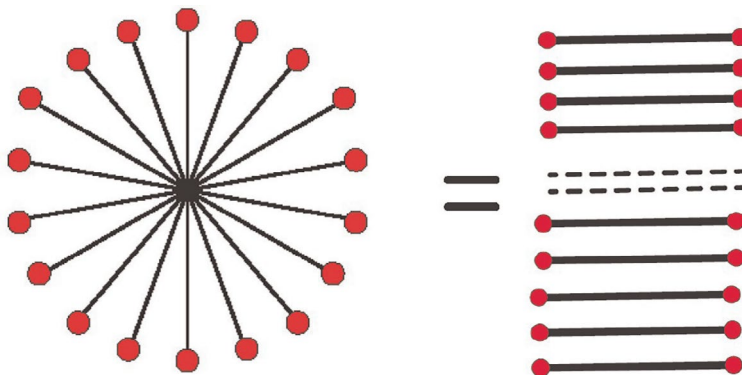


Figure 6.
 In our diagrammatic analysis the right hand side of the figure yields $1 + 1 + 1, \dots, 1 = 17$ qubits as the entanglement of formation, being the sum of 17 two-qubit entanglements of formation. There are 18 multi-party entangled qubits in the left-hand side.

where N is the number of discrete points in bijective transformations (this number N is conveniently taken as prime integers).

7.1 Two-point joint distributions

We have a joint distribution in p -space as,

$$|p'\rangle|p''\rangle = \frac{1}{\sqrt{N}} \sum_{q'} \exp\left(-\frac{i}{\hbar} p' \cdot q'\right) |q'\rangle \frac{1}{\sqrt{N}} \sum_{q''} \exp\left(-\frac{i}{\hbar} p'' \cdot q''\right) |q''\rangle. \quad (62)$$

Therefore, for a qubit or a two-state system, we write,

$$|p\rangle = \frac{1}{\sqrt{2}} \sum_{q=0}^1 \exp\left(-\frac{i}{\hbar} p \cdot q\right) |q\rangle. \quad (63)$$

Consider the *joint distribution* of two qubits in “Bloch-function” space. We can form 4 joint distributions of *Bloch-function* in what follows. To derive these, first, we write the following matrix-representation and Hadamard-transformation identity,

$$\begin{aligned}
 & \pi\hbar \begin{pmatrix} |0\rangle \\ |1\rangle \end{pmatrix} \otimes \pi\hbar \begin{pmatrix} |0\rangle \\ |1\rangle \end{pmatrix} \\
 &= \frac{1}{\sqrt{2}} \frac{1}{\sqrt{2}} \begin{pmatrix} (|0\rangle + |1\rangle) \\ (|0\rangle - |1\rangle) \end{pmatrix} \otimes \begin{pmatrix} (|0\rangle + |1\rangle) \\ (|0\rangle - |1\rangle) \end{pmatrix}.
 \end{aligned} \tag{64}$$

We will denote the joint distribution in p -space as $\mathcal{D}(p_1, p_2, \dots, p_n)$. We will denote these 4 “Bloch-function” distributions by the standard notations for the Bell basis in the literature, namely, Φ^+ , Φ^- , Ψ^+ and Ψ^- . Then, we have

$$\mathcal{D}(0, 0) = \frac{1}{\sqrt{2}} \{\Phi^+ + \Psi^+\}, \quad \mathcal{D}(1, 1) = \frac{1}{\sqrt{2}} (\Phi^+ - \Psi^+), \tag{65}$$

$$\mathcal{D}(0, 1) = \frac{1}{\sqrt{2}} (\Phi^- - \Psi^-), \quad \mathcal{D}(1, 0) = \frac{1}{\sqrt{2}} (\Phi^- + \Psi^-). \tag{66}$$

7.2 Three-point joint distributions

Similarly, for three-fold joint distribution in p -space, we have,

$$\begin{aligned}
 |p_1\rangle |p_2\rangle |p_3\rangle &= \frac{1}{\sqrt{N}} \sum_{q_1} \exp\left(-\frac{i}{\hbar} p_1 \cdot q_1\right) |q_1\rangle \\
 &\times \frac{1}{\sqrt{N}} \sum_{q_2} \exp\left(-\frac{i}{\hbar} p_2 \cdot q_2\right) |q_2\rangle \\
 &\times \frac{1}{\sqrt{N}} \sum_{q_3} \exp\left(-\frac{i}{\hbar} p_3 \cdot q_3\right) |q_3\rangle.
 \end{aligned} \tag{67}$$

Again, in matrix form, we express the above equation as

$$\begin{aligned}
 & \pi\hbar \begin{pmatrix} |0\rangle \\ |1\rangle \end{pmatrix} \otimes \pi\hbar \begin{pmatrix} |0\rangle \\ |1\rangle \end{pmatrix} \otimes \pi\hbar \begin{pmatrix} |0\rangle \\ |1\rangle \end{pmatrix} \\
 &= \frac{1}{\sqrt{2}} \begin{pmatrix} 1 & 1 \\ 1 & -1 \end{pmatrix} \begin{pmatrix} |0\rangle \\ |1\rangle \end{pmatrix} \otimes \frac{1}{\sqrt{2}} \begin{pmatrix} 1 & 1 \\ 1 & -1 \end{pmatrix} \begin{pmatrix} |0\rangle \\ |1\rangle \end{pmatrix} \otimes \frac{1}{\sqrt{2}} \begin{pmatrix} 1 & 1 \\ 1 & -1 \end{pmatrix} \begin{pmatrix} |0\rangle \\ |1\rangle \end{pmatrix}, \\
 &= \frac{1}{\sqrt{2}} \frac{1}{\sqrt{2}} \frac{1}{\sqrt{2}} \begin{pmatrix} (|0\rangle + |1\rangle) \\ (|0\rangle - |1\rangle) \end{pmatrix} \otimes \begin{pmatrix} (|0\rangle + |1\rangle) \\ (|0\rangle - |1\rangle) \end{pmatrix} \otimes \begin{pmatrix} (|0\rangle + |1\rangle) \\ (|0\rangle - |1\rangle) \end{pmatrix}.
 \end{aligned} \tag{68}$$

From Eq. (68), we can define 8 joint distributions in p -space, namely, $\mathcal{D}(0,0,0)$, $\mathcal{D}(0,0,1)$, $\mathcal{D}(0,1,0)$, $\mathcal{D}(0,1,1)$, $\mathcal{D}(1,0,0)$, $\mathcal{D}(1,0,1)$, $\mathcal{D}(1,1,0)$, and $\mathcal{D}(1,1,1)$. We obtained,

$$\mathcal{D}(0,0,0) = \frac{1}{\sqrt{4}} \{(\Theta_3^+ + \Gamma^+ + \Xi^+ + \Omega^+)\}, \tag{69}$$

$$\mathcal{D}(0,0,1) = \frac{1}{\sqrt{4}} \{(\Theta_3^- + \Gamma^- + \Xi^- + \Omega^-)\}, \tag{70}$$

$$\mathcal{D}(0,1,0) = \frac{1}{\sqrt{4}} \{\Theta_3^- - \Xi^- + \Gamma^- - \Omega^-\}, \tag{71}$$

$$\mathcal{D}(0,1,1) = \frac{1}{\sqrt{4}} \{ \Theta_3^+ - \Gamma^+ - \Omega^+ + \Xi^+ \}, \quad (72)$$

$$\mathcal{D}(1,0,0) = \frac{1}{\sqrt{4}} \{ \Theta_3^- + \Omega^- + \Gamma^- + \Xi^- \}, \quad (73)$$

$$\mathcal{D}(1,0,1) = \frac{1}{\sqrt{4}} \{ \Theta_3^+ - \Xi^+ + \Omega^+ - \Gamma^+ \}, \quad (74)$$

$$\mathcal{D}(1,1,0) = \frac{1}{\sqrt{4}} \{ \Theta_3^+ - \Xi^+ - \Omega^+ + \Gamma^+ \}, \quad (75)$$

$$\mathcal{D}(1,1,1) = \frac{1}{\sqrt{4}} \{ \Theta_3^- + \Xi^- - \Omega^- - \Gamma^- \}. \quad (76)$$

In Eqs. (69)–(76), we made use of the following relations:

$$\frac{1}{\sqrt{2}} (|0\rangle|0\rangle|0\rangle + |1\rangle|1\rangle|1\rangle) = \Theta_3^+, \quad \frac{1}{\sqrt{2}} (|0\rangle|0\rangle|1\rangle + |1\rangle|1\rangle|0\rangle) = \Gamma^+, \quad (77)$$

$$\frac{1}{\sqrt{2}} (|0\rangle|1\rangle|0\rangle + |1\rangle|0\rangle|1\rangle) = \Omega^+, \quad \frac{1}{\sqrt{2}} (|0\rangle|1\rangle|1\rangle + |1\rangle|0\rangle|0\rangle) = \Xi^+, \quad (78)$$

$$\frac{1}{\sqrt{2}} (|0\rangle|0\rangle|0\rangle - |1\rangle|1\rangle|1\rangle) = \Theta_3^-, \quad \frac{1}{\sqrt{2}} (|0\rangle|0\rangle|1\rangle - |1\rangle|1\rangle|0\rangle) = \Gamma^-, \quad (79)$$

$$\frac{1}{\sqrt{2}} (|0\rangle|1\rangle|0\rangle - |1\rangle|0\rangle|1\rangle) = \Omega^-, \quad \frac{1}{\sqrt{2}} (|0\rangle|1\rangle|1\rangle - |1\rangle|0\rangle|0\rangle) = \Xi^-. \quad (80)$$

A crucial observation is that only even (+) combinations of entangled basis states correspond to joint distributions and entanglements, and similarly only odd (−) combinations of entangled basis states correspond to joint distributions and entanglements as well. This claim will become clear when we discuss the basic characterization of entanglements and of entanglement measure, which have concurrency⁵ equals 1.

8. Chiral degrees of freedom and entangled qubits

Observe that the pseudo-spin variables in semiconductor Bloch equation is defined by the following expressions,

$$S_0 = \rho_{cc} + \rho_{vv}, \quad (81)$$

$$S_x = \rho_{vc} + \rho_{cv}, \quad (82)$$

$$S_y = -i(\rho_{vc} - \rho_{cv}), \quad (83)$$

$$S_z = \rho_{cc} - \rho_{vv}. \quad (84)$$

This maps to

⁵ Concurrency is one of the most important characterization of entangled qubits, to be discussed in more details below.

$$e_0 = |\Phi^+\rangle = \frac{1}{\sqrt{2}}(|1\rangle|1\rangle + |0\rangle|0\rangle), \quad (85)$$

$$e_x = |\Psi^+\rangle = \frac{1}{\sqrt{2}}(|0\rangle|1\rangle + |1\rangle|0\rangle), \quad (86)$$

$$ie_y = i|\Psi^-\rangle = \frac{1}{\sqrt{2}}(|0\rangle|1\rangle - |1\rangle|0\rangle), \quad (87)$$

$$e_z = |\Phi^-\rangle = \frac{1}{\sqrt{2}}(|1\rangle|1\rangle - |0\rangle|0\rangle). \quad (88)$$

We refer to the basis (e_0, e_x, e_y, e_z) as the pseudo-spin component basis, which differ from the Bell basis in $|\Psi^-\rangle$ by the factor i in $|\Psi^-\rangle$. An important observation that follows from this is that the entangling of chiral degrees of freedom creates another chiral degrees of freedom, e.g., Eqs. (69)–(76).

This is a very important observation which will aid in understanding the *entanglement-induced delocalization*, in topological insulators treated by the quantum transport approach in Ref. [6].

9. The concurrence concept and emergent qubit

By virtue of our diagrammatic construction, coupled with discrete phase space Hadamard transformation, in deriving the entangled basis states, the concurrence concept defined by Wootters [2, 3], as well as the two-state (qubit) properties of entangled multi-partite qubits, naturally coincides with the mathematical description of our physical model of qubit entanglement. In other words, the essence of the quantum description of an entangled qubits in **Figure 1** consists of the superposition of product ‘site states’ and their corresponding translated ‘site states’ of all qubits. This means a superposition of the two states of the entangled two qubits of **Figure 1**. One observe that irrespective of how many qubits are entangled, the resulting entangled state is an *emergent* two-state system and therefore behave just like one qubit with two-states, namely, the first state and its *translated* state [4]. Therefore its associated entropy is just one⁶.

The concept of concurrence is basically contained by construction of our physical model of qubit entanglement. It is defined by

$$|\langle\Psi|\tilde{\Psi}\rangle| = C, \quad (89)$$

where C is the quantitative value of concurrence. This number lies between 0 and 1, $0 \leq C \leq 1$. Here $\tilde{\Psi}$ is the corresponding translated qubits of Ψ .

10. A natural measure of entanglement

The two properties of any entangled qubits, namely, concurrence and its *emergent* qubit behavior, lead Wootters [2, 3] to introduce a measure of entanglement, as incorporated in the two formulas,

⁶ This is also deduced when concurrence $C = 1$ [3].

$$E(C) = H\left(\frac{1}{2} + \frac{1}{2}\sqrt{1 - C^2}\right), \quad (90)$$

$$H(x) = -x \ln x - (1 - x) \ln(1 - x). \quad (91)$$

Equation (90) basically say that if there is complete concurrence, i.e., $C = 1$, then Eq. (91) says that the system behave as an emergent qubit or two-state system, as depicted clearly in our diagrams. Thus, for maximally entangled multi-partite qubits, we have $C = 1$,

$$E(C) = H\left(\frac{1}{2}\right), \quad (92)$$

$$H\left(\frac{1}{2}\right) = \frac{1}{2} \ln 2 + \frac{1}{2} \ln 2, = 1. \quad (93)$$

affirming that entangled qubits behave as a two-state system or as an *emergent qubit*, yielding entropy equals one.

10.1 Entropic distance in entanglement measure

From the above developments, one can introduce an entanglement entropic distance by the formula

$$\mathcal{E} = |Tr(\rho \ln \rho) - 1|, \quad (94)$$

where $Tr(\rho \ln \rho)$ is evaluated using Eqs. (90) and (91). This distance has a range: $0 \leq \mathcal{E} \leq 1$. When the concurrence, $C = 1$, $Tr(\rho \ln \rho) = 1 = H\left(\frac{1}{2}\right)$, then we have the entropy-distance from maximally entangled state, $\mathcal{E} = 0$. When $C = 0$, $Tr(\rho \ln \rho) = 0 = H(1)$, then we have the entropy-distance from maximally entangled state, $\mathcal{E} = 1$.

An example where the $C < 1$ may occur in the following singlet state, with less entanglement,

$$|\psi\rangle = \alpha|01\rangle + \beta|10\rangle, \quad (95)$$

where

$$\alpha^2 + \beta^2 = 1. \quad (96)$$

Then

$$\begin{aligned} C &= |\langle\psi||\tilde{\psi}\rangle| = (\alpha\langle 01| + \beta\langle 10|)(\alpha|10\rangle + \beta|01\rangle), \\ &= \alpha\beta + \beta\alpha \leq 1. \end{aligned} \quad (97)$$

11. Mixed states and pure states

In discussing mixed and pure states, one makes use of density-matrix operators. This is the domain of abstract statistical treatment usually found in the literature, perhaps following the statistical tradition of Bell's theorem. To elucidate the basic

physics, we will here avoid abstract statistical treatment and only discuss specific situations and examples.

11.1 Mixed states and mixed entanglements

Consider the maximally mixed state of a triplet system,

$$\hat{\rho}_W = \frac{1}{2}(|00\rangle\langle 00| + |11\rangle\langle 11|). \quad (98)$$

We obtain the mixed entanglements given by,

$$\hat{\rho}_B = \frac{1}{2}(|\Phi^+\Phi^+\rangle\langle\Phi^+\Phi^+| + |\Phi^-\Phi^-\rangle\langle\Phi^-\Phi^-|). \quad (99)$$

Similarly, consider the maximally mixed state of a singlet system,

$$\hat{\rho}_W = \frac{1}{2}(|01\rangle\langle 01| + |10\rangle\langle 10|). \quad (100)$$

We obtain the mixed entanglements given by

$$\hat{\rho}_B = \frac{1}{2}(|\Psi^+\Psi^+\rangle\langle\Psi^+\Psi^+| + |\Psi^-\Psi^-\rangle\langle\Psi^-\Psi^-|). \quad (101)$$

11.2 Mixed state from pure state (entangled state)

Consider the example of a bipartite of two qubit system. Consider a pure entangled state,

$$|\psi\rangle = \frac{1}{\sqrt{2}}(|00\rangle + |11\rangle). \quad (102)$$

Then the density matrix is,

$$\rho = \frac{1}{2}(|00\rangle + |11\rangle)(\langle 00| + \langle 11|), \quad (103)$$

where the first qubit belongs to party A and the second qubit belongs to party B .⁷ We have

$$\rho^2 = \rho, \quad (104)$$

so that Eq. (103) is a pure state. Again, we have, by tracing the party B we obtain,

$$\begin{aligned} \rho_A &= \text{Tr}_B \rho, \\ &= \frac{1}{2}(|0_A\rangle\langle 0_A| + |1_A\rangle\langle 1_A|). \end{aligned} \quad (105)$$

⁷ What we mean by party A and B is in the general sense since any entangled number of qubits behave as an emergent qubit.

Now clearly

$$\rho_A^2 = \frac{1}{2}\rho_A, \quad (106)$$

so that ρ_A is not a pure state but mixed, i.e., a mixture of two pure states, $|0_A\rangle$ and $|1_A\rangle$.⁸ Note that the mixed states density matrix do not possess *off-diagonal elements*. The tracing operation basically eliminates the contribution of the “*off-diagonal*” terms. From the last identity, the eigenvalues of ρ_A is $\frac{1}{2}$ and since the subsystem A is an emergent qubit, in general with two distinct states, then eigenvalues of ρ_A corresponds to $\frac{1}{2}$ of our first example above. Thus we refer to ρ_A as “uniformly” mixed often referred to as “*maximally mixed*” with the initial state $|\psi\rangle$ as “*maximally entangled*”.

12. Concluding remarks

The inverter-chain rigid-coupling mechanical model of entanglement link has been demonstrated to faithfully implement the discrete phase space viewpoint [4]. The crucial observation that arise from this inverter-chain link model is that any multi-partite qubit entangled system has the property of an *emergent* qubit, which has been rigorously justified. This readily lead us to the equality relations of the entropy of entanglement formation in the so-called monogamy inequality of entanglement formation, using statistical arguments [5] discussed in the literature. In this paper, mixed states and mixed entanglements are related by the Hadamard transformations [7]. In addition, we show that mixed state can be extracted from pure entangled state, where the party A or B need not be a single qubit themselves but can each be an entangled multi-partite qubit system, respectively, by virtue of *emergent* qubit property of entangled qubit systems. We find that joint distributions in quantum mechanics have inherent entanglement properties.

The natural measure of entanglement is based on entropy of entanglement formation, concurrence, and entropic distance from maximally entangled reference.

⁸ If the parties A and B are entangled states, then what we have obtain are also mixed entanglement through the inverse Hadamard transformation.

Author details


Felix A. Buot^{1,2}

1 C&LB Research Institute, Carmen, Cebu, Philippines

2 Department of Physics, LCFMNN, TCSE Group, University of San Carlos,
Cebu City, Philippines

*Address all correspondence to: felixa.buot@gmail.com

IntechOpen

© 2023 The Author(s). Licensee IntechOpen. This chapter is distributed under the terms of the Creative Commons Attribution License (<http://creativecommons.org/licenses/by/3.0>), which permits unrestricted use, distribution, and reproduction in any medium, provided the original work is properly cited. 

References

- [1] Einstein A, Podolsky B, Rosen N. Can quantum-mechanical description of physical reality be considered complete? *Physics Review*. 1935;**47**:777
- [2] Hill S, Wootters WK. Entanglement of a pair of quantum bits. *Physical Review Letters*. 1977;**78**:5022
- [3] Wootters WK. Entanglement of a pair of quantum bits. *Physical Review Letters*. 1998;**80**:2245
- [4] Buot FA, Elnar AR, Maglasang G, Galon CM. A mechanical implementation and diagrammatic calculation of entangled basis states. *arXiv:2112.10291 [cond-mat.mes-hall]*. 2021
- [5] Kim JS. Entanglement of formation and monogamy of multi-party quantum entanglement. *Scientific Reports*. 2021; **11**:2364. DOI: 10.1038/s41598-021-82052-3
- [6] Buot FA, Rivero KB, Otadoy RES. Generalized nonequilibrium quantum transport of spin and pseudospins: Entanglements and topological phases. *Physica B*. 2019;**559**:42-61
- [7] Buot FA. *Nonequilibrium Quantum Transport Physics in Nanosystem*. Hackensack, NJ, USA: World Scientific; 2009, and references therein

Perspective Chapter: On the Contradiction between Special Relativity and Quantum Entanglement

Yoram Kirsh

Abstract

Demonstrations of quantum entanglement (QE), which confirm the violation of Bell's inequality, indicate that under certain conditions action at a distance is possible. This consequence seems to contradict the relativistic principle of causality, which asserts that an effect never precedes its cause, in any reference frame. By analyzing a numerical example of Bell's experiment with entangled pairs of photons, we show how observers in two inertial reference frames can disagree about the causality relation between two events. One observer claims that event 1 is the cause of event 2, while the other claims that event 1 is the result of event 2. The solution we suggest to the paradox is that in entangled systems, one can find pairs of "entangled events" which have symmetrical causality relations. Each of the events can serve as a cause or as an effect, depending on the frame of reference in which they are observed.

Keywords: quantum entanglement, EPR paradox, special relativity, Bell's inequality, entangled events

1. Introduction

Recently, several independent "loophole-free Bell violation" experiments were reported (*e.g.* [1–3]). These works, as well as previous demonstrations of quantum entanglement (QE) since the pioneering work of Freedman and Clauser [4], have shown that under certain conditions, action at a distance between entangled systems is possible. A straightforward interpretation of the results is that faster-than-light (FTL) or *superluminal* communication is feasible. This consequence may seem to contradict an established tenet of Special Relativity (SR) that claims that FTL transfer of information violates causality and is therefore impossible. The purpose of this chapter was to examine in detail where the conflict arises and to propose a possible solution to the paradox.

In fact, the paradox was already hidden in the Einstein-Podolsky-Rosen (EPR) thought experiment [5]. If two identical particles, *A* and *B*, move in opposite directions after a brief interaction which ensured that $\mathbf{v}_B = -\mathbf{v}_A$, and if at a specific moment, t_0 , when *A* and *B* are far apart, the position of *A* and the momentum of *B* are measured,

one can know both the position and the momentum of A at t_0 , since $\mathbf{p}_A = -\mathbf{p}_B$. The authors claimed that this thought experiment contradicted Heisenberg's uncertainty principle, and consequently that quantum mechanics (QM) is incomplete.

In addition to this explicit criticism against QM, another claim can be based on the EPR thought experiment, concerning an inconsistency between QM and SR. Suppose we perform a very accurate measurement of the magnitude of the momentum of A and find that it is \mathbf{p}_A . According to the uncertainty principle, the measurement changes the state of A so that the uncertainty in its location becomes infinite, or very large (since $\Delta p \times \Delta x \approx \hbar$). But since A and B are entangled, the measurement should change the state of B as well. If we now measure \mathbf{p}_B we should certainly get $\mathbf{p}_B = -\mathbf{p}_A$ while the uncertainty in the location of B becomes infinite, or very large. This is a substantial change in the wave function Ψ_B , which prior to the measurement on A , could be presented by a wave packet in which both Δx_B and Δp_B were finite.

The question is, how is it possible that an operation made on A instantly influences the state of B which, in principle, could be thousands of kilometers away from A . The effect of the measurement on A on the state of B is immediate, since the time interval Δt between the measurements on A and on B can be arbitrarily short. It seems to contradict SR which claims that no interaction can travel faster than the speed of light.

2. The EPR paradox in the spin version

An alternative version of the EPR paradox is based on measuring the spin direction, instead of momentum and location [6]. In this version, A and B are particles with spin $1/2$, which were created with opposite spins (e.g., by the decay of a particle with spin 0). They arrive at two detectors D_A and D_B where their spin directions are measured with respect to an arbitrary z -axis. Due to the conservation of angular momentum, if the spin of A is found to be positive ($|+\frac{1}{2}\rangle$), then the spin of B must be negative ($|-\frac{1}{2}\rangle$), and vice versa. This is truly unrelated to the distance that separates the particles at the moment of measurement.

If we repeat the measurement but measure both spins along the x -axis (perpendicularly to the z -axis), the result will be the same. If the spin of A is found to be $+\frac{1}{2}$, the measured spin of B will be $-\frac{1}{2}$, and vice versa. The results can be explained in two different ways.

1. The particles are entangled in such a way that when one spin is measured, the other spin becomes its opposite. The quantum state of the system, which could be a combination of $|+\frac{1}{2}\rangle$ and $|-\frac{1}{2}\rangle$ for both particles prior to the measurement, collapses into $|+\frac{1}{2}\rangle$ for particle A and $|-\frac{1}{2}\rangle$ for particle B (or vice versa) because of the measurement. This is the QM or the Copenhagen explanation.
2. The two particles were created with definite (opposite) spins around any axis in space we may choose. This is "the hidden variable" explanation.

Both explanations seem to be problematic. In order to illustrate the problem with the first explanation, let us assume that particle A arrives at the detector D_A and after a short time interval, Δt , particle B arrives at the detector D_B . The information about the measured spin of A should travel from D_A to D_B faster than the speed of light, since the distance between them can be many kilometers, while Δt can be arbitrarily small. This seems to violate SR.

According to the second explanation, no information is transferred from one detector to the other. However, we have to assume that each of the two particles is created with definite eigenvalues of both S_z and S_x . But, according to QM, two perpendicular components of the angular momentum cannot be simultaneously in defined states. If a particle has a definite spin direction relative to the z -axis, its spin direction on the x -axis should be a superposition of $|+\frac{1}{2}\rangle$ and $|-\frac{1}{2}\rangle$ so that a measurement can give each state with equal probabilities. If the information about the results of potential measurements of the spin along any arbitrary axis exists prior to the measurement, then that information must somehow be concealed. Hence, this model was dubbed “hidden variables.”

3. Bell’s experimental setup for photons

Until the article of John Stewart Bell [7], no experiment was made in order to find out which of the two explanations is true, since they were thought to be indistinguishable in terms of experimental results. Bell pointed out that the two explanations predict the same results if D_A and D_B are oriented in the same direction in space. However, the results predicted by the two explanations may differ, if the detectors measure the spins in different directions. Bell adopted the spin example advocated by Bohm and Aharonov [6], but since most experiments were made with photons (where the polarization of the photon substitutes the spin component), it will be more convenient in the ensuing discussion to present Bell’s thought experiment with photons. The following scheme, depicted in **Figure 1**, is a simplified version of the two-channel experimental setup first employed by Aspect et al. [8].

A source (S) emits two photons, A and B , which travel in opposite directions and have the same polarization state. The photons reach two detectors (e.g., sensitive photomultipliers), D_A and D_B , which are able to detect single photons. In front of each detector, there is a polarizer (P_A and P_B). If the photon passes the polarizer and arrives at the detector, the event is registered as 1. If the photon is stopped by the polarizer and does not reach the detector, the event is recorded as 0.

Let us assume first that the axes of both polarizers are oriented in the z direction, as shown in **Figure 1**. Since the two photons were emitted with the same polarization, we can assume that there will be perfect correspondence between the results recorded by

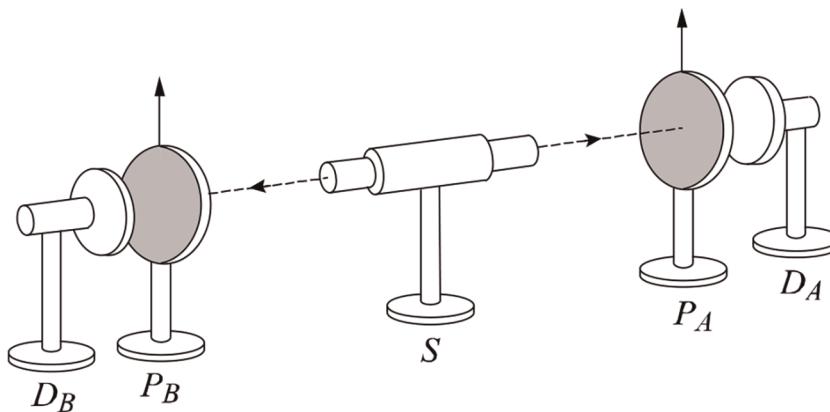


Figure 1.
 The setup for Bell’s experiment with photons.

the two detectors: if one detector records the series: 1, 0, 0, 1, 0, 1..., the second detector will record exactly the same series. On the other hand, if polarizer P_A is oriented in the z direction while polarizer P_B is oriented in the x direction, there will be a perfect mismatch between the results: if D_A records 1 then D_B will record 0, and vice versa.

Suppose that there is an angle θ between the two polarizers. We define a “matching function” $F(\theta)$, which is the ratio of the number of matches between the two detectors to the total number of readings, in a long series of measurements. We also define a “mismatch function” $E(\theta)$ as the percentage of mismatches between the two detectors. It’s easy to see that:

$$E(\theta) = 1 - F(\theta) \quad (\text{for any } \theta) \quad (1)$$

$$F(\theta = 0^\circ) = 1; \quad E(\theta = 0^\circ) = 0 \quad (2)$$

$$F(\theta = 90^\circ) = 0; \quad E(\theta = 90^\circ) = 1 \quad (3)$$

Let us consider the case of $\theta = 0^\circ$. The correlation between D_A and D_B (Eq. (2)) comes as no surprise if the initial polarization of the pair of photons is parallel to the z -axis ($|z\rangle$) or to the x -axis ($|x\rangle$). However, we expect to get the same correlation, even when the initial polarization of the photons forms an arbitrary angle ϕ ($0^\circ < \phi < 90^\circ$) with the z -axis. In this case, the initial polarization prior to the measurement can be considered as a superposition of $|z\rangle$ and $|x\rangle$, and the measurement actually causes the collapse of the wave function of each photon to one of the eigenstates, $|z\rangle$ or $|x\rangle$. As mentioned above, the fact that in two remote locations, the collapse is to the same eigenstate can be explained in two alternative ways: the QM interpretation (which involves an immediate action at a distance) or the hidden-variable model.

4. Bell’s inequality and Bell’s theorem

Let us explore the following four-stage thought experiment, which will lead us to Bell’s Inequality.

Stage 1: P_A and P_B both point in the z direction ($\theta = 0$), as shown in **Figure 2-1**. Two entangled photons are emitted from the source. Photon A arrives at P_A while photon B arrives at P_B . The readings of the two detectors will be the same all the time, therefore $E(\theta) = 0$.

Stage 2: P_B is rotated counterclockwise at an angle θ ($0^\circ < \theta < 45^\circ$, e.g., $\theta = 15^\circ$), as shown in **Figure 2-2**. Once more, two photons are emitted from the source. Let us assume that photon A passes through P_A and reaches D_A . The probability that photon B will reach D_B is no longer 100%; sometimes it will arrive at D_B and sometimes it will not. In some cases, photon A will be blocked while photon B arrives at D_B . Therefore, $E(\theta)$, which corresponds to the average mismatch between D_A and D_B , is no longer 0.

Stage 3: P_B is restored to its previous position (parallel to the z -axis) while P_A is rotated clockwise at the same angle θ , as shown in **Figure 2-3**. The situation is symmetrical to **Figure 2-2**, and we expect the average mismatch to be $E(\theta)$ as in Stage 2.

Stage 4: We leave P_A as in Stage 3, i.e., skewed at an angle θ clockwise. We rotate P_B anticlockwise at the same angle θ . The angle between the two polarizers is now 2θ , as shown in **Figure 2-4**. We repeat the series of measurements that were performed in the previous stages. The mismatch between D_A and D_B is now $E(2\theta)$.

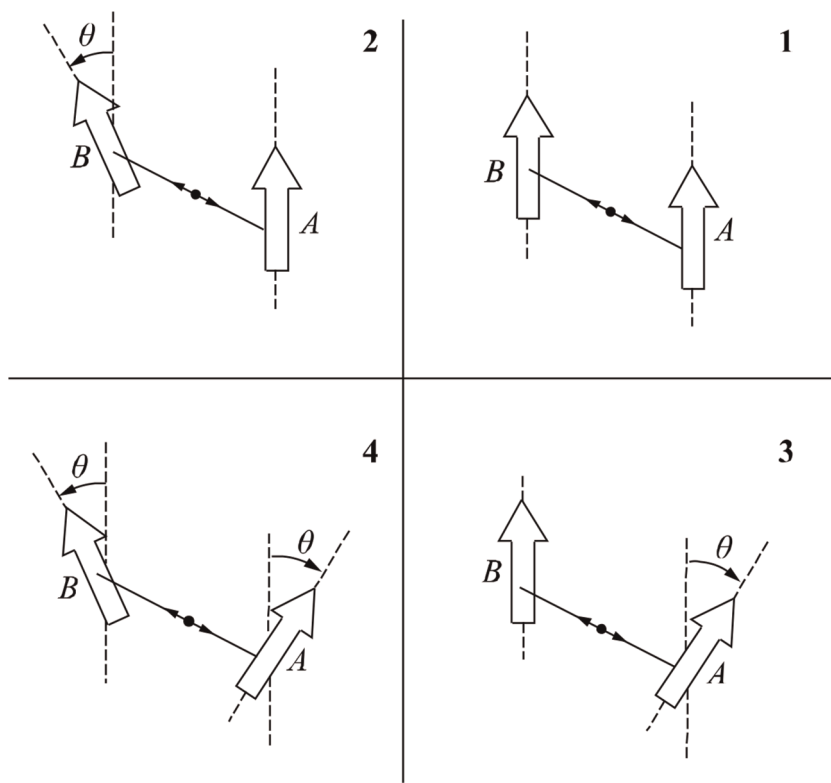


Figure 2.
 A four-stage thought experiment that leads to Bell's inequality.

We shall now see that the two models, which explain the correlation between the readings of D_A and the readings of D_B , provide different predictions about the relationship between $E(2\theta)$ and $E(\theta)$. Therefore, by measuring $E(\theta)$ and $E(2\theta)$ for various values of θ , it can be determined as to which of the two models is correct.

According to the hidden-variable model—that rejects action at a distance—there is no connection between the two polarizers. There is no way that polarizer P_A could sense the state of polarizer P_B . Therefore, the rotation of polarizer P_B between Stage 3 and Stage 4 cannot affect polarizer P_A . Consequently, at Stage 4, polarizer P_A will continue to pass or block photons with the same rate of mismatch which we would get if P_B stayed upright. In other words, at Stage 4, the mismatch between the series a (which shows the readings of D_A) and a hypothetical series c (which represents the results we would get from D_B at Stage 4, if P_B remained upright) is still $E(\theta)$.

By the same token, the mismatch between c and b (the actual readings of D_B at Stage 4) will also be $E(\theta)$. One might conclude that the mismatch between a and b will be the sum of the mismatch between a and c and the mismatch between b and c , namely, that $E(2\theta) = 2E(\theta)$. However, this conclusion is too hasty. In some cases, an element in a will be the opposite of the corresponding element in c , and the same element in b will also be the opposite of the element in c . In this case, the elements in a and in b will be identical. Therefore, the average mismatch between a and b at Stage 4, namely $E(2\theta)$, can be $2E(\theta)$ but can also be smaller than $2E(\theta)$. We can write:

$$E(2\theta) \leq 2E(\theta) \left[\text{Bell's inequality} \right] \quad (4)$$

We can demonstrate the relation between $E(2\theta)$ and $2E(\theta)$ by the following example. Let us assume that.

$$c = 0, 0, 1, 0, 1, 0, 1, 1, 0, 1, 1, 0 \quad (5)$$

In order to create series a , we duplicate c but randomly change 4 of the 12 digits. To create series b , we once more duplicate c and randomly change 4 of the 12 digits. The mismatch between c and a as well as between c and b will be $1/3$.

$$E(c, a) = E(c, b) = 1/3 \quad (6)$$

If the elements of c , which were changed to create b , were different from the elements of c which were changed to create a , the mismatch between a and b will be $2/3$. However, if the same elements were changed in both cases, the mismatch between a and b will be 0. In the general case, we can write:

$$E(a, b) \leq 2/3 \quad (7)$$

In correspondence with Eq. (4). Eq. (4) is Bell's inequality for the specific experimental procedure described above. According to Bell's theorem, Eq. (4) would be verified experimentally if the hidden-variable model is true. On the other hand, if Bell's inequality is violated, then the QM model is true.

5. $E(\theta)$ according to quantum mechanics

We can go on and evaluate $E(\theta)$ according to the traditional interpretation of QM. Let us assume that in Stage 2 of the thought experiment described in Section 4, photon A passes through P_A and reaches D_A . This means that the polarization of photon A is parallel to the z -axis. Since the two photons are entangled, this is also the polarization of photon B . The angle between the axes of P_A and P_B is θ . Therefore, the polarization of photon B is skewed relatively to P_B at an angle θ .

According to Malus's law, when a polarized beam of light hits a perfect polarizer, the intensity of the light that passes through the polarizer is given by:

$$I = I_0 \cos^2 \theta \quad (8)$$

where I_0 is the initial intensity and θ is the angle between the light's direction of polarization and the axis of the polarizer.

When we regard the beam as a stream of photons, we can ascribe to each photon a defined direction of polarization which creates an angle θ with P_B . According to Eq. (8), out of N photons, approximately $N \cos^2 \theta$ will pass P_B and about $N \sin^2 \theta$ will be blocked. The probability that a single photon will reach D_A or D_B , while its companion will be blocked at the other detector is therefore $\sin^2 \theta$, and this will be the average mismatch rate in a long series of measurements¹. Thus, according to QM, at Stages 2 and 3:

¹ If photon A is blocked, the probability that photon B will pass is $\cos^2(90^\circ - \theta) = \sin^2 \theta$

$$E(\theta) = \sin^2 \theta \text{ (Stages 2 and 3)} \quad (9)$$

In Stage 4, the angle between the polarizers is 2θ and, according to QM, the mismatch rate will be:

$$E(2\theta) = \sin^2 2\theta \quad (10)$$

If, for example, $\theta = 30^\circ$, we shall get in Stages 2 and 3 a mismatch rate of:

$$E(30^\circ) = \sin^2(30^\circ) = 0.5^2 = 0.25 \quad (11)$$

while in Stage 4 the mismatch rate will be:

$$E(60^\circ) = \sin^2(60^\circ) = 0.75 \quad (12)$$

In this case, $E(2\theta) > 2E(\theta)$ in contrast to Bell's inequality (Eq. (4)). Indeed, it's easy to prove that $E(2\theta) > 2E(\theta)$ for any θ in the range: $0^\circ < \theta < 45^\circ$.

To prove this, we notice that:

$$\sin^2(2\theta) = 4 \sin^2(\theta) \times \cos^2(\theta) \quad (13)$$

In the range $0^\circ \leq \theta \leq 45^\circ$, the function $\cos^2(\theta)$ is a monotonically descending function, which has a minimum at $\theta = 45^\circ$, where $\cos^2(\theta) = 0.5$. At that point:

$$\sin^2(2\theta) = 4\sin^2(\theta) \times 0.5 = 2 \sin^2(\theta) \quad (\theta = 45^\circ) \quad (14)$$

namely, for $\theta = 45^\circ$, $E(2\theta) = 2E(\theta)$. If $0^\circ < \theta < 45^\circ$ then $\cos(2\theta) > 0.5$ and $\sin^2(2\theta) > 2\sin^2(\theta)$, which means that $E(2\theta) > 2E(\theta)$, in contrast with Bell's inequality.

Figure 3 depicts $E(\theta)$ according to the QM description ($E(\theta) = \sin^2 \theta$) in the range $0^\circ \leq \theta \leq 90^\circ$. On the straight line (described by $E(\theta) = \theta/90^\circ$), the relation between $E(\theta)$ and $E(2\theta)$ is: $E(2\theta) = 2E(\theta)$. One can see that in the range $0^\circ < \theta < 45^\circ$, the function $E(\theta) = \sin^2 \theta$ (which represents QM's results) lies below the straight line, while Bell's inequality Eq. (4) is valid only for points that are above the straight line. Thus, by performing the experiment described in Section 4, one can find out whether the QM model or the hidden-variable model is correct.

In a pioneering work of Freedman and Clauser [4], an experiment similar to the thought experiment described above was performed. They measured the polarization correlation of two entangled photons emitted in an atomic cascade of calcium. The wavelengths of the photons were 551.3 nm and 422.7 nm. The measurements were made at nine different angles in the range $0^\circ \leq \theta \leq 90^\circ$. The results were in agreement with quantum mechanics and violated Bell's inequality to a high statistical accuracy. Actually, the curve describing the results (**Figure 3** in [4]) is similar to $E(\theta) = \sin^2 \theta$ in **Figure 3** above, except for the values on the vertical axis which reflect the fact that the efficiency of the detectors was less than 100%. The authors considered the results as strong evidence against local hidden-variable theories.

Over the years, additional experiments demonstrated clearly the violation of Bell's inequality. It was established that in experiments such as those described in the EPR and Bell's papers, a measurement performed on one particle does affect the other particle which can be far away. The effect is immediate, indicating that a single

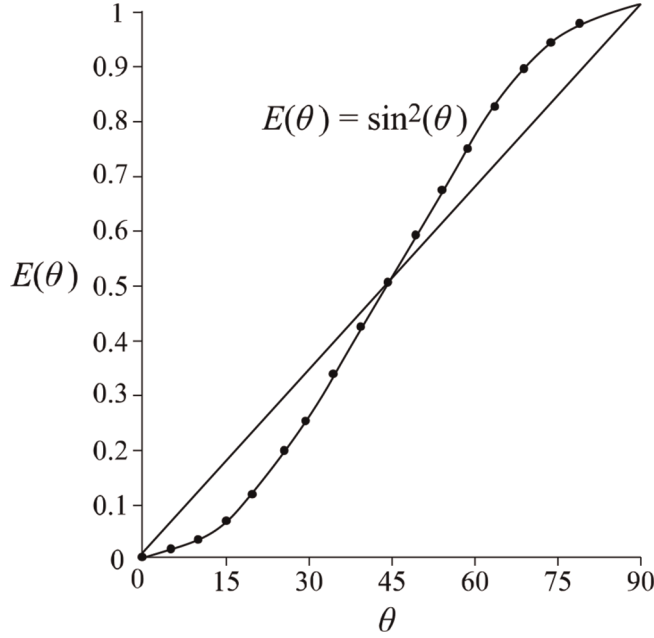


Figure 3.
The points depict $E(\theta)$ according to quantum mechanics (QM) ($E(\theta) = \sin^2 \theta$). On the straight line (described by $E(\theta) = \theta/90^\circ$), $E(2\theta) = 2E(\theta)$.

unified wave function continues to describe the two particles even when they are far apart. Thus, a measurement performed on one particle causes the collapse of the wave function in the other one as well. In order to resolve the contradiction between this action at a distance and SR, we have to see why the contradiction arises in the first place.

6. Special relativity and action at a distance

Let S and S' denote two inertial reference frames. S' is moving with respect to S at a constant velocity v along the x -axis. At time $t = 0$, the spatial axes and clocks of S and S' coincide. Suppose that an event that occurred in S , at point x_1 in time t_1 creates a signal that travels at a velocity u . The signal arrives at point x_2 in time t_2 and creates a second event there (e.g., turning on a lamp). The coordinates and times of the two events in S' are (x'_1, t'_1) and (x'_2, t'_2) . According to the Lorentz transformation:

$$t'_1 = \gamma \left(t_1 - \frac{vx_1}{c^2} \right); \quad t'_2 = \gamma \left(t_2 - \frac{vx_2}{c^2} \right) \quad (15)$$

Where $\gamma = 1/(1-v^2/c^2)^{1/2}$. From (15), we get:

$$\Delta t' = \gamma (\Delta t - v\Delta x/c^2) \quad (16)$$

Where $\Delta t' = t'_2 - t'_1$; $\Delta t = t_2 - t_1$; $\Delta x = x_2 - x_1$.

Since $\Delta x = u\Delta t$, we can write:

$$\Delta t' = \gamma \Delta t (1 - uv/c^2) \quad (17)$$

If the signal velocity u is greater than the speed of light ($u > c$), we can define a reference frame S' that moves at a velocity v which is smaller than c but close enough to c so that $uv/c^2 > 1$ (in order for that to happen, v should meet the condition $c > v > c^2/u$). The expression $(1 - uv/c^2)$ in Eq. (17) will be negative, and therefore if Δt is positive, $\Delta t'$ should be negative and vice versa. Thus, in S' , event 1 will occur after event 2 and an observer in S' would see the effect precede its cause. For example, let $u = 1.1c$ and $\Delta x = c \times 1$ s while $v = 0.98c$ ($\gamma = 5.025$). With these values:

$$\Delta t = \Delta x/u = 0.9091 \text{ s.}$$

$$\Delta t' = 5.025 \times 0.9091(1 - 0.98 \times 1.1) = -0.356 \text{ s.}$$

The minus sign indicates that the order of events in S and S' is reversed. According to an observer in S' , event 1 (which is the cause of event 2) occurred 0.356 s after event 2. The assumption that a signal can travel faster than the speed of light leads to a violation of the relativistic principle of causality, which asserts that an effect never precedes its cause, in any reference frame. This is why SR forbids instantaneous action at a distance as well as traveling of matter, energy, or information at speeds greater than the speed of light.

In order to demonstrate the inconsistency of Bell-like experiments with SR, let us return to Stage 1 in the experiment described in Section 4. Both polarizers P_A and P_B are oriented in the z direction ($\theta = 0$), as shown in **Figure 2-1**. Thus, the readings of the two detectors are the same all the time and $E(\theta) = 0$. Let us assume that D_A , D_B , and the source are on the x -axis of a rest frame S . The source is at $x_0 = 0$ and the coordinates of D_A and D_B are:

$$x_1 = x(D_A) = 15 \text{ m}; x_2 = x(D_B) = -15.3 \text{ m} \quad (18)$$

In order to facilitate the calculations, we redefine our unit of length so that $c = 3 \times 10^8$ m/s exactly. We denote by t_1 and t_2 the times of two events. **Event 1**: "Photon A reached P_A and then D_A registered 0 or 1," **Event 2**: "Photon B reached P_B and then D_B registered 0 or 1." It's easy to see that:

$$t_1 = 50 \text{ ns}; t_2 = 51 \text{ ns} \quad (19)$$

Before checking the times in another frame, S' , let us discuss the following question: Can an observer in S consider event 2 as the result of event 1? I claim that she can. The two events can be considered a combination of cause and effect for the following reasons.

1. In frame S , event 1 precedes event 2 by 1 ns.
2. Prior to the occurrence of event 1, the reading of D_B could be either 0 or 1 in equal probabilities. After event 1 takes place, the reading of D_B is definitely determined.
3. If D_A was removed after the photons left the source, and before they reached the polarizers, the reading of D_B could be either 0 or 1 in equal probabilities. The fact that D_A operated and registered the arriving photon influenced the reading of D_B .

Therefore, event 2 can be considered the result of event 1. An argument against this claim is that the two events are separated by a space-like interval. According to SR, only if two events are separated by a time-like or light-like interval can one event influence the other. However, it can be claimed that the concept of causality is metaphysically prior to the relativistic restrictions. Actually, it was argued that many standard philosophical theories would treat the relationship between such two events as causal, despite the contradiction with SR [9].

Let us assume a second frame S' which is moving with respect to S in the negative direction of the x -axis at a velocity $v = -0.6c$. Let us assume that when the two photons are ejected from the source, the clocks at S and S' show $t = t' = 0$, and the origins coincide. By using the Lorentz transformation (Eq. 15), we find:

$$t'_1 = 100 \text{ ns}; \quad t'_2 = 25.5 \text{ ns} \quad (20)$$

Thus, in S' event 2 occurs before event 1, although we defined event 1 as the cause of event 2. Actually, since the velocity of the signal which carries the information between D_A and D_B is infinite, the paradox appears for v as small as $|v| \approx 0.01c$ for the numerical values of the example above. In general, it occurs whenever:

$$-v \geq \frac{t_2 - t_1}{x_1 - x_2} c^2 \quad (21)$$

7. Solutions to the paradox

Several solutions can be offered for the contradiction, which was demonstrated in the previous section between SR and Bell-like experiments. Ballentine and Jarrett [10] suggested a distinction between a “strong” locality principle and a “weak” one that is needed to satisfy the demands of relativity. They claimed that QM satisfies the latter and therefore there is no contradiction between QM and SR. Instead, one can argue that we do not have two separate events here but only one spatially extended but indivisible event which is “the collapse of the wave function which represents the polarization of the two photons” ([9], p. 41). Another alternative is to formulate a theory of causation which requires some conditions which two events need to fulfill in order to represent a cause-and-effect relationship, and then show that these conditions are not realized here ([9], p. 42).

The solution, which I suggest to the paradox, is based on the following principles:

1. Event 1 and event 2, in the example discussed in Section 6, are two distinct and separate events that occur at different points in space-time.
2. There is a cause-and-effect connection between the two events.
3. According to an observer in S , event 2 is a result of event 1.
4. According to an observer in S' , on the other hand, event 1 is a result of event 2.
5. The disagreement between the two observers does not violate the causality principle of SR, since in this particular case the cause-and-effect relationship

between the two events is symmetrical: each of them can be regarded as a result of the other, depending on the frame of reference in which they are observed.

Usually, when there is a causal relationship between two remote events, they are physically different. That's why the effect cannot precede its cause in any reference frame. For example, if event 1 is the ejection of a signal from point (x_1, y_1, z_1, t_1) and event 2 is the arrival of the signal to point (x_2, y_2, z_2, t_2) where it turns on a lamp, we demand that, in any reference frame, $t_2 > t_1$. This demand is fulfilled only if the velocity of the signal does not exceed the speed of light, as shown in Section 6.

However, in Bell-like experiments, like the one described in Section 4, there is no physical difference between the two events: they are totally symmetrical. Each of them can serve as a cause or as an effect, depending on the frame of reference in which they are observed. If event 1 is observed before event 2, event 1 is the cause and event 2 is the result. If the order of times is reversed, then event 2 is the cause and event 1 is the result.

It is customary to think that the causal relation between two events can be one of the four types:

1. Event 2 is a result of event 1.
2. Event 1 is a result of event 2.
3. Both events have a common cause.
4. There is no causal relation between the two events.


The analysis of the ostensible contradiction between Bell's theorem and SR indicates that there is an additional possibility. In entangled systems, one can find pairs of "entangled events" which have symmetrical cause-and-effect relations. Each of them can appear to be the cause of the other, depending on the frame of reference in which they are observed. This fifth possibility solves the paradox which the action at a distance creates. Experimental results (e.g., [11]) can be interpreted as supporting this suggestion.

Author details

Yoram Kirsh
The Open University of Israel, Raanana, Israel

*Address all correspondence to: yoramk@openu.ac.il

IntechOpen

© 2023 The Author(s). Licensee IntechOpen. This chapter is distributed under the terms of the Creative Commons Attribution License (<http://creativecommons.org/licenses/by/3.0>), which permits unrestricted use, distribution, and reproduction in any medium, provided the original work is properly cited. 

References

- [1] Hensen B et al. Loophole-free Bell inequality violation using electron spins separated by 1.3 kilometres. *Nature*. 2015;**526**:682-686. Available from: <https://www.nature.com/articles/nature15759>
- [2] Giustina M et al. A significant-loophole-free test of Bell's theorem with entangled photons. *Physical Review Letters*. 2015;**115**:250401
- [3] Shalm LK et al. A strong loophole-free test of local realism. *Physical Review Letters*. 2015;**115**:250402
- [4] Freedman SJ, Clauser JF. Experimental test of local hidden-variable theories. *Physical Review Letters*. 1972;**28**:938-941. DOI: 10.1103/PhysRevLett.28.938
- [5] Einstein A, Podolsky B, Rosen N. Can quantum-mechanical description of physical reality be considered complete? *Physical Review*. 1935;**47**:777-780. DOI: 10.1103/PhysRev.47.777
- [6] Bohm D, Aharonov Y. Discussion of experimental proof for the paradox of Einstein, Rosen, and Podolsky. *Physical Review*. 1957;**108**:1070-1076
- [7] Bell JS. On the Einstein-Podolsky-Rosen paradox. *Physics*. 1964;**1**:195-200. Available from: https://cds.cern.ch/record/111654/files/vol1p195-200_001.pdf
- [8] Aspect A, Grangier P, Roger G. Experimental realization of Einstein-Podolsky-Rosen-Bohm gedankenexperiment: A new violation of Bell's inequalities. *Physical Review Letters*. 1982;**49**:91-94
- [9] Butterfield J. David Lewis meets John Bell. *Philosophy of Science*. 1992;**59**: 26-43
- [10] Ballentine LE, Jarrett JP. Bell's theorem: Does quantum mechanics contradict relativity? *American Journal of Physics*. 1987;**55**:696-701. DOI: 10.1119/1.15059
- [11] Goswami K et al. Indefinite causal order in a quantum switch. *Physical Review Letters*. 2018;**121**:090503

Phenomenology of Heavy Quark at the LHC

Rachid Benbrik and Mohammed Boukidi

Abstract

In the Standard Model, the Higgs boson is responsible for giving particles mass through a process called the Higgs mechanism. However, the interactions between the Higgs boson and usual quarks are determined by Yukawa couplings, which means that the strength of their interactions depends on their mass. In contrast, vector-like quarks are expected to have a more “vector” coupling with the Higgs boson, which would make their interactions independent of their mass. This property could potentially make them easier to detect experimentally. In this chapter, we develop the theoretical framework of such exotic heavy quarks both in the standard model and beyond it such as the two Higgs doublets model (2HDM). This chapter introduces a Lagrangian which follows the most generic concept of the Standard Model which is consistent with the basics, and then we explore the consequences of identifying the eigenstates and interactions with SM-VLQ. We also provide a detailed description of the full interaction in the 2HDM mass basis. We shortly comment on the production of heavy quark pairs at the LHC.

Keywords: exotic particles, vector-like quark, LHC, Higgs, SM

1. Introduction

The introduction of vector quarks into the realm of particle physics represents a departure from the conventional characteristics of Standard Model (SM) quarks on multiple intriguing fronts. In stark contrast to their SM counterparts, vector quarks typically do not acquire masses through Yukawa couplings with a Higgs doublet, a feature that resonates with the experimental observations of the Higgs boson [1, 2]. This distinct trait opens up new avenues for exploration. What further sets vector quarks apart is their remarkable capacity for mixing with SM quarks. This mixing dynamic has profound implications, altering their couplings with essential bosons like the Z , W , and Higgs bosons [3]. Such mixing represents a straightforward mechanism for breaking the Glashow-Iliopoulos-Maiani mechanism, a tantalizing prospect that holds the potential for ushering in novel phenomena in low-energy physics [4]. However, the allure of vector quarks goes beyond these unique traits. Two primary theoretical motivations underpin their extensive study. Firstly, they play a pivotal role in the intricate dance of electroweak symmetry breaking, offering a promising avenue for explaining the observed light mass of the Higgs boson [5]. This becomes

particularly compelling within theoretical frameworks that posit the Higgs as a pseudo Goldstone boson [6].

Secondly, vector-like quarks emerge organically as fermion resonances within theories that delve into the nuanced realm of partial flavor composition within the Standard Model. In both of these theoretical scenarios, substantial mixing between the novel vector quarks and the third family of SM quarks, often dubbed “top partners,” takes center stage [7–10]. Notably, the presence of vector quarks is not confined to a single theoretical framework but extends its reach into diverse models. These encompass small Higgs and composite Higgs models, as well as their holographic counterparts [11]. Consequently, the study of vector quarks not only enriches our understanding of particle physics but also offers a tantalizing glimpse into the potential extensions and augmentations of the Standard Model, unearthing the profound intricacies that underlie the fundamental forces shaping the universe’s particle interactions.

Simultaneously, it is worth noting that testing quantum entanglement directly in proton-proton (pp) collisions at the Large Hadron Collider (LHC) poses a formidable challenge due to the macroscopic and complex nature of these interactions [12]. Quantum entanglement typically manifests at the microscopic scale, involving the correlation of properties between individual or pairs of particles. Nevertheless, researchers at the LHC can indirectly explore aspects related to quantum entanglement [13–15]. They may investigate the correlations and angular momentum conservation among particles produced in these high-energy collisions [16]. While not direct evidence of entanglement, these studies shed light on the quantum dynamics governing the particle interactions. Additionally, the search for new, exotic particles beyond the Standard Model is a primary mission of the LHC [17]. These hypothetical particles might exhibit quantum properties, including entanglement, which could be uncovered through their distinctive decay patterns and behaviors. Although the LHC primarily serves as a platform for fundamental particle physics research, it contributes to our broader comprehension of quantum mechanics and its role in the universe’s fundamental fabric [18, 19].

1.1 From weak eigenstates to mass eigenstates and mixing angles

Let us consider a general 2×2 Hermitian matrix of the form:

$$\mathcal{M} = \begin{pmatrix} a & b \\ \bar{b} & M \end{pmatrix}, \quad (1)$$

Where a, b, c , and d are complex numbers. In order to diagonalize the above matrix with the aid of the unitary matrix \mathcal{U} , we seek a diagonal matrix $\mathcal{M}_{\text{diag}}$ such that:

$$\mathcal{U}\mathcal{M}\mathcal{U}^\dagger = \mathcal{M}_{\text{diag}} \quad (2)$$

Here \mathcal{U}^\dagger denotes the conjugate transpose of \mathcal{U} . We adopt the following form for the unitary matrix \mathcal{U} :

$$\mathcal{U} = \begin{pmatrix} \cos \theta & -\sin \theta e^{i\varphi} \\ \sin \theta e^{-i\varphi} & \cos \theta \end{pmatrix}, \quad (3)$$

where θ and φ are real parameters. We determine these parameters by requiring that \mathcal{U} diagonalizes \mathcal{M} . Specifically, we choose θ and φ such that:

$$\tan(2\theta) = \frac{2|b|}{M-a} \quad \text{and} \quad \varphi = \arg(b), \quad (4)$$

We proceed to substitute the matrices \mathcal{U} , \mathcal{U}^\dagger , and \mathcal{M} into the equation for diagonalization, which we then simplify as follows:

$$\begin{aligned} \mathcal{U}\mathcal{M}\mathcal{U}^\dagger &= \begin{pmatrix} c & -se^{i\varphi} \\ se^{-i\varphi} & c \end{pmatrix} \begin{pmatrix} a & b \\ \bar{b} & M \end{pmatrix} \mathcal{U}^\dagger \\ &= \begin{pmatrix} ca - s|b| & cb - sMe^{i\varphi} \\ sae^{-i\varphi} + c\bar{b} & s|b| + cM \end{pmatrix} \begin{pmatrix} c & se^{i\varphi} \\ -se^{-i\varphi} & c \end{pmatrix} \\ &= \begin{pmatrix} c^2a - sc|b| - sc|b| + s^2M & scae^{i\varphi} - s^2b + c^2b - scMe^{i\varphi} \\ scae^{-i\varphi} + c^2\bar{b} - s^2\bar{b} - scMe^{-i\varphi} & s^2a + sc|b| + sc|b| + c^2M \end{pmatrix} \end{aligned} \quad (5)$$

Here, $c = \cos \theta$, $s = \sin \theta$, and \bar{b} denotes the complex conjugate of b .

To simplify the (1,2) entry, we utilize the fact that \mathcal{M} is Hermitian along with the following relationship derived from Eq. (1):

$$\frac{2sc}{c^2 - s^2} = \frac{2|b|}{M-a} \quad (6)$$

This yields the following equations:

$$\begin{aligned} (1, 2) &= sc(a - M)e^{i\varphi} + (c^2 - s^2)b \\ &= \frac{b}{M-a}(a - M)(c^2 - s^2)e^{i\varphi} + (c^2 - s^2)b \\ &= 0 \end{aligned} \quad (7)$$

$$(2, 1) = (1, 2)^* = 0 \quad (8)$$

$$(1, 1) = c^2a + s^2M - 2sc|b| \quad (9)$$

$$(2, 2) = s^2a + c^2M + 2sc|b| \quad (10)$$

We shall invoke the definition of the matrix \mathcal{M} , previously established as follows:

$$\mathcal{M} = \begin{pmatrix} y_{33} & y_{34} \\ 0 & M \end{pmatrix} \quad (11)$$

Utilizing the aforementioned definition of \mathcal{M} , the products $\mathcal{M}\mathcal{M}^\dagger$ and $\mathcal{M}^\dagger\mathcal{M}$ can be computed as:

$$\mathcal{M}\mathcal{M}^\dagger = \begin{pmatrix} |y_{33}|^2 + |y_{34}|^2 & y_{34}M \\ y_{34}M & M^2 \end{pmatrix} \quad \text{where} \quad \mathcal{U}_L = \begin{pmatrix} \cos \theta_L & -\sin \theta_L e^{i\varphi_L} \\ \sin \theta_L e^{-i\varphi_L} & \cos \theta_L \end{pmatrix} \quad (12)$$

$$\mathcal{M}^\dagger\mathcal{M} = \begin{pmatrix} |y_{33}|^2 & y_{33}^*y_{34} \\ y_{33}y_{34}^* & M^2 + |y_{34}|^2 \end{pmatrix} \quad \text{where} \quad \mathcal{U}_R = \begin{pmatrix} \cos \theta_R & -\sin \theta_R e^{i\varphi_R} \\ \sin \theta_R e^{-i\varphi_R} & \cos \theta_R \end{pmatrix} \quad (13)$$

The mixing angles θ_L and θ_R can be expressed as follows:

$$\begin{cases} \tan(2\theta_L) = \frac{2|y_{34}|M}{M^2 - |y_{33}|^2 - |y_{34}|^2} & \text{where } \varphi_L = \arg(y_{34}) \\ \tan(2\theta_R) = \frac{2|y_{33}y_{34}|}{M^2 + |y_{34}|^2 - |y_{33}|^2} & \text{where } \varphi_R = \arg(y_{33}^*y_{34}) \end{cases} \quad (14)$$

Let us define a new matrix \mathcal{M} with a distinct element configuration from the previous one:

$$\mathcal{M} = \begin{pmatrix} y_{33} & 0 \\ y_{43} & M \end{pmatrix} \quad (15)$$

Upon calculating the products $\mathcal{M}^{\mathcal{M}}$ and $\mathcal{M}^\dagger \mathcal{M}$, we obtain two matrices as a result:

$$\mathcal{M}\mathcal{M}^\dagger = \begin{pmatrix} |y_{33}|^2 & y_{33}y_{43}^* \\ y_{33}^*y_{43} & M^2 + |y_{43}|^2 \end{pmatrix} \quad \mathcal{M}^\dagger \mathcal{M} = \begin{pmatrix} |y_{33}|^2 + |y_{43}|^2 & y_{43}^*M \\ y_{43}M & M^2 \end{pmatrix} \quad (16)$$

From the above expressions, we can extract the mixing angles θ_L and θ_R , as well as the phases φ_L and φ_R .

$$\begin{cases} \tan(2\theta_L) = \frac{2|y_{33}y_{43}|}{M^2 + |y_{43}|^2 - |y_{33}|^2} & \text{where } \varphi_L = \arg(y_{33}y_{43}^*) \\ \tan(2\theta_R) = \frac{2|y_{43}|M}{M^2 - |y_{33}|^2 - |y_{43}|^2} & \text{where } \varphi_R = \arg(y_{33}^*) \end{cases} \quad (17)$$

2. Framework of SM + VLQs singlet

In the basis of weak eigenstates (t, T) , where t represents the standard model top quark, the matrix describing the masses of the top quark and vector-like quarks (VLQ) [20] can be expressed as follows

$$\mathcal{M} = \begin{pmatrix} y_{33} \frac{v}{\sqrt{2}} & y_{34} \frac{v}{\sqrt{2}} \\ 0 & M \end{pmatrix} \quad (18)$$

The aforementioned mass matrix clearly indicates that the physical mass of the heavy top quark, m_T , differs from the mass parameter M due to the mixing of the weak eigenstates t and T . To obtain the physical states $(t_{L,R}, T_{L,R})$ in terms of the gauge eigenstates $(\tilde{t}_{L,R}, \tilde{T}_{L,R})$, the mass matrix \mathcal{M} can be diagonalized through a bi-unitary transformation, as described in Section 1.

$$\begin{pmatrix} t_{L,R} \\ T_{L,R} \end{pmatrix} = \mathcal{U}_{L,R} \begin{pmatrix} \tilde{t}_{L,R} \\ \tilde{T}_{L,R} \end{pmatrix} \quad (19)$$

Where the rotation matrices \mathcal{U}_L and \mathcal{U}_R corresponding to left-handed and right-handed rotations, respectively, can be defined as follows:

$$\mathcal{U}_{L,R} = \begin{pmatrix} \cos(\theta_{L,R}) & -\sin(\theta_{L,R})e^{i\varphi_{L,R}} \\ \sin(\theta_{L,R})e^{-i\varphi_{L,R}} & \cos(\theta_{L,R}) \end{pmatrix} \quad (20)$$

In regards to the mixing angles, it is important to note that θ_L and θ_R are not considered independent parameters. This can be deduced from the bi-unitary transformations, which yield the following relationships:

$$\tan 2\theta_L = \left(\frac{2|y_{34}|\frac{v}{\sqrt{2}}M}{M^2 - |y_{33}|^2\frac{v^2}{2} - |y_{34}|^2\frac{v^2}{2}} \right), \quad \tan 2\theta_R = \left(\frac{|y_{33}y_{34}|v^2}{M^2 + |y_{34}|^2\frac{v^2}{2} - |y_{33}|^2\frac{v^2}{2}} \right) \quad (21)$$

Here y_{33} is assumed to be real, $\varphi_L = \arg(y_{34})$ and $\varphi_R = \arg(y_{33}^*y_{34})$.

Based on the aforementioned relation in Section 1, namely $\mathcal{U}_L \mathcal{M} \mathcal{U}_R^\dagger = \mathcal{M}_{diag}$, we can introduce the following notations:

$$\bar{u}_L^0 \mathcal{M} u_R^0 = \bar{u}_L^0 \mathcal{U}_L^\dagger \mathcal{M}_{diag} \mathcal{U}_R u_R^0 \Rightarrow \begin{cases} u_{L,R} = \mathcal{U}_{L,R} u_{L,R}^0 \\ u_{L,R}^0 = \mathcal{U}_{L,R}^\dagger u_{L,R} \end{cases} \quad (22)$$

2.1 Modified gauge boson couplings

The couplings of the W boson to the top quark (t) and its heavy partner (T) with the bottom quark (b) can be expressed in terms of the left-handed up-type quark mixing matrix \mathcal{U}_L , as follows (**Figure 1**).

$$\begin{pmatrix} \bar{u}_{L3}^0 & \bar{u}_{L4}^0 \end{pmatrix} \begin{pmatrix} 1 & 0 \end{pmatrix} b_L = \begin{pmatrix} \bar{t}_L & \bar{T}_L \end{pmatrix} \mathcal{U}_L \begin{pmatrix} 1 \\ 0 \end{pmatrix} b_L \quad (23)$$

where

$$\mathcal{U}_L \begin{pmatrix} 1 \\ 0 \end{pmatrix} = \begin{pmatrix} c_L \\ s_L e^{-i\varphi_L} \end{pmatrix} \quad (24)$$

Using these expressions, we obtain the following couplings:

$$V_{tb} = c_L, \quad \text{and} \quad V_{Tb} = s_L e^{-i\varphi_L} \quad (25)$$

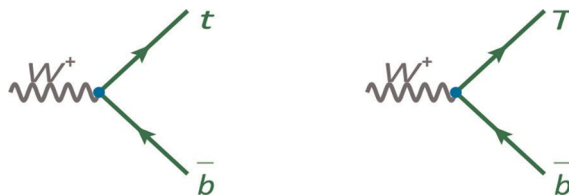
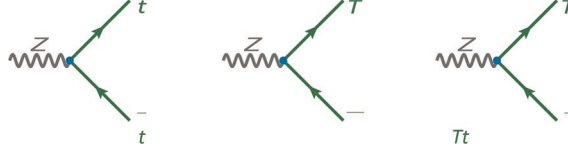


Figure 1.
 Typical Feynman diagram of the W boson couplings to the top quark (t) and its heavy partner (T) with the bottom quark (b).


Figure 2.

Typical Feynman diagram of the Z boson couplings to pairs of top (t) and top partner (T).

The neutral current expression can be employed to describe the neutral couplings of the Z boson to pairs of top (t) and top partner (T) (**Figure 2**).

$$(\bar{u}_{L3}^0 \quad \bar{u}_{L4}^0) \begin{pmatrix} 1 & 0 \\ 0 & 0 \end{pmatrix} \begin{pmatrix} u_{L3}^0 \\ u_{L4}^0 \end{pmatrix} = (\bar{t}_L \quad \bar{T}_L) \mathcal{U}_L \begin{pmatrix} 1 & 0 \\ 0 & 1 \end{pmatrix} \mathcal{U}_L^\dagger \begin{pmatrix} t_L \\ T_L \end{pmatrix} \quad (26)$$

The computation of the product yields the following relationships:

$$(\bar{u}_{L3}^0 \quad \bar{u}_{L4}^0) \begin{pmatrix} 1 & 0 \\ 0 & 0 \end{pmatrix} \begin{pmatrix} u_{L3}^0 \\ u_{L4}^0 \end{pmatrix} = (\bar{t}_L \quad \bar{T}_L) \mathcal{U}_L \begin{pmatrix} 1 & 0 \\ 0 & 1 \end{pmatrix} \mathcal{U}_L^\dagger \begin{pmatrix} t_L \\ T_L \end{pmatrix} \quad (27)$$

The aforementioned equations can be employed to define the following couplings:

$$X_{tt} = c_L^2, \quad X_{TT} = s_L^2, \quad X_{Tt} = c_L s_L e^{-i\varphi_L} \quad (28)$$

2.2 Modified Higgs couplings

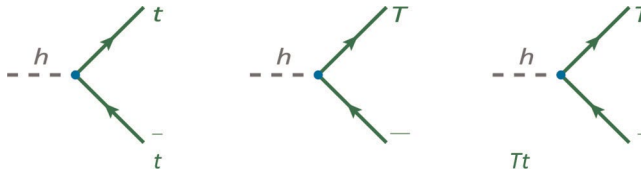
The neutral Higgs couplings to top (t) and top partner (T) pairs can be derived from the following equations (**Figure 3**):

$$\mathcal{M} = \begin{pmatrix} \frac{y_{33}}{\sqrt{2}} & \frac{y_{34}}{\sqrt{2}} \\ 0 & 0 \end{pmatrix} = \begin{pmatrix} \frac{y_{33}}{\sqrt{2}} & \frac{y_{34}}{\sqrt{2}} \\ 0 & \frac{M^0}{v} \end{pmatrix} - \begin{pmatrix} 0 & 0 \\ 0 & \frac{M^0}{v} \end{pmatrix} = \frac{M}{v} - \frac{M^0}{v} \begin{pmatrix} 0 & 0 \\ 0 & 1 \end{pmatrix} \quad (29)$$

Then we compute:

$$(\bar{u}_{L3}^0 \quad \bar{u}_{L4}^0) \mathcal{M} \begin{pmatrix} u_{R3}^0 \\ u_{R4}^0 \end{pmatrix} = (\bar{u}_{L3}^0 \quad \bar{u}_{L4}^0) \frac{M}{v} \begin{pmatrix} u_{R3}^0 \\ u_{R4}^0 \end{pmatrix} - \frac{M^0}{v} (\bar{u}_{L3}^0 \quad \bar{u}_{L4}^0) \begin{pmatrix} 0 & 0 \\ 0 & 1 \end{pmatrix} \begin{pmatrix} u_{R3}^0 \\ u_{R4}^0 \end{pmatrix} \quad (30)$$

Further simplifying the above equation, we get:


Figure 3.

Typical Feynman diagram of the Higgs boson h couplings to pairs of top (t) and top partner (T).

$$(\bar{t}_L \quad \bar{T}_L) \frac{1}{v} \begin{pmatrix} m_t & 0 \\ 0 & M \end{pmatrix} \begin{pmatrix} t_R \\ T_R \end{pmatrix} - \frac{M^0}{v} (\bar{t}_L \quad \bar{T}_L) \mathcal{U}_L \begin{pmatrix} 0 & 0 \\ 0 & 1 \end{pmatrix} \mathcal{U}_R^+ \begin{pmatrix} t_R \\ T_R \end{pmatrix} \quad (31)$$

$$\begin{pmatrix} c_L & -s_L e^{i\varphi_L} \\ s_L e^{-i\varphi_L} & c_L \end{pmatrix} \begin{pmatrix} 0 & 0 \\ 0 & 1 \end{pmatrix} \mathcal{U}_R^+ = \begin{pmatrix} 0 & -s_L e^{i\varphi_L} \\ 0 & c_L \end{pmatrix} \begin{pmatrix} c_R & s_R e^{i\varphi_R} \\ -s_R e^{-i\varphi_R} & c_R \end{pmatrix} \quad (32)$$

$$= \begin{pmatrix} s_L s_R e^{i(\varphi_L - \varphi_R)} & -s_L c_R e^{i\varphi_L} \\ -c_L s_R e^{-i\varphi_R} & c_L c_R \end{pmatrix} \quad (33)$$

Applying the aforementioned transformation yields the following couplings:

$$y_{tH} = c_L^2, \quad (34)$$

$$y_{TTH} = s_L^2, \quad (35)$$

$$y_{tH}^L = \frac{m_t}{m_T} s_L c_L e^{i\phi}, \quad y_{TtH}^R = s_L c_L e^{i\phi}. \quad (36)$$

2.3 Framework of SM + VLQs doublet

Let us start with the Yukawa Lagrangian:

$$\mathcal{L} = -y_{4j}^u \begin{pmatrix} \bar{u}_{L4}^0 & \bar{d}_{L4}^0 \end{pmatrix} u_{Rj}^0 \tilde{\Phi} - y_{4j}^d \begin{pmatrix} \bar{u}_{L4}^0 & \bar{d}_{L4}^0 \end{pmatrix} d_{Rj}^0 \Phi + h.c. \quad (37)$$

The matrix describing the masses the vector-like quarks (VLQ) can be expressed as follows:

$$\mathcal{M}^u = \begin{pmatrix} y_{33}^u \frac{v}{\sqrt{2}} & 0 \\ y_{43}^u \frac{v}{\sqrt{2}} & \mathcal{M}^0 \end{pmatrix} \equiv \begin{pmatrix} W_{33}^u & 0 \\ W_{43}^u & \mathcal{M}^0 \end{pmatrix} ; \quad \mathcal{U}_L^u \mathcal{M}^u \mathcal{U}_R^{u+} = \mathcal{M}_{diag}^u \quad (38)$$

$$\mathcal{M}^d = \begin{pmatrix} y_{33}^d \frac{v}{\sqrt{2}} & 0 \\ y_{43}^d \frac{v}{\sqrt{2}} & \mathcal{M}^0 \end{pmatrix} \equiv \begin{pmatrix} W_{33}^d & 0 \\ W_{43}^d & \mathcal{M}^0 \end{pmatrix} ; \quad \mathcal{U}_L^d \mathcal{M}^d \mathcal{U}_R^{d+} = \mathcal{M}_{diag}^d \quad (39)$$

The rotation matrices \mathcal{U}_L^q and \mathcal{U}_R^q corresponding to left-handed and right-handed rotations, respectively, can be defined as follows:

$$\mathcal{U}_{L,R}^q = \begin{pmatrix} c_{L,R}^q & -s_{L,R}^q e^{i\varphi_{L,R}^q} \\ s_{L,R}^q e^{-i\varphi_{L,R}^q} & c_{L,R}^q \end{pmatrix} \quad (40)$$

$$\begin{cases} u_{L,R} = \mathcal{U}_{L,R}^u u_{L,R}^0, & u_{L,R}^0 = \mathcal{U}_{L,R}^{u\dagger} u_{L,R} \\ d_{L,R} = \mathcal{U}_{L,R}^d d_{L,R}^0, & d_{L,R}^0 = \mathcal{U}_{L,R}^{d\dagger} d_{L,R} \end{cases} \quad (41)$$

2.3.1 Charged currents

The Yukawa Lagrangian of charged currents may be expressed as follows:

$$\mathcal{L} = \frac{-g}{\sqrt{2}} [\bar{u}_{L4}^0 \gamma^\mu d_{L4}^0 + \bar{u}_{R4}^0 \gamma^\mu d_{R4}^0 + \bar{u}_{L3}^0 \gamma^\mu d_{L3}^0] W_\mu^+ + hc. \quad (42)$$

The Left-Handed (LH) terms can be represented as follows:

$$\begin{pmatrix} \bar{u}_{L3}^0 & \bar{u}_{L4}^0 \end{pmatrix} \begin{pmatrix} 1 & 0 \\ 0 & 1 \end{pmatrix} \gamma^\mu \begin{pmatrix} d_{L3}^0 \\ d_{L4}^0 \end{pmatrix} = (\bar{t}_L \quad \bar{T}_L) \mathcal{U}_L^\mu \begin{pmatrix} 1 & 0 \\ 0 & 1 \end{pmatrix} \mathcal{U}_L^{d+} \gamma^\mu \begin{pmatrix} b_L \\ B_L \end{pmatrix} \quad (43)$$

$$\begin{pmatrix} c_L^u & -s_L^u e^{i\varphi_L^u} \\ s_L^u e^{-i\varphi_L^u} & c_L^u \end{pmatrix} \begin{pmatrix} c_L^d & c_L^d e^{i\varphi_L^d} \\ -s_L^d e^{-i\varphi_L^d} & c_L^d \end{pmatrix} = \begin{pmatrix} c_L^u c_L^d + s_L^u s_L^d e^{i(\varphi_L^u - \varphi_L^d)} & c_L^u s_L^d e^{i\varphi_L^d} - s_L^u c_L^d e^{i\varphi_L^u} \\ s_L^u c_L^d e^{-i\varphi_L^u} - c_L^u s_L^d e^{-i\varphi_L^d} & s_L^u s_L^d e^{i(\varphi_L^d - \varphi_L^u)} + c_L^u c_L^d \end{pmatrix} \quad (44)$$

Applying the aforementioned transformation yields the following couplings:

$$y_{tbW^+}^L = c_L^u c_L^d + s_L^u s_L^d e^{i(\varphi_L^u - \varphi_L^d)}, \quad (45)$$

$$y_{TbW^+}^L = s_L^u c_L^d e^{-i\varphi_L^u} - c_L^u s_L^d e^{-i\varphi_L^d}, \quad (46)$$

$$y_{tBW^+}^L = c_L^u s_L^d e^{i\varphi_L^d} - s_L^u c_L^d e^{i\varphi_L^u}, \quad (47)$$

$$y_{TBW^+}^L = c_L^u c_L^d + s_L^u s_L^d e^{-i(\varphi_L^u - \varphi_L^d)}. \quad (48)$$

The Right-Handed (RH) terms can be represented as follows:

$$\begin{pmatrix} \bar{u}_{R3}^0 & \bar{u}_{R4}^0 \end{pmatrix} \begin{pmatrix} 0 & 0 \\ 0 & 1 \end{pmatrix} \gamma^\mu \begin{pmatrix} d_{R3}^0 \\ d_{R4}^0 \end{pmatrix} = (\bar{t}_R \quad \bar{T}_R) \mathcal{U}_R^\mu \begin{pmatrix} 0 & 0 \\ 0 & 1 \end{pmatrix} \mathcal{U}_R^{d+} \gamma^\mu \begin{pmatrix} b_L \\ B_L \end{pmatrix} \quad (49)$$

$$\begin{pmatrix} c_R^u & -s_R^u e^{i\varphi_R^u} \\ s_R^u e^{-i\varphi_R^u} & c_R^u \end{pmatrix} \begin{pmatrix} 0 & 0 \\ 0 & 1 \end{pmatrix} \mathcal{U}_R^{d+} = \begin{pmatrix} 0 & -s_R^u e^{i\varphi_R^u} \\ 0 & c_R^u \end{pmatrix} \begin{pmatrix} c_R^d & s_R^d e^{i\varphi_R^d} \\ -s_R^d e^{-i\varphi_R^d} & c_R^d \end{pmatrix} \\ = \begin{pmatrix} s_R^u s_R^d e^{i(\varphi_R^u - \varphi_R^d)} & -s_R^u c_R^d e^{i\varphi_R^u} \\ -c_R^u s_R^d e^{-i\varphi_R^d} & c_R^u c_R^d \end{pmatrix} \quad (50)$$

Upon performing the calculations, the aforementioned transformation yields the expression for the following couplings:

$$y_{tbW^+}^R = s_R^u s_R^d e^{i(\varphi_R^u - \varphi_R^d)}, \quad (51)$$

$$y_{TbW^+}^R = -c_R^u s_R^d e^{-i\varphi_R^d}, \quad (52)$$

$$y_{tBW^+}^R = -s_R^u c_R^d e^{i\varphi_R^u}, \quad (53)$$

$$y_{TBW^+}^R = c_R^u c_R^d. \quad (54)$$

2.3.2 Neutral currents

The Yukawa Lagrangian of neutral currents may be expressed as follows:

$$\mathcal{L} = \frac{-g}{2c_W} [\bar{u}_{Li}^0 \gamma^\mu u_{Li}^0 - \bar{d}_{Li}^0 \gamma^\mu d_{Li}^0 + \bar{u}_{R4}^0 \gamma^\mu u_{R4}^0 - \bar{d}_{R4}^0 \gamma^\mu d_{R4}^0] z_\mu + J_{EM}^\mu, \quad \text{with } i = 3, 4 \quad (55)$$

The Left-Handed (LH) terms can be represented as follows:

$$\begin{aligned} (\bar{u}_{L3}^0 \quad \bar{u}_{L4}^0) \begin{pmatrix} 1 & 0 \\ 0 & 1 \end{pmatrix} \gamma^\mu \begin{pmatrix} u_{L3}^0 \\ u_{L4}^0 \end{pmatrix} &= (\bar{t}_L \quad \bar{T}_L) \mathcal{U}_L^u \begin{pmatrix} 1 & 0 \\ 0 & 1 \end{pmatrix} \mathcal{U}_L^{u\mu} \begin{pmatrix} t_L \\ T_L \end{pmatrix} \\ &= (\bar{t}_L \quad \bar{T}_L) \gamma^\mu \begin{pmatrix} t_L \\ T_L \end{pmatrix} etc \end{aligned} \quad (56)$$

Applying the aforementioned transformation yields the following couplings:

$$y_{ttZ}^L = y_{bbZ}^R = 1, \quad (57)$$

$$y_{TTZ}^L = y_{TTZ}^R = 1 \quad (58)$$

$$y_{tTZ}^L = y_{bBZ}^L = 0. \quad (59)$$

The Right-Handed (RH) terms can be represented as follows:

$$\begin{aligned} \mathcal{U}_R^u \begin{pmatrix} 0 & 0 \\ 0 & 1 \end{pmatrix} \mathcal{U}_R^{u\dagger} &= \begin{pmatrix} c_R^u & -s_R^u e^{i\varphi^u} \\ s_R^u e^{-i\varphi^u} & c_R^u \end{pmatrix} \begin{pmatrix} 0 & 0 \\ 0 & 1 \end{pmatrix} \mathcal{U}_R^{u\dagger} \\ &= \begin{pmatrix} 0 & -s_R^u e^{i\varphi^u} \\ 0 & c_R^u \end{pmatrix} \begin{pmatrix} c_R^u & s_R^u e^{i\varphi^u} \\ -s_R^u e^{-i\varphi^u} & c_R^u \end{pmatrix} \\ &= \begin{pmatrix} s_R^{u^2} & -s_R^u c_R^u e^{i\varphi^u} \\ -s_R^u c_R^u e^{-i\varphi^u} & c_R^{u^2} \end{pmatrix} \equiv X^u \end{aligned} \quad (60)$$

After performing the requisite calculations, the aforementioned transformation leads to the expression of the following couplings:

$$y_{ttZ}^R = s_R^{u^2} \quad (61)$$

$$y_{TTZ}^R = c_R^{u^2} \quad (62)$$

$$y_{tTZ}^R = -s_R^u c_R^u e^{i\varphi_R^u} \quad (63)$$

$$y_{bbZ}^R = s_R^{d^2}, \quad (64)$$

$$y_{BBZ}^R = c_R^{d^2}, \quad (65)$$

$$y_{bBZ}^R = -s_R^d c_R^d e^{i\varphi_R^d}. \quad (66)$$

2.3.3 Modified Higgs couplings

$$\mathcal{L} = -(\bar{u}_{L3}^0 \quad \bar{u}_{L4}^0) \begin{pmatrix} y_{33}^u & 0 \\ y_{34}^u & 0 \end{pmatrix} \frac{H}{\sqrt{2}} + (u \rightarrow d) + hc \quad (67)$$

$$\begin{pmatrix} \frac{y_{33}^u}{\sqrt{2}} & 0 \\ \frac{y_{43}^u}{\sqrt{2}} & 0 \end{pmatrix} = \frac{1}{v} \begin{pmatrix} \frac{y_{33}^u}{\sqrt{2}} & 0 \\ \frac{y_{43}^u}{\sqrt{2}} & M^0 \end{pmatrix} \begin{pmatrix} 1 & 0 \\ 0 & 0 \end{pmatrix} = \frac{1}{v} \mathcal{M}^u \begin{pmatrix} 1 & 0 \\ 0 & 0 \end{pmatrix} \quad (68)$$

$$\begin{aligned}
 \mathcal{U}_L^u \frac{1}{v} \mathcal{M}^u \begin{pmatrix} 1 & 0 \\ 0 & 0 \end{pmatrix} \mathcal{U}_R^{u+} &= \frac{1}{v} \mathcal{U}_L^u \mathcal{M}^u \mathcal{U}_R^{u+} \mathcal{U}_R^u \begin{pmatrix} 1 & 0 \\ 0 & 0 \end{pmatrix} \mathcal{U}_R^{u+} \\
 &= \frac{1}{v} \mathcal{M}_{diag}^u \mathcal{U}_R^u \left[1 - \begin{pmatrix} 0 & 0 \\ 0 & 1 \end{pmatrix} \right] \mathcal{U}_R^{u+} \\
 &= \frac{1}{v} \mathcal{M}_{diag}^u (1 - X^u)
 \end{aligned} \tag{69}$$

Upon completing the necessary calculations, the resulting transformation yields the following couplings:

$$y_{tH}^R = c_R^{u^2} \tag{70}$$

$$y_{TTH}^R = s_R^{u^2} \tag{71}$$

$$y_{tTH}^L = s_R^u c_R^u e^{i\phi_u}, \quad y_{tTH}^R = \frac{m_t}{m_T} (s_R^u c_R^u e^{i\phi_u}) \tag{72}$$

$$y_{bbH}^R = c_R^{d^2}, \tag{73}$$

$$y_{BBH}^R = s_R^{d^2}, \tag{74}$$

$$y_{bBH}^R = s_R^d c_R^d u e^{i\phi_d}, \quad y_{bBH}^R = \frac{m_t}{m_T} (s_R^d c_R^d e^{i\phi_d}). \tag{75}$$

In **Figure 4**, we depict the branching ratios (\mathcal{BR} s) of three decay channels, namely $T \rightarrow W^+b$, tZ , and th , as a function of the top quark partner mass m_T , at a fixed s_L for SM + T representation (left) and at a fixed s_R^u and s_R^d for SM + TB representation (right). It can be observed from both panels that the $T \rightarrow W^+b$ decay mode exhibits dominance over other modes throughout the entire mass spectrum of T , ranging from 300 to 3000 GeV.

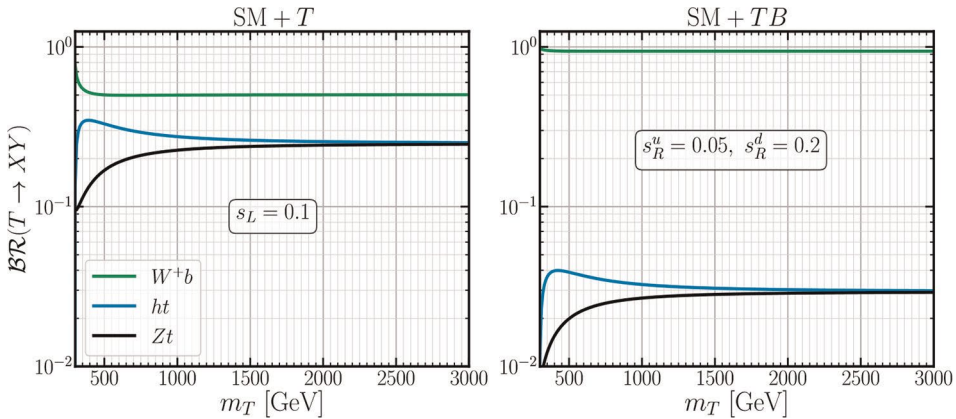


Figure 4. $BR(T \rightarrow XY)$ as a function of m_T for SM + T (left) and SM + TB (right).

3. 2HDM + VLQs singlet: concepts and formulations

The most general renormalizable potential, of 2HDM + VLQ [21, 22], which is invariant under $SU(2) \otimes U(1)$ can be written as

$$\begin{aligned} V(\phi_1, \phi_2) = & m_1^2 \phi_1^\dagger \phi_1 + m_2^2 \phi_2^\dagger \phi_2 + (m_{12}^2 \phi_1^\dagger \phi_2 + h.c.) + \lambda_1 (\phi_1^\dagger \phi_1)^2 + \lambda_2 (\phi_2^\dagger \phi_2)^2 \\ & + \lambda_3 (\phi_1^\dagger \phi_1) (\phi_2^\dagger \phi_2) + \lambda_4 (\phi_1^\dagger \phi_2) (\phi_2^\dagger \phi_1) + [\lambda_5 (\phi_1^\dagger \phi_2)^2 + h.c.] \\ & + \phi_1^\dagger \phi_1 [\lambda_6 (\phi_1^\dagger \phi_2) + h.c.] + \phi_2^\dagger \phi_2 [\lambda_7 (\phi_1^\dagger \phi_2) + h.c.] \end{aligned} \quad (76)$$

where $\phi_i, i = 1, 2$ are complex $SU(2)$ doublets

$$\phi_1 = \begin{pmatrix} G^+ \\ \frac{v + \phi_1^0 + iG^0}{\sqrt{2}} \end{pmatrix}, \quad \phi_2 = \begin{pmatrix} H^+ \\ \frac{\phi_2^0 + iA}{\sqrt{2}} \end{pmatrix} \quad (77)$$

The physical CP-even scalars h and H are mixtures of $\phi_{1,2}^0$:

$$\begin{pmatrix} h \\ H \end{pmatrix} = \begin{pmatrix} s_{\beta\alpha} & s_{\beta\alpha} \\ c_{\beta\alpha} & -s_{\beta\alpha} \end{pmatrix} \begin{pmatrix} \phi_1^0 \\ \phi_2^0 \end{pmatrix} \quad (78)$$

where: $s_{\beta\alpha} = \sin(\beta - \alpha)$, $c_{\beta\alpha} = \cos(\beta - \alpha)$.
we write:

$$\tilde{\phi}_1 = \begin{pmatrix} \frac{v + \phi_1^0 - iG^0}{\sqrt{2}} \\ -G^- \end{pmatrix}, \quad \tilde{\phi}_2 = \begin{pmatrix} \frac{\phi_2^0 - iA}{\sqrt{2}} \\ -H^- \end{pmatrix} \quad (79)$$

where $\tilde{\phi}_i = i\tau_2 \phi_i^*$ ($i = 1, 2$), .

we add the Lagrangian of Yukawa interaction for the heavy Quark $T_{L,R}^0$ and $B_{L,R}^0$:

$$\begin{aligned} -\mathcal{L}_Y^H \supset & y_t \overline{Q}_L^0 \tilde{\phi}_2 T_R^0 + \lambda_t \overline{Q}_L^0 \tilde{\phi}_1 T_R^0 + M_T \overline{T}_L^0 T_R^0 + y_b \overline{Q}_L^0 (\sigma_1 \tilde{\phi}_2) B_R^0 \\ & + \lambda_b \overline{Q}_L^0 (\sigma_1 \tilde{\phi}_1) B_R^0 + M_B \overline{B}_L^0 B_R^0 + Hc \end{aligned} \quad (80)$$

where $\overline{Q}_L^0 = (\overline{t}_L^0, \overline{b}_L^0)$, and $\sigma_1 = \begin{pmatrix} 0 & 1 \\ 1 & 0 \end{pmatrix}$.

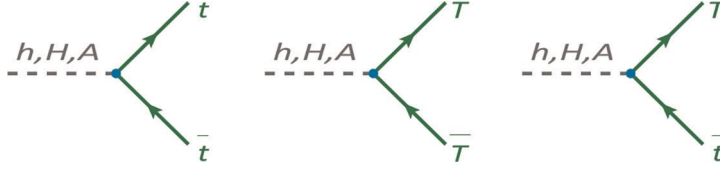
3.1 Neutral Higgs couplings

- For the Light-Light couplings of Top quarks to the triplets Higgs h, H , and A (Figure 5)

$$y_{htt} = (s_{\beta\alpha} + c_{\beta\alpha} \cot \beta) c_L^2 \quad (81)$$

$$y_{Htt} = (c_{\beta\alpha} - s_{\beta\alpha} \cot \beta) c_L^2 \quad (82)$$

$$y_{Att} = -\cot \beta c_L^2 \quad (83)$$


Figure 5.

Typical Feynman diagram of the Higgs bosons h , H and A couplings to pairs of top (t) and top partner (T).

- For the heavy-heavy couplings of Top quarks to the triplets Higgs h , H , and A

$$y_{hTT} = (s_{\beta\alpha} + c_{\beta\alpha} \cot \beta) s_L^2 \quad (84)$$

$$y_{HTT} = (c_{\beta\alpha} - s_{\beta\alpha} \cot \beta) s_L^2 \quad (85)$$

$$y_{ATT} = -\cot \beta s_L^2 \quad (86)$$

- For the Light-heavy left and right couplings of Top quarks to the triplets Higgs h , H , and A

$$\begin{aligned} y_{htT}^L &= (s_{\beta\alpha} + c_{\beta\alpha} \cot \beta) \frac{m_t}{m_T} c_L s_L e^{i\phi} y_{htT}^R = (s_{\beta\alpha} + c_{\beta\alpha} \cot \beta) c_L s_L e^{i\phi} \\ y_{HtT}^L &= (c_{\beta\alpha} - s_{\beta\alpha} \cot \beta) \frac{m_t}{m_T} c_L s_L e^{i\phi} y_{HtT}^R = (c_{\beta\alpha} - s_{\beta\alpha} \cot \beta) c_L s_L e^{i\phi} \\ y_{AtT}^L &= -\cot \beta \frac{m_t}{m_T} c_L s_L e^{i\phi} y_{AtT}^R = -\cot \beta c_L s_L e^{i\phi} \end{aligned} \quad (87)$$

3.2 Charged Higgs couplings

The couplings of the charged Higgs boson H^\pm to the top quark (t) and its heavy partner (T) with the bottom quark (b) can be expressed as follows (**Figure 6**):

$$y_{tbH^+}^L = c_L, \quad y_{tbH^+}^R = 1 \quad (88)$$

$$y_{TbH^+}^L = s_L, \quad y_{TbH^+}^R = 0 \quad (89)$$

4. 2HDM + VLQs doublet case

4.1 Neutral Higgs couplings

Following the methodology outlined in the preceding section, the Higgs coupling can be determined within the framework of the 2HDM + TB [23, 24] as follows:


Figure 6.

Typical Feynman diagram of the charged Higgs boson H^+ couplings to the top quark (t) and its heavy partner (T) with the bottom quark (b).

- For the Light-Light couplings of Top quarks to the triplets Higgs h , H , and A

$$y_{htt} = (s_{\beta\alpha} + c_{\beta\alpha} \cot \beta) c_R^{u^2} \quad (90)$$

$$y_{Htt} = (c_{\beta\alpha} - s_{\beta\alpha} \cot \beta) c_R^{u^2} \quad (91)$$

$$y_{Att} = -\cot \beta c_R^{u^2} \quad (92)$$

- For the heavy-heavy couplings of Top quarks to the triplets Higgs h , H , and A

$$y_{hTT} = (s_{\beta\alpha} + c_{\beta\alpha} \cot \beta) s_R^{u^2} \quad (93)$$

$$y_{HTT} = (c_{\beta\alpha} - s_{\beta\alpha} \cot \beta) s_R^{u^2} \quad (94)$$

$$y_{ATT} = -\cot \beta s_R^{u^2} \quad (95)$$

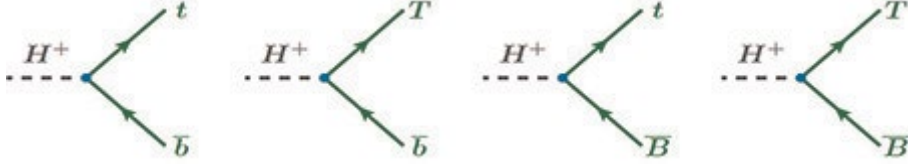
- For the Light-heavy left and right couplings of Top quarks to the triplets Higgs h , H , and A

$$\begin{aligned} y_{htT}^L &= (s_{\beta\alpha} + c_{\beta\alpha} \cot \beta) s_R^u c_R^u e^{i\phi_u} y_{htT}^R = (s_{\beta\alpha} + c_{\beta\alpha} \cot \beta) \frac{m_t}{m_T} s_R^u c_R^u e^{i\phi_u} \\ y_{HtT}^L &= (c_{\beta\alpha} - s_{\beta\alpha} \cot \beta) s_R^u c_R^u e^{i\phi_u} y_{HtT}^R = (c_{\beta\alpha} - s_{\beta\alpha} \cot \beta) \frac{m_t}{m_T} s_R^u c_R^u e^{i\phi_u} \\ y_{AtT}^L &= -\cot \beta s_R^u c_R^u e^{i\phi_u} y_{AtT}^R = -\cot \beta \frac{m_t}{m_T} s_R^u c_R^u e^{i\phi_u} \end{aligned} \quad (96)$$

4.2 Charged Higgs couplings

Let us start with the Yukawa Lagrangian (**Figure 7**):

$$\begin{aligned} \mathcal{L} &= -y_{ij}^u \bar{q}_{Li} u_{Rj} \epsilon H_u^* + y_{ij}^{d*} \bar{q}_{Li} d_{Rj} \epsilon H_d^* - y_{4j}^{u*} \bar{Q}_L u_{Rj} \epsilon H_u^* + y_{4j}^{d*} \bar{Q}_L d_{Rj} \epsilon H_d^* + h.c. \\ &= -y_{ij}^{u*} \begin{pmatrix} \bar{u}_{Li}^0 & \bar{d}_{Li}^0 \end{pmatrix} \begin{pmatrix} H_u^{0*} \\ -H_u^+ \end{pmatrix} u_{Rj}^0 + y_{ij}^{d*} \begin{pmatrix} \bar{u}_{Li}^0 & \bar{d}_{Li}^0 \end{pmatrix} \begin{pmatrix} H_d^- \\ -H_d^{0*} \end{pmatrix} u_{Rj}^0 \\ &\quad - y_{4j}^{u*} \begin{pmatrix} \bar{u}_{L4}^0 & \bar{d}_{L4}^0 \end{pmatrix} \begin{pmatrix} H_u^{0*} \\ -H_u^+ \end{pmatrix} u_{Rj}^0 + y_{4j}^{d*} \begin{pmatrix} \bar{u}_{L4}^0 & \bar{d}_{L4}^0 \end{pmatrix} \begin{pmatrix} H_d^- \\ -H_d^{0*} \end{pmatrix} u_{Rj}^0 \\ &= -y_{ij}^{u*} \begin{pmatrix} \bar{u}_{Li}^0 & \bar{d}_{Li}^0 \end{pmatrix} \begin{pmatrix} \frac{1}{\sqrt{2}} [\cos \alpha h^0 + \sin \alpha H_1^0 - i (\sin \beta G^0 + \cos \beta P_1^0)] \\ -(\sin \beta G^+ + \cos \beta H^+) \\ -(\cos \beta G^- + \sin \beta H^-) \end{pmatrix} u_{Rj}^0 \\ &\quad + y_{ij}^{d*} \begin{pmatrix} \bar{u}_{Li}^0 & \bar{d}_{Li}^0 \end{pmatrix} \begin{pmatrix} -\frac{1}{\sqrt{2}} [-\sin \alpha h^0 + \cos \alpha H_1^0 + i (\cos \beta G^0 - \sin \beta P_1^0)] \\ -(\sin \beta G^+ + \cos \beta H^+) \\ -(\cos \beta G^- + \sin \beta H^-) \end{pmatrix} u_{Rj}^0 \\ &\quad - y_{4j}^{u*} \begin{pmatrix} \bar{u}_{L4}^0 & \bar{d}_{L4}^0 \end{pmatrix} \begin{pmatrix} \frac{1}{\sqrt{2}} [\cos \alpha h^0 + \sin \alpha H_1^0 - i (\sin \beta G^0 + \cos \beta P_1^0)] \\ -(\sin \beta G^+ + \cos \beta H^+) \\ -(\cos \beta G^- + \sin \beta H^-) \end{pmatrix} u_{Rj}^0 \\ &\quad + y_{4j}^{d*} \begin{pmatrix} \bar{u}_{L4}^0 & \bar{d}_{L4}^0 \end{pmatrix} \begin{pmatrix} -\frac{1}{\sqrt{2}} [-\sin \alpha h^0 + \cos \alpha H_1^0 + i (\cos \beta G^0 - \sin \beta P_1^0)] \\ -(\sin \beta G^+ + \cos \beta H^+) \\ -(\cos \beta G^- + \sin \beta H^-) \end{pmatrix} u_{Rj}^0 \end{aligned} \quad (97)$$


Figure 7.

Typical Feynman diagram of the charged Higgs boson H^\pm couplings to the top quark (t) and its heavy partner (T) with the bottom quark (b) and its heavy partner (B).

If we select only the H^\pm particle, the result is:

$$\begin{aligned}
 \mathcal{L} \supset & y_{ij}^{u*} \begin{pmatrix} \bar{u}_{Li}^0 & \bar{d}_{Li}^0 \end{pmatrix} \begin{pmatrix} 0 \\ \cos\beta H^+ \end{pmatrix} u_{Rj}^0 \\
 & + y_{ij}^{d*} \begin{pmatrix} \bar{u}_{Li}^0 & \bar{d}_{Li}^0 \end{pmatrix} \begin{pmatrix} \sin\beta H^- \\ 0 \end{pmatrix} u_{Rj}^0 \\
 & + y_{4j}^{u*} \begin{pmatrix} \bar{u}_{L4}^0 & \bar{d}_{L4}^0 \end{pmatrix} \begin{pmatrix} 0 \\ \cos\beta H^+ \end{pmatrix} u_{Rj}^0 \\
 & + y_{4j}^{d*} \begin{pmatrix} \bar{u}_{L4}^0 & \bar{d}_{L4}^0 \end{pmatrix} \begin{pmatrix} \sin\beta H^- \\ 0 \end{pmatrix} u_{Rj}^0 \\
 & \supset y_{ij}^{u*} \cos\beta H^\pm \bar{d}_{Li}^0 u_{Rj}^0 + y_{ij}^{d*} \sin\beta H^\pm \bar{u}_{Li}^0 d_{Rj}^0 \\
 & + y_{4j}^{u*} \cos\beta H^\pm \bar{d}_{L4}^0 u_{Rj}^0 + y_{4j}^{d*} \sin\beta H^\pm \bar{u}_{L4}^0 d_{Rj}^0 \\
 & \supset y_{ij}^{u*} \cos\beta H^\pm \bar{d}_{Li}^0 u_{Rj}^0 + y_{4j}^{u*} \cos\beta H^\pm \bar{d}_{L4}^0 u_{Rj}^0 \\
 & + y_{ij}^{d*} \sin\beta H^\pm \bar{u}_{Li}^0 d_{Rj}^0 + y_{4j}^{d*} \sin\beta H^\pm \bar{u}_{L4}^0 d_{Rj}^0
 \end{aligned} \tag{98}$$

Subsequently, we can express the Yukawa Lagrangian of the charged Higgs boson as follows:

$$\mathcal{L} = \begin{pmatrix} \bar{u}_{L3}^0 & \bar{u}_{L4}^0 \end{pmatrix} \begin{pmatrix} y_{33}^d & 0 \\ y_{43}^d & 0 \end{pmatrix} \begin{pmatrix} d_{R3}^0 \\ d_{R4}^0 \end{pmatrix} \sin\beta H^\pm + \begin{pmatrix} \bar{d}_{L3}^0 & \bar{d}_{L4}^0 \end{pmatrix} \begin{pmatrix} y_{33}^u & 0 \\ y_{43}^u & 0 \end{pmatrix} \begin{pmatrix} u_{R3}^0 \\ u_{R4}^0 \end{pmatrix} \cos\beta H^\pm \tag{99}$$

$$\begin{pmatrix} y_{33}^d & 0 \\ y_{43}^d & 0 \end{pmatrix} = \frac{\sqrt{2}}{v} \left[\begin{pmatrix} \frac{y_{33}^d v}{\sqrt{2}} & 0 \\ \frac{y_{43}^d v}{\sqrt{2}} & \frac{y_{44}^d v}{\sqrt{2}} \end{pmatrix} - \begin{pmatrix} 0 & 0 \\ 0 & M^0 \end{pmatrix} \right] = \frac{\sqrt{2}}{v} \mathcal{M}^d - \frac{M^0 \sqrt{2}}{v} \begin{pmatrix} 0 & 0 \\ 0 & 1 \end{pmatrix} \tag{100}$$

$$\begin{aligned}
 \mathcal{U}_L^u \left[\frac{\sqrt{2}}{v} \mathcal{M}^d - \frac{M^0 \sqrt{2}}{v} \begin{pmatrix} 0 & 0 \\ 0 & 1 \end{pmatrix} \right] \mathcal{U}_R^{d\dagger} &= \frac{\sqrt{2}}{v} \mathcal{U}_L^u \left[\mathcal{U}_L^{d\dagger} \mathcal{U}_L^d \mathcal{M}^d \mathcal{U}_R^{d\dagger} \mathcal{U}_R^d - M^0 \begin{pmatrix} 0 & 0 \\ 0 & 1 \end{pmatrix} \right] \mathcal{U}_R^{d\dagger} \\
 &= \frac{\sqrt{2}}{v} \mathcal{U}_L^u \mathcal{M}_{diag}^d \underbrace{\mathcal{U}_R^d \mathcal{U}_R^{d\dagger}}_{=1} - M^0 \frac{\sqrt{2}}{v} \mathcal{U}_L^u \begin{pmatrix} 0 & 0 \\ 0 & 1 \end{pmatrix} \mathcal{U}_R^{d\dagger} \\
 &= \frac{\sqrt{2}}{v} \left(A \times \mathcal{M}_{diag}^d - m_B B \right)
 \end{aligned} \tag{101}$$

with

$$\begin{aligned} A &= \mathcal{U}_L^u \mathcal{U}_L^{d\dagger} \\ &= \begin{pmatrix} c_L^u & -s_L^u e^{i\phi_u} \\ s_L^u e^{-i\phi_u} & c_L^u \end{pmatrix} \begin{pmatrix} c_L^d & s_L^d e^{i\phi_d} \\ -s_L^d e^{-i\phi_d} & c_L^d \end{pmatrix} \\ &= \begin{pmatrix} c_L^u c_L^d + s_L^u s_L^d e^{i(\phi_u - \phi_d)} & c_L^u s_L^d e^{i\phi_d} - c_L^d s_L^u e^{i\phi_u} \\ c_L^d s_L^u e^{-i\phi_u} - c_L^u s_L^d e^{-i\phi_d} & s_L^u s_L^d e^{i(\phi_d - \phi_u)} + c_L^u c_L^d \end{pmatrix} \end{aligned} \quad (102)$$

$$\begin{aligned} B &= \mathcal{U}_L^u \begin{pmatrix} 0 & 0 \\ 0 & 1 \end{pmatrix} \mathcal{U}_R^{d\dagger} \\ &= \begin{pmatrix} c_L^u & -s_L^u e^{i\phi_u} \\ -s_R^d e^{-i\phi_u} & c_L^u \end{pmatrix} \begin{pmatrix} 0 & 0 \\ 0 & 1 \end{pmatrix} \mathcal{U}_R^{d\dagger} \\ &= \begin{pmatrix} 0 & -s_L^u e^{i\phi_u} \\ 0 & c_L^u \end{pmatrix} \begin{pmatrix} c_R^d & s_R^d e^{i\phi_d} \\ -s_R^d e^{i\phi_d} & c_R^d \end{pmatrix} \\ &= \begin{pmatrix} s_L^u s_R^d e^{i(\phi_u - \phi_d)} & -c_R^d s_L^u e^{i\phi_u} \\ -c_L^u s_R^d e^{-i\phi_d} & c_L^u c_R^d \end{pmatrix} \end{aligned} \quad (103)$$

Now we can define the Matrix M^u as follows:

$$\begin{aligned} M^u &= A \times \mathcal{M}_{diag}^d - m_B B \\ &= \begin{pmatrix} [c_L^u c_L^d + s_L^u s_L^d e^{i(\phi_u - \phi_d)}] & m_b - m_B s_L^u s_R^d e^{i(\phi_u - \phi_d)} & [c_L^u s_L^d e^{i\phi_d} - c_L^d s_L^u e^{i\phi_u}] & m_B + m_B c_R^d s_L^u e^{i\phi_u} \\ [c_L^d s_L^u e^{-i\phi_u} - c_L^u s_L^d e^{-i\phi_d}] & m_b + m_B c_L^u s_R^d e^{-i\phi_d} & [s_L^u s_L^d e^{i(\phi_d - \phi_u)} + c_L^u c_L^d] & m_B - m_B c_L^u c_R^d \end{pmatrix} \end{aligned} \quad (104)$$

Similarly, the matrix M^d can be defined in the same manner as M^u .

$$M^d = \begin{pmatrix} [c_L^d c_L^u + s_L^d s_L^u e^{i(\phi_d - \phi_u)}] & m_t - m_T s_L^d s_R^u e^{i(\phi_d - \phi_u)} & [c_L^d s_L^u e^{i\phi_u} - c_L^u s_L^d e^{i\phi_d}] & m_T + m_T c_R^u s_L^d e^{i\phi_d} \\ [c_L^u s_L^d e^{-i\phi_d} - c_L^d s_L^u e^{-i\phi_u}] & m_t + m_T c_L^d s_R^u e^{-i\phi_u} & [s_L^d s_L^u e^{i(\phi_u - \phi_d)} + c_L^d c_L^u] & m_T - m_T c_L^d c_R^u \end{pmatrix} \quad (105)$$

Finally, the charged Higgs couplings can be defined as follows:

- For the coupling $H^\pm tb$:

$$\mathcal{Y}_{H^+tb}^L = c_L^d c_L^u + \frac{s_L^d}{s_L^u} \left(s_L^u{}^2 - s_R^u{}^2 \right) e^{i(\phi_u - \phi_d)} \quad (106)$$

$$\mathcal{Y}_{H^+tb}^R = \frac{m_b}{m_t} \left[c_L^u c_L^d + \frac{s_L^u}{s_L^d} \left(s_L^d{}^2 - s_R^d{}^2 \right) e^{i(\phi_u - \phi_d)} \right] \quad (107)$$

- For the coupling $H^\pm Tb$:

$$y_{H^+Tb}^L = c_L^d c_L^u + \frac{s_L^d}{s_L^u} \left(s_L^{u^2} - s_R^{u^2} \right) e^{-i\phi_d^*} \quad (108)$$

$$y_{H^+Tb}^R = \frac{m_b}{m_T} \left[c_L^u c_L^d + \frac{s_L^u}{s_L^d} \left(s_L^{d^2} - s_R^{d^2} \right) e^{-i\phi_d} \right] \quad (109)$$

- For the coupling H^+tB

$$y_{H^+tB}^L = \frac{m_t}{m_B} \left[c_L^u c_L^d e^{i\phi_d} + \frac{c_L^d}{s_L^u} \left(s_L^{d^2} - s_R^{d^2} \right) e^{i\phi_u} \right] \quad (110)$$

$$y_{H^+tB}^R = c_L^d c_L^u + \frac{s_L^d}{s_L^u} \left(s_L^{u^2} - s_R^{u^2} \right) e^{\phi_u} \quad (111)$$

- For the coupling $H^\pm tB$:

$$y_{H^+tb}^L = s_L^d s_L^u e^{i(\phi_d - \phi_u)} + \frac{c_L^d}{c_L^u} \left(s_R^{u^2} - s_L^{u^2} \right) \quad (112)$$

$$y_{H^+tb}^R = \frac{m_B}{m_T} \left[s_L^u s_L^d e^{i(\phi_d - \phi_u)} + \frac{c_L^u}{c_L^d} \left(s_R^{d^2} - s_L^{d^2} \right) e^{i(\phi_u - \phi_d)} \right] \quad (113)$$

Figure 8 presents the branching ratios ($\mathcal{BR}s$) for all open decay channels, including $T \rightarrow W^+b$, tZ , th , H^+b , Ht , and At , as a function of the mass of the top quark partner m_T . The left panel illustrates the singlet representation 2HDM + T , with fixed values for m_h , m_H , m_A , $\tan \beta$, and s_L , while the right panel depicts the 2HDM + TB representation with the same fixed 2HDM parameters in addition to s_R^u and s_R^d .

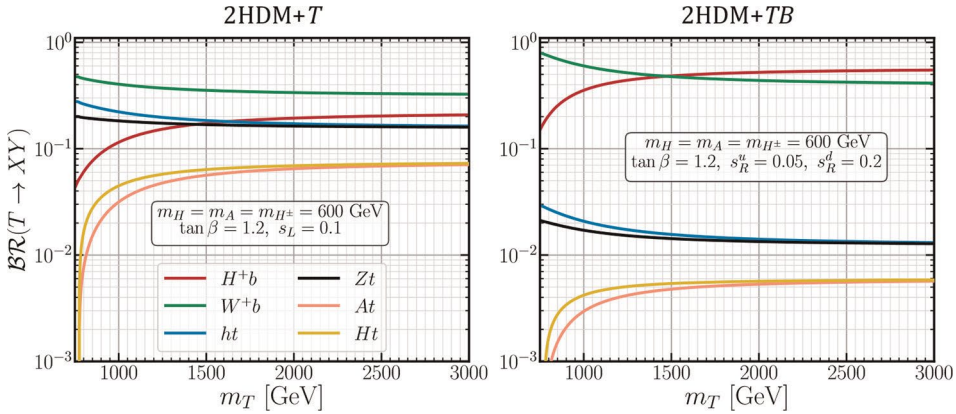


Figure 8. $BR(T \rightarrow XY)$ as a function of m_T for 2HDM + T (left) and 2HDM + TB (right).

5. Summary of gauge interactions

5.1 Light–light interactions

$$\begin{aligned}
 \mathcal{L}_W &= -\frac{g}{\sqrt{2}}\bar{t}\gamma^\mu (y_{tb}^L P_L + y_{tb}^R P_R)bW_\mu^+ + H.c., \\
 \mathcal{L}_Z &= -\frac{g}{2c_W}\bar{t}\gamma^\mu (y_{tt}^L P_L + y_{tt}^R P_R - 2Q_t s_W^2)tZ_\mu \\
 &\quad -\frac{g}{2c_W}\bar{b}\gamma^\mu (-y_{Zbb}^L P_L - y_{bb}^R P_R - 2Q_b s_W^2)bZ_\mu + H.c., \\
 \mathcal{L}_h &= -\frac{gm_t}{2M_W}y_{tt}^h\bar{t}th^0 - \frac{gm_b}{2M_W}y_{bb}^h\bar{b}bh^0 + H.c., \\
 \mathcal{L}_H &= -\frac{gm_t}{2M_W}y_{tt}^H\bar{t}tH^0 - \frac{gm_b}{2M_W}y_{bb}^H\bar{b}bH^0 + H.c., \\
 \mathcal{L}_A &= -i\frac{gm_t}{2M_W}y_{tt}^{A\tau}\gamma_5 tA + i\frac{gm_b}{2M_W}y_{bb}^A\bar{b}\gamma_5 bA + H.c., \\
 \mathcal{L}_{H^+} &= -\frac{gm_t}{\sqrt{2}M_W}\bar{t}(\cot\beta y_{tb}^L P_L + \tan\beta y_{tb}^R P_R)bH^+ + H.c.
 \end{aligned} \tag{114}$$

5.2 Heavy-heavy interactions

$$\begin{aligned}
 \mathcal{L}_W &= -\frac{g}{\sqrt{2}}\bar{Q}\gamma^\mu (y_{QQ}^L P_L + y_{QQ}^R P_R)Q'W_\mu^+ + H.c., \\
 \mathcal{L}_Z &= -\frac{g}{2c_W}\bar{Q}\gamma^\mu (\pm y_{QQ}^L P_L \pm y_{QQ}^R P_R - 2Q_Q s_W^2)QZ_\mu \\
 \mathcal{L}_h &= -\frac{gm_Q}{2M_W}y_{QQ}^h\bar{Q}Qh^0 + H.c., \\
 \mathcal{L}_H &= -\frac{gm_Q}{2M_W}y_{QQ}^H\bar{Q}QH^0 + H.c., \\
 \mathcal{L}_A &= \pm i\frac{gm_Q}{2M_W}y_{QQ}^A\bar{Q}\gamma_5 QA + H.c., \\
 \mathcal{L}_{H^+} &= -\frac{gm_Q}{\sqrt{2}M_W}\bar{Q}(\cot\beta y_{QQ}^L P_L + \tan\beta y_{QQ}^R P_R)QH^+ + H.c.
 \end{aligned} \tag{115}$$

5.3 Light-heavy interactions

$$\begin{aligned}
 \mathcal{L}_W &= -\frac{g}{\sqrt{2}}\bar{Q}\gamma^\mu (y_{Qq}^L P_L + y_{Qq}^R P_R)qW_\mu^+ \\
 &\quad -\frac{g}{\sqrt{2}}\bar{q}\gamma^\mu (y_{qQ}^L P_L + y_{qQ}^R P_R)QW_\mu^+ + H.c. \\
 \mathcal{L}_Z &= -\frac{g}{2c_W}\bar{q}\gamma^\mu (\pm y_{qQ}^L P_L \pm y_{qQ}^R P_R)QZ_\mu + H.c. \\
 \mathcal{L}_h &= -\frac{gm_T}{2M_W}\bar{t}(Y_{ht}^L P_L + y_{ht}^R P_R)Th^0 \\
 &\quad -\frac{gm_B}{2M_W}\bar{b}(y_{hb}^L P_L + y_{hb}^R P_R)Bh^0 + H.C. \\
 \mathcal{L}_H &= -\frac{gm_T}{2M_W}\bar{t}(Y_{Ht}^L P_L + y_{Ht}^R P_R)TH^0 \\
 &\quad -\frac{gm_B}{2M_W}\bar{b}(y_{Hb}^L P_L + y_{Hb}^R P_R)BH^0 + H.C. \\
 \mathcal{L}_A &= i\frac{gm_T}{2M_W}\bar{t}(Y_{At}^L P_L - Y_{At}^R P_R)TA \\
 &\quad -i\frac{gm_B}{2M_W}\bar{b}(y_{Ab}^L P_L - y_{Ab}^R P_R)BA + H.C. \\
 \mathcal{L}_{H^+} &= -\frac{gm_T}{\sqrt{2}M_W}\bar{T}(\cot\beta y_{Tb}^L P_L + \tan\beta y_{Tb}^R P_R)bH^+ \\
 &\quad -\frac{gm_B}{\sqrt{2}M_W}\bar{t}(\cot\beta y_{tb}^L P_L + \tan\beta y_{tb}^R P_R)BH^+ + H.c.,
 \end{aligned} \tag{116}$$

6. Vector-like quarks pair production at the LHC

The production process of vector-like quark pairs (VLQs) is an essential mechanism for investigating the properties of these hypothetical particles and for understanding the behavior of high energy interactions. A key benefit of VLQ pair production is its model independence, since it depends only on the masses of the VLQs and the energy of the colliding particles. At hadron colliders [25, 26], the extra-heavy quarks are able to get paired production because of their unique gauge couplings with the gluons.

In **Figure 9**, a typical Feynman diagram of pair-produced vector-like quarks $Q(\equiv T, B, X, Y)$ is shown.

The expression for the total inclusive $t\bar{t}$ production cross-section can be written as follows, as described in [27]:

$$\sigma_{\text{tot}}(pp \rightarrow T\bar{T}) = \sum_{ij} \int_0^{\beta_{\text{max}}} d\beta \Phi_{ij}(\beta, \mu_F^2) \hat{\sigma}_{ij}(\beta, m^2, \mu_F^2, \mu_R^2) \quad (117)$$

Here, the indices i and j enumerate all possible initial state particles; β_{max} is defined as $\sqrt{1 - 4m^2/s}$, where \sqrt{s} is the centre-of-mass energy of the hadron collider; and $\beta = \sqrt{1 - \rho}$, where $\rho \equiv 4m^2/s$, is the relative velocity of the final state top quarks with pole mass m and partonic centre-of-mass energy \sqrt{s} .

The function Φ is the partonic flux and is given by:

$$\Phi_{ij}(\beta, \mu_F^2) = \frac{2\beta}{1 - \beta^2} \mathcal{L}_{ij} \left(\frac{1 - \beta \max}{1 - \beta}, \mu_F^2 \right) \quad (118)$$

Here, \mathcal{L} is the usual partonic luminosity, defined as:

$$\mathcal{L}(x, \mu_F^2) = x (f_i \otimes f_j)(x, \mu_F^2) \quad (119)$$

The renormalization and factorization scales are denoted by μ_R and μ_F , respectively. Setting $\mu_F = \mu_R = m$, the NNLO (next-to-next-to-leading order) partonic cross-section can be expanded as follows:

$$\hat{\sigma}_{ij}(\beta) = \frac{\alpha_s^2}{m^2} \left(\sigma_{ij}^{(0)} + \alpha_s \sigma_{ij}^{(1)} + \alpha_s^2 \sigma_{ij}^{(2)} + \mathcal{O}(\alpha_s^3) \right) \quad (120)$$

In the above equation, α_s represents the renormalized $\overline{\text{MS}}$ coupling, considering the presence of $N_L = 5$ active flavors at scale $\mu_R^2 = m^2$. Moreover, the functions $\sigma_{ij}^{(n)}$ solely depend on the value of β .

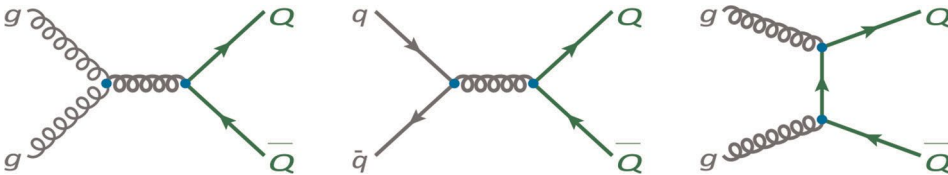


Figure 9.
Typical Feynman diagram of pair-produced vector-like quarks $Q(\equiv T, B, X, Y)$.

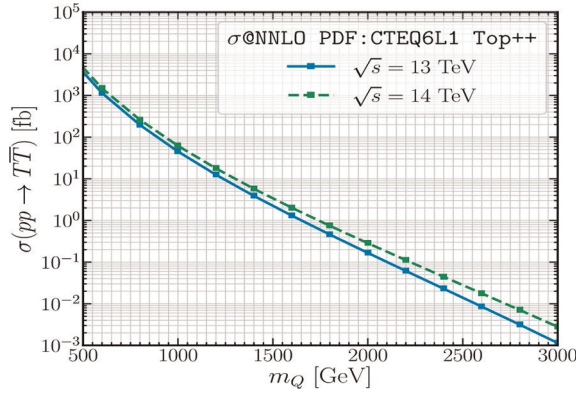


Figure 10.
 Production cross section for pair-produced vector-like quarks T at the LHC. In green (blue) we show the NNLO cross section for 14 TeV (13 TeV) Centre of mass energy computed by top++ [28].

In **Figure 10**, we present the production cross-section at the next-to-next-to-leading order (NNLO) of vector-like quark T pairs produced at the Large Hadron Collider (LHC), as a function of their masses m_Q . The curves are depicted in green and blue, corresponding to centre of mass energies of 14 and 13 TeV, respectively.

7. Conclusions

In this chapter, we focus on the Lagrangian framework that adheres to the fundamental principles of the standard model, exploring its consequences by determining eigenstates and interactions with SM-VLQ. We provide a comprehensive examination of the full interaction within the mass basis of 2HDM. Additionally, we touch upon the pair production of heavy quarks at the LHC, operating at energies of 13 and 14 TeV, underlining the importance of these endeavors in advancing our understanding of the fundamental forces and particles shaping the universe.

Simultaneously, the pursuit of heavy quarks, which share quantum characteristics like spin and electric charge with their standard model counterparts, is highly motivated. These quarks are abundantly produced within the LHC, and their discovery would mark a monumental advancement in particle physics. Although current experimental searches for vector-like quarks at CERN's LHC have not yielded conclusive evidence, the quest continues, holding the potential to usher in a new era of particle physics research. In this context, researchers at the LHC grapple with the challenge of directly testing quantum entanglement in proton-proton collisions, which is complicated by the macroscopic nature of these interactions. Quantum entanglement, typically a phenomenon observed at the microscopic scale, involves correlations between particles or pairs of particles. While the LHC's experiments may not provide direct proof of entanglement, they indirectly explore related aspects by studying correlations and angular momentum conservation among particles generated during collisions.

Appendix: heavy quark decay widths

The partial widths for T decays, including all possible mixing terms, are

$$\begin{aligned}
 \Gamma(T \rightarrow W^+ b) &= \frac{g^2}{64\pi M_W^2} \lambda(m_T, m_b, M_W)^{1/2} \left\{ \left(|y_{Tb}^L|^2 + |y_{Tb}^R|^2 \right) \right. \\
 &\quad \times \left[1 + r_W^2 - 2r_b^2 - 2r_W^4 + r_b^4 + r_W^2 r_b^2 \right] - 12r_W^2 r_b |y_{Tb}^L| |y_{Tb}^{R*}| \left. \right\}, \\
 \Gamma(T \rightarrow Zt) &= \frac{g}{128\pi c_W^2 M_Z^2} \lambda(m_T, m_t, M_Z)^{1/2} \left\{ \left(|y_{tT}^L|^2 + |y_{tT}^R|^2 \right) \right. \\
 &\quad \times \left[1 + r_Z^2 - 2r_t^2 - 2r_Z^4 + r_t^4 + r_Z^2 r_t^2 \right] - 12r_Z^2 r_t |y_{tT}^L| |y_{tT}^{R*}| \left. \right\}, \\
 \Gamma(T \rightarrow Ht) &= \frac{g^2}{128\pi M_W^2} \lambda(m_T, m_t, M_H)^{1/2} |y_{tT}^H|^2 (1 + 6r_t^2 - r_H^2 + r_t^4 - r_t^2 r_H^2),
 \end{aligned} \tag{121}$$

and for the 2HDM- T quark they are completely analogous, with $r_x \equiv m_x/m_Q$, where $x = t, b, W, Z, H$ and Q is the heavy quark, and

$$\lambda(x, y, z) \equiv (x^4 + y^4 + z^4 - 2x^2 y^2 - 2x^2 z^2 - 2y^2 z^2). \tag{122}$$


Author details

Rachid Benbrik^{*†} and Mohammed Boukidi[†]
 Polydisciplinary Faculty, Laboratory of Fundamental and Applied Physics,
 Cadi Ayyad University, Safi, Morocco

^{*}Address all correspondence to: r.benbrik@uca.ac.ma

[†] These authors contributed equally.

IntechOpen

© 2023 The Author(s). Licensee IntechOpen. This chapter is distributed under the terms of the Creative Commons Attribution License (<http://creativecommons.org/licenses/by/3.0>), which permits unrestricted use, distribution, and reproduction in any medium, provided the original work is properly cited. 

References

- [1] Aad G et al. Observation of a new particle in the search for the standard model Higgs boson at the large hadron collider. *Physics Letters B*. 2012;**716**(1): 1-29
- [2] Chatrchyan S et al. Observation of a new boson at a mass of 125 GeV with the CMS experiment at the LHC. *Physics Letters B*. 2012;**716**(1):30-61
- [3] Buchkremer M et al. Vector-like quarks and Higgs effective couplings. *Journal of High Energy Physics*. 2012; **2012**(9):1-34
- [4] Glashow SL, Iliopoulos J, Maiani L. Weak interactions with lepton-hadron symmetry. *Physical Review D*. 1970;**2**(7):1285-1292
- [5] Chatrchyan S et al. Study of the mass and spin-parity of the Higgs boson candidate via its decays to Z boson pairs. *Physical Review Letters*. 2012;**110**(8): 081803
- [6] Contino R, Servant G. Discovering the top partners at the LHC using same-sign dilepton final states. *Journal of High Energy Physics*. 2010;**2010**(6): 1-30
- [7] ATLAS collaboration, Aad G, et al. Search for pair production of heavy top-like quarks decaying to a high-pT W boson and a b quark in the lepton plus jets final state at $\sqrt{s} = 7$ TeV with the ATLAS detector. *Physics Letters*. 2013; **B718**:1284-1302, 1210.5468, arXiv: 1210.5468 [hep-ex]
- [8] CMS collaboration, Chatrchyan S, et al. Search for pair produced fourth-generation up-type quarks in pp collisions at $\sqrt{s} = 7$ TeV with a lepton in the final state. *Physics Letters*. 2012; **B718**:307-328, arXiv:1209.0471 [hep-ex]
- [9] Matsedonskyi O, Panico G, Wulzer A. On the interpretation of top partners searches. *JHEP*. 2014;**12**:97
- [10] Aguilar-Saavedra JA. Identifying top partners at LHC. *JHEP*. 2009;**11**:030, arXiv:0907.3155 [hep-ex]
- [11] Contino R et al. Holography for fermions. *Journal of High Energy Physics*. 2006;**2006**(5):1-27
- [12] Aaboud M et al. Measurement of the correlation between the polar angles of leptons from top quark decays in the helicity basis at 7 TeV using the ATLAS detector. *Physics Letters B*. 2016;**757**: 236-256
- [13] Varma M, Baker OK. Quantum Entanglement in Top Quark Pair Production. [arXiv:2306.07788 [hep-ph]]
- [14] Aguilar-Saavedra JA. Post-decay quantum entanglement in top pair production. [arXiv:2307.06991 [hep-ph]]
- [15] Dong Z, Gonçalves D, Kong K, Navarro A. When the Machine Chimes the Bell: Entanglement and Bell Inequalities with Boosted $t\bar{t}$. [arXiv: 2305.07075 [hep-ph]]
- [16] CMS Collaboration. Measurement of long-range near-side two-particle angular correlations in pp collisions at 7 TeV. *Physical Review Letters*. 2013; **111**(12):122301
- [17] CERN. Large Hadron Collider (LHC). n.d. Available from: <https://home.cern/science/accelerators/large-hadron-collider> (<https://home.cern/science/accelerators/large-hadron-collider>)
- [18] Aaboud M et al. Measurement of the W boson polarisation in $t\bar{t}$ events from

pp collisions at 8 TeV in the lepton + jets channel with ATLAS. The European Physical Journal C. 2017;77(4):264

[19] Aad G et al. (ATLAS Collaboration). Measurements of the Higgs boson production and decay rates and constraints on its couplings from a combined ATLAS and CMS analysis of the LHC pp collision data at 7 and 8 TeV. Journal of High Energy Physics. 2015; **2015**(8):1

[20] Aguilar-Saavedra JA, Benbrik R, Heinemeyer S, Pérez-Victoria M. Handbook of vectorlike quarks: Mixing and single production. Physics Review. 2013;**D88**(9):094010, arXiv:1306.0572 [hep-ex]

[21] Arhrib A, Benbrik R, King SJD, Manaut B, Moretti S, Un CS. Phenomenology of 2HDM with vectorlike quarks. Physics Review. 2018; **D97**:095015, arXiv:1607.08517 [hep-ex]

[22] Benbrik R, Kuutmann EB, Buarque Franzosi D, Ellajosyula V, Enberg R, Ferretti G, et al. Signatures of vector-like top partners decaying into new neutral scalar or pseudoscalar bosons. JHEP. 2020;5:28, arXiv:1907.05929 [hep-ex]

[23] Benbrik R, Boukidi M, Moretti S. Probing light charged Higgs bosons in the 2-Higgs doublet model type-II with vector-like quarks. arXiv:2211.07259 [hep-ex].

[24] Arhrib A, Benbrik R, Boukidi M, Enberg R, Manaut B, Moretti S, et al. Anatomy of vector-like top-quark models in the alignment limit of the 2-Higgs doublet model type-II

[25] ATLAS collaboration, Aaboud M, et al. Combination of the searches for pair-produced vector-like partners of the third-generation quarks at $\sqrt{s} = 13$ TeV

with the ATLAS detector. Physical Review Letters. 2018;**121**(21):211801, arXiv:1808.02343 [hep-ex]

[26] CMS Collaboration. Search for pair production of vector-like quarks in leptonic final states in proton-proton collisions at $\sqrt{s} = 13$ TeV. arXiv: 2209.07327 [hep-ex]

[27] Czakon M, Fiedler P, Mitov A. Total top-quark pair-production cross section at hadron colliders through $O(\alpha_s^4)$. Physical Review Letters. 2013;**110**: 252004, arXiv:1303.6254 [hep-ex]

[28] Czakon M, Mitov A. Top++: A program for the calculation of the top-pair cross-section at hadron colliders. Computer Physics Communications. 2014;**185**:2930, arXiv:1112.5675 [hep-ex]

The Electromagnetic Inter-Nucleon Quark-to-Quark Bond and Its Effect on the Nuclear Force

Nancy Lynn Bowen

Abstract

This chapter discusses the electromagnetic forces inside a nucleus. Previous nuclear theories have ignored the electromagnetic force or treated it as a minor component, considering only Coulomb forces between protons. Since quarks are the centers for both the electric charge and the magnetic dipole moments within a nucleon, such assumptions are not valid. Since the electromagnetic interaction between inter-nucleon quarks may be formidable, electromagnetism can, indeed, be the force holding the nucleons together in a nucleus. Thus, the electromagnetic forces within a nucleus should not be ignored, but rather given the foremost of consideration—specifically with regard to nuclear behavior. New understandings are gained by applying the laws of electromagnetism to the nuclear structure inside an atomic nucleus. In this chapter, historic misunderstandings are debunked and clarified—including the supposed limitations of the electromagnetic force, the miscalculated violations of uncertainty principles, and the misconceived lowest-energy shape of the nuclides.

Keywords: quarks, electromagnetics, nuclear structure, nuclear binding energy, nuclear behavior

1. Introduction

The development of a proper theory of the Nuclear Force has occupied nuclear physicists for over eight decades as one of the main topics of physics research in the twentieth and twenty-first centuries. Currently, there is no singular model of the Nuclear Force that can explain all nuclear behaviors [1, 2]. A successful model of the Nuclear Force should explain the more salient nuclear behaviors: the shape of binding energy curve, particle decay, large quadrupole moments, and excited energy states.

The emphasis of this chapter is electromagnetics; however, the concepts of quantum physics are not ignored or contradicted in any way, and they are properly included in this examination of nuclear behavior.

1.1 Definition and clarification of terms

The Nuclear Force binds the nucleons inside the nucleus. Historically, the Nuclear Force was called the “Strong Nuclear Force,” one of four forces of nature, along with the Gravitational Force, the Electromagnetic Force, and the Weak Nuclear Force. After the discovery of quarks, the “Chromodynamic Force” was identified as the force holding the quarks together inside a nucleon. Later, the Chromodynamic Force was renamed the “Strong Nuclear Force,” considered to be the force responsible for binding the sub-nucleon particles together inside a nucleon. The force holding the nucleons together in a nucleus was renamed the “Nuclear Force.”

To add to this confusion, there is a model of the Nuclear Force called the “Residual Chromodynamic Force,” also known as the “Residual Strong Force.” Because of this model, and its association with chromodynamics, the Nuclear Force was thought to be a subset of the Chromodynamic Force. The Strong Nuclear Force is now considered to have two parts: the Chromodynamic Force, holding the quarks inside a nucleon, and the Nuclear Force, holding the nucleons inside a nucleus.

To avoid confusion regarding these forces, the term “Strong Nuclear Force” is not used in this chapter. Rather the term “Chromodynamic Force” is used to describe the force holding the quarks together in a nucleon, and the term “Nuclear Force” is used to describe the force holding the nucleons together in a nucleus.

2. Brief review of other models of the nuclear force

There are a number of models of the Nuclear Force, each of which can explain a limited range of nuclear behavior. The current state of the theory for the Nuclear Force is simply a study of the various models, with no one single model being able to explain the majority of the observed behaviors in an atomic nucleus.

The Liquid Drop Model, developed in 1929, claims that the nucleons bind to their closest neighbors, similar to a drop of liquid. This concept is based on empirical data for the binding energy curve, wherein the binding energy per nucleon is relatively constant. Used in conjunction with the Liquid Drop Model is the Weizsäcker formula [3]. This formula is a mathematical equation that is simply a curve-fitting estimate for the experimental binding energy. It uses five parameters and conditional logic to obtain the best fit to the experimental binding curve, duplicating the experimental binding energies to within a few percent. The Liquid Drop Model assumes that the nucleus is spherical in shape, without any consideration for other shapes. It does not explain excited states, large quadrupole moments, or nuclear particle decay.

The Nuclear Shell Model was developed in 1949 [4], and it mimics the Electronic Shell Model for electrons around an atom. The Nuclear Shell Model attempts to explain the minor deviations that were observed, in the 1940s, between the experimental data and the Weizsäcker formula. At that time, with only a limited amount of experimental data, there were notable deviations that were observed at “magic” numbers. However, when utilizing the current data, these minor deviations are revealed to be either non-existent, relatively minor, or related to obscure behavior [5]. The Shell Model uses the Pauli Exclusion Principle to predict the spins of the various atomic nuclides; however, these predictions are accurate only when the Nilsson terms are included [6]. The Nilsson terms, often referred to as “spaghetti plots” due to their complicated natures, provide two or three different empirical terms per nuclide in

order to match the experimental spin data to the theory [7]. The Shell Model does not explain particle decay or large quadrupole moments.

There are several Independent Particle Models [8] of the Nuclear Force. These models hypothesize that nucleons are confined inside a 3-D potential energy well, with no interaction among the nucleons. Although such a concept is unrealistic, it is employed to make the mathematics of the Schrödinger equation easier to solve. Depending on the atomic nuclide being studied, the Independent Particle Models alter the shape of the 3-D potential energy well within the Schrödinger equation, using numerous empirically selected variables to allow the models to duplicate the excited states of the nuclide. These models replicate large quadrupole moments only if the potential energy well is modeled as a 3-D ellipsoid, rather than a sphere. These models do not attempt to explain particle decay or the binding energy curve.

The Alpha-Cluster Model of 1938 [9] explained the stronger binding energy, observed for the nuclei with an integer number of alpha segments, claiming that alpha particles were formed as clusters inside a nucleus. This model was recently extended beyond the alpha nuclei and renamed the Clustering Model [10], with much recent research in the field of a nuclear clustering. According to this model, clusters of nucleons link together to form a chain-like structure. There is much experimental and theoretical evidence that atomic nuclides are made of clusters of alpha particles, as well as other types of segments. Recent research regarding the Clustering Model has indicated that clustering structures do indeed exist within nuclei [11, 12].

The Residual Color Model (also known as the Residual Chromodynamic Model or Residual Strong Force Model) is a theoretical model of the Nuclear Force, postulating the exchange of virtual pi-mesons as the binding force between nucleons [13]. In this model, the Nuclear Force is related to the Chromodynamic Force, but with four notable exceptions: it acts outside rather than inside the nucleons, it is a short-range force, it has different mediating particles, and it has a significantly lower strength. The Residual Color Force bonds a quark in one nucleon to a quark in another nucleon, thereby binding the two nucleons together. The Residual Color Model asserts that each nucleon is bonded to its nearest neighbors, similar to the Liquid Drop Model. The derivation of this residual force is mathematically difficult, even for only two nucleons. Only the smallest atomic nuclides have been simulated; however, these simulations resulted in significantly large errors. Thus, this model is unable to predict nuclear behavior. It should be noted that the computer simulations for the Residual Color Model used inflated quark masses, much larger than the theoretical mass of a “naked” quark. This mass inflation of the quarks was done to aid in the convergence of the simulations, since the simulations with small quark masses would not converge. Also, the use of inflated quark masses avoids a violation of Copenhagen interpretation of the Heisenberg uncertainty principle. Fortunately, there is some validity to this mass inflation of the quarks, related with the Constituent Quark Model.

In the Constituent Quark Model [14], the nucleons consist of three constituent quarks that are “dressed” with gluons and quark-antiquark pairs, thereby significantly increasing the effective mass of the quarks. If the quarks could be isolated from each other, then their chromodynamic binding energy could be experimentally measured. The quark rest masses would be the sum of the chromodynamic binding energy plus the rest mass of the nucleon. Unfortunately, the chromodynamic binding energy of the quarks is unknown. However, it is known to be at least as large as the amount of energy required to make a nucleon spontaneously emit a meson. (The actual binding energy could be much larger than this amount.) From this minimum estimate of the chromodynamic binding energy, the minimum value for the quark mass can be

determined: the minimum mass of each dressed quark is between 300 and 400 MeV/ c^2 . The inflated quark masses used in the Residual Color Model are consistent with the minimum values for a dressed quark.

3. A brief review of quarks

In 1964, the concept of quarks was introduced by Gell-Mann and Zweig [15, 16], stating that the proton and neutron are non-elementary particles. A proton is made of two up quarks and one down quark. A neutron is made of two down quarks and one up quark. The terms “up” and “down” are simply quantum attributes, unrelated to vertical orientation. Up-quarks have an electrical charge that is $+2/3$ of an elementary charge, and down-quarks have an electric charge that is $-1/3$ of an elementary charge. The electrical charge and magnetic moments of a nucleon are confined to the quarks, rather than being homogeneously distributed throughout the nucleon. Quarks have the attributes of mass, spin, electric charge, magnetic moments, and a quantum attribute called “color,” which is unrelated to visual color.

Illustrated in **Figure 1** are shorthand symbolic representations of the proton and neutron, showing the up- and down-quarks. In this representation, the up-quarks have a “++” charge, and the down-quarks have a “-” charge ($2/3$ and $-1/3$ of an elementary charge, respectively). The colors in these illustrations do not relate to the Chromodynamic Force, rather the colors are used to distinguish between the up- and down-quarks. The dots for the quarks do not represent the relative quark size, but rather are sized for easy viewing. The magnetic dipole moments of the quarks, not shown, are perpendicular to the page.

Gell-Mann stated that quark charges are localized, and Richard Feynman asserted that high-energy experiments proved the reality of quarks. Feynman surmised that the quarks have a distribution of position and momentum, like any other particle, and he correctly believed that the diffusion of quark momentum explained diffractive scattering. James Bjorken proposed that point-like partons would imply certain relations in deep inelastic scattering of electrons and protons, relations that were verified in experiments at Stanford Linear Accelerator in 1969 [17].

The deep inelastic scattering experiments indicate that the quarks have a confined three-dimensional spatial distribution for their position. Specifically, the quarks are not moving with a simple random motion throughout the entire volume of the nucleon, rather there is a physical separation of the quarks, as illustrated in **Figure 2a**.

The quarks exist as individual and definitive particles, as in **Figure 2a**, with each quark having a relative charge distribution in three-dimensional space and each quark

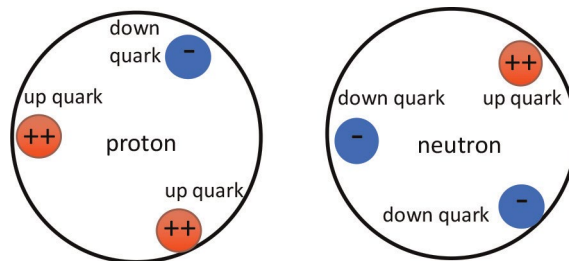


Figure 1.
Shorthand simplified representations of a proton and neutron.

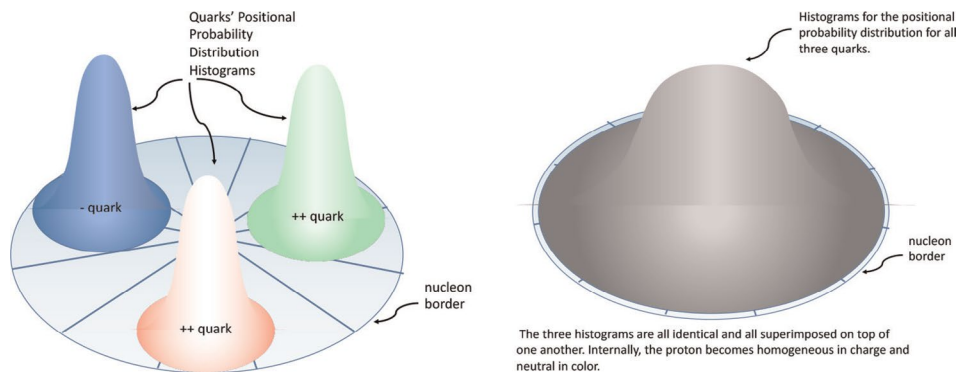


Figure 2.
 In 2a, (left) the quark probability distributions are distinct and separate. In 2b, (right) is an illustration of an incorrect probability distribution of the three quarks, superimposed on one another and coincident with the nucleon boundary, causing a homogeneous charge and a neutral color.

being separate and distinct from the other quarks. Nucleons do not have a homogeneous charge or neutral gray color throughout their volumes. This incorrect hypothetical situation is illustrated in **Figure 2b**, shown as a comparison with **Figure 2a**.

A quote about the Laureates, who won the 1990 Nobel Prize for their deep elastic experiments at the Stanford Linear Accelerator, describes this concept.

“Earlier investigations of the proton at low energies had shown that this ought to be ‘soft’ with a relatively even internal distribution of its electrical charge. This year’s Laureates therefore had reason to believe there would be a decline in the probability of photon absorption (low number of events). But they found instead a high probability level (many events), i.e. there seemed to be something small and “hard” inside the proton.”

“Thus the new investigations gave the surprising result that the electrical charge within the proton is concentrated to smaller components of negligible size.”

“This unexpected discovery by the 1990 Laureates was noted immediately by certain skilled theoreticians, chiefly R.P. Feynman and J.D. Bjorken. The result was first interpreted within the framework of what is termed the parton model, which, however, soon came to be identified with the quark model.”

Thus, the quark probability distributions are not merged together, but rather they are individual and distinct distributions, as shown in **Figure 2a**.

3.1 The chromodynamic, nuclear, and electromagnetic forces on quarks

The Chromodynamic Force is much stronger than the Nuclear Force, by several orders of magnitude. However, an actual definitive measurement of its strength has not been made, because particle physicists are unable to separate the quarks from a nucleon. The Chromodynamic Force is thought to be similar to the force of a spring—the further it is stretched from its neutral point, the stronger it pulls back. Presently, there are numerous models of what comprises the mass of a nucleon. These models of the nucleon describe: the number of quarks inside a nucleon, what constitutes the mass of a nucleon, and what gives the nucleon its spin. Some models claim there are several

hundred non-valence quarks and gluons inside a nucleon. For the Electromagnetic Model of the Nuclear Force, only the three valence quarks are considered. The Chromodynamic Force is the force inside of the protons and neutrons, and it confines and contains the quarks therein. The Chromodynamic Force abruptly neutralizes itself, falling to zero near the edge of the nucleon. Therefore, the quantum color of a quark strongly affects the other quarks inside that same nucleon; however, the quantum color of a quark does not affect quarks within other nucleons.

Conversely, the Electromagnetic Force does not abruptly neutralize itself at the edge of the nucleon. Rather, the Electromagnetic Force is completely unaffected by the nucleon boundary. These Electromagnetic Forces have an influence on all of the other quarks within the entire atomic nucleus, attracting or repulsing the other quarks within an atomic nucleus, depending on the polarity of the associated electric charges and magnetic dipoles. As a result, a quark inside of one nucleon feels the electromagnetic influences of a quark from another nucleon. Those same two quarks are contained and confined within their respective nucleons by the Chromodynamic Force; however, outside of their respective nucleons, the quarks are able to influence one another due to their electromagnetic forces.

3.2 Quarks and the electromagnetic bond

For the Electromagnetic Model, the nuclear bond is between two quarks forming the bond—a positively charged up quark from one nucleon and a negatively charged down quark from another nucleon. The concept of a nuclear bond is similar to the electronic bonds among the atoms of a molecule. In electronic molecular bonding of atoms, one atom cannot bond to an indefinite number of other atoms. Similarly, one nucleon cannot bond to an indefinite number of other nucleons. The number of bonds is limited by the number of quarks available for bonding. Thus with only three valence quarks, each nucleon can bond only to three other nucleons.

Prior to the 1960s, the proton was incorrectly thought to be homogeneously charged, and to be an elementary particle, with no sub-particles inside of it. As a result, the strongest electrical energy between two such protons was thought to be about 10^{-13} joules. The experimental energy required to free a single nucleon from an atomic nucleus is much larger than this. For this reason, the Nuclear Force was believed to be much stronger than the Electromagnetic Force. As a result, this incorrect concept of a homogeneously charged elementary proton created the erroneous limitation for the maximum strength of the Electromagnetic Force. Unfortunately, this incorrect concept is still often perpetuated.

Mathematically, in the limit as the distance goes to zero, the electromagnetic energy goes to infinity. Hence, the electromagnetic energy can be extremely large if the quarks are close enough to each other. Since the electric charge of the nucleons resides only within the quarks, a quark from one nucleon can bond electromagnetically with a quark in another nucleon, and the resulting force between two such quarks can be large enough to be the Nuclear Force.

3.3 Slight conceptual change to the inter-nucleon quark-to-quark bonding

If the Nuclear Force is dependent on the up and down flavor of quarks, rather than on the color of the quarks, then many problems are resolved, and many questions can be answered [18]. This one simple conceptual change to the Residual Color Model makes an extremely important difference in the understanding of the Nuclear Force.

Specifically, the concept is that a down-quark is attracted to an up-quark, but not to another down-quark. Similarly, an up-quark is attracted to down-quark, but not to another up-quark. The Nuclear Force is simply the attraction between an up-quark in one nucleon and a down-quark in another nucleon. When a bond is made between these two quarks in two different nucleons, the nucleons themselves become bonded. This bond lowers the overall energy of the nuclide as compared with its constituent parts, thereby giving the nuclide a higher binding energy.

This one simple conceptual change, that the Nuclear Force is dependent upon the up/down polarity rather than the quantum color of the quark, explains why a system of six protons and six neutrons is at a lower energy (and at a higher binding energy) than five protons and seven neutrons. It is because six protons and six neutrons form one bond for every pair of up-down quarks. There are 18 up-quarks and 18 down-quarks in the system of six protons and six neutrons; thus, there are 18 pairs of up-down quarks and 18 bonds. However, for five protons and seven neutrons, there are 19 down-quarks and 17 up-quarks. Thus, only 17 bonds are formed, and two quarks remain unbonded. The nucleus with five protons and seven neutrons is at a higher overall energy (and at a lower binding energy) than the system of six protons and six neutrons. With this simple change, it is now understood why a nucleon only bonds to its nearest neighbors—a nucleon can only bond three times because it only has three quarks available for bonding.

This concept also explains the first term of the Weizsäcker formula; it is because of the limited number of possible bonds for each nucleon. Also, this simple change of concept explains the asymmetry force of the Weizsäcker formula—the greatest number of bonds occurs when there are equal numbers of up-quarks and down-quarks, which means an equal number of protons and neutrons. The Coulomb energy term of the Weizsäcker formula is also easily explained as being related to the electrical energy of the net positive charges within a nucleus.

Furthermore, due to the inter-nucleon up-to-down quark bonding with three possible bonds per nucleon, there is a predilection for the formation of an alpha segment, made of two neutrons and two protons. This predilection explains the pairing term in the Weizsäcker formula, giving a higher binding energy (and a lower overall energy) when N and Z are even. The highest binding energy occurs when there are an even numbers of protons and an even number of neutrons, allowing for the formation of alpha segments. The “surface” term of the Weizsäcker formula is related to the two unbonded up quarks on the ends of the chain-like configuration and the two unbonded down quarks in the middle open-alpha segment. (The reason for these unbonded quarks will be explained later.)

Thus, for this one simple change—that the inter-nucleon quark-to-quark bond is related to up/down flavor rather than to color—the five terms of the Weizsäcker formula can be understood as a direct consequence of the inter-nucleon up-to-down quark bonding. Simple calculations show that the concept of inter-nucleon up-to-down quark bonding reproduces the binding energy curve surprisingly well [18]. If the force between the inter-nucleon quarks is assumed to be the Electromagnetic Force, then more rigorous calculations can be made, as done in Section 5.

4. Quarks and the Copenhagen interpretation of uncertainty principles

It is shown here that there is no violation of the Copenhagen interpretation of the Heisenberg uncertainty principle. An example calculation is done to illustrate this. However, some definitions, explanations, and equations are discussed first.

The original derivation of the Heisenberg uncertainty principle states that if the two variables, position and momentum, are measured simultaneously, then the uncertainty of the measurement must be greater than $\hbar/2$, shown in Eq. (1).

$$\sigma_x \eta_p \geq \hbar/2 \quad (1)$$

Here, σ_x is the noise in the error of the measurement of position, and η_p is the resultant disturbance in the momentum, as a result of the measurement [19]. This equation and these definitions of the variables represent the original form for the Heisenberg uncertainty principle. The Copenhagen interpretation, however, does not involve laboratory measurements. The Copenhagen interpretation claims that the existence of a quantum system—whether observed or not—cannot exist in a state that is more precise than the Heisenberg limit. This changes the original Heisenberg uncertainty principle from that of Eq. (1) to that of Eq. (2),

$$\sigma_x \sigma_p \geq \hbar/2 \quad (2)$$

where σ_x is the standard deviation of the position probability distribution of the particle, and σ_p is the standard deviation of the momentum probability distribution of the particle.

There are probability distributions for position and momentum for each quark. Associated with these probability distributions are the quantum Expectation Values for position and momentum, which are essentially the mean position and momentum of a quark. The mean value for position is a summation of all the possible values that the position can have, with each value being weighted according to the probability $P(x)$ of that value occurring. To normalize these probability distributions, this is divided by the total number of events, which is the summation of $P(x)$. For a smooth distribution, the summation is replaced by an integral, as shown in Eq. (3):

$$\text{Mean of } x = \frac{\int_{-\infty}^{\infty} x P(x) dx}{\int_{-\infty}^{\infty} P(x) dx} \quad (3)$$

In a quantum mechanical calculation, the probability function $P(x)$ of the particle is the complex conjugate of the wave function times the original wave function. The wave function $\Psi(x, t)$ of the particle is found by solving the Schrödinger equation with the appropriate boundary conditions. For the Expectation Value of position, the probability distribution is multiplied by x , then integrated. Since the overall probability of the particle's position within infinity is unity, the integral in the denominator of Eq. (3) is defined to be one. Thus, for quantum mechanics, the Expectation Value of the position x is as shown in Eq. (4):

$$\text{Expectation Value of } x = \int_{-\infty}^{\infty} \Psi^*(x, t) x \Psi(x, t) dx \quad (4)$$

Since the denominator is defined as one, it is no longer explicitly necessary for the equation. A similar operation is done to find for the Expectation Value of momentum.

As mentioned previously, in the computer simulations of the Residual Color Force Model, the mass of the bare “naked” quarks was inflated to avoid non-convergence. This inflated mass also avoided a violation of the Copenhagen interpretation of the Heisenberg uncertainty principle—since for “dressed” quarks, the quantum uncertainty principles are not inherently violated. This larger mass is thought to be due to either relativistic speeds or to a quantum energy associated with the gluons. If relativistic speeds are involved, then the dressed quarks would also have a significant uncertainty in their momentum probability distribution. Regardless, the Chromodynamic Force is considered to be strong enough to confine the quarks inside the nucleus, despite relativistic speeds.

Due to their vibrations and quantum fluctuations, the quarks have a quantum probability distribution in three dimensions for both space and momentum. Thus, the quarks are not in a fixed or static position relative to each other. Rather there are probability distributions for their relative positions and momentums. When the positions are averaged over spacetime, the Expectation Values of the three quarks appear to be in point-like spatial positions, relative to each other.

This is an important concept: the Expectation Value of the three-dimensional spatial positions of the three quarks inside a nucleon can be modeled as point-like positions with respect to each other. At any given instant in time, there is an uncertainty in the position and momentum of the quarks. Although the spatial and momentum probability distributions are not point-like, the positional Expectation Values do appear as point-like positions.

Several experimental studies have been conducted to measure the radial charge distribution inside a proton and neutron [20–22]. The resulting radial charge densities are shown in **Figure 3**.

As seen in the **Figure 3**, these experiments indicate that there is zero charge density at the center of both the proton and neutron—consistent with the quarks having a probability distribution situated more toward the periphery. Using these experimentally determined charge distributions, the quark probability distributions can be found by solving for the up and down probability distributions necessary to achieve these same charge distributions [23]. These quark probability distributions are shown in **Figure 4**.

As can be seen, the quarks are not homogeneously distributed throughout the entire volume of the nucleon. Their mean position is approximately 0.8 femtometers

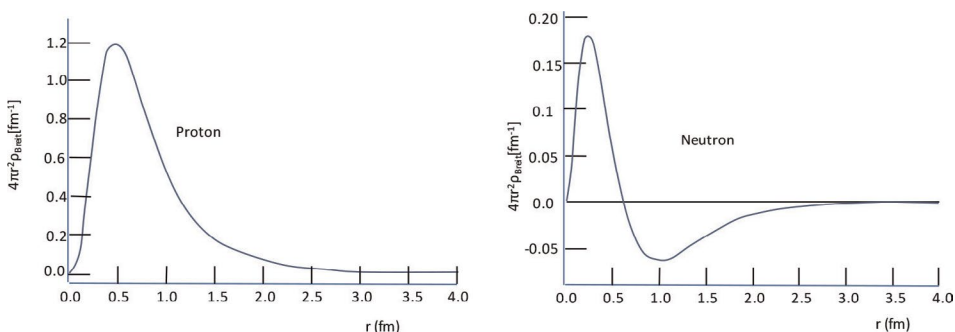


Figure 3.
 Experimental data for the radial charge symmetry of the proton and neutron. Note the difference in the vertical axis.

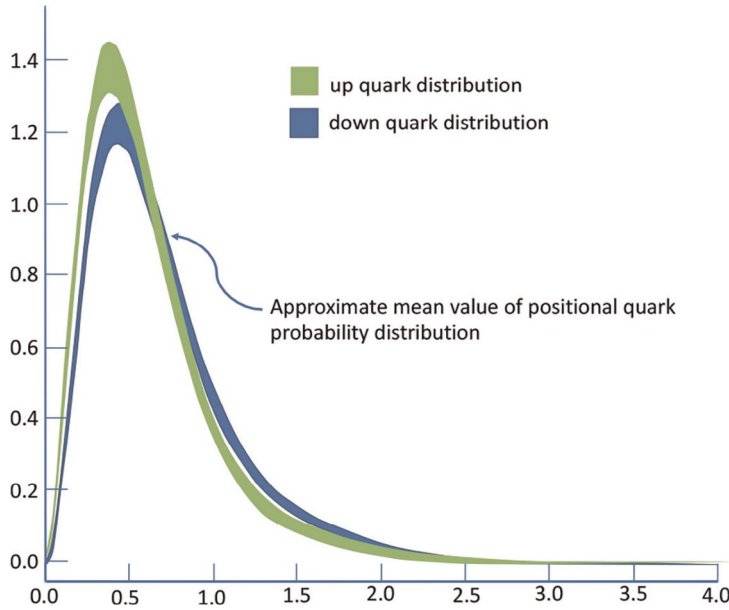


Figure 4. Up-quark and down-quark orbital radial distributions. The mean value of the quarks position is roughly at 0.8 femtometers from the center.

from the center, in agreement with the calculations of this paper. (Note, these distributions are radial densities.)

While it is not possible to definitively calculate the combined uncertainty in space and momentum, by using reasonable values for these standard deviations, some estimates can be made to determine if the quarks fit within the confines of quantum uncertainty principles.

If the quarks inside a proton cannot be unbound by the addition of 139.6 MeV of energy, then the binding mass is at least this 139.6 MeV/c². The chromodynamic binding mass is subtracted from the masses of the three isolated quarks. In other words, the total mass of the three quarks is equal to the rest mass of the nucleon plus the chromodynamic binding mass. This information gives us a lower limit to the masses of the three constituent quarks. This calculation is shown in Eq. (5), where the mass of a proton is 938.3 MeV/c².

$$\sum Mass_{constituent\ parts} \geq 938.3 \frac{MeV}{c^2} + 139.6 \frac{MeV}{c^2} \geq 1077.9 \frac{MeV}{c^2} \quad (5)$$

Assuming there are no other massive particles, as yet undiscovered, inside the proton, this gives the sum of the masses of the three quarks to be at least 1077.9 MeV/c². This indicates that each of the effective masses of the three constituent quarks is at least 350 MeV/c² = 6.4 × 10⁻²⁸ kg in mass. (Most likely, they are more massive than this.) Regardless of whether this constituent quark mass is the rest mass of the three “dressed” quarks or a relativistically inflated mass of the “naked” quarks, this value of 6.4 × 10⁻²⁸ kg is a reasonable estimate for the lower limit of the quark mass. Also, this value is in good agreement with the Constituent Quark Model and the computer simulations used in the Residual Quark Model.

A reasonable estimate for the standard deviation of the quark vibrational velocity distribution is about 0.8 times the speed of light. Thus, $\sigma_v = 0.8c = 2.4 \times 10^8$ m/sec. This gives, σ_p , the standard deviation for the quark momentum as: $\sigma_p = (2.4 \times 10^8 \text{ m/sec})(6.4 \times 10^{-28} \text{ kg}) = 1.54 \times 10^{-19} \text{ kg-m/sec}$. A reasonable estimate for the standard deviation of the spatial distribution, σ_x , is about $\frac{1}{4}$ the diameter of the nucleon. Thus, $\sigma_x = (\frac{1}{4})(1.68 \text{ fm}) = 0.42 \times 10^{-15} \text{ m}$.

Using these reasonable estimates and the lower limit of the quark mass, the product of the two standard deviations falls within the limits of the Heisenberg uncertainty principle, as shown in Eq. (6).

$$\sigma_x \sigma_p = (0.42 \times 10^{-15} \text{ m})(1.54 \times 10^{-19} \text{ kg m/sec}) = 6.45 \times 10^{-35} \geq \hbar/2 \quad (6)$$

Thus, using these reasonable estimates for the uncertainties, the product is above the Heisenberg limit; there is no violation of the Copenhagen interpretation. Furthermore, the binding mass is very likely to be more than $139.6 \text{ MeV}/c^2$, which means that the product of the uncertainties is even larger. Also, the vibrational speed of the quarks could easily exist within the realm of relativistic speeds, again increasing the uncertainty product. Both considerations make a violation of the Copenhagen interpretation less likely. Hence, the concept of a quark that “appears” to be a point-like electric charge and magnetic moment is fundamentally allowed.

5. Calculations of the energies within the nucleus

For this calculation, the energies that are taken into consideration are the centrifugal energy, electric energy, and magnetic energy. The electric charges and magnetic dipole moments of the nucleons are contained in the quarks. Since the electric charges and magnetic dipole moments reside in the quarks, it can easily be realized that the electromagnetic forces between an up-quark and a down-quark are strong enough to bind the two nucleons together. No other force, different from the electromagnetic force, is needed to account for the strong bond between nucleons. **Figure 5** shows this electromagnetic bond. Also present is the magnetic force, perpendicular to the page, but not shown.

The force binding these two nucleons need not be anything other than the electromagnetic forces between the up- and down-quarks.

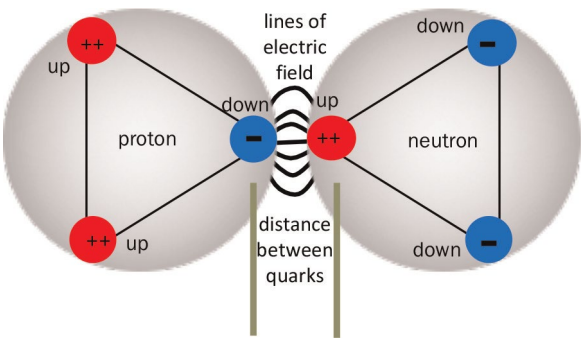


Figure 5.
The electromagnetic bond between quarks.

5.1 The electric energy

The electric energy [24] between two charged particles is shown in Eq. (7):

$$Energy_{12} = \frac{q_1 q_2}{(4\pi\epsilon_0)(distance_{12})} \quad (7)$$

where $distance_{12}$ is the distance between particles 1 and 2, and q_1 and q_2 are the electric charges on particles 1 and 2. For additional charges, the total electric energy is the double summation over all pairs of charges, as shown in Eq. (8).

$$E_{electric_total} = \sum_{i=1}^{n-1} \sum_{j=i+1}^n \frac{q_i q_j}{(4\pi\epsilon_0)(distance_{ij})} \quad (8)$$

5.2 The magnetic energy

The magnetic energy [25, 26] between two magnets has vector and positional dependence. Given two magnets, with magnetic moments μ_1 and μ_2 , the magnetic field of magnet₁ is determined at the location of the magnet₂. This vector field is symbolized as B_{12} , as shown in Eq. (9).

$$\vec{B}_{12} = \frac{\mu_0}{4\pi} \left\{ \frac{3(\vec{\mu}_2 \cdot \vec{r}_{21}) \vec{r}_{21} - r_{21}^2 (\vec{\mu}_2)}{r_{21}^5} \right\} \quad (9)$$

The resultant energy, $U_{magnetic12}$, is the negative dot product of the vector of the magnetic moment μ_2 with the vector of B_{12} , as shown in Eq. (10).

$$U_{magnetic12} = -\vec{\mu}_2 \cdot \vec{B}_{12} \quad (10)$$

For a collection of magnets, the total magnetic energy is the double summation over all pairs of magnets, as shown in Eq. (11).

$$U_{magnetic_total} = \sum_{i=1}^{n-1} \sum_{j=i+1}^n -\vec{\mu}_i \cdot \vec{B}_{ij} \quad (11)$$

where \vec{B}_{ij} is the vector magnetic field established by the i th magnet at the location of the j th magnet.

Combining Eqs. (9)–(11), the total electromagnetic energy of a distribution of charges and magnets is shown in Eq. (12):

$$U_{EM_total} = \sum_{i=1}^{n-1} \sum_{j=i+1}^n \frac{q_i q_j}{(4\pi\epsilon_0)(r_{ij})} + \sum_{i=1}^{n-1} \sum_{j=i+1}^n \frac{\mu_0}{4\pi} \left\{ \frac{3(\vec{\mu}_j \cdot \vec{r}_{ji})(\vec{\mu}_i \cdot \vec{r}_{ji}) - r_{ji}^2 (\mu_i \cdot \mu_j)}{r_{ji}^5} \right\} \quad (12)$$

Due to the vector properties of this energy, the lowest energy configuration for two magnets is a stacked bond, in which the magnetic moments of the magnets are

oriented in the same direction, stacked one atop the other, and as close as physically possible. A side-by-side bond is with anti-parallel magnetic moments, oriented side by side, and as close as physically possible. An angled bond gives intermediate results. From quantum field theory, it is known that quarks behave as point-like Dirac particles, each having their own inherent magnetic moment [27].

5.3 The centrifugal energy

The kinetic energy of spin must be properly included in the total energy of a nuclide. A rotating rigid object comprises numerous individual particles that orbit about a central axis of rotation. The kinetic energy of this orbital movement, E_{orbital} , is related to the angular velocity, ω , and to the moment of inertia, I_{orbital} , shown in Eq. (13):

$$E_{\text{orbital}} = \frac{1}{2}I\omega^2 = \frac{1}{2}L^2/I_{\text{orbital}} \quad (13)$$

where L is the orbital angular momentum of the object. Note that $L = \omega I_{\text{orbital}}$. Putting these concepts into the quantum realm of nuclear physics [28], the equation for the quantum orbital angular momentum, L , is shown in Eq. (14):

$$L = \hbar\sqrt{l(l+1)} \quad (14)$$

where l is the value of the quantum number for the orbital angular momentum. Combining Eqs. (13) and (14) yields Eq. (15).

$$E_{\text{orbital}} = \frac{\frac{1}{2}L^2}{I_{\text{orbital}}} = \frac{\frac{1}{2}(\hbar^2[l(l+1)])}{I_{\text{orbital}}} \quad (15)$$

5.4 The total binding energy

The total binding energy can be calculated using these equations. There is only one parameter that must be selected, and that is the minimum distance between the inter-nucleon quarks, as shown previously in **Figure 5**, between two bonded quarks of two different nucleons. The value of 2.11082×10^{-16} meters is used to match the experimental data. This value gives excellent matching to the experimental binding energy, as seen in Section 7. The calculated binding energy is the difference of the total energies of the configuration and the total energies of the isolated constituent parts, shown in Eq. (16).

$$U_{\text{binding energy}} = U_{\text{total of configuration}} - U_{\text{total of constituent parts}} \quad (16)$$

Note that a positive binding energy lowers the total energy and mass of the configuration, as compared with the individual constituent parts.

5.5 Nuclear bonds and the quantum hard-core repulsion

The Pauli Exclusion principle states that nucleons cannot overlap in their physical dimensions; this is also known as the hard-core repulsion. For this reason, a pair of double-bonded nucleons, defined as two nucleons bonded twice to each other, is not

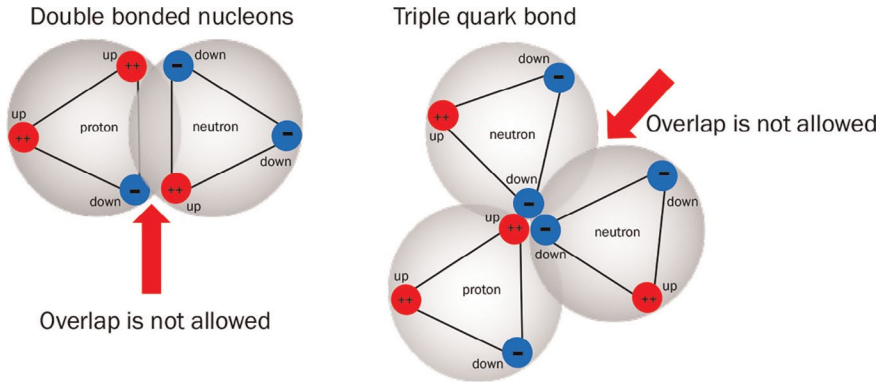


Figure 6. Left is an illustration of a double bond between a proton and neutron. Right is a triple-quark bond.

allowed. Similarly, a triple-quark bond, defined as three quarks attempting to bond together, is not allowed. These conditions are illustrated in **Figure 6**.

6. The determination of the lowest energy configurations

The lowest energy configurations of the atomic nuclei are determined by using the laws and equations for electromagnetics and angular momentum, as applied to the quarks within a structured nucleus. The position of each quark is defined in a matrix with xyz spatial coordinates and an electric charge value of either $-1/3$ or $+2/3$ of an elementary charge. The value of the magnetic moment and the three-dimensional vector direction of each magnetic moment are also included in the matrix. Based on the physical constraints of the configuration, a determination is made as to whether the magnetic bond is stacked, angled, or side by side.

The various possible configurations are tested to determine which configuration is the lowest energy state. As a result, every nucleus in this paper is in its lowest energy state in accordance with the rules for electromagnetic and spin energies. Also, double-bonded nucleons or triple-quark bonds are not allowed.

The atomic nuclides from hydrogen ^2H up to Copernicium ^{283}Cn have been simulated and placed in their lowest energy configuration. For this lowest energy configuration, a pattern emerges from ^{12}C upward, as discussed below.

The nucleons bond together to form the various basic clusters or segments; these segments subsequently bond together to form the larger atomic nuclides. For the lowest energy configuration, these basic segments bond together in a chain-like configuration, in strong agreement with the Cluster Model.

For stable atomic nuclides, the alpha segment predominates. When there are only three possible bonds per nucleon, the alpha segment is the lowest energy configuration for two protons and two neutrons.

6.1 Alpha segments predominate

The nuclear bond is an attractive electromagnetic bond between the up-quark in one nucleon and the down-quark in another nucleon. This bond lowers the overall energy of the atomic nucleus, similar to the way that chemical bonds between the atoms lower the overall energy of a molecule. The number of times that an atom can

bond to another atom is limited by the number of valence electrons available for bonding. Similarly, the number of bonds for each nucleon is limited by the number of valence quarks available for bonding. Thus, with only three valence quarks, each nucleon can only bond three times. Two quarks, one from each of the two nucleons, are needed to form one bond. If every quark were fully bonded in an atomic nucleus, there would be three bonds for every two nucleons.

The alpha segment is predominant because there are only three bonds for each nucleon. Each nucleon can bond a maximum of three times, causing the nucleons to cluster into alpha segments. If there were only two bonds within each nucleon, they would simply string together as shown in **Figure 7a**. As can be seen in that illustration, each hypothetical proton and neutron can bond only twice. A structure similar to a string of beads is formed.

With three bonds allowed for each nucleon, the protons and neutrons form alpha segments, as shown in **Figure 7b**. This results in clusters of alpha segments, linked together in a chain-like structure.

If there were more bonds within each proton or neutron, the predominant cluster would be something larger than the alpha segment. For example, with five possible bonds per nucleon, the predominant structure inside such a hypothetical atomic nucleus would be ${}^6\text{Li}$, as seen in **Figure 7c**.

Experimentally, it is known that segments, such as a ${}^6\text{Li}$ segment, are not the predominant structure of atomic nuclei, but rather the alpha particle predominates. This can be seen in the scallop-like pattern of the curve of binding energy and in the prevalence of alpha decay for the larger radioactive nuclides. The predominance of the alpha segment strongly implies that there are only three bonds per nucleon, as is expected for a nucleon having three valence quarks.

An important observation to make can be seen in the representation of the alpha segments, shown in **Figure 7b**. This nuclide represents oxygen ${}^{16}\text{O}$. The left side of the oxygen ${}^{16}\text{O}$ configuration would have an unbonded positively charged up-quark on

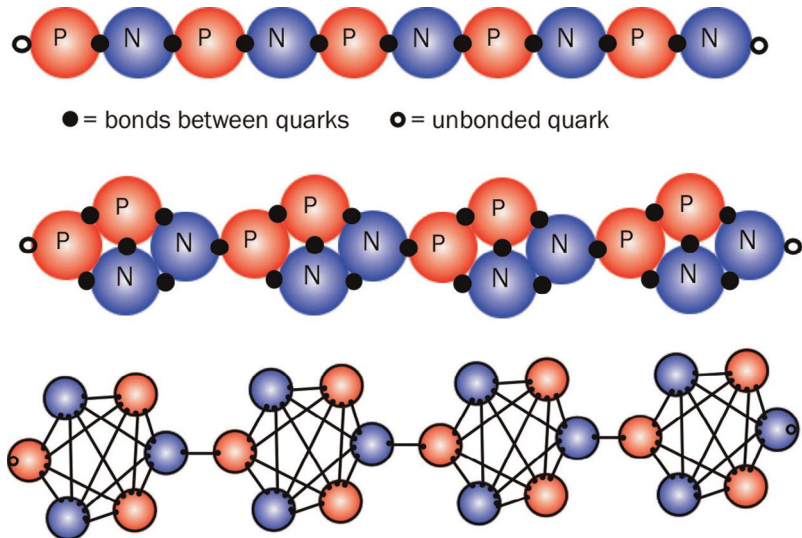


Figure 7.
(a) Hypothetical nuclear bonding if there were only two bonds for each proton and neutron. (b) Nuclear bonding with three bonds for each proton and neutron. (c) Hypothetical nuclear bonding if there were five bonds for each proton and neutron.

the end, and the right side would have an unbonded negatively charged down-quark on the end. This charge polarity causes an electric dipole moment in the configuration. However, quantum mechanics states there can be no net electric dipole moment within a nuclide [29].

Thus, to prevent this dipole, a bond is broken in one of the alpha segments. This broken bond creates an alpha segment, called an open-alpha segment, which bonds to the rest of the chain via its positive quarks, causing there to be two unbonded down-quarks in its center. This allows a negative charge to be situated near the center of the configuration and also spreads out the net positive charge of the nuclide. Both ends of the chain terminate with a positive charge, and there is no dipole moment.

The lowest energy configuration is one that maximizes the number of up-to-down quark bonds. To reduce the Coulomb energy, the lowest energy configuration spreads out the net positive charge as much as possible, while still maintaining the bonds. Any negative charge, such as an unbonded down-quark of an extra neutron, is situated in what would otherwise be the highest concentration of positive charge.

6.2 Spherical nuclides and the deformation parameter

Thus, the lowest energy configuration of any atomic nuclide is not a sphere. Rather, the electric force of the net positive charge within a nucleus attempts to spread apart that net positive charge as much as possible, without breaking the bonds. This forms a clustered, chain-like structure. When considering the electric force, a spherical shape for a net positively charged nuclide is exactly the opposite of its lowest energy shape.

There is much experimental evidence to substantiate this non-spherical shape. For example, the deformation parameter is a measure of an atomic nuclide's non-spherical shape. The experimentally known deformation parameters are shown in **Figure 8**. If the nuclides were spherical, then all of the deformation parameters seen in

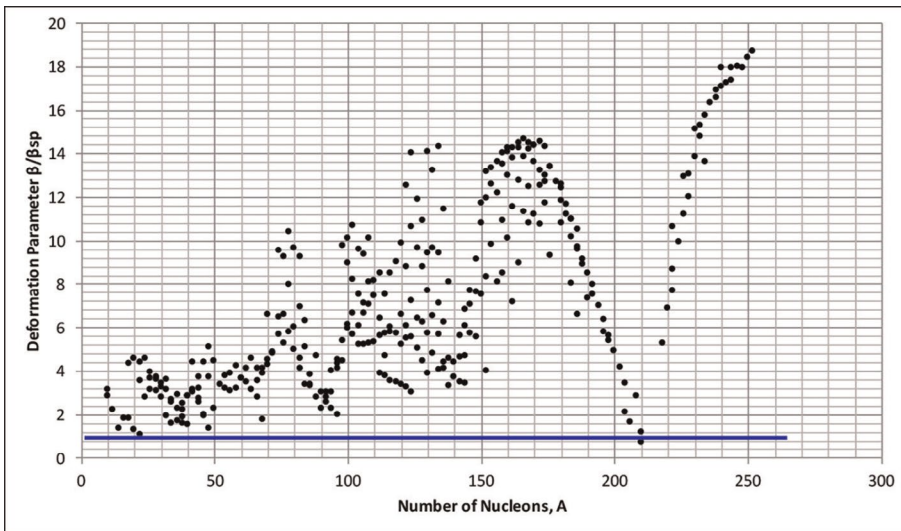


Figure 8. The ratio of the experimental nuclear deformation parameter divided by the predicted deformation parameter of the Shell Model, indicated by the blue line at the value 1.

Figure 8 should be less than 1, indicated by the blue line. However, they are much higher. (All data for **Figure 8** were extracted from reference [30].)

The deformation parameters are much larger than the Shell Model can explain. This theoretical discrepancy with the empirical data is also true of electric quadrupole moments. Note that the distortion from a spherical shape does not appear in just a few small isolated regions of the nuclear table; rather it covers the entire range of the table. These large experimentally measured deformation parameters for the vast majority of atomic nuclides invalidate the concept of spherical atomic nuclides, in conflict with any model that pre-assumes a spherical shape, as is commonly done in many previous models [31].

For example, when researchers interpret the scattering data from an experimentally probed atomic nucleus, the shape of the atomic nucleus is pre-assumed to be a spherical shape, prior to interpreting the data. Furthermore, only the electric monopole moment is considered. For this pre-assumed spherical shape, the best value of its radius is forced-fit to the data, without any consideration that a different shape may be possible [32].

6.3 The patterns of the lowest energy configurations

For stable atomic nuclides with $A \geq 12$, the lowest-energy configurations follow a pattern, as might be expected. Nuclides below $A = 12$ cannot follow the pattern, simply because there are not enough nucleons to do so. For stable nuclides, with $A \geq 12$, the pattern is as follows.

- Alpha segments predominate within the configuration. For every two protons and two neutrons, an alpha segment is formed.
- There is an open-alpha segment near the center of the configuration.
- There is a triton segment, made of two neutrons and one proton, with an unbonded down quark, included in all stable nuclides with odd Z (with the exception of ^{14}N).
- For stable atomic nuclides with $N > Z$, the extra neutrons are positioned in the location that would otherwise have the highest positive electric charge density.
- For stable atomic nuclides smaller than bismuth ^{209}Bi , the excess neutrons are positioned between the alpha segments.

For unstable nuclides, the pattern is as follows:

- For unstable nuclides larger than ^{209}Bi , the extra neutrons are forced to double up between the alpha segments. There are no stable nuclides with doubled-up neutrons in their configuration.
- In the lowest energy state for radioactive nuclides above the nuclear drip line (either having excess protons or not having enough neutrons), the net positive charge of the nuclide is spread out as much as possible.

- For radioactive nuclides below the nuclear drip line, the excess neutrons, with their negatively charged unbonded down quarks, are spread out as much as possible.
- These chain-like configurations may also curve or curl depending on the orientation of the constraints on the magnetic bonds between the segments. For example, a helix shape may form.

7. Summary of the electromagnetic force within the nucleon

- The electromagnetic force is valid inside the atomic nucleus.
- The electric charge and the magnetic dipole moment of the nucleons are contained within the quarks.
- Within a single nucleon, the three quarks have a spatial quantum probability distribution relative to each other. (An equilateral triangle is assumed for simplicity.)
- There are three possible bonds per nucleon, one for each quark.
- An up-quark and a down-quark, one from two different nucleons, are needed for one bond.
- The configuration, with the lowest electromagnetic energy plus spin kinetic energy, is assumed for the ground state.
- The kinetic energy of the quantum angular momentum of the nucleus [33, 34] is properly taken into account.
- There is a minimum distance between two quarks of two different nucleons, consistent with the hard core repulsion.
- The hard core repulsion of the nucleons prevents a nucleon from bonding more than once to another nucleon. Double-bonded nucleons and triple-quark bonds are not allowed.

Once the lowest energy configurations are determined, there remains only one parameter to be selected for the best fit to the binding energy data—namely, the “minimum quark-to-quark distance.” This model has only one parameter to determine, whereas the Weizsäcker formula uses five empirically fit parameters and a conditional logic statement to achieve its mathematical curve fitting. The electromagnetic model of the Nuclear Force is able to get comparable results with only one parameter.

Over a thousand different configurations for different atomic nuclides have been computer modeled using this method to calculate the binding energy based on electromagnetics. These include stable and unstable atomic nuclides; large, medium, and small atomic nuclides; and ground and excited states. These detailed calculations have been done for every atomic nuclide shown in **Figure 9**. Each atomic nuclide is placed in the lowest-energy configuration; then the electromagnetic energy of the configuration is calculated, and the binding energy is determined.

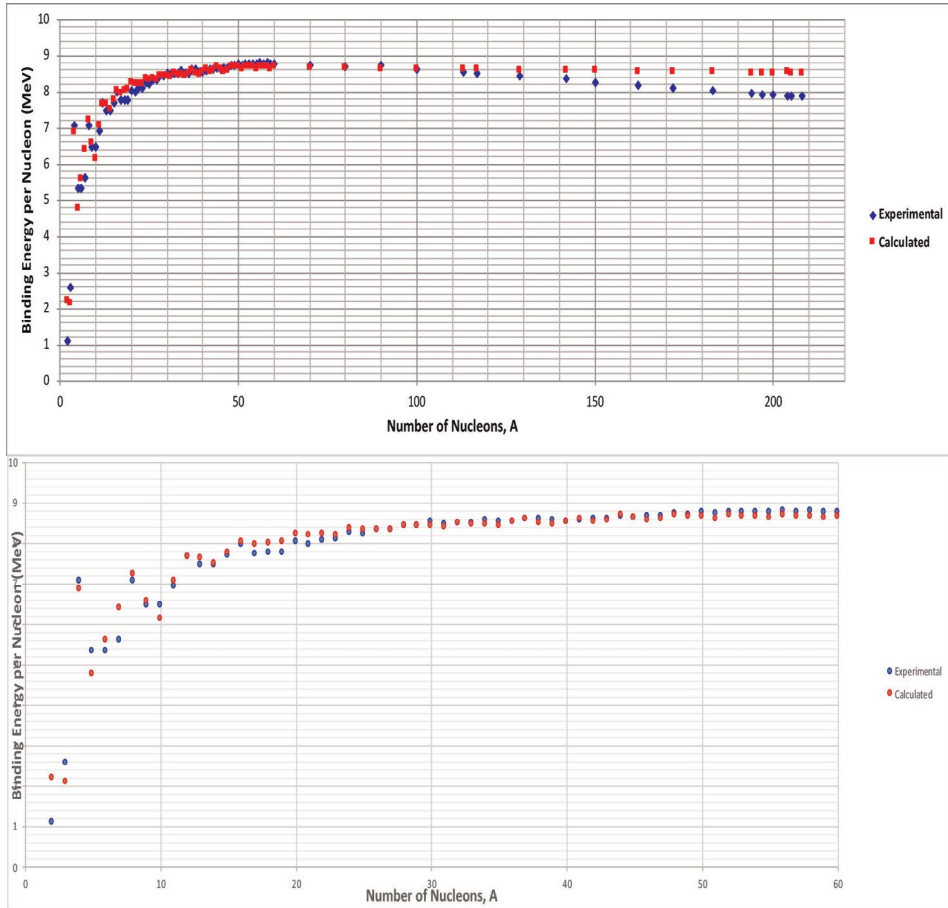


Figure 9.
 (a) Binding energy per nucleon versus A , for both calculated and experimental data, from $A = 2$ to $A = 208$.
 (b) Binding energy per nucleon versus A , for both calculated and experimental data, from $A = 2$ to $A = 60$.

The value for the minimum distance between quarks is 2.11082×10^{-16} meters. The resulting binding energy curve is shown in **Figure 9**. The top pane shows all the points from $A = 2$ to $A = 208$. The lower pane shows only the points from $A = 2$ to $A = 60$, for ease of viewing the details. As can be seen, there is excellent agreement in the reproduction of the experimental data.

Most of the atomic nuclides fall within a 1 or 2% error. For the atomic nuclides with large A , the predicted downward slope is not as severe as is experimentally observed. For these larger atomic nuclides, the worst error is 8.32% for ^{204}Pb . (Experimental data are extracted from reference [35].) Using electromagnetic equations, atomic nuclides as large as copernicium ^{283}Cn have been easily modeled.

By applying the electromagnetic forces to the quarks and nucleons within a nucleus, new insights about many other behaviors of the Nuclear Force can be achieved. For example, by examining the electromagnetic forces that could possibly cause violations of the hard-core repulsion—such as a nuclide attempting to form either a double-bonded nucleons or triple-quark bonds—this model can potentially explain the nuclear behaviors of neutron ejection, proton ejection, and alpha decay.

Also, by considering configurations that are not the lowest energy state, new insights can be provided about the nuclear behaviors of these excited states and their

isomeric transitions. Understanding how the electromagnetic forces within a nuclide might change after the occurrence of beta decay also allows for many interesting and discerning insights.

8. Conclusions

This chapter acts as an introduction to the electromagnetic behaviors inside the atomic nucleus. It also serves to clarify the important role of electromagnetics and to debunk the historical misconceptions regarding the electromagnetic forces inside an atomic nucleus. Rather than disregarding the electromagnetic forces and energies of the quarks, when taken into full account and understanding, the electromagnetic forces inside a nucleus can explain much about nuclear behavior. It is the intent of this chapter to highlight the role of electromagnetics, as a topic of nuclear physics that deserves further analysis and serious consideration. By recognizing the Electromagnetic Forces within the nuclear structure, a better understanding of nuclear behavior can be obtained.

The Electromagnetic Model of the Nuclear Force asserts that the electromagnetic properties of the quarks are the force binding the nucleons together, via an inter-nucleon quark-to-quark bond. The ground state configurations of hundreds of atomic nuclides, from ^2H to ^{283}Cn , have been determined and computer-simulated. The calculated binding energies agree with the experimental binding energies to within a few percent. These computations are done by using only one selected parameter. No previous theoretical model of the Nuclear Force is able to demonstrate such an accurate prediction of binding energy with only one parameter.


With this understanding that the electromagnetic properties of the quarks are what that bind the nucleons together in a nucleus, the Nuclear Force is directly unified to the Electromagnetic Force.

Author details

Nancy Lynn Bowen
Colorado Mountain College, Glenwood Springs, CO, USA

*Address all correspondence to: nbowen@coloradomtn.edu

IntechOpen

© 2023 The Author(s). Licensee IntechOpen. This chapter is distributed under the terms of the Creative Commons Attribution License (<http://creativecommons.org/licenses/by/3.0>), which permits unrestricted use, distribution, and reproduction in any medium, provided the original work is properly cited. 

References

- [1] Eisberg R, Resnick R. Quantum Physics of Atoms, Molecules, Solids, Nuclei, and Particles. New York: Wiley; 1985. p. 509
- [2] Lilley J. Nuclear Physics Principles and Applications. Chichester: Wiley; 2001. p. 35
- [3] Von Weizsäcker CF. Zur theorie der kernmassen. Zeitschrift für Physik. 1935; **96**(7–8):431-458. (in German)
- [4] Mayer MG, Jensen JHD. Elementary Theory of Nuclear Shell Structure. New York: Wiley; 1955
- [5] Bowen NL. An examination of the updated empirical data in support of the shell model. Journal of Condensed Matter Nuclear Science. 2020;**33**:224
- [6] Nilsson SG. Binding states of individual nucleons in strongly deformed nuclei. Det Kongelige Danske Videnskabernes Selskab. Matematisk-fysiske Meddelelser. 1955; **29**:16
- [7] Brown BA, Wildenthal BH. Status of the nuclear shell model. Annual Review of Nuclear and Particle Science. 1988;**38**: 29-66
- [8] Mukhin K. Experimental Nuclear Physics, Volume 1, Physics of Atomic Nucleus. Moscow: Mir Publishers; 1987. p. 133
- [9] Hafstad LR, Teller E. The alpha-particle model of the nucleus. Physics Review. 1938;**54**:681
- [10] Brink DM. History of cluster structure in nuclei. Journal of Physics: Conference Series. 2008;**111**:012001. DOI: 10.1088/1742-6596/111/1/012001
- [11] Ichikawa T, Maruhn JA, Itagaki N, Ohkubo S. Linear chain structure of four- α clusters in ^{16}O . Physics Review Letters. 2011;**107**:112501
- [12] Beck C. Present status of nuclear cluster physics and experimental perspectives. Journal of Physics: Conference Series. 2014;**569**:012002. DOI: 10.1088/1742-6596/569/1/012002
- [13] Vayenas G, Souentie S. Gravity, Special Relativity and the Strong Force. New York: Springer; 2012. pp. 25-27
- [14] Griffiths D. Introduction to Elementary Particles. New Jersey: Wiley-VCH; 2008. p. 135
- [15] Gell-Mann M. A schematic model of baryons and mesons. Physics Letters. 1964;**8**(3):214-215. DOI: 10.1016/S0031-9163(64)92001-3
- [16] Zweig G. An $\text{SU}(3)$ Model for Strong Interaction Symmetry and Its Breaking. CERN-TH-401. 1964. Available from: <https://cds.cern.ch/record/570209>
- [17] Friedman JI, Kendall HW. Deep inelastic electron scattering. Annual Review of Nuclear Science. 1972;**22**:203
- [18] Bowen NL. The inter-nucleon up-to-down quark bond and its implications for nuclear binding. In: Szadkowski ZP, editor. Quantum Chromodynamic. London: IntechOpen; 2020. DOI: 10.5772/intechopen.94377
- [19] Heisenberg W. Quantum theory and measurement. In: Wheeler JA, Zurek WH, editors. Princeton, NJ: Princeton University Press. pp. 62-84 [Translation into English by J. A. Wheeler and W. H. Zurek, 1981. Originally published under the title,

“Über den anschaulichen Inhalt der quantentheoretischen Kinematik und Mechanik,” *Zeitschrift für Physik*, 43, 172-98 (1927)]

[20] Hasell DK et al. The BLAST experiment. *Nuclear Instrument Mathematics*. 2009;**A603**:247. DOI: 10.1016/j.nima.2009.01.131

[21] Hasell DK et al. Spin-dependent electron scattering from polarized protons and deuterons with the BLAST experiment at MIT-Bates. *Annual Review of Nuclear Particle Science*. 2011; **61**:409-433

[22] Hata H, Murata M, Yamato S. Chiral currents and static properties of nucleons in holographic QCD. *Physical Review D*. 2008;**78**:086006. DOI: 10.1103/PhysRevD.78.086006

[23] Smith TP. The anatomy of a neutron. *American Scientist*. 2010;**98**:478-485. Available from: <http://www.jstor.org/stable/25766725>. [Accessed: 21 June 2022]

[24] Lorrain P, Corson D. *Electromagnetic Fields and Waves*. San Francisco: Freeman and Company; 1970. pp. 72-76

[25] Owen GE. *Electromagnetic Theory*. Boston: Allen and Bacon, Inc.; 1963. p. 205

[26] Yosida K. *Theory of Magnetism*. New York: Springer; 1996. p. 13

[27] Peskin ME, Schroeder DV. *An Introduction to Quantum Field Theory*. Reading, MA: Perseus Books; 1995. pp. 175-198

[28] Krane KS. *Introductory Nuclear Physics*. New York: Wiley; 1988. pp. 34-37

[29] Bertulani CA. *Nuclear Physics in a Nutshell*. Princeton, New Jersey: Princeton University Press; 2007. p. 105

[30] Raman S, Nestor CW, Tikkanen P. Transition probability from the ground to the first 2^+ state of even-even nuclides. In: Pritychenko B, editor. *Atomic Data and Nuclear Data Tables*. Vol. 78. Cambridge, MA: Elsevier Inc.; 2001. pp. 1-128

[31] Krane KS. *Introductory Nuclear Physics*. New York: Wiley; 1988. pp. 49-57

[32] De Vries H, De Jager CW, De Vries C. Nuclear charge-density-distribution parameters from elastic electron scattering. *Atomic Data and Nuclear Data Tables*. 1987;**36**:495-536

[33] Krane KS. *Introductory Nuclear Physics*. New York: Wiley; 1988. p. 144

[34] Bertulani CA. *Nuclear Physics in a Nutshell*. Princeton, NJ: Princeton University Press; 2007. p. 155

[35] National Nuclear Data Center. Available from: The NuDat 2 database, <http://www.nndc.bnl.gov/nudat2/> [Accessed: 04 October 2021]

Exploring Strange Entanglement: Experimental and Theoretical Perspectives on Neutral Kaon Systems

*Nahid Binandeh Dehaghani, A. Pedro Aguiar and
Rafal Wisniewski*

Abstract

This chapter provides an in-depth analysis of the properties and phenomena associated with neutral K-mesons. Kaons are quantum systems illustrating strange behaviors. We begin by examining the significance of strangeness and charge parity violation in understanding these particles. The concept of strangeness oscillations is then introduced, explaining oscillations between K^0 and \bar{K}^0 states. The regeneration of K_S is investigated, uncovering the underlying mechanisms involved. The discussion moves on to quasi-spin space, exploring its bases and their implications. The entangled states of kaon pairs (K^0, \bar{K}^0) are considered, with a focus on maximally entangled neutral kaons and nonmaximally entangled states. Decoherence effects on entangled kaons are examined, utilizing the density matrix description to capture the dynamics. A dedicated decoherence parameter is introduced to quantify the impact of decoherence. Furthermore, the chapter investigates the loss of entanglement through measures such as von Neumann entanglement entropy, entanglement of formation, and concurrence. These measures provide insights into quantifying and characterizing entanglement in the context of neutral kaons. Through this comprehensive exploration of properties, phenomena, and entanglement dynamics, this chapter aims to pointing out recent works on neutral kaons, contributing to advancements in particle physics.

Keywords: decoherence, entanglement, K-meson, open quantum system, particle physics, strange particles

1. Introduction

Quantum entanglement, being among the most counterintuitive and subtle foundational elements of quantum mechanics, pertains to the correlations observed

between distant components of certain composite systems. This intriguing phenomenon was brought to light by the pioneering work of Einstein, Podolsky and Rosen (EPR) in [1] and Schrödinger in [2], who uncovered a “spooky” characteristic of quantum machinery, better featured as nonlocality in the correlations of an EPR pair. Well-known and valuable tools for exploring this nonlocality are obtained by means of the subsequent development of initial Bell inequalities [3], and their subsequently reformulated variations [4, 5]. Experimental tests have consistently demonstrated the violation of Bell inequalities [6, 7], indicating the failure of local realistic theories and affirming the nonlocal nature of the universe.

Consequently, there is considerable interest in exploring the EPR-Bell correlations of measurements in various branches of physics, including particle physics. As a result, several pioneering researchers in particle physics have proposed investigating EPR-entangled massive particles, such as neutral kaons [8–10]. They referred to the unique characteristics of individual neutral kaon states, which exhibit various rare phenomena such as strangeness oscillation, small mass splitting, different lifetimes between the physical states, violations of two primary symmetries: charge parity (CP) and time reversal (T), regeneration when traversing a slab of material, and most notably, strange entanglement. Neutral kaons exhibit a unique form of entanglement known as strange entanglement, referring to the specific entanglement between two neutral kaons [11].

Numerous studies have been conducted to test quantum mechanics in the neutral kaon systems and search for CPT violation through neutral-meson oscillations. Notably, a significant focus on CP, T, and CPT violation in the neutral kaon system was first conducted at CERN in the CPLEAR experiment [12]. Additional contributions came from experiments such as NA48 and NA62 [13], which played key roles in discovering direct CP violation, yielding crucial experimental results. Moreover, experiments like KLOE [14], conducted at the DAΦNE collider, and its successor KLOE-2 [15], at the Frascati National Laboratory, achieved enhanced precision in investigating CPT violations and conducting quantum decoherence tests. The LHCb experiment, located at CERN’s Large Hadron Collider (LHC) [16], and KOTO, performed at the Japan Proton Accelerator Research Complex (J-PARC) [17], were among the other experiments which significantly contributed to our understanding of strange entanglement in neutral kaon system, providing valuable insights into the properties and behavior of entangled kaon states.

The investigation of the evolution of an entangled kaon system subjected to decoherence is a crucial aspect. This analysis is carried out by studying the system’s behavior over time using the so-called master equation as time progresses, the level of decoherence in the initially entangled kaon system increases, leading to a loss in the system’s entanglement. This reduction in entanglement can be accurately assessed in the field of quantum information, where the degree of entanglement in a state is quantified using specific measures, such as entropy of entanglement, concurrence, and entanglement of formation. These measures are widely employed for quantifying quantum entanglement. The unique characteristics of strange entanglement exhibited by neutral kaons, distinct from any other system, enable the exploration of novel phenomena. Considering the high importance of strange entanglement, a significant portion of the chapter is dedicated to exploring the stability of the entangled quantum system and examining the potential occurrence of decoherence due to interactions with its surrounding environment. We aim to understand the extent of these effects and their impact on entanglement by focusing on the correlation between decoherence and the loss of entanglement.

The structure of the chapter is as follows: In Section II, we review the strange behavior of neutral kaons through several phenomena, that is, strangeness and CP violation, strangeness oscillation, and regeneration. Section III introduces the bases in quasi-spin formalism, including the strangeness basis, free-space basis, and inside-matter basis. In Section IV, entangled states of kaon pairs are studied in two main subsections, that is, maximally and nonmaximally entangled states. In the next section, the effects of decoherence on entangled kaons are studied. The density matrix description of entangled kaon system is introduced, and its evolution is studied through the Gorini-Kossakowski-Sudarshan-Lindblad equation. In section VI, the decline in entanglement is quantitatively measured, and explicit evidence of the loss of entanglement is provided. The chapter ends with a conclusion and an overview of prospective research challenges.

1.1 Notation

The ket symbol is used to denote a column vector in a Hilbert space, indicating the quantum state of the particle, that is, $|K^0\rangle$ represents the state vector of a neutral kaon particle. The bra vector is used to describe the dual space or the bra state in quantum mechanics. In the case of a neutral kaon, $\langle K^0|$ represents the bra vector corresponding to the quantum state of the neutral kaon particle. We use the superscript \dagger to show the conjugate transpose of a matrix (or vector). The symbol \otimes indicates the tensor product, and \oplus the direct sum. For A and B being operators, we use the notation $[A, B] = AB - BA$, and $\{A, B\} = AB + BA$. The expression $A(t = t_i; t_r)$ represents the state (or probability) A at a specific time, where the time t is equal to t_i , and t_r represents a specific reference time. For a generic function $f(t)$, its derivative with respect to time is denoted by $\dot{f}(t)$. For a composite system consisting of subsystem A and subsystem B , the partial trace over subsystem B is denoted as tr_B . The imaginary unit is shown by $i = \sqrt{-1}$.

2. Properties of the neutral kaons

Kaons are the lightest strange mesons whose quark content is understood as $u\bar{s}$, $s\bar{u}$, $d\bar{s}$ for the charged kaons $K^+(494\text{MeV}/c^2)$ and $K^-(494\text{MeV}/c^2)$, and the neutral kaon $K^0(498\text{MeV}/c^2)$, respectively [18]. Neutral K-mesons exhibit fascinating quantum phenomena that showcase their peculiar and intriguing behavior. In the following, we study notable instances that exemplify this strangeness.

2.1 Strangeness and charge parity violation

The neutral kaon and its antiparticle $\bar{K}^0(498\text{MeV}/c^2) = s\bar{d}$ are distinguished by a quantum number \mathcal{S} , known as strangeness, such that $\mathcal{S}|K^0\rangle = +|K^0\rangle$, and $\mathcal{S}|\bar{K}^0\rangle = -|\bar{K}^0\rangle$. Kaons are pseudoscalar particles with a total spin of 0 and parity $P = -1$ ($J^P = 0^-$). They exhibit charge conjugation symmetry (C), which corresponds to the transformation $K^0 \rightleftharpoons \bar{K}^0$. Hence, for the joint transformation, one can write

$$CP|K^0\rangle = -|\bar{K}^0\rangle, \quad CP|\bar{K}^0\rangle = -|K^0\rangle \quad (1)$$

From a theoretical point of view, in order to obtain the CP eigenstates, one can implement the superposition of \bar{K}^0 and K^0 as

$$|K_1^0\rangle = \frac{1}{\sqrt{2}}(|K^0\rangle - |\bar{K}^0\rangle), \quad |K_2^0\rangle = \frac{1}{\sqrt{2}}(|K^0\rangle + |\bar{K}^0\rangle). \quad (2)$$

where $CP|K_1^0\rangle = +|K_1^0\rangle$, $CP|K_2^0\rangle = -|K_2^0\rangle$. The state K_1 principally decays to two pions while K_2 primarily decays to three pions, which occurs around 600 times slower in comparison to the decay of K_1 into two pions. The reason why this decay occurs so slowly is due to the fact that the mass of K_2 is a bit greater than the total masses of the three pions. Strangeness is not conserved in weak interactions; moreover, such interactions are CP-violating. The observation of these two modes of decay led to the establishment of the existence of two weak eigenstates of the neutral kaons, called K_L (K-long, T) and K_S (K-short, θ). The weak eigenstates are slightly different in mass, $\Delta m = m(K_L) - m(K_S) = 3.49 \times 10^{-12} \text{ MeV}$, however, they differ considerably in their lifetimes and decay modes. The state (K_S) is a combination of K_2 (K_1) with a small portion of K_1 (K_2), expressed as

$$|K_S\rangle = \frac{1}{\sqrt{|p|^2 + |q|^2}}(p|K^0\rangle - q|\bar{K}^0\rangle) \quad |K_L\rangle = \frac{1}{\sqrt{|p|^2 + |q|^2}}(p|K^0\rangle + q|\bar{K}^0\rangle) \quad (3)$$

where $p = 1 + \varepsilon$ and $q = 1 - \varepsilon$, with ε being the complex CP-violating parameter that is the same for K_L and K_S , that is, $\varepsilon_L = \varepsilon_S = \varepsilon$. According to the CPT Theorem [19], since CP symmetry is violated, time reversal (T) symmetry must also be violated to maintain the overall CPT symmetry. The decay of K_L (long-lived neutral kaon) is dominantly governed by CP violation, similar to the decay of K_2 . The primary decay mode of K_L is the three-pion decay, represented as $K_L \rightarrow 3\pi$, with a lifetime of approximately $\tau_L = 5.17 \times 10^{-8}$ seconds. Similarly, K_S (short-lived neutral kaon) predominantly decays via the strong interaction, similar to the decay of K_1 . The main decay mode of K_S is the two-pion decay, denoted as $K_S \rightarrow 2\pi$, with a lifetime of approximately $\tau_S = 8.954 \times 10^{-11}$ seconds. It is important to note that while the dominant decay mode of K_L is $K_L \rightarrow 3\pi$, there is also a small amount of CP-violating decay observed, specifically $K_L \rightarrow 2\pi$ [20].

2.2 Strangeness oscillation

The two kaons K^0 and \bar{K}^0 transfer to common states, and subsequently, they mix, meaning that they oscillate between K^0 and \bar{K}^0 before they decay. Consider the time-dependent Schrödinger equation for the state vector $|\psi(t)\rangle$ as

$$i\hbar|\dot{\psi}(t)\rangle = H|\psi(t)\rangle \quad (4)$$

where \hbar is the plank constant, and H is the non-Hermitian effective mass Hamiltonian describing the decay characteristics and strangeness oscillations of kaons, defined as

$$H = M - \frac{i}{2}\Gamma \quad (5)$$

whose eigenstates are K_S and K_L . The matrices M , related to mass, and Γ , a decay-matrix, are 2×2 Hermitian expressed as

$$M = \begin{pmatrix} M_{11} & M_{12} \\ M_{12}^* & M_{11} \end{pmatrix}, \quad \Gamma = \begin{pmatrix} \Gamma_{11} & \Gamma_{12} \\ \Gamma_{12}^* & \Gamma_{11} \end{pmatrix}, \quad (6)$$

$$\text{in which } \begin{cases} M_{11} = \frac{1}{2}(m_L + m_S) \\ M_{12} = \frac{1}{2}(m_L - m_S) \end{cases} \text{ and } \begin{cases} \Gamma_{11} = \frac{\hbar}{2}(\Gamma_L + \Gamma_S) \\ \Gamma_{12} = \frac{\hbar}{2}(\Gamma_L - \Gamma_S) \end{cases}, \text{ with } \Gamma_j = \tau_j^{-1}, j = S, L.$$

$$\text{The eigenvalues of } H \text{ satisfy } \begin{cases} H|K_S(t)\rangle = \left(m_S - \frac{i\hbar}{2}\Gamma_S\right)|K_S(t)\rangle \\ H|K_L(t)\rangle = \left(m_L - \frac{i\hbar}{2}\Gamma_L\right)|K_L(t)\rangle \end{cases}. \text{ The system evolves}$$

exponentially; that is, the solutions to the Hamiltonian are obtained as

$$|K_S(t)\rangle = e^{-\left(\frac{i}{\hbar}m_S + \frac{\Gamma_S}{2}\right)t}|K_S(t=0)\rangle, \quad |K_L(t)\rangle = e^{-\left(\frac{i}{\hbar}m_L + \frac{\Gamma_L}{2}\right)t}|K_L(t=0)\rangle \quad (7)$$

Subsequently, one can find the solution for K^0 and \bar{K}^0 as

$$\begin{aligned} |K^0(t)\rangle &= \frac{1}{2}\left(e^{-\left(\frac{i}{\hbar}m_S + \frac{\Gamma_S}{2}\right)t} + e^{-\left(\frac{i}{\hbar}m_L + \frac{\Gamma_L}{2}\right)t}\right)|K^0\rangle + \frac{q}{2p}\left(-e^{-\left(\frac{i}{\hbar}m_S + \frac{\Gamma_S}{2}\right)t} + e^{-\left(\frac{i}{\hbar}m_L + \frac{\Gamma_L}{2}\right)t}\right)|\bar{K}^0\rangle \\ |\bar{K}^0(t)\rangle &= \frac{p}{2q}\left(-e^{-\left(\frac{i}{\hbar}m_S + \frac{\Gamma_S}{2}\right)t} + e^{-\left(\frac{i}{\hbar}m_L + \frac{\Gamma_L}{2}\right)t}\right)|K^0\rangle + \frac{1}{2}\left(e^{-\left(\frac{i}{\hbar}m_S + \frac{\Gamma_S}{2}\right)t} + e^{-\left(\frac{i}{\hbar}m_L + \frac{\Gamma_L}{2}\right)t}\right)|\bar{K}^0\rangle \end{aligned} \quad (8)$$

Suppose an experiment in which a beam of pure K^0 is produced at $t = t_i$, where t_i is the initial time, via the strong interaction. The probability of observing a K^0 in the beam at a subsequent time t is determined by

$$\begin{aligned} |\langle K^0 | K^0(t) \rangle|^2 &= \frac{1}{4}\left(e^{\left(\frac{i}{\hbar}m_S - \frac{\Gamma_S}{2}\right)t} + e^{\left(\frac{i}{\hbar}m_L - \frac{\Gamma_L}{2}\right)t}\right)\left(e^{-\left(\frac{i}{\hbar}m_S + \frac{\Gamma_S}{2}\right)t} + e^{-\left(\frac{i}{\hbar}m_L + \frac{\Gamma_L}{2}\right)t}\right) \\ &= \frac{1}{4}\left(e^{-\Gamma_S t} + e^{-\Gamma_L t} + 2e^{-\frac{t}{2}(\Gamma_S + \Gamma_L)}\cos\left(\frac{t(m_L - m_S)}{\hbar}\right)\right) \end{aligned} \quad (9)$$

where the third term shows interference, which is the reason for an oscillation in the K^0 beam [18]. By following the same procedure, one can compute the probability of observing \bar{K}^0 particles in a beam at a later time, given that the beam initially consists of K^0 particles. Therefore,

$$|\langle \bar{K}^0 | K^0(t) \rangle|^2 = \frac{1}{4}\frac{|q|^2}{|p|^2}\left(e^{-\Gamma_S t} + e^{-\Gamma_L t} - 2e^{-\frac{t}{2}(\Gamma_S + \Gamma_L)}\cos\left(\frac{t(m_L - m_S)}{\hbar}\right)\right) \quad (10)$$

The K^0 beam oscillates with frequency $f = \frac{(m_L - m_S)}{2\pi}$, with $(m_L - m_S)\tau_S = 0.47$. The probability of finding a K^0 or \bar{K}^0 from an initially pure K^0 beam is shown in **Figure 1**.

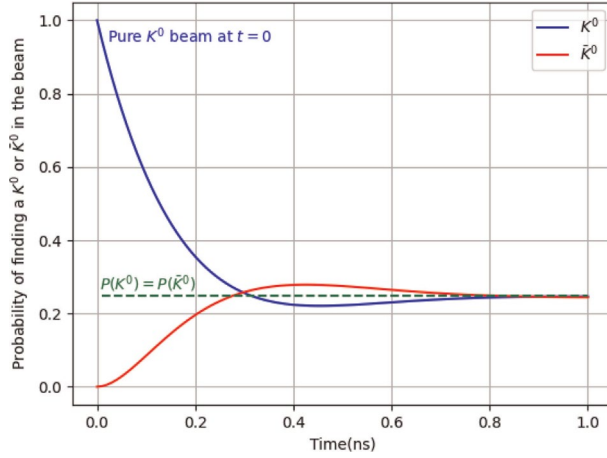


Figure 1.

Probability of finding a K^0 or \bar{K}^0 state in an initially produced K^0 beam over time.

The plank constant \hbar is considered as a unit for convenience. The oscillation becomes apparent when considering times on the order of a few τ_S , before all K_S mesons have decayed and only K_L mesons remain in the beam. Therefore, in a beam initially consisting of only K^0 mesons at $t = 0$, the presence of the \bar{K}^0 is observed at a distance from the production source through its equal probability of being found in the K_L meson. A similar phenomenon occurs when starting with a \bar{K}^0 beam [21].

Over time, the composition of the beam undergoes variations in strangeness due to the different nature of K^0 and \bar{K}^0 particles. This intriguing phenomenon is commonly referred to as strangeness oscillations, reflecting the oscillating strangeness content within the beam. In a broader context, this fascinating occurrence is known as flavor oscillations.

2.3 Regeneration of K_S

A beam of K-meson decays in flight after a few centimeters, so the short-lived kaon state K_S disappears, and only a pure beam of long-lived K_L is left. By shooting the K_L beam into a block of matter, which is usually regarded as a composition of protons and neutrons for all practical purposes, then the K^0 and \bar{K}^0 components of the beam interact dissimilarly with matter, which also causes the loss of quantum coherence between them. The K^0 particle engages in quasi-elastic scattering interactions with nucleons, while \bar{K}^0 has the ability to produce hyperons. Since the emerging beam contains various different linear combinations of K^0 and \bar{K}^0 , that is, a mixture of K_L and K_S , the K_S would eventually be regenerated in the beam [22].

3. Bases in quasi-spin space

The “quasi-spin” picture for kaons, initially proposed by Lee and Wu [23] and later developed by Lipkin [24], offers notable advantages when compared to spin- $\frac{1}{2}$ particles or photons with vertical (V)/horizontal (H) polarization. The strangeness

eigenstates K^0 and \bar{K}^0 are regarded as members of a quasi-spin doublet, where $K^0 = \begin{pmatrix} 1 \\ 0 \end{pmatrix}$ (or V polarized photon) and $\bar{K}^0 = \begin{pmatrix} 0 \\ 1 \end{pmatrix}$ (or H polarized photon) are considered as the quasi-spin states up $|\uparrow\rangle_z$ and down $|\downarrow\rangle_z$, respectively. All operators acting in the quasi-spin space can be expressed by Pauli matrices, that is, σ_x , σ_y , σ_z . The strangeness operator S is identified by σ_z , that is,

$$\sigma_z |K^0\rangle = +|K^0\rangle, \quad \sigma_z |\bar{K}^0\rangle = -|\bar{K}^0\rangle, \quad (11)$$

the CP operator with $-\sigma_x$, and the CP violation is relative to σ_y . This formalism is suitable for all two-level quantum systems. In this regard, the Hamiltonian in Eq. (5) can be implemented as

$$H = \alpha I + \beta(\sin \theta \sigma_x + \cos \theta \sigma_y) \quad (12)$$

where $\alpha = \frac{1}{2}(m_L + m_S - \frac{1}{2}(\Gamma_L + \Gamma_S))$, $\beta = \frac{1}{2}(m_L - m_S - \frac{1}{2}(\Gamma_L - \Gamma_S))$, and the phase θ corresponds to the CP parameter ε such that $e^{i\theta} = \frac{1-\varepsilon}{1+\varepsilon}$.

Overall, in the quasi-spin formalism, we may work with one of the following bases [25]:

- Strangeness basis $\{K^0, \bar{K}^0\}$: This basis is well-suited for examining electromagnetic and strong interaction processes that conserve strangeness, including the formation of $K^0 \bar{K}^0$ systems from nonstrange initial states, for instance $e^+ e^- \rightarrow \phi(1020) \rightarrow K^0 \bar{K}^0$ or $p \bar{p} \rightarrow K^0 \bar{K}^0$, and the detection of neutral kaons through strong kaon-nucleon interactions. This is an orthonormal basis, that is, $\langle K^0 | \bar{K}^0 \rangle = 0$.
- Free-space basis: $\{K_S, K_L\}$: In the quasi-spin space, the weak interaction eigenstates are similar to the CP eigenstates $|K_1\rangle$ and $|K_2\rangle$. However, the K_S, K_L basis provides a useful framework for analyzing the propagation of particles in free space while the CP basis is particularly suited for studying weak kaon decays. This basis is quasi-orthonormal with $\langle K_S | K_S \rangle = \langle K_L | K_L \rangle = 1$, and $\langle K_S | K_L \rangle = \langle K_L | K_S \rangle = \frac{\varepsilon + \varepsilon^*}{1 + |\varepsilon|^2} \simeq 0$.
- Inside-matter basis: $\{K'_S, K'_L\}$: The behavior of neutral kaons as they travel through a homogeneous medium of nucleonic matter, serving as both a regenerator and an absorber is determined by the medium Hamiltonian, which includes an extra strong interaction term as

$$H_{\text{medium}} = H - \frac{2\pi\nu}{m_K} \begin{pmatrix} f_0 & 0 \\ 0 & \bar{f}_0 \end{pmatrix} \quad (13)$$

where ν indicates the nucleonic density of the homogeneous medium, m_K is the mean value of $K_{S,L}$ mass, f_0 and \bar{f}_0 show the forward scattering amplitudes for K^0 and \bar{K}^0 , respectively. The $|K'_L\rangle$ and $|K'_S\rangle$ are the eigenstates of H_{medium} expressed as

$$|K'_L\rangle = \frac{1}{\sqrt{1+|r\bar{\rho}|^2}} \left(|K^0\rangle + r\bar{\rho} |\bar{K}^0\rangle \right), \quad |K'_S\rangle = \frac{1}{\sqrt{1+|r(\bar{\rho})^{-1}|^2}} \left(|K^0\rangle - r(\bar{\rho})^{-1} |\bar{K}^0\rangle \right) \quad (14)$$

where the dimensionless regenerator parameter ρ , the auxiliary parameter $\bar{\rho}$ and its inverse $(\bar{\rho})^{-1}$ are introduced as

$$\rho \equiv \frac{\pi\nu}{m_K} \frac{f_0 - \bar{f}_0}{m_L - m_S - \frac{i}{2}(\Gamma_L - \Gamma_S)} \quad (15)$$

$$\bar{\rho} \equiv \sqrt{1 + 4\rho^2} + 2\rho, \quad (\bar{\rho})^{-1} = \sqrt{1 + 4\rho^2} - 2\rho$$

and $r = \frac{1-\epsilon}{1+\epsilon}$. This basis is also quasi-orthonormal.

$$\langle K'_S | K'_L \rangle = \langle K'_L | K'_S \rangle^* = \frac{1 - |r|^2 (\bar{\rho}^* / \bar{\rho})}{\sqrt{1 + |r\bar{\rho}|^2} \sqrt{1 + |r/\bar{\rho}|^2}} \quad (16)$$

Two limiting cases exist:

1. For a very low density medium: $|K'_S\rangle \rightarrow |K_S\rangle$ and $|K'_L\rangle \rightarrow |K_L\rangle$
2. For extremely high density media: $|K'_L\rangle \rightarrow |\bar{K}^0\rangle$ and $|K'_S\rangle \rightarrow |K^0\rangle$

4. Entangled states of kaon pairs

In general terms, we classify a state as entangled when it cannot be expressed as a convex combination of product states, otherwise it is separable [26]. Quantum entanglement, as a central feature of quantum mechanics, is a phenomenon where two or more particles can become correlated in such a way that the properties of one particle are immediately affected by the properties of the other particle, regardless of the distance between them. In quantum information, entanglement is regarded as a resource. Hence, one is interested in maximally entangled quantum states. To this end, we investigate the entangled states of kaon pairs in two main class, that is, maximally and nonmaximally entangled states.

4.1 Maximally entangled neutral kaons

The spin-singlet states, initially proposed by Bohm, are the most commonly studied and simplest form of bipartite states. These states involve a pair of spin-1/2 particles. In analogy to the standard Bohm state, we consider entangled states of $K^0 \bar{K}^0$ [21, 27]. In both cases of Φ -resonance decays and s-wave proton-antiproton annihilation, the process begins at time, $t = 0$ with an initial state denoted as $|\phi(0)\rangle$ with global spin, charge conjugation, and parity $J^{PC} = 1^{--}$ expressed as

$|\phi(t=0)\rangle = \frac{1}{\sqrt{2}} \left(|K^0\rangle_l \otimes |\bar{K}^0\rangle_r - |\bar{K}^0\rangle_l \otimes |K^0\rangle_r \right)$, which can further be written in free-space basis as

$$|\phi(t=0)\rangle = \frac{1+|\varepsilon|^2}{\sqrt{2}(1-\varepsilon^2)} \left[|K_S\rangle_l \otimes |K_L\rangle_r - |K_L\rangle_l \otimes |K_S\rangle_r \right] \quad (17)$$

The neutral kaons separate and can be observed both to the left (l) and right (r) of the source. The weak interactions, which violate CP symmetry, come into play only in Eq. (17). It is worth noting that this state is both antisymmetric and maximally entangled in the two observable bases. Consequently, any measurements performed will consistently yield left–right anticorrelated outcomes. After production, the left-moving and right-moving kaons undergo evolution as described by Eq. (7) for respective proper times t_l and t_r . This formal evolution results in the formation of the “two-times” state. Therefore,

$$|\phi(t_l, t_r)\rangle = \frac{1}{\sqrt{2}} e^{-(\Gamma_S t_l + \Gamma_L t_r)/2} \left(|K_S\rangle_l \otimes |K_L\rangle_r - e^{(i\Delta m + \Delta\Gamma/2)\Delta t} |K_L\rangle_l \otimes |K_S\rangle_r \right) \quad (18)$$

where $\Delta t = t_l - t_r$, $\Delta m = m_L - m_S$, $\Delta\Gamma = \Gamma_L - \Gamma_S$, and $\varepsilon \rightarrow 0$. Equivalently, Eq. (18) can be written in strangeness basis

$$\begin{aligned} |\phi(t_l, t_r)\rangle = & \frac{1}{2\sqrt{2}} e^{-(\Gamma_S t_l + \Gamma_L t_r)/2} \left(\left(1 - e^{(i\Delta m + \Delta\Gamma/2)\Delta t} \right) \left(|K^0\rangle_l \otimes |K^0\rangle_r - |\bar{K}^0\rangle_l \otimes |\bar{K}^0\rangle_r \right) \right. \\ & \left. + \left(1 - e^{(i\Delta m + \Delta\Gamma/2)\Delta t} \right) \left(|K^0\rangle_l \otimes |\bar{K}^0\rangle_r - |\bar{K}^0\rangle_l \otimes |K^0\rangle_r \right) \right) \end{aligned} \quad (19)$$

Typically, it is common to examine two-kaon states at a unique time, that is, $t \equiv t_r = t_l$. In this scenario, we have the following equation

$$\begin{aligned} |\phi(t, t)\rangle &= \frac{1}{\sqrt{2}} e^{-(\Gamma_S + \Gamma_L)t/2} \left(|K^0\rangle_l \otimes |\bar{K}^0\rangle_r - |\bar{K}^0\rangle_l \otimes |K^0\rangle_r \right) \\ &= \frac{1}{\sqrt{2}} e^{-(\Gamma_S + \Gamma_L)t/2} \left(|K_S\rangle_l \otimes |K_L\rangle_r - |K_L\rangle_l \otimes |K_S\rangle_r \right) \end{aligned} \quad (20)$$

exhibiting similar maximal entanglement and anticorrelations over time.

4.2 Nonmaximally entangled states

In addition to the previously discussed maximally entangled state of kaons, there is interest in exploring other nonmaximally entangled states for testing the local realism versus Quantum Mechanics theories. To prepare these states, we begin with the initial state described in Eq. (17). A thin and homogeneous regenerator is positioned along the right beam, as close as possible to the source of the two-kaon state. If the regenerator is placed in close proximity to this origin and the proper time (Δt) required for the right-moving neutral kaon to pass through the regenerator is sufficiently short, that is, much smaller than τ_S , weak decays can be neglected, and the resulting state after traversing the thin regenerator is obtained as

$$|\phi(\Delta t)\rangle = \frac{1}{\sqrt{2}}(|K_S\rangle \otimes |K_L\rangle - |K_L\rangle \otimes |K_S\rangle + \eta(|K_S\rangle \otimes |K_S\rangle - |K_L\rangle \otimes |K_L\rangle)) \quad (21)$$

The regeneration effects are designated by $\eta = i\rho(\Delta m - \frac{i}{2}\Delta\Gamma)\Delta t$. One may note the difference between Eqs. (20) and (21) at made by the terms linear in η . To intensify that difference, let the state Eq. (21) propagate in free space up to a proper time $\tau_S \leq T \leq \tau_L$, so

$$|\phi(T)\rangle = \frac{e^{-(\Gamma_L\tau_l + \Gamma_S\tau_r)/2}}{\sqrt{2}}(|K_S\rangle \otimes |K_L\rangle - |K_L\rangle \otimes |K_S\rangle - \eta(e^{-(i\Delta m + \Delta\Gamma/2)T}|K_L\rangle \otimes |K_L\rangle - e^{(i\Delta m + \Delta\Gamma/2)T}|K_S\rangle \otimes |K_S\rangle)) \quad (22)$$

Eq. (22) shows that the $|K_L\rangle \otimes |K_L\rangle$ component has exhibited remarkable resilience against weak decays compared to the accompanying terms $|K_S\rangle \otimes |K_L\rangle$ and $|K_L\rangle \otimes |K_S\rangle$, resulting in its significant enhancement. Conversely, the $|K_S\rangle \otimes |K_S\rangle$ component has experienced substantial suppression and can therefore be disregarded provided that $T \gg \tau_S$. By normalizing Eq. (22) to the surviving pairs, one obtains

$$|\Phi\rangle = \frac{1}{\sqrt{2 + |R_L|^2 + |R_S|^2}}(|K_S\rangle \otimes |K_L\rangle - |K_L\rangle \otimes |K_S\rangle + R_L|K_L\rangle \otimes |K_L\rangle + R_S|K_S\rangle \otimes |K_S\rangle) \quad (23)$$

in which $R_L = -re^{-(i\Delta m + \Delta\Gamma/2)T}$, $R_S = re^{(i\Delta m + \Delta\Gamma/2)T}$. The state Φ , which is nonmaximally entangled, encompasses all pairs of kaons wherein both the left and right partners persist until the common proper time T . Due to the specific normalization of Φ , kaon pairs exhibiting decay of one or both members prior to time T need to be identified and excluded. This exclusion occurs before any measurement utilized in a Bell-type test, rendering this approach a “preselection” procedure rather than a “postselection” one, thereby avoiding any conflicts between local realism and quantum mechanics. Upon the establishment of the state $|\Phi\rangle$, it becomes essential to examine alternative joint measurements on each corresponding pair of kaons when conducting a Bell-type test.

5. Decoherence effects on entangled kaons

Exploring the factors that could potentially lead to decoherence of entangled kaons is of high importance [21, 28–31]. Besides, the decoherence allows us to gather insights into the quality of the entangled state. In the subsequent analysis, we explore potential decoherence effects that may arise from interactions between the quantum “system” and its surrounding “environment,” as shown in **Figure 2**. Decoherence effects are mainly divided into two groups: standard and nonstandard [21]. Examples of “standard” decoherence effects can be found in various sources, including:

- Strong interaction scatterings of kaons with nucleons
- Weak interaction decays
- Noise from the experimental setup

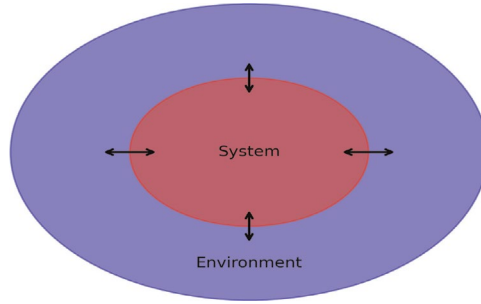


Figure 2.
 The overall system can be divided into two components: the system of interest, referred to as the “system”, and the surrounding “environment”.

Nonstandard decoherence effects are due to the fundamental modifications of quantum mechanics, such as:

- Influence of quantum gravity [32–34]
- Quantum fluctuations in the space-time structure at Planck mass scale [35]
- Dynamical state-reduction theories [36]

5.1 Density matrix description of entangled kaon system

We will now delve into the decoherence model within the Hilbert space $\mathcal{H} = \mathbb{C}^2$, which represents a two-dimensional complex vector space. Our analysis will specifically focus on the usual effective mass Hamiltonian, as denoted by Eq. (5). Here, it is supposed that CP invariance is not violated as in the case of CPLEAR experiment [12], whose data are not sensitive to the impacts of CP violation. Therefore, $p = q = 1$ meaning that

$$|K_1^0\rangle \equiv |K_S\rangle, \quad |K_2^0\rangle \equiv |K_L\rangle, \quad \langle K_S|K_L\rangle = 0 \quad (24)$$

We can effectively track the evolution of the density operator ρ by employing the so-called Gorini-Kossakowski-Sudarshan-Lindblad equation representing the dynamics of a subsystem within a Markovian system as the entire system expressed as [37],

$$\dot{\rho}(t) = \mathcal{L}\rho(t) = -i(H\rho(t) - \rho(t)H^\dagger) + \underbrace{\sum_j \left(L_j \rho(t) L_j^\dagger - \frac{1}{2} \{ L_j^\dagger L_j, \rho(t) \} \right)}_{\mathcal{D}(\rho)} \quad (25)$$

in which \mathcal{L} is the Liouville superoperator, and L_j is the Lindblad (or jump) operator. The effect of decoherence is added by the dissipation term $\mathcal{D}(\rho)$, for which we consider the following ansatz [30],

$$\mathcal{D}(\rho) = \frac{\lambda}{2} \sum_j [P_j, [P_j, \rho]] \quad \text{with} \quad P_j = |K_j\rangle\langle K_j|, \quad j = S, L \quad (26)$$

where $\lambda \geq 0$ is the decoherence parameter. Eq. (26) shows a special case of dissipation where $L_j = \sqrt{\lambda}P_j$. Therefore, for the elements of the density operator $\rho(t) = \sum_{i,j=S,L} \rho_{ij}(t) |K_i\rangle\langle K_j|$, we attain

$$\begin{aligned}\rho_{SS}(t) &= \rho_{SS}(0)e^{-\Gamma_S t} \\ \rho_{LL}(t) &= \rho_{LL}(0)e^{-\Gamma_L t} \\ \rho_{LS}(t) &= \rho_{LS}(0)e^{-i(m_L - m_S) - \Gamma - \lambda)t}\end{aligned}\quad (27)$$

where $\Gamma = \frac{1}{2}(\Gamma_S + \Gamma_L)$.

Consider the maximally entangled state Eq. (20) at initial time $t = 0$ as

$$|\psi^-\rangle = \frac{1}{\sqrt{2}}(|e_1\rangle - |e_2\rangle) \quad (28)$$

where $|e_1\rangle = |K_S\rangle_l \otimes |K_L\rangle_r$ and $|e_2\rangle = |K_L\rangle_l \otimes |K_S\rangle_r$. The total system Hamiltonian is then described by a tensor product of the one-particle Hilbert spaces as $H = H_l \otimes I_r + I_l \otimes H_r$ with l and r denoting the direction of the moving particles. The state in Eq. (28) is a Bell state [38–40] and is equivalently expressed by the density operator

$$\rho(0) = \frac{1}{2}(|e_1\rangle\langle e_1| + |e_2\rangle\langle e_2| - |e_1\rangle\langle e_2| - |e_2\rangle\langle e_1|) \quad (29)$$

In this case, the projectors are $P_1 = |e_1\rangle\langle e_1|$ and $P_2 = |e_2\rangle\langle e_2|$, which project to the eigenstates of two-particle Hamiltonian. Therefore, the element-wise time evolution obtained from Eq. (25) with the ansatz Eq. (26) is expressed as

$$\begin{aligned}\dot{\rho}_{ij}(t) &= -2\Gamma\rho_{ij}(t) & \text{for } i = j : \rho_{ij}(t) &= \rho_{ij}(0)e^{-2\Gamma t} \\ \dot{\rho}_{ij}(t) &= -(2\Gamma + \lambda)\rho_{ij}(t) & \text{for } i \neq j : \rho_{ij}(t) &= \rho_{ij}(0)e^{-(2\Gamma + \lambda)t}\end{aligned}\quad (30)$$

From Eq. (29), we already know $\rho_{11}(0) = \rho_{22}(0) = \frac{1}{2}$ and $\rho_{12}(0) = \rho_{21}(0) = -\frac{1}{2}$. As a result, we acquire the time-varying density operator as the following:

$$\rho(t) = \frac{1}{2}e^{-2\Gamma t}(|e_1\rangle\langle e_1| + |e_2\rangle\langle e_2| - e^{-\lambda t}(|e_1\rangle\langle e_2| + |e_2\rangle\langle e_1|)) \quad (31)$$

From Eq. (25), it follows that $\rho(t) = e^{\mathcal{L}t}\rho(0)$. This means that the initial state $\rho(0)$ is transformed to $\rho(t)$ by the completely positive and trace-preserving (CPTP) map $\mathcal{V}(t) = e^{\mathcal{L}t}$ generated by the superoperator \mathcal{L} [41, 42]. Note that while $\mathcal{V}(t)$ should satisfy trace-preserving characteristics, the non-Hermitian nature of the system Hamiltonian results in a deviation from the property of trace preservation. Specifically, we observe that $\text{tr}(\rho(0)) = 1$ but $\text{tr}(\rho(t)) = e^{-2\Gamma t}$, in other words, $\text{tr}(\dot{\rho}(t)) \neq 0$. The issue arising from the non-Hermitian Hamiltonian in this particular system has been addressed in previous studies [43, 44]. By introducing certain modifications to the Hilbert space and the dynamical equation, one can effectively work with this Hamiltonian. Therefore, the Hilbert space \mathcal{H} of the system is extended by adding the Hilbert space \mathcal{H}_0 which corresponds to the decay states resulting from the dissipation, so $\mathcal{H}_{\text{tot}} = \mathcal{H} \oplus \mathcal{H}_0$. By using the effective mass Hamiltonian defined in Eq. (5), the dynamical equation is then expressed as

$$\dot{\rho}(t) = -i[M, \rho(t)] - \left\{ \frac{1}{2} \Gamma, \rho(t) \right\} \quad (32)$$

Let define $B : \mathcal{H} \rightarrow \mathcal{H}_0$, and $\Gamma = B^\dagger B$, then we obtain $\text{tr}(\dot{\rho}) = -\text{tr}(B^\dagger B \rho(t)) \neq 0$. By adding $B\rho(t)B$ to Eq. (32), such that $\dot{\rho}(t) = -i[M, \rho(t)] - \left\{ \frac{1}{2} \Gamma, \rho(t) \right\} + B\rho(t)B$, then $\text{tr}(\dot{\rho}(t)) = 0$, meaning that the trace of $\rho(t)$ is preserved.

5.1.1 Purity

Decoherence arises exclusively from the influence of the factor $e^{-\lambda t}$ on the off-diagonal elements. Hence, for $t = 0$, the density operator corresponds to a pure state; however, for $t > 0$ and $\lambda \neq 0$, the state $\rho(t)$ does not exhibit a pure state anymore. As time elapses and environmental factors come into play, the quantum effects, characterized by coherences, gradually fade away, giving rise to the phenomenon of decoherence.

In quantum mechanics, and particularly in the field of quantum information theory, the purity of a quantum state described by the density operator is defined as $\mathcal{P}(t) = \text{tr}(\rho^2(t))$. The purity expresses a measure of quantum states and provides information regarding the degree of mixture in a given state. Here, the purity of $\rho(t)$ is [31],

$$\mathcal{P}(t) = \frac{1}{2} e^{-4\Gamma t} (1 + e^{-2\lambda t}) \quad (33)$$

that is, for $t = 0$, $\mathcal{P}(t) = 1$, and for $t > 0$, $\mathcal{P}(t) < 1$. We can conclude that the evolution of $\rho(t)$ transfers from a pure state to a mixed state is due to the occurrence of decoherence phenomenon. In addition, the purity of a normalized quantum state satisfies $\frac{1}{2} \leq \mathcal{P}(t) \leq 1$ for a state defined upon a two-dimensional Hilbert space. However, in this case, the value of $\mathcal{P}(t)$ can be less than $\frac{1}{2}$. It happens when one of the conditions of the density operator is not satisfied for $t > 0$, that is, $\text{tr}(\rho(t)) \neq 1$.

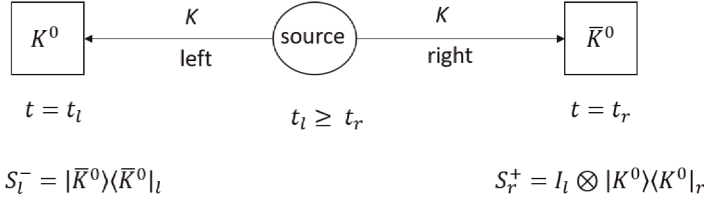
5.2 Decoherence parameter associated with entangled kaon system

In the CPLEAR experiment, as described in [12], entangled kaons are generated. Subsequently, the strangeness content (S) of the right-moving and left-moving particles is measured at time $t = t_r$ and $t = t_l$, respectively. Consider a specific scenario where the detection reveals that a \bar{K}^0 is observed at the right side at time $t = t_r$, while a K^0 is detected at the left side at time $t = t_l$, where $t_r \leq t_l$. We indicate two operators S_r^+ and S_l^- to represent the measurement of strangeness at the right and left sides, respectively (see **Figure 3**). After the measurement occurred at the right side, the density operator of the left-moving particle turned out to be.

$$\rho_l(t = t_r; t_r) = \text{tr}_r(S_r^+ \rho(t_r)) \quad (34)$$

From here, the probability of this case becomes [31],

$$P(\bar{K}^0, t_l; K^0, t_r) = \text{tr}(S_l^- \rho_l(t_l; t_r)) = \text{tr}(\text{tr}_r(S_r^+ \rho(t_r))) \quad (35)$$


Figure 3.

We consider a case that \bar{K}^0 and K^0 are detected at the right side at $t = t_r$ and left side at $t = t_l$, respectively, where $t_l \geq t_r$. The operators S_r^+ and S_l^- correspond to strangeness measurement at the right and left sides.

In the following, we obtain $P(\bar{K}^0, t_l; K^0, t_r)$. For the other cases, the same procedure can be employed. In order to determine Eq. (35), one can use $|K_S\rangle$ and $|K_L\rangle$ as the basis and write Eq. (34) as

$$\rho_l(t = t_r; t_r) = \frac{1}{4} e^{-2\Gamma t_r} (|K_S\rangle\langle K_S|_l + |K_L\rangle\langle K_L|_l - e^{-\lambda t_r} (|K_S\rangle\langle K_L|_l + |K_L\rangle\langle K_S|_l)) \quad (36)$$

Suppose the density operator related to a left-moving particle is expressed as

$$\begin{aligned} \rho_l(t; t_r) = & \rho_{SS}(t; t_r) |K_S\rangle\langle K_S|_l + \rho_{SL}(t; t_r) |K_S\rangle\langle K_L|_l \\ & + \rho_{LS}(t; t_r) |K_L\rangle\langle K_S|_l + \rho_{LL}(t; t_r) |K_L\rangle\langle K_L|_l \end{aligned} \quad (37)$$

which is supposed to evade decoherence for the time interval $t > t_r$. Therefore, it evolves according to $\dot{\rho}_l(t; t_r) = -i(H\rho_l(t; t_r) - \rho_l(t; t_r)H^\dagger)$. Hence, the following equation is obtained

$$\begin{aligned} \dot{\rho}_l(t; t_r) = & -\Gamma_S \rho_{SS}(t; t_r) |K_S\rangle\langle K_S|_l + (i\Delta m - \Gamma) \rho_{SL}(t; t_r) |K_S\rangle\langle K_L|_l \\ & - (i\Delta m + \Gamma) \rho_{LS}(t; t_r) |K_L\rangle\langle K_S|_l - \Gamma_L \rho_{LL}(t; t_r) |K_L\rangle\langle K_L|_l \end{aligned} \quad (38)$$

Let us assume that C_{ij} with $i, j = S, L$ is constant, so

$$\begin{aligned} \rho_{SS}(t; t_r) &= C_{SS} e^{-\Gamma_S t}, & \rho_{LL}(t; t_r) &= C_{LL} e^{-\Gamma_L t}, \\ \rho_{SL}(t; t_r) &= C_{SL} e^{(i\Delta m - \Gamma)t}, & \rho_{LS}(t; t_r) &= C_{LS} e^{-(i\Delta m + \Gamma)t} \end{aligned} \quad (39)$$

From our knowledge of Eqs. (36) and (37), the values of C_{ij} and subsequently $\rho_{ij}(t; t_r)$ can be obtained. Finally, by replacing $t = t_l$, we attain $P(\bar{K}^0, t_l; K^0, t_r)$.

Explicitly, by assuming that $\Delta t = t_l - t_r$, we have the following results

$$\begin{aligned} P(K^0, t_l; \bar{K}^0, t_r) &= P(\bar{K}^0, t_l; K^0, t_r) \\ &= \frac{1}{8} e^{-2\Gamma t_r} (e^{-\Gamma_S \Delta t} + e^{-\Gamma_L \Delta t} + 2e^{-\lambda t_r} \cos(\Delta m \Delta t) e^{-\Gamma \Delta t}) \end{aligned} \quad (40)$$

$$\begin{aligned} P(K^0, t_l; K^0, t_r) &= P(\bar{K}^0, t_l; \bar{K}^0, t_r) \\ &= \frac{1}{8} e^{-2\Gamma t_r} (e^{-\Gamma_S \Delta t} + e^{-\Gamma_L \Delta t} - 2e^{-\lambda t_r} \cos(\Delta m \Delta t) e^{-\Gamma \Delta t}) \end{aligned} \quad (41)$$

Let consider $\Delta t = 0$, that is, $t_l = t_r = t$, then from Eq. (40), one obtains

$$P(K^0, t_l; \bar{K}^0, t_r) = P(\bar{K}^0, t_l; K^0, t_r) = \frac{1}{4}e^{-2\Gamma t}(1 - e^{-\lambda t}) \quad (42)$$

which is in contradiction to the pure quantum mechanical EPR-correlations. The asymmetry of probabilities is the captivating factor of interest, as it directly responds to the interference term and can be quantified by means of experimental measurements. In the realm of pure quantum mechanics, where a system does not experience decoherence, we encounter this phenomenon by A^{QM} expressed as

$$\begin{aligned} A^{QM}(t_l, t_r) &= \frac{P(K^0, t_l; \bar{K}^0, t_r) + P(\bar{K}^0, t_l; K^0, t_r) - P(K^0, t_l; K^0, t_r) - P(\bar{K}^0, t_l; \bar{K}^0, t_r)}{P(K^0, t_l; \bar{K}^0, t_r) + P(\bar{K}^0, t_l; K^0, t_r) + P(K^0, t_l; K^0, t_r) + P(\bar{K}^0, t_l; \bar{K}^0, t_r)} \\ &= \frac{\cos(\Delta m \Delta t)}{\cosh\left(\frac{1}{2}\Delta\Gamma\Delta t\right)} \end{aligned} \quad (43)$$

in which $\Delta\Gamma = \Gamma_L - \Gamma_S$. In the decoherence model of entangled kaon system, since it is not known which particle will first be detected, t_r in Eqs. (40) and (41) need to be replaced by $\tau = \min(t_r, t_l)$. By inserting Eqs. (40) and (41), we obtain

$$A^\lambda(t_l, t_r) = A^{QM}(t_l, t_r)e^{-\lambda\tau} \quad (44)$$

which indicates that the decoherence effect represented by $e^{-\lambda\tau}$ is dependent on the time of the first detected kaon.

The decoherence model in Eq. (44) can be introduced in a phenomenological way, where the decoherence parameter λ corresponds to an effective decoherence parameter ζ as $\zeta(t_l, t_r) = 1 - e^{-\lambda\tau}$. Apparently, the value of $\zeta = 0$ represents pure quantum mechanics and $\zeta = 1$ corresponds to complete decoherence or spontaneous factorization of the wave function (Schrödinger-Furry hypothesis). By means of standard least squares method [45, 46], $\zeta = 0.13 \pm 0.865$ is obtained in [31], which is in agreement with the results obtained from the effective variance method, where $\zeta = 0.13^{+0.16}_{-0.15}$ [47, 48] correspondent to $\lambda = (1.84^{+2.17}_{-2.50}) \times 10^{-12} \text{MeV}$. The value of both parameters is compatible with quantum mechanics, that is, $\zeta = 0$ and $\lambda = 0$ far away from the total decoherence, that is, $\zeta = 1$ or $\lambda = \infty$. It indicates that the interaction between the system and its environment has negligible influence on the system. As a result, the quantum properties related to the entanglement of the strangeness are preserved without significant alteration.

6. Loss of entanglement

As time progresses, the degree of decoherence in the initially fully entangled $K^0\bar{K}^0$ system increases, leading to a decrease in the system's entanglement. This loss of entanglement, defined as the disparity between an entanglement value and its maximum unity, can be precisely measured [21, 49]. In the realm of quantum information, the quantification of entanglement in a state is assessed by employing specific measures designed for quantifying entanglement. In this context, entropy plays a pivotal

role. The entropy serves as a measure of the level of uncertainty or lack of knowledge associated with a quantum state. If the quantum state is pure, maximum information about the system is provided; however, mixed states only offer partial information. The entropy quantifies the extent to which maximal information is absent. In the following, we focus on the three most important and widely used entanglement measures: Von Neumann entanglement entropy, entanglement of formation, and concurrence. When the interest is focused on the effect of decoherence, one needs to compensate for the decay up to time t to attain a proper density operator for the kaon system. Therefore, we divide the state Eq. (31) with its trace, that is,

$$\rho_N(t) = \frac{\rho(t)}{\text{tr}(\rho(t))}.$$

6.1 Von Neumann entanglement entropy

Von Neumann's entropy of the quantum state is expressed as

$$S(\rho_N(t)) = -\text{tr}(\rho_N(t) \log_d \rho_N(t)) \quad (45)$$

where d is the dimension of the Hilbert space, that is, for the Hilbert space of a qubit $d = 2$, hence $0 < S(\rho_N(t)) < 1$. For $t = 0$, the entropy is zero, meaning that the state is pure and also maximally entangled. However, as $t \rightarrow \infty$, the entropy approaches to one, that is, the system becomes mixed. The von Neumann entropy is a good criterion of entanglement, specifically for pure quantum states [21, 30, 50].

The bipartite von Neumann entanglement of its reduced states [51]. This entropy can be defined as the von Neumann entropy of any of its reduced states. This definition holds true because both reduced states have the same value, as can be demonstrated through the Schmidt decomposition of the state with respect to the bipartition. Consequently, the outcome remains unchanged regardless of the specific reduced state chosen. Generally, two subsystems are maximally entangled when their reduced density operators are maximally mixed. In our case, the left- (subsystem l) and right- (subsystem r) propagating kaons are our subsystems. Therefore, the reduced density operators are defined as

$$\rho_N^l(t) = \text{tr}_r(\rho_N(t)), \quad \rho_N^r(t) = \text{tr}_l(\rho_N(t)) \quad (46)$$

The von Neumann entropy of $\rho_N^l(t)$ (or $\rho_N^r(t)$) provides the uncertainty in the subsystem l (or r) before measuring the subsystem r (or l). In the case of the kaon system, we have

$$S(\rho_N^l(t)) = S(\rho_N^r(t)) = 1 \quad \forall t \geq 0 \quad (47)$$

which are independent of the decoherence parameter λ , meaning that the correlation stored in the entire system is lost to the environment and not to the subsystems.

6.2 Entanglement of formation

Entanglement entropy is also known as the entanglement of formation for pure states. It is possible to express any density matrix as a collection of pure states forming an ensemble $\rho_i = |\psi_i\rangle\langle\psi_i|$, with each pure state having a corresponding probability p_i ,

that is $\rho = \sum_i p_i \rho_i$. For mixed states, entanglement of formation can be generalized by defining a quantity minimized over all the ensemble realizations of the mixed state. For the kaon system, we have

$$E_f(\rho) = \min \sum_i p_i S(\rho_i^l) \quad (48)$$

The entanglement of formation can be simplified to $E_f(\rho) \geq \mathcal{E}(f(\rho))$ by introducing the lower bound of $E_f(\rho)$, given by

$$\begin{aligned} \mathcal{E}(f(\rho)) &= H\left(\frac{1}{2} + \sqrt{f(\rho)(1-f(\rho))}\right) \quad \text{for } f(\rho) \geq \frac{1}{2} \\ \mathcal{E}(f(\rho)) &= 0 \quad \text{for } f(\rho) < \frac{1}{2} \end{aligned} \quad (49)$$

where $f(\rho) = \max \langle e | \rho | e \rangle$, known as the fully entangled fraction of ρ , is the maximum overall completely entangled states $|e\rangle$, and

$$H(x) = -x \log_2 x - (1-x) \log_2 (1-x). \quad (50)$$

For our model, the lower bound expressed for $E_f(\rho)$ is saturated, that is, $E_f(\rho) = \mathcal{E}(f(\rho))$. Therefore, one can calculate the entanglement of formation simply by computing $\mathcal{E}(f(\rho))$ [21].

The fully entangled fraction of $\rho_N(t)$ is $f(\rho_N(t)) = \frac{1}{2}(1 + e^{-\lambda t}) \geq 0$. Therefore, the entanglement of formation for the $K^0 \bar{K}^0$ is assessed in terms of $E_f(\lambda)$ as

$$E_f(\lambda) = -\frac{1 + \sqrt{1 - e^{-2\lambda t}}}{2} \log_2 \frac{1 + \sqrt{1 - e^{-2\lambda t}}}{2} - \frac{1 - \sqrt{1 - e^{-2\lambda t}}}{2} \log_2 \frac{1 - \sqrt{1 - e^{-2\lambda t}}}{2} \quad (51)$$

From which one can obtain the entanglement loss $L_E(t)$ as

$$\begin{aligned} L_E(t) &= 1 - E(\rho_N(t)) \\ &\simeq \frac{\lambda}{\ln 2} t = \frac{1}{\ln 2} \xi(t) = 1.44 \xi(t) \end{aligned} \quad (52)$$

approximated for small values of λ . Eq. (52) shows that the entanglement loss equals the weighted amount of decoherence.

6.3 Concurrence

Wootters and Hill, in their research publications [52–54], discovered a relation between entanglement of formation and a measure known as concurrence. This connection allows the expression of entanglement of formation for a general mixed state ρ of two qubits in terms of the concurrence as

$$E_f(\rho) = \mathcal{E}(C(\rho)) = H\left(\frac{1}{2} + \frac{1}{2} \sqrt{1 - C^2(\rho)}\right) \quad (53)$$

with $0 \leq C(\rho) \leq 1$. As The function $\mathcal{E}(C(\rho))$ is monotonically increasing from 0 to 1 as $C(\rho)$ goes from 0 to 1.

The concurrence $C(\rho)$ is defined as $C(\rho) \equiv \max \{0, \lambda_1 - \lambda_2 - \lambda_3 - \lambda_4\}$ with λ_i 's representing the square roots of the eigenvalues, in decreasing order, of $R = \rho \tilde{\rho}$ matrix where $\tilde{\rho}$ is the spin-flipped state of ρ defined as

$$\tilde{\rho} = (\sigma_y \otimes \sigma_y) \rho^* (\sigma_y \otimes \sigma_y) \quad (54)$$

The complex conjugate of ρ , that is, ρ^* is taken in the basis $\{|\uparrow\uparrow\rangle, |\uparrow\downarrow\rangle, |\downarrow\uparrow\rangle, |\downarrow\downarrow\rangle\}$. In our model, since $\rho_N(t)$ is not variant under spin flip, hence $R = \rho_N^2$, and the concurrence is

$$C(\rho_N(t)) \equiv \max \{0, e^{-\lambda t}\} = e^{-\lambda t} \quad (55)$$

Hence, $L_C(t)$ is computed as

$$L_C(t) = 1 - C(\rho_N(t)) = 1 - e^{-\lambda t} = \xi(t) \quad (56)$$

The value of $L_C(t)$ is precisely equivalent to decoherence $\xi(t)$, describing the factorization of the initial spin-singlet state to the state $|K_S\rangle_l \otimes |K_L\rangle_r$ or $|K_S\rangle_l \otimes |K_L\rangle_r$. In both cases, Eqs. (52) and (56) show that the loss of entanglement is equivalent to decoherence and increases linearly with time [30]. In **Figure 4**, we show the loss of information by the von Neumann entropy $S(\lambda)$ in comparison with the loss of entanglement of formation $L_E(t)$ depending on the normalized time τ of the propagating $K^0 \bar{K}^0$ system for the experimental mean value $\lambda = 1.84 \times 10^{-12} \text{ MeV}$, and the upper bound $\lambda = 4.34 \times 10^{-12} \text{ MeV}$ of the decoherence parameter. The rate of increase in the loss of entanglement of formation is slower as time progresses, indicating the amount of resources required to create a specific entangled state. In the overall state, the level of entanglement decreases until separability is achieved, which occurs exponentially fast as time approaches infinity. In the CPLEAR experiment, where the propagation of one kaon for 2 cm corresponds

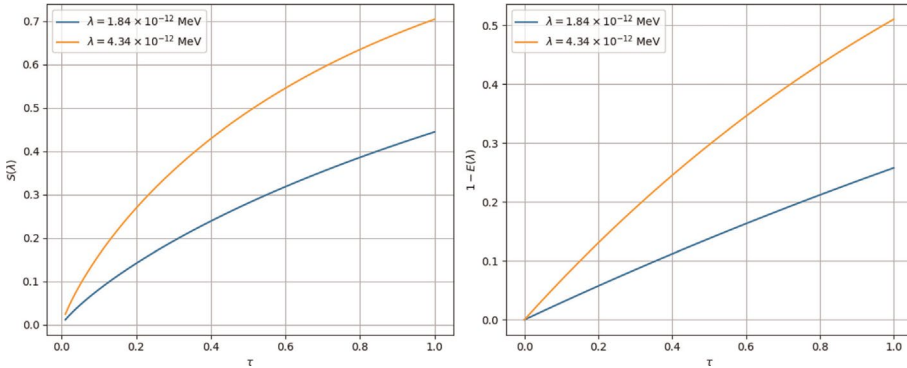


Figure 4. The time dependence of von Neumann entropy and the loss of entanglement of formation for two values of λ . The time t is normalized versus τ_S , that is, $\tau = \frac{t}{\tau_S}$.

to the propagation time $\tau = 0.55$, until an absorber measures it, the loss of entanglement is approximately 0.18 and 0.38 for the mean value and upper bound of λ , respectively.

7. Conclusions

This chapter has provided a comprehensive analysis of the properties and phenomena associated with neutral K-mesons, highlighting their intriguing and often puzzling behaviors. We began by emphasizing the significance of strangeness and charge parity violation in the understanding of these particles. Next, the concept of strangeness oscillations, exemplified by the oscillations between K^0 and \bar{K}^0 states, was introduced and thoroughly explored. We delved into the regeneration of K_S and unraveled the underlying mechanisms that govern these oscillations, shedding light on the intricate dynamics involved. Next, we examined the quasi-spin space and its bases, unraveling their implications and providing insights into the entangled states of kaon pairs, particularly focusing on both maximally and nonmaximally entangled neutral kaons. This exploration has broadened our understanding of the entanglement properties exhibited by these particles. Furthermore, we dedicated significant attention to the study of decoherence effects on entangled kaons. Through the use of density matrix formalism, we captured the dynamic nature of decoherence and introduced a dedicated parameter to quantify its impact. Measures such as von Neumann entanglement entropy, entanglement of formation, and concurrence were employed to explore the loss of entanglement, providing valuable tools for characterizing and quantifying entanglement in the context of neutral kaons. However, several intriguing questions for future research remain open.

8. Outlook

The study of kaon entanglement and decoherence raises a host of intriguing open questions that drive ongoing research and exploration. How do environmental interactions, such as scattering or absorption, impact the entanglement and coherence properties of neutral kaons? Can we develop methods to quantify and control these effects? Additionally, investigating entanglement dynamics in multipartite kaon systems, involving more than two neutral kaons, presents an exciting avenue of research. How does multipartite entanglement and its degradation relate to the underlying interactions and dynamics? Developing novel experimental techniques and theoretical models to explore these phenomena could shed light on the intricate nature of entanglement in kaon systems.

Furthermore, the generation and manipulation of entangled kaon states offer intriguing possibilities. Can we create specific entanglement patterns or preserve entanglement over extended timescales? Understanding and enhancing entanglement in kaon systems could have implications for quantum information processing and communication. The role of entanglement in comprehending and quantifying CP violation in kaon systems is another crucial aspect. How does entanglement contribute to our understanding of the underlying mechanisms driving CP violation? Exploring connections between the entanglement properties of neutral kaons and other areas of physics, such as quantum information theory, quantum field theory, or

quantum gravity, holds promise for uncovering fundamental principles and phenomena.

Additionally, the presence of decoherence poses significant challenges. How does decoherence affect the entanglement properties of neutral kaons? Can we develop techniques to mitigate or minimize its detrimental effects and preserve entanglement over longer durations? Exploring the entanglement and coherence properties of neutral kaons within nonstandard models beyond the Standard Model of particle physics could provide insights into new physics and phenomena. Moreover, extending the study of entanglement and decoherence to other meson systems or particles with similar characteristics is a compelling direction. How do the entanglement properties differ or align between different types of particles? Finally, experimental methodologies and theoretical frameworks for directly observing or measuring entanglement in kaon systems, as well as exploring the implications of entanglement for quantum computing and communication, open up exciting possibilities for practical applications in quantum technologies.

These open questions highlight the ongoing exploration and research endeavors, presenting intriguing avenues for further investigation and potential breakthroughs.

Acknowledgements

The authors gratefully acknowledge the financial support provided by the Foundation for Science and Technology (FCT/MCTES) within the scope of the PhD grant 2021.07608.BD, the Associated Laboratory ARISE (LA/P/0112/2020), the R&D Unit SYSTEC through Base (UIDB/00147/2020) and Programmatic (UIDP/00147/2020) funds and project RELIABLE - Advances in control design methodologies for safety-critical systems applied to robotics (PTDC/EEI-AUT/3522/2020), all supported by national funds through FCT/MCTES (PIDDAC). The work has been done in honor and memory of Professor Fernando Lobo Pereira.

Conflict of interest

The authors declare no conflict of interest.

Author details


Nahid Binandeh Dehaghani^{1*}, A. Pedro Aguiar¹ and Rafal Wisniewski²

1 Research Center for Systems and Technologies (SYSTEC), ARISE and the Electrical and Computer Engineering Department, Faculty of Engineering, University of Porto, Porto, Portugal

2 Department of Electronic Systems, Aalborg University, Aalborg, Denmark

*Address all correspondence to: nahid@fe.up.pt

IntechOpen

© 2023 The Author(s). Licensee IntechOpen. This chapter is distributed under the terms of the Creative Commons Attribution License (<http://creativecommons.org/licenses/by/3.0>), which permits unrestricted use, distribution, and reproduction in any medium, provided the original work is properly cited. 

References

- [1] Einstein A, Podolsky B, Rosen N. Can quantum-mechanical description of physical reality be considered complete? *Physical Review*. 1935; **47**:777-780. DOI: 10.1103/physrev.47.777
- [2] Schrödinger E. Die gegenwärtige situation in der Quantenmechanik. *Naturwissenschaften*. 1935; **23**:844-849. DOI: 10.1007/bf01491987
- [3] Bell JS. *Physics*. Reprinted in *JS Bell, Speakable and Unspeakable in Quantum Mechanics*. 2nd ed. Vol. 1. Cambridge University Press; 1964, 1987. pp. 195. DOI: 10.1017/CBO9780511815676
- [4] Clauser JF, Horne MA. Experimental consequences of objective local theories. *Physical Review D*. 1974; **10**:526. DOI: 10.1103/physrevd.10.526
- [5] Wigner EP. On hidden variables and quantum mechanical probabilities. In: *Part I: Particles and Fields. Part II: Foundations of Quantum Mechanics*. Berlin, Heidelberg: Springer-Verlag; 1997. pp. 515-523. DOI: 10.1007/978-3-662-09203-3_56
- [6] Aspect A, Dalibard J, Roger G. Experimental test of Bell's inequalities using time-varying analyzers. *Physical Review Letters*. 1982; **49**:1804. DOI: 10.1103/physrevlett.49.1804
- [7] Tittel W, Brendel J, Zbinden H, Gisin N. Violation of Bell inequalities by photons more than 10 km apart. *Physical Review Letters*. 1998; **81**:3563. DOI: 10.1103/physrevlett.81.3563
- [8] Feynman RP, Leighton RB, Sands M. *The Feynman Lectures on Physics*. Reading, MA: Addison-Wesley Pub. Co.; 1963. DOI: 10.1063/1.3051743
- [9] Lee TD. *Particle Physics and Introduction to Field Theory*. Chur, Switzerland: Harwood Academic Publishers; 1981. DOI: 10.1201/b16972-2
- [10] Okun LB. *Leptons and Quarks*. North-Holland: Elsevier; 2013. DOI: 10.1016/b978-0-444-86924-1.50031-3
- [11] Bernabeu J, Di Domenico A. Can future observation of the living partner post-tag the past decayed state in entangled neutral K mesons? *Physical Review D*. 2022; **105**:116004. DOI: 10.1103/physrevd.105.116004
- [12] Apostolakis A, Aslanides E, Backenstoss G, Bargassa P, Behnke O, Benelli A, et al. An EPR experiment testing the non-separability of the K0K0 wave function. *Physical Review B*. 1999; **422**:339-348. DOI: 10.1016/S0370-2693(97)01545-1
- [13] Bizzeti A. Recent results from the NA62 and NA48/2 experiments at CERN. *Nuclear and Particle Physics Proceedings*. 2023; **324**:113-118. DOI: 10.1016/j.nuclphysbps.2023.01.023
- [14] Aloisio A, Ambrosino F, Antonelli A, Antonelli M, Bacci C, Bencivenni G, et al. Recent results from KLOE at DAΦNE. *Nuclear Physics B – Proceedings Supplements*. 2002; **111**: 213-218. DOI: 10.1016/S0920-5632(02)01708-5
- [15] Gauzzi P, Perez del Rio E. The KLOE-2 experiment at DAΦNE. *EPJ Web Conference*. 2019; **212**:01002. DOI: 10.1051/epjconf/201921201002
- [16] Aaij R, Beaucourt L, Chefdeville M, Decamp D, Déléage N, et al. LHCb detector performance. *International Journal of Modern Physics A*. 2015; **30**:

1530022. DOI: 10.1142/S0217751X15300227

[17] Yamanaka T et al. The J-PARC KOTO experiment. *Progress of Theoretical and Experimental Physics*. 2012;**2012**:02B006. DOI: 10.1093/ptep/pts057

[18] Martin BR, Shaw G. *Particle Physics*. Chichester, United Kingdom: John Wiley & Sons; 2016. DOI: 10.1063/1.2808907

[19] Greaves H, Thomas T. *Studies in History and Philosophy of Science Part B: Studies in History and Philosophy of Modern Physics*. Vol. 45. Elsevier; 2014. pp. 46-65. DOI: 10.1016/j.shpsb.2013.10.001

[20] Griffiths D. *Introduction to Elementary Particles*. Wiley-VCH Verlag GmbH & Co. KGaA; 2004. DOI: 10.1002/9783527618460

[21] Bertlmann RA. Entanglement, Bell inequalities and decoherence in particle physics. *Quantum Coherence: From Quarks to Solids*. 2006;**2006**:1-45. DOI: 10.1007/11398448_1

[22] Pais A, Piccioni O. Note on the decay and absorption of the θ^0 . *Physical Review*. 1995;**100**:1487-1489. DOI: 10.1103/PhysRev.100.1487

[23] Lee TD, Wu CS. Weak interactions (second section) chapter 9: Decays of neutral K mesons. *Annual Review of Nuclear Science*. 1966;**16**:511-590. DOI: 10.1007/978-1-4612-5397-6_27

[24] Lipkin HJ. CP violation and coherent decays of kaon pairs. *Physical Review*. 1968;**176**:1715. DOI: 10.1103/physrev.176.1715

[25] Bramon A, Escribano R, Garbarino G. A review of Bell inequality

tests with neutral kaons. *Handbook on Neutral Kaon Interferometry at a Φ Factory*. 2007;**2007**:217-254

[26] Bruß D. Characterizing entanglement. *Journal of Mathematical Physics*. 2002;**43**:4237-4251. DOI: 10.1364/icqi.2001.t4

[27] Bramon A, Garbarino G, Hiesmayr BC. Quantum marking and quantum erasure for neutral kaons. *Physical Review Letters*. 2004; **92**:020405. DOI: 10.1103/physrevlett.92.020405

[28] Di Domenico A. Search for CPT violation and decoherence effects in the neutral kaon system. *Journal of Physics: Conference Series*. 2009;**171**:012008. DOI: 10.1088/1742-6596/171/1/012008

[29] Di Domenico A. Latest results on kaon physics at KLOE-2. *JACoW*. 2023; **eeFACT2022**:30-34. DOI: 10.18429/JACoW-eeFACT2022-TUXAS0101

[30] Bertlmann RA, Durstberger K, Hiesmayr BC. Decoherence of entangled kaons and its connection to entanglement measures. *Physical Review A*. 2003;**68**:012111. DOI: 10.1103/physreva.68.012111

[31] Syahbana A, Zen FP, Dwiputra D. Study of entangled K-meson and its decoherence. *Indonesian Journal of Physics*. 2022;**33**:39-44. DOI: 10.5614/itb.ijp.2022.33.1.4

[32] Rovelli C. *Quantum Gravity*. Cambridge, United Kingdom: Cambridge University Press; 2004. DOI: 10.1017/cbo9780511755804

[33] Kiefer C. *Why Quantum Gravity?* Berlin, Heidelberg: Springer-Verlag; 2007. DOI: 10.1093/acprof:oso/9780199212521.003.01

- [34] Gambini R, Porto RA, Pullin J. Fundamental decoherence from quantum gravity: A pedagogical review. *General Relativity and Gravitation*. 2007;**39**:1143-1156. DOI: 10.1007/s10714-007-0451-1
- [35] Sivaram C. What is special about the planck mass? arXiv Preprint. 2007. DOI: 10.48550/arXiv.0707.0058
- [36] Pearle P. Combining stochastic dynamical state-vector reduction with spontaneous localization. *Physical Review A*. 1989;**39**:2277. DOI: 10.1103/physreva.39.2277
- [37] Dehaghani NB, Pereira FL, Aguiar AP. Quantum control modelling, methods, and applications. *Extensive Reviews*. 2022;**2**:75-126. DOI: 10.21467/exr.2.1.5037
- [38] Nielsen MA, Chuang IL. *Quantum Computation and Quantum Information*. Cambridge: Cambridge University Press; 2010. DOI: 10.1017/cbo9780511976667
- [39] Kurgalin S, Borzunov S. *Concise Guide to Quantum Computing*. Switzerland: Springer; 2021. DOI: 10.1007/978-3-030-65052-0
- [40] Zaman F, Jeong Y, Shin H. Counterfactual Bell-state analysis. *Scientific reports*. 2018;**8**:14641. DOI: 10.1038/s41598-018-32928-8
- [41] Breuer HP, Petruccione F. *The Theory of Open Quantum Systems*. USA: Oxford University Press; 2007. DOI: 10.1093/acprof:oso/9780199213900.001.0001
- [42] Manzano D. A short introduction to the Lindblad master equation. *AIP Advances*. 2020;**2020**:10. DOI: 10.1063/1.5115323
- [43] Caban P, Rembieliński J, Smoliński KA, Walczak Z. Unstable particles as open quantum systems. *Physical Review A*. 2005;**72**:032106. DOI: 10.1103/physreva.72.032106
- [44] Bertlmann RA, Grimus W, Hiesmayr BC. Open-quantum-system formulation of particle decay. *Physical Review A*. 2006;**73**:054101. DOI: 10.1103/physreva.73.054101
- [45] Barlow RJ. *Statistics: A Guide to the Use of Statistical Methods in the Physical Sciences*. Chichester: Wiley; 1993. DOI: 10.2307/1269014
- [46] Bevan A. *Statistical Data Analysis for the Physical Sciences*. New York: Cambridge University Press; 2013. DOI: 10.1017/CBO9781139342810
- [47] Bertlmann RA, Grimus W, Hiesmayr BC. Quantum mechanics, Furry's hypothesis, and a measure of decoherence in the K0 system. *Physical Review D*. 1999;**60**:114032. DOI: 10.1103/physrevd.60.114032
- [48] Bertlmann RA, Zeilinger A. *Quantum [Un]Speakables II. The Frontiers Collection*. 2017
- [49] Hiesmayr BC. *The Puzzling Story of the Neutral Kaon System: Or What We Can Learn from Entanglement* [Ph.D. thesis]. Austria: University of Vienna; 2002
- [50] Varizi AD. *Open Quantum System Approach to Neutral Kaon Interferometry* [Ph.D. thesis]. Brazil: Universidade Federal de Minas Gerais; 2017
- [51] Bennett CH, DiVincenzo DP, Smolin JA, Wootters WK. Mixed-state entanglement and quantum error correction. *Physical Review A*. 1996;**54**:3824. DOI: 10.1103/physreva.54.3824

[52] Wootters WK. Entanglement of formation of an arbitrary state of two qubits. *Physical Review Letters*. 1998;**80**: 2245. DOI: 10.1103/physrevlett.80.2245

[53] Hill SA, Wootters WK. Entanglement of a pair of quantum bits. *Physical Review Letters*. 1997;**78**:5022. DOI: 10.1103/physrevlett.78.5022

[54] Wootters WK. Entanglement of formation and concurrence. *Quantum Information and Computation*. 2001;**1**: 27-44. DOI: 10.26421/qic1.1-3

Section 3

Interdisciplinarity

Perspective Chapter: Why Do We Care about Violating Bell Inequalities?

Christopher G. Timpson

Abstract

High energy experiments present an exciting new regime in which to explore the violation of Bell inequalities by nature. There are two main reasons why one is interested in Bell inequality violation. The first is that—for suitable experimental configurations—Bell inequality violation can indicate the failure of the condition of *Local Causality*, which condition is a natural way of capturing the desideratum of no superluminal action-at-a-distance. The second is that Bell inequality violation is an *Entanglement Witness*. I review both of these reasons for interest, and suggest that high energy experiments plausibly involve the latter rather more than the former, at least as currently configured.

Keywords: Bell inequality, entanglement witness, high energy, local causality, nonlocality

1. Introduction

Recently there have been both a number of proposals for, and actual experimental tests of, Bell inequality violation in high energy experiments (see e.g., [1–3]). This is an important new regime for exploring entanglement and Bell inequality violation, involving very different length-scales from the current state of the art in Bell experiments (compare [4]). It offers the promise of new insights into quantum correlations and entanglement at the femtometre scale, and will help us in our concrete understanding of the behaviour of relativistic quantum fields.

But at the same time, it is noteworthy that despite its now being nearly 60 years since Bell's seminal paper [5], and despite the award of the 2022 Nobel prize to Aspect, Clauser and Zeilinger for their experimental work demonstrating Bell inequality violation, there is still considerable controversy over what Bell inequality violation really means, and why we should care about it [6, 7].

Here I will review the meaning of Bell inequalities and the significance of their violation, distinguishing two distinct broad areas of interest:

1. Tests of whether the world is nonlocal, or more precisely, is not *locally causal* [8], and

2. Tests of whether a multipartite system described by quantum mechanics is in an entangled state or not (that is, the use of Bell inequalities as *entanglement witnesses* [9]).

In the high energy Bell tests, the latter notion is certainly in play and it is important. As we shall see, however, it is an open question the extent to which the criteria for providing a test of the first kind are satisfied in high energy experiments.

2. Bell correlations and entangled states

For Schrödinger, entanglement was *the* characteristic feature of quantum theory, that feature which ‘enforces its entire departure from classical lines of thought’ [10]. Feynman, by contrast, insisted that it was the concept of superposition, as manifested in the two-slit experiment, that was ‘the heart of quantum mechanics. In reality, it contains the only mystery ...’ [11]. Reassuringly, we need not see these two claims as being as much in dispute as one might initially suppose: for entanglement can be understood simply as genuinely multi-particle superposition.

Thus, given some system A with a Hilbert space \mathcal{H}_A and a set of basis states $\{|\phi_i\rangle \in \mathcal{H}_A\}$, $\langle \phi_i | \phi_j \rangle = \delta_{ij}$, then A is in a superposition with respect to that basis *iff* its state vector $|\psi\rangle \in \mathcal{H}_A$ is given by:

$$|\psi\rangle = \sum_i c_i |\phi_i\rangle, \quad (1)$$

where more than one of the coefficients c_i is non-zero.

Now consider a second system, B , with \mathcal{H}_B ; $\{|\chi_j\rangle \in \mathcal{H}_B\}$, $\langle \chi_j | \chi_k \rangle = \delta_{jk}$. The pair of systems AB will be (pure state) entangled *iff* their joint state $|\Psi\rangle \in \mathcal{H}_A \otimes \mathcal{H}_B$ *cannot* be written as a product, i.e.:

$$|\Psi\rangle \neq |\phi\rangle |\chi\rangle, \quad (2)$$

for any $|\phi\rangle, |\chi\rangle$ in $\mathcal{H}_A, \mathcal{H}_B$, respectively. If the joint state *could* be written as a product $|\phi\rangle |\chi\rangle$, then even though $|\phi\rangle$ might be a superposition with respect to some basis of interest for \mathcal{H}_A , and $|\chi\rangle$ might be a superposition with respect to some basis of interest for \mathcal{H}_B , we would not have *multiparticle* superposition: each particle individually would merely be in its own superposition. By contrast if we have a state of the form:

$$|\Psi\rangle = \sum_i c_i |\phi_i\rangle |\chi_i\rangle, \quad (3)$$

with more than one c_i non-zero, then it cannot be written as a product, and we have genuinely multiparticle superposition: a superposition of the product basis $|\phi_i\rangle |\chi_i\rangle$ for the two systems.

We can immediately see that something interesting is going on with an entangled state like (3).

Take a somewhat simplified case for illustrative purposes: suppose the states $|\phi_i\rangle$ corresponded to states with compact spatial support within a small width Δ around a location which is i units along the x -axis (with a unit length being $> 2\Delta$, say), and similarly, suppose that the states $|\chi_i\rangle$ corresponded to states with the same width but at a location $i + 2$ units along the x -axis. Then if we think that being in an eigenstate of the operator corresponding to some physical quantity is both necessary and sufficient for a system's having a definite value of that property, our pair of systems in the state given by (3) will definitely be two units of length apart from one another, whilst neither system A , nor system B , individually has any definite location of its own. This is a very striking, and non-classical, kind of holism about quantum property possession: the properties possessed by the whole system are not determined by properties possessed by the sub-systems, even for such a simple and important property as position. To take another, very familiar, example, consider the singlet state of a pair of spin-half particles:

$$|\Psi^-\rangle = \frac{1}{\sqrt{2}}(|\uparrow\rangle|\downarrow\rangle - |\downarrow\rangle|\uparrow\rangle). \quad (4)$$

This is of the form (3) and clearly an entangled state. In this case, the two spins are definitely in opposite directions, without there being a fact about which direction, if any, each individual spin is pointing in. Again: we have properties of the whole which are not determined by the properties of the parts, in a way which is not possible classically.

Even if we do not think that a system's being in an eigenstate of the operator corresponding to some quantity implies that the system actually has a definite value of that quantity, but (as in some approaches to understanding quantum theory, e.g. [12]) restrict ourselves to the weaker claim that it merely implies that a suitable measurement interaction will give a particular result with probability one, entangled states remain strikingly non-classical and of great interest. An entangled state such as (3) is a pure state of the theory: it is not composed (in the theory) of a statistical mixture of more fine-grained states. Yet it will both give rise to non-trivial probabilities (i.e. those other than 0 and 1) for all observables for each system taken individually, whilst also providing *correlations* between measurement results on the two sides. This is not possible classically: in a classical probabilistic theory, pure states cannot give rise to correlations. (Consider two classical bits: we can only make a correlated state by producing a mixture of two of the pairs of bit values, e.g. by tossing a fair coin and producing (pure) bit values 01 on heads and 10 on tails, say).

The definition of pure state entanglement above can be generalised in two different directions: we can define entanglement for non-pure, i.e., mixed states, and we can define it for multipartite systems, i.e. those with a number of components $N > 2$, rather than just for bipartite ($N = 2$) systems.

A mixed state of a bipartite system AB , represented by a density operator ρ_{AB} , is an entangled state *iff* it cannot be written in the form:

$$\rho_{AB} = \sum_i \lambda_i \rho_A^i \otimes \rho_B^i, \quad (5)$$

where $\rho_{A/B}^i$ are density operators on $\mathcal{H}_{A/B}$ respectively and the λ_i are convex coefficients: real numbers $0 \leq \lambda_i \leq 1$ which sum to one: $\sum_i \lambda_i = 1$.

A state in the form (5) with only one term in the sum is called a product state; one with two or more terms is called *seperable* (or sometimes *classically correlated*). If we include pure state density operators ($\rho^2 = \rho$) in our reckoning then this definition of entanglement covers both pure and mixed state cases.

The state $\rho_{1\dots N}$ of an N -party system is N -party entangled *iff* it cannot be expressed as a convex sum of the form:

$$\rho_{1\dots N} = \sum_i \lambda_i \rho^i, \quad (6)$$

where each ρ^i can be factorised into products states of less than N parties. An N -party system may be $M < N$ -party entangled, even if it has no M -party subsystem whose reduced state is itself M -party entangled [13].

The GHZ state:

$$|\Psi^{\text{GHZ}}\rangle = \frac{1}{\sqrt{2}}(|\uparrow\rangle|\uparrow\rangle \dots |\uparrow\rangle + |\downarrow\rangle|\downarrow\rangle \dots |\downarrow\rangle) \quad (7)$$

is a familiar example of an N -party state which is fully N -party entangled.

2.1 The Einstein-Podolsky-Rosen argument

Nowadays, entanglement is a workhorse of quantum information science, essential for entanglement-assisted communication (e.g. quantum teleportation), quantum computation, and quantum cryptography [14]. But it was first explicitly put to work by Einstein in his debates with Bohr on the completeness of quantum theory [15].

In these debates, Einstein would formulate thought experiments designed to illustrate that there was some knowable physical fact which a description according to the rules of quantum theory would leave out [16]. Bohr typically responded by arguing that the measurements involved in the putative experiments must be disturbing (due, as he was wont to say, to ‘the finiteness of the quantum of action’ [15, 17]) and hence they did not after all reveal that there were some knowable physical facts which the quantum description left out.

Einstein brilliantly realised that the correlations encapsulated in entangled states could transform this debate [18]. If we consider an experiment in which the measurement is performed on one half of a spatially separated entangled pair, and we ask about the physical features of the other half, then Bohr would be able to maintain his disturbance-on-measurement doctrine only at the cost of invoking some form of action-at-a-distance. The measurement on one side would have to disturb the physical features of the far side.

Thus the argument of the famous Einstein-Podolsky-Rosen (EPR) paper [19] was to the conclusion of a dilemma: either quantum theory is incomplete—it does not describe all the knowable physical features of systems—or it is nonlocal: it involves instantaneous action-at-a-distance. Einstein, for obvious reasons, preferred the first horn of the dilemma.

As formulated in the EPR paper (Einstein himself would prefer simpler, later, presentations [18, 20]) the argument used an important principle, the *EPR criterion of reality*:

'If, without in any way disturbing a system, we can predict with certainty (i.e., with probability equal to unity) the value of a physical quantity, then there exists an element of reality corresponding to that quantity.' [19]

Consider the singlet state (4) above, and suppose that Alice, in one lab, holds one half of a pair of systems in this state, whilst Bob, in a distant lab, holds the other. If Alice were to measure spin in the z -direction, say, she would get either the outcome spin-up with 0.5 probability, or the outcome spin-down, with 0.5 probability. Suppose she gets spin-up. As soon as she has her measurement result, she knows that a measurement on Bob's system in the z -direction would now with certainty give a spin-down outcome. From the EPR criterion we can infer that there is an element of reality of Bob's system corresponding to this spin value. Alternatively we might simply note that following Alice's measurement, to get the correct probabilities for measurement results on Bob's system, we now need to assign it the state $|\downarrow_z\rangle$. Either way, the supposedly complete quantum state (4) misses something out: it does not include an element of reality corresponding to spin down in the z direction for Bob's system, and it does not assign the state $|\downarrow_z\rangle$. So either the quantum description is missing things out, or the result of Alice's measurement is to change the features of Bob's system, e.g., in the instantaneous change of the state of his system from $\rho_B = 1/2(|\uparrow\rangle\langle\uparrow| + |\downarrow\rangle\langle\downarrow|)$ to $|\downarrow_z\rangle\langle\downarrow_z|$.

Bohr's reply to EPR [21] is generally felt to be somewhat obscure [15, 22, 23] but a summary version would be that—for all its plausibility—he rejected the EPR criterion of reality.

One simple way of taking this is as a rejection of the idea that the changing of the probabilities for the outcomes of measurements on Bob's far system, given Alice's nearby action, need correspond to the changing of any intrinsic physical feature of Bob's system. (Nonlocal action, note, would require changes in the locally defined—the intrinsic—properties of the far system).

In turn, an extreme way of implementing this thought is to step back from the idea that the formalism of quantum theory, and in particular the quantum state, provides much in the way of description of the actual microphysical world in the first place. For example, if one took the (controversial) view that quantum states are no more than compendia of probabilities for the observable macroscopic results of measurement interactions, for ensembles of similarly prepared systems [12], and do not purport to describe microphysical reality, then one would not be troubled by the change in the state of Bob's system from $1/2(|\uparrow\rangle\langle\uparrow| + |\downarrow\rangle\langle\downarrow|)$ to $|\downarrow_z\rangle\langle\downarrow_z|$. Since quantum states, on this view, do not describe the actual microphysical properties of individual quantum systems, such a change in the state would not correspond to a change in the properties of any system, hence not to a nonlocal change. On the other hand, it might be felt that stepping back so far from quantum theory's having descriptive microphysical content would be to throw the baby out with the bathwater.

2.2 Bell's theorem

In any case: the EPR argument was, as we have seen, an argument about the content of quantum theory, over whether the theory was incomplete or was nonlocal. Bell changed things completely. His concern was not whether some particular theory (e.g. standard quantum theory) was nonlocal. His question was rather whether *the world* is nonlocal. That is, does any empirically adequate theory of the world—any

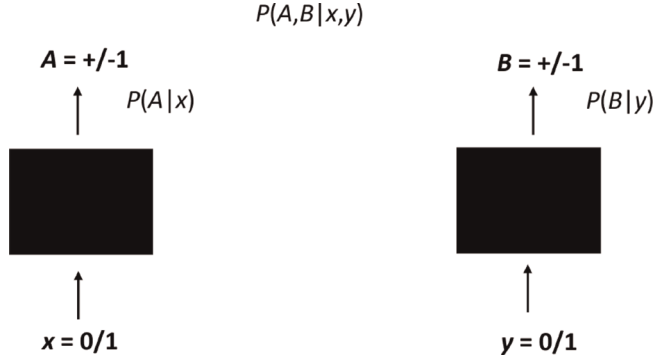


Figure 1. Correlation boxes. For randomly chosen input values x, y we gather output values A, B and estimate the individual and joint probabilities $P(A|x), P(B|y)$ and $P(AB|xy)$ respectively.

theory which will account for the experimental results—have to include nonlocality within it?¹ He was able to address this question by beginning from a suitably theory-independent starting place.²

Thus let us frame the question of the existence of various correlations operationally. Suppose we begin with a pair of black boxes 1 and 2, where box 1 takes an input bit value $x = 0, 1$ and outputs a value $A = \pm 1$ with some probability distribution $P(A|x)$, and box 2 takes an input value $y = 0/1$ and outputs a value $B = \pm 1$ with probability distribution $P(B|y)$ (**Figure 1**).

Suppose that we run a large number of repeated trials using these boxes, choosing input values x and y randomly and independently of each other. Gathering the input and output data, we will be able to estimate the underlying probability distributions. Suppose furthermore that when we gather the statistics we find there to be correlations between the outputs of the boxes, so that:

$$P(AB|xy) \neq P(A|x)P(B|y). \quad (8)$$

We can explore the idea that these correlations are due, and due only, to some further variable λ connecting the boxes. If they are, then when we condition on this further variable, the joint probability for A and B should factorise:

$$P(AB|xy\lambda) = P(A|x\lambda)P(B|y\lambda). \quad (9)$$

Call this the *factorisability condition*. We have been supposing that the input values x and y are chosen independently of each other. If they are, additionally, independent of the new variable λ (too)

$$P(\lambda|xy) = P(\lambda), \quad (10)$$

a condition we may label λ -*independence*, then the joint probability for the outcomes can be expressed as:

¹ Bell's thinking became increasingly general as it developed. By 1975 it had reached its fully mature form. See [24] for an account of the developments.

² Of course, there is no *entirely* theory neutral starting place for science; it is a matter of degree. Bell was able to formulate a sufficiently theory-independent framework to show something interesting and important.

$$P(AB|xy) = \int P(A|x\lambda)P(B|y\lambda)P(\lambda)d\lambda. \quad (11)$$

Call a joint probability which can be expressed in the form (11) *Bell correlated*.

If the probabilities for the behaviour of our boxes are Bell correlated, then a number of interesting inequalities—called Bell inequalities [5]—follow. For example, if we define the expectation value (equivalently, the correlation function) for the outputs of our boxes for various inputs as:

$$E(x, y) = \sum_{AB} ABP(AB|xy), \quad (12)$$

then one such is:

$$|E(x = 0, y = 0) + E(x = 0, y = 1) + E(x = 1, y = 0) - E(x = 1, y = 1)| < 2. \quad (13)$$

This is known as the Clauser-Horne-Shimony-Holt (CHSH) inequality [25]; it is a particular Bell inequality. Nowadays, a menagerie of different Bell inequalities is available, for example allowing different numbers of inputs and outputs, and numbers of boxes greater than two [26]. They all follow from the assumption that the salient joint probabilities can be expressed in the form (11).

But why should we care about this? Why should we care whether our boxes are Bell correlated or not; whether they satisfy a Bell inequality or not?

We care when we embed the boxes in a relativistic spacetime, and the choice of x and the outcome A occur at spacelike separation from the choice of y and the outcome B .

Start with the idea that correlations should be explicable, and start with the idea that:

‘The direct causes (and effects) [of events] are nearby, and even the indirect causes (and effects) are no further away than permitted by the velocity of light.’ [27]

This is Bell’s principle of *Local Causality*. It incorporates both the idea that causal relations are mediated (a causal link between distant events a and b will be made up of a causal chain of events between a and b , so the causal link does not obtain at a distance) and the constraint from relativity theory that the speed of light is the upper bound on the propagation of causal influence.

We need to formulate the principle mathematically to deploy it in our theories. This Bell did as follows [8, 27]:

If we consider an event A in spacetime (an event such as one our boxes producing a particular output on a particular occasion), then a full specification (or a sufficient specification) M of facts on a spacelike hypersurface through the past lightcone of A will render facts N associated with any other region of spacetime probabilistically irrelevant to A (see **Figure 2**). Thus:

$$P(A|MN) = P(A|M). \quad (14)$$

This is the formal statement of Local Causality.

Applying it to the case—call it the standard configuration—in which we have embedded our correlation boxes within spacetime, with the choice of x and the output

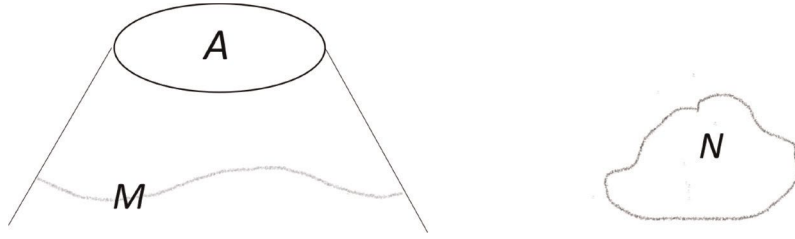


Figure 2.
Local causality. A sufficient specification of facts on the surface M renders facts within N probabilistically irrelevant to the event A : $P(A|MN) = P(A|M)$.

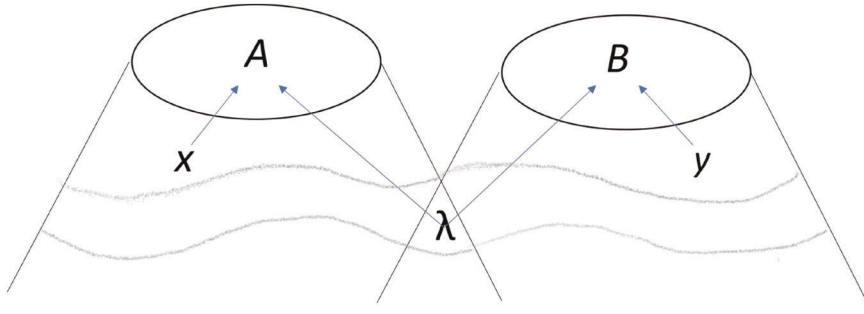


Figure 3.
A spacetime picture of the Bell experiment in standard configuration. λ specifies facts in a spacetime region cutting through the union of the past light cones of A and B , including where they overlap.

A at spacelike separation from the choice of y and the output B , and with λ a full or sufficient specification of facts in a spacetime region cutting through the past light cones of A, B , including where they overlap (see **Figure 3**), Local Causality will imply the factorisability condition (9).³

Given too that x and y can be taken as free variables—or sufficiently free variables (we will return to this)— λ -independence will also hold, and so the CHSH inequality will follow for the outputs of our boxes.

Bell's theorem is the claim that correlations in a standard-configuration experiment satisfying Local Causality and λ -independence will also satisfy a Bell inequality. It follows that any theory which predicts that the results of correlation experiments in standard configuration can violate a Bell inequality must also violate Local Causality, λ -independence, or both.

We know that the CHSH inequality has been shown to be violated for high quality experiments in standard configuration (e.g. [4, 28]), and we very reasonably believe that in these experiments, it was possible to choose the input variables x and y independently. Accordingly it seems we must conclude that *Local Causality fails*.

This is often taken to lead to two further conclusions (very distinct from one another):

³ By coarse-graining λ by integrating over its values in certain regions, we can obtain if we wish variables which correspond just to the part of the hypersurface where the past light cones of A, B , overlap; just to the part within the remainder of the past light cone of A ; and just to the part within the remainder of the lightcone of B .

- Quantum mechanics is nonlocal; and
- *The world* is nonlocal.

3. Now for some controversy

These conclusions are remarkable in reach and content, but the path that led to them seems clear enough. How can there be any controversy regarding the meaning of Bell inequality violation?

The simplest place to begin is by noting that certain ways of understanding quantum theory would seem already to provide counterexamples to the last two conclusions of the previous section.

Note to begin that we did not (as Bell was himself very aware) need experimental violation of Bell inequalities to conclude that quantum theory is not locally causal. The quantum probabilities for the correlation experiments are given by:

$$P(AB|xy\lambda) = \langle \Psi | P_x^A \otimes P_y^B | \Psi \rangle, \quad (15)$$

where P_x^A is the projector (or more generally, positive operator) associated with the value A for measurement of quantity x , and P_y^B similarly, and λ captures that we have prepared state $|\Psi\rangle$ for our bipartite system. It is automatic that this quantity will not factorise whenever $|\Psi\rangle$ is entangled.

Meanwhile, approaches to quantum theory which take its content to be mainly operational—capturing the statistics of macroscopic measurement results, say, rather than describing physical features of quantum systems—or that otherwise step back from the detailed description of a mind-independent physical world can still count as local. There are even ways—at least one—of taking quantum theory to be descriptive of the detailed microphysical features of the world and of individual quantum systems whilst still remaining local: the Everett (Many Worlds) interpretation of the theory is generally taken to be local [24, 29].

This raises the question of how failure of the specific condition of Local Causality relates to the presence of nonlocality, and especially to the presence of any nonlocality we might find worrying or problematic.

It is helpful to note that we can distinguish between two different notions, each of which can be thought to fall under the more general heading of ‘nonlocality’ (the distinction goes back to Einstein in fact [20], though my terminology is not quite his):

- *Dynamical nonlocality*—there are changes in *locally defined* (intrinsic) properties in some region due to spacelike happenings elsewhere. (This is a notion of genuine superluminal action).
- *Kinematical nonlocality*—the states assigned to unions of spacetime regions are not determined by the states assigned to the individual regions. (This is often known as the failure of *separability*).

Certainly in quantum mechanics when we have a failure of separability in the sense that we have an entangled state for a pair of systems, and when those two systems are spatially separated, we will also have a failure of separability in the sense of kinematical nonlocality. Perhaps other, post-quantum, theories might similarly be

kinematically nonlocal. Kinematical nonlocality is certainly a striking and non-classical feature, but it seems perfectly coherent theoretically (it is an actual feature in quantum theory) and in and of itself it does not give rise to any problems of consistency with relativity (though we should note that a kinematically nonlocal theory will still need to allow a rich-enough range of locally defined properties given by the states of individual regions, as is achieved in quantum theory via use of the reduced density operator [30]). If kinematical nonlocality can be combined with the *absence* of any dynamical nonlocality then we may have a perfectly satisfactory theory, consistent with relativity, and perhaps one which can violate a Bell inequality unproblematically.

On the other hand, Bell's intuitive prose statement of Local Causality did seem to capture our notions of dynamical locality consistent with relativity, and his reasoning from this statement to the factorisability condition seems simple and sound. What, if anything, can have gone wrong with it?

To make this question more pointed, suppose that we did try to appeal to a mere failure of kinematical locality, rather than a failure of dynamical locality, to explain Bell-inequality violation. How would this failure of kinematical locality actually help? We may grant there to be non-separable features in the joint past of Alice and Bob's correlation experiments, but surely we can just condition on these and include them within λ [31]? Then a Bell inequality should still hold, and kinematical nonlocality will not have helped us to violate it.

3.1 Looking at the examples

To unpick these puzzles, let us look a little more closely at how the proposed examples of local understandings of quantum theory work. We can discern three kinds of example.

The first kind of example we are already familiar with from what I called the 'extreme' way of offering a response to EPR in wake of Bohr. It is the kind of view which retreats from the idea that quantum theory, and the quantum state, provide us with means of describing the microphysical world. Instead the formalism of the theory is seen as a device for organising our experimental interactions with the world, and quantum probabilities only pertain to the behaviour of measuring devices which can be characterised non-quantum mechanically and at the macroscopic level. The only role of the quantum state is to furnish these probabilities; it does not describe actual features of quantum systems. Such views [12] can be called *operationalist* (foregrounding operational procedures in the lab) or *anti-realist* in the sense that they depart from a scientific realist conception of our physical theories. In a scientific realist conception, the aim of science is to provide us with a literally true description of the what the mind-independent world is like in both its directly observable and non-directly observable features, and as applied to quantum theory, it would require us to interpret at least a large part of the quantum formalism as directly representing facts about the microphysical systems from which the world is built.

In a sufficiently operationalist or anti-realist interpretation of a theory, the notion of (dynamical) locality will itself be given a suitably operationalist understanding. Since the theory is not in the business of describing microphysical goings-on in individual runs of an experiment, but rather in the business of codifying statistical features, non-microphysically characterised, of repeated runs of experiments, the notion of dynamical locality will be spelt out in statistical, operational, terms: a theory will be (operationally) nonlocal *iff* it is *signalling*, where a theory is signalling *iff* operational procedures confined to one spacetime region produce a change in the statistics for measurement outcomes in a spacelike region.

Quantum theory itself is rather obviously *non-signalling* since the reduced density operator for a far system is unchanged by any operation one can perform on a nearby system. A sufficiently operationalist interpretation of quantum theory, therefore, will—by the relevant estimation—count as dynamically local despite predicting Bell inequality violation.

Notably, such an approach does not explain how Bell inequality violation comes about in experiments, it just asserts that it does. It gives-up on the idea of explaining physically how correlated measurement results turn out as they do on individual runs of an experiment, as part more broadly of relinquishing descriptive ambitions for quantum theory. Remaining fastidiously aloof from describing microphysical systems, it will remain equally aloof from causal description of events involving those systems, hence Bell's prose statement of the principle of Local Causality above will not apply straightforwardly, if at all. But as remarked before in the context of the EPR argument, taking so stringently thin a notion of the content of quantum theory as this may be depriving ourselves of too much that we need.

The second kind of example may agree with the prose statement of Local Causality, but instead raise trouble for the mathematical expression of the principle in terms of probabilities as in Eq. (14) and Eq. (9). In particular, one might offer a notion of probability according to which changes in the probabilities assigned by Alice to the possible results of measurements on Bob's distant system do not count as changes in any objective, or in any localised, feature of his system. If changes in the probabilities pertaining to a system need not correspond to changes in objective or in localised features of the system, then the inference from changes in the probabilities to causal consequences in the world is rendered shaky.

It is tempting to think that there is a single correct, best, probability distribution for what the results of measurement on a given system should be, a probability distribution fixed by the features of the system and its immediate surroundings (perhaps including the features of any measurement device with which it is about to interact). In the quantum case, it is very tempting to think that this single correct, best, probability distribution is given by what the correct quantum state (pure or mixed) that this system should be assigned is.

But it might be argued, as in [32, 33] that there is no single set of probabilities which should be assigned to a given system; the physical features of a system, or more generally, the physical features of the world in the past light cone of a system, need not determine a single, univocal, probability for the results of measurement on that system. It will follow that there is not a single quantum state that should be assigned to a system either. Thus Alice following her spin measurement on her half of the entangled pair shared with Bob correctly assigns to Bob's system the pure state $|\downarrow_z\rangle$, but this assignment is not made correct by any feature intrinsic to (locally defined for) Bob's system; it is made correct by what Alice has learnt at her location. Bob, correctly, and unimprovably (for now) at his location, not missing any physical feature intrinsic to his system, continues to assign the mixed state to his system.

In this kind of view, the full specification of physical facts on some spacelike hypersurface do not determine *univocal* and ideally best probabilities for each event on future spacelike hypersurfaces, so we cannot straightforwardly draw causal inferences from the probabilities assigned to an occurrence changing when conditioned on facts pertaining to a spacelike separated region.

In [32, 33] probabilities (and quantum states) are objective, even if they are not univocal (because relational). A rather different picture is given in QBism [34], where again there are not univocal probabilities, and there are not unique quantum states for

systems, but this time because probabilities (and quantum states) are viewed as subjective, in the sense of being expressions of individual agents's degrees of belief. Again, this renders the probabilistic formulation of Local Causality as ineligible to express causal notions.

The third example is the particular concrete example given by the Everettian (Many Worlds) approach to quantum mechanics and it is quite unlike the first two kinds of example. Unlike these, in the Everettian approach, the quantum state (of the universe!) is unique, objective, and intended to be part of the detailed description of individual quantum mechanical systems. It is a thorough-going scientific realist approach to understanding quantum theory. But, it is generally held to be a dynamically local theory, indeed it will satisfy the prose statement of Local Causality, since in Everett, the state of any spacetime region will be fixed by the state on a spacelike surface cutting the past light cone of that region.

A number of tightly-interconnected factors seem to be involved in the Everett approach being able to violate Bell inequalities whilst remaining dynamically local:

1. Though the quantum state is real in the sense of playing a central role in describing real features of the world, it does not collapse on measurement, so there are no dynamically nonlocal changes in the state. Instead the state evolves by unitary dynamics given by a local Hamiltonian.
2. Apart from some background spacetime structure, all the remaining physical ontology (physical features of the world) supervenes on the quantum state and its evolution. (Nothing extra is added, such as hidden variables which might need to be pushed-about dynamically nonlocally.)
3. The theory is emphatically kinematically non-local, since entanglement between different spatially separated regions is generic.
4. There is non-uniqueness of measurement outcomes (different outcomes of a given measurement, in different worlds which have branched from the measurement). We do not need to guarantee single correlated outcomes on a given run of the experiment, at the expense of other possible outcomes: all the outcomes are realised.

It is an interesting open question whether any theory which is suitably scientific realist, which is dynamically local, which is kinematically nonlocal, and yet which can violate a Bell inequality (without λ -dependence), is also one in which uniqueness of measurement outcomes will fail. That is, do the features which co-occur in the Everett interpretation *have* to co-occur?

In any case: the clearest lesson from reflecting on the Everett example seems to be that in a theory which is kinematically non-local, the probabilistic formulation of Local Causality may again not be an appropriate way of expressing the prose formulation of Local Causality [24].

3.2 Summing-up this controversy

Though they incorporate, or express, a range of very different philosophical approaches, perhaps the simplest, quick, way to understand these controversies is to discern an ambiguity (deliberately planted there) in my earlier statement of Bell's

theorem. I said that the theorem was the claim that correlations in a standard-configuration experiment satisfying Local Causality and λ -independence will also satisfy a Bell inequality. But which version of Local Causality? The initial, intuitive, prose version? Or the mathematical formulations, Eqs. (9) and (14)? No one could deny the content of the theorem if we meant the latter. But as we have seen, there are a number of routes by which one might endorse the prose version of the principle, but not agree with its mathematical formulation, thus not agree with the claim, if Local Causality in the prose formulation is intended.

Still: the class of theories for which the mathematical formulation is a good way of expressing Local Causality is very broad and important. So the claim that Bell inequality violation in nature shows that Local Causality, as mathematically expressed, is not true, is still very deep, remarkable, and powerful.

3.3 ‘Local causality’ vs. ‘local realism’

It is rather common to find Bell’s results discussed under the heading of ‘Local Realism’ instead of ‘Local Causality’. This alternative terminology may perhaps be traced back to [35, 36], but it can be highly, and distractingly, controversial. For some, asserting that Bell inequality violation (for standard configuration experiments, etc.) rules out Local Realism invites the prospect that locality might be salvaged by jettisoning a(n allegedly atavistic) realism assumption. For others, such a contention must be quite mistaken, for Bell’s reasoning *did not* and *need not* make any appeal to any assumptions beyond locality (Local Causality) itself [37–39].

There is some truth in both contentions, but there is no doubt that ‘Local Causality’ is the better terminology, for it does not invite the confusions that ‘Local Realism’ does.

We have already seen that some dialling-down of realist, descriptive, ambitions for physics does allow scope for evading inferences to the presence of dynamical nonlocality (action at a distance) both in the context of the original EPR argument (recalling the tenor of Bohr’s response), and in one of the routes we explored for resisting the idea that the mathematical and the prose formulations of Local Causality aptly express conditions for dynamical locality in all contexts. So some realist commitment is involved as part of the background of Local Causality’s expressing an interesting physical feature. But what is the realism in Local Realism supposed to be?

For some it is just a generic commitment to the notion of scientific realism along the lines introduced above. Thus Clauser and Shimony: ‘Realism is a philosophical view, according to which external reality is assumed to exist and have definite properties, whether or not they are observed by someone.’ [35]. On other occasions, realism is taken to be the logically much stronger—or more specific—view that all physical quantities (e.g. all quantities represented by self-adjoint operators in quantum mechanics) have a definite value for what the result of measuring them on some occasion would be, even if they were not in fact measured on that occasion [36]. The latter is a stronger view since it commits to there being hidden variables which are deterministic (fixing definite measurement outcomes), whereas in the former view it could be that there are independently existing properties of the world but that they only (in general) furnish non-deterministic probabilities for measurement outcomes. Further, the latter reading suggests definite values for all physical quantities simultaneously, where one might take the external world to have real mind-independent features at all times, but perhaps only for a subset of the physical quantities.

The strong view (realism as deterministic hidden variables) is too narrow. Local Causality covers a broader range of theories than this (and it needs to, to be applicable to realistic experimental scenarios). But if we relax merely to the broader view (scientific realism as applied in the quantum context) then we find examples of theories which are (dynamically) local and realist in this sense, but which can violate Bell inequalities: the Many Worlds approach. So locality and realism (in this broader sense) do not entail Bell inequalities; while locality and realism (taken in the narrower sense) does not cover all cases. We should simply drop ‘Local Realism’ and stick with ‘Local Causality’.

4. Back to λ -independence

If our correlation experiments were not in standard configuration, then it would be easy for them to produce Bell inequality violating results without there needing to be any failure of local causality, or any other non-classical funny-business. For example, if the setting— x , say—on one side was not at spacelike separation from the setting or outcome on the other, then there would be plenty of time for a classical sub-luminal, or a lightlike, channel to connect the two sides. Bob’s box would then be able to take both x and y as inputs, and locally mimic failure of local causality. (The response function which captures the behaviour of Bob’s box can now be of the form $P(B|x, y, \lambda) \neq P(B|x, \lambda)$ consistently with local causality.) This additional channel connecting the two sides of the experiment might not be obvious to us, but it could certainly be there. Requiring that the experiment be in the standard configuration rules out there being any such channel, on pain of inconsistency with relativity.

It is also extremely important that there actually be a choice of x and y values when the experiment is run. If x and y took the same fixed values across all runs of the experiment then we would not have any interesting correlations. Any correlations in the outputs ($P(AB) \neq P(A)P(B)$) could readily be accounted for by a purely locally causal mechanism. More subtly, if x and y choices were made on each run, but we happened to know in advance what they would be, it would again be possible to mimic failure of local causality locally: we could adjust the other input to the boxes, via λ , to make it look as if local causality were failing when it was not. This brings us back to the question of λ -independence.

It will be recalled that λ -independence ((10) above) was an essential ingredient in arriving at Bell-correlations ((11) above) and thus in deriving Bell inequalities. We are used to the idea that we can often have a good deal of control over at least some of the parameters which are involved in our experiments. We are also used to the idea that, in general, separate systems will not be correlated with one another unless they have had some explicit interaction in the past, often, in the recent past. Accordingly, if when constructing our correlation experiment we have taken pains that the process by which the x input value is selected is independent of other things, and the process by which the y input value is selected is independent of other things, then it will seem reasonable to assume a) that x and y are not correlated with each other (in fact we can explicitly check whether $P(xy) = P(x)P(y)$) and b) that, crucially, they are not correlated with anything else important for the results of the experiment. With these precautions, then, λ -independence seems a safe assumption.

On the other hand, if this condition fails, then locally causal theories could produce arbitrary correlations—whether the quantum correlations, or even stronger

correlations, which maximally violate the CHSH inequality (the Popescu-Rohrlich correlations [40]). To see this, let us consider a simple example.

Suppose we have a theory which is deterministic in the sense that specification of all the facts on a spacelike hypersurface which cuts through the past light cone of some event fixes all the facts to the future of that surface within the lightcone in question. By construction such a theory will be locally causal. It will also automatically violate λ -independence. To see this, consider that in such a theory both x and y will be functions of λ —call them $f(\lambda)$ and $g(\lambda)$ respectively. Then we can consider the set Λ_{xy} of all those values of λ which would give rise to some specific x, y pair:

$$\Lambda_{xy} = \{\lambda | f(\lambda) = x, g(\lambda) = y\}. \quad (16)$$

Given some specific x, y in some run of the experiment, then, λ in that run will be constrained to lie within Λ_{xy} , which is a strict subset of the set Λ of all values of λ , which means that λ -independence fails. Knowing the values of x, y we know that λ must be within a specific subset of values. Letting χ_{xy} be the characteristic function of the set Λ_{xy} (giving value 1 if $\lambda \in \Lambda_{xy}$ and 0 otherwise), we have that:

$$P(\lambda | xy) = \frac{\chi_{xy}(\lambda)P(\lambda)}{P(xy)} \neq P(\lambda). \quad (17)$$

With the λ -dependence of this deterministic theory in hand, we can now see how to produce arbitrary correlations (this kind of construction seems first explicitly to have been noted, for quantum correlations, in [41]). We just need to put an appropriate probability distribution over the initial set of λ s.

Note that in this theory, not only x and y but also the outcomes A and B will be functions of λ . We can thus further refine the Λ_{xy} with a partition:

$$\Lambda_{xy} = \bigcup_{AB} \Lambda_{xy}^{AB}, \quad (18)$$

where the Λ_{xy}^{AB} are the sets of all λ values which produce the specific values x, y, A, B . (Note, $\Lambda_{xy}^{AB} \cap \Lambda_{x'y'}^{A'B'} = \emptyset$).

Taking χ_{xy}^{AB} to be the characteristic function of the set Λ_{xy}^{AB} , the joint probability $P(ABxy\lambda)$ will be given by:

$$P(ABxy\lambda) = \chi_{xy}^{AB}(\lambda)P(\lambda). \quad (19)$$

Suppose that it is the quantum correlations which we want to recover. Then we need merely postulate a $P(\lambda)$ which is such that the correct weight gets given to the sets Λ_{xy}^{AB} . Thus we choose $P(\lambda)$ such that:

$$P(\lambda \in \Lambda_{xy}^{AB}) = \int \chi_{xy}^{AB}(\lambda)P(\lambda)d\lambda = \langle \Psi | P_x^A \otimes P_y^B | \Psi \rangle P(xy). \quad (20)$$

The correlation probabilities in this theory will be given by:

$$P(AB|xy) = \int \frac{\chi_{xy}^{AB}(\lambda)P(\lambda)}{P(xy)}d\lambda. \quad (21)$$

For the weights on Λ_{xy}^{AB} given by $P(\lambda)$ satisfying (20) we will immediately obtain $\langle \Psi | P_x^A \otimes P_y^B | \Psi \rangle$ as desired. By choosing different weights on the Λ_{xy}^{AB} we can obtain any desired correlations.

The λ -dependence of this deterministic theory was of a rather strong kind, with λ fixing x and y . It is also possible to pursue the more subtle question of how little λ -dependence is required in order to reproduce certain correlations locally causally. For example [42] shows that at most one bit of correlation (as measured by the mutual information) between λ and one of the measurement settings is sufficient in order to be able to reproduce any correlations which could be generated by quantum measurements on a singlet state (see also [43]). In the other direction, interestingly, [44] shows that if one's theory retains a little λ independence, in the sense that given λ s do not absolutely rule out particular x , y s, then there is a Bell inequality which would be violated for a less than maximally entangled quantum state, but which this λ -dependent theory would not be able to violate.

4.1 Effective λ -independence

The discussion so far of the λ -dependence of the deterministic theory leaves us with something of a puzzle. Earlier we noted that, having taken care to apply certain precautions, it would be perfectly reasonable to believe that λ -independence was satisfied for one's experiment in standard configuration. But as we have just seen, if there is an underlying deterministic theory, then λ -dependence is obligatory. And it seems a perfectly reasonable thought that there might be some (perhaps as yet to be discovered) deterministic theory underlying quantum theory.

The key to resolving this conundrum is to recognise that what is important is *effective* λ -independence, as opposed to what might be called *absolute* or *fine-grained* λ -independence. (I take this to be one of the key lessons from—and an area of agreement within—the exchange between Bell and Clauser, Horne and Shimony [45].)

When considering the behaviour of some physical system—for example one of our black boxes—it may well be (at least for the sake of argument) that there is some fully deterministic theory in the background, which gives us a detailed λ which is sufficient entirely to fix the system's behaviour. Yet that physical system may in a certain sense be insensitive to λ . That is, although λ fully fixes the behaviour, the system might behave in much the same way, or exactly the same way, for a range of values of λ . In other words, the behaviour of the system may best be characterised as responsive to some coarse-grained variables, corresponding to some coarse-graining of Λ .

Let us introduce the notation $\bar{\lambda}$ for new variables given by some minimal coarse-graining of Λ (e.g., averaging values of λ within some small ϵ -volume of Λ). Considering now the boxes in our correlation experiment, suppose them to be governed by a locally causal theory; their behaviour will be captured by the response functions:

$$P(A|Bxy\lambda) = P(A|x\lambda), \text{ and} \quad (22)$$

$$P(B|Axy\lambda) = P(B|y\lambda). \quad (23)$$

Suppose now that the boxes are insensitive to fine-grained λ . There will be some coarse-grained $\bar{\lambda}$ which screens-off λ in the response functions:

$$P(A|x\bar{\lambda}) = P(A|x\lambda); \quad (24)$$

$$P(B|y\bar{\lambda}) = P(B|y\lambda). \quad (25)$$

Now it may be that at this coarse-grained level, $\bar{\lambda}$ -independence will hold— $P(\bar{\lambda}|xy) = P(\bar{\lambda})$ —even if λ independence does not. Then we will again have Bell correlated joint probabilities, and Bell inequalities will hold for our locally causal theory:

$$P(AB|xy) = \int P(A|x\bar{\lambda})P(B|y\bar{\lambda})P(\bar{\lambda})d\bar{\lambda}. \quad (26)$$

Say that *effective* λ -independence holds, iff there is some minimally coarse-grained $\bar{\lambda}$ which screens-off λ in the measurement response functions and for which $\bar{\lambda}$ -independence holds.

Effective λ -independence can certainly hold in a deterministic theory, and in the circumstances relevant to our experiment in standard configuration we would expect it to do so. Reflect that many and various different processes could be selected which produce the x and y input values for the experiment (and we can check to see whether it makes any difference to the presence of Bell-inequality violation which process is used). These processes could be of the kind where we have very good reason to believe that the dynamics (whatever it is) leading-up to the production of the value is extremely complicated (as for example in a pseudo-random-number-generator), so that an exact specification of the final state of the choosing-device would be necessary to determine its initial state, whilst the value produced itself is a very coarse-grained function of the final state of the choosing-device. In this circumstance, we can envisage that if there is an underlying deterministic theory, its sets Λ_{xy} are highly fibrillated and interwoven with one another. Then knowing the exact λ would still fix which Λ_{xy} we were in. But even a slightly coarse-grained $\bar{\lambda}$ would not pin down any Λ_{xy} : within the small ϵ -ball some (approximately) equal-measured subset of each Λ_{xy} might be present. Thus $\bar{\lambda}$ -independence would hold.

Important as it is, this is not enough for effective λ -independence to hold. For that we also need that $\bar{\lambda}$ screens-off λ in the response functions. However, given the enormous variety of ways (ways which we can to some extent choose between), and the enormous complexity of ways (which we can to some extent ensure), in which any fine-grained λ s can be connected to x and y values, it would be extraordinary if the response functions were always sensitive to the fineness of grain of λ required to fix x and y . In other words, it would be extraordinary if $\bar{\lambda}$ did not screen-off λ in the response functions, and thus effective λ -independence hold. (Plausibly, it would be far more extraordinary than Local Causality's failing.)

Bell in [46] talks about input x and y variables, when they are produced by plausible randomisation processes, being 'sufficiently free variable[s] for the purposes at hand'. I take the notion of effective λ -independence just outlined to be a way of capturing this notion of 'sufficiently free'. There may be some description (e.g. the envisaged underlying deterministic one) in which x and y are not free variables, since they are correlated with, or caused by, something else. But that need not stop them being effectively, or sufficiently, free; and the degree of coarseness of grain of λ which both screens-off λ in the measurement response functions and delivers $\bar{\lambda}$ -independence captures the relevant metric for sufficient freedom.

4.2 The question of λ -independence in the case of high energy experiments

So far, then, we have reassured ourselves that in the standard configuration for the correlation experiment, and if one has taken trouble that the procedures for selection of x and y values are one from some number of suitably randomising procedures—or otherwise give us a high degree of confidence that the selection processes are independent of other aspects of the experiment—we may be confident that λ -independence, or effective λ -independence, holds.

It is sometimes suggested, however, that there may be special reasons even so why (effective) λ -independence might fail, thus allowing us to avoid the conclusion that the world is not locally causal, despite Bell inequality violation. Such special reasons might include the thought that backwards causation might be possible, so that we should not rule out the possibility that Alice and Bob selecting their x and y values could affect the value of λ in the past (e.g. [47, 48]) or that a particular form of deterministic hidden variable theory might naturally give rise to λ -dependence [49]. In each of these cases (as also in [50]) we face the question of whether there is more reason to believe that these special reasons obtain than to believe that effective λ -independence does. Given the strength of the general physical grounds for believing effective λ -independence obtains, the general view is against these special reasons.

Throughout our discussion of (effective) λ -independence, however, it was extremely important that the processes which produced the selection of x and y values were separately identifiable and understandable to the extent that we could have confidence that the values produced were (at least effectively) independent of each other and of other features which might be important in the experiment. By controlling and probing the behaviour of these processes, we could come to a very high degree of confidence that such independence obtains. In terms of a causal diagram (rather than just a spacetime diagram) where arrows indicate the presence of causal influence and the absence of arrows its absence, we need a causal structure as given in **Figure 4a**.

Let us now turn (finally) to some more specific aspects of Bell tests in high energy experiments. Here (as in e.g. [1–3]) we envisage a high-energy collision product which itself decays into two parts, where conservation principles will ensure that the two parts are in a suitable entangled state. For example for a Higgs particle (spinless) decaying into a W^\pm pair, the spin state of the W^\pm pair should be close to a singlet state [1]. (The spin state in top/anti-top quark pair production is also a very

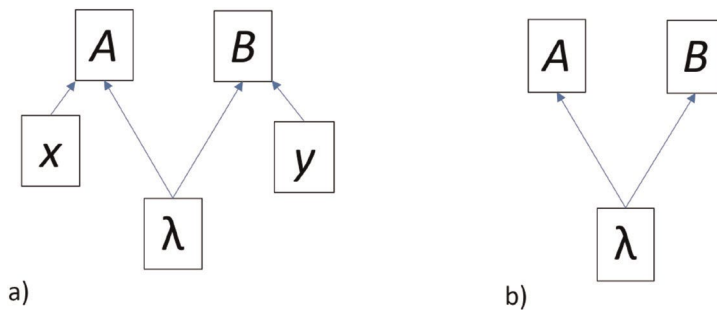


Figure 4. Causal diagrams for correlation experiments. In a) we have standard configuration with x and y values independently selected, independent of λ (and outside the forward light cone of the preparation event for the systems measured). In b) there is no independent selection of x , y values.

interesting case [51, 52]). These entangled decay products separate with opposite momenta, and then themselves decay further, where these final decay products are then detected, and from their angular spread, the spin of the parent (entangled) particle inferred.

It will be noticed immediately that we do not have a part of this process which provides an external choice of measurement on the particles in the entangled state (corresponding to a choice of x and y). The decay of each particle into the finally detected products is spontaneous (or is a matter of the interaction of the particles with the quantum fields immediately surrounding them) rather than being selected or being a matter of choice. We do not have an independently identifiable and controllable process in the experiment which is determining what measurement is made and whose features we can separately study and ascertain. The causal structure of the experiment seems to be of the form of **Figure 4b** rather than **Figure 4a**.

How much of a problem is that? From the point of view of performing an ideal test of whether the world is not locally causal, it is a significant problem. We no longer have a sufficient guarantee that (effective) λ -independence will hold since we no longer have independent access to whatever it might be that is determining x and y values. If we are attempting experimentally to constrain the features of a general class of theories, we need to consider the possibility that there might be some hidden variables underlying our entangled state for the W^\pm particles, which were carried along by the two particles as they separated, and which in due course told the particles when and how to decay. In that case we would have strong λ -dependence, no reason to believe that effective λ -independence obtained, and the theory giving us these hidden variables could perfectly well be locally causal while still giving us Bell inequality violation.

It is a different case if we are assuming quantum theory to be the true theory of the world. Then we might see the quantum description of the experiment giving us an analogue of, or perhaps an instance of, a choice of x and y values independent of the features of the particles being measured: we might look to the particles' decay being caused by their interaction with the quantum fields surrounding them, and we might see this as a process which we have good reason to believe is intrinsically random and not such as to give rise to λ -dependence. Indeed, we might see such interactions with local quantum fields as being much like the use of pseudo-random-number-generators in a traditional Bell experiment.⁴ However, if, as in an ideal Bell test, we are interested in establishing general truths about the world (about how things have to be in broad classes of theories in order for them to be empirically adequate) then we cannot assume quantum theory as a whole, or even too-large chunks of it. Thus we cannot assume that the process leading to the entangled particles' final decays are driven by suitably random and independent processes just because they would be if quantum theory were true. The main point at issue is: how much can we infer about the world irrespective of whether quantum theory is true? (Recall: quantum theory itself is automatically not locally causal. We want to know how much we can pin down experimentally the different question of whether *the world* is not locally causal.)

Of course: we do use theory in our assessment of the functioning of pseudo-random-number-generators in standard Bell tests too. It is not that no aspect of our ideal Bell experiment can use theory. But so far as possible, the theory used should be independent of the theory being tested, and so far as possible, we should have detailed

⁴ I owe this observation to Alan Barr.

experimental access to the functioning of the various devices we use in our experiment, including whatever it is that is selecting x and y values.

To sum-up then. High energy experimental tests of Bell inequalities, at least as currently configured and conceived, do not seem to give us sufficient guarantee that (effective) λ -independence should hold since we do not have independent access to, or independent understanding of, the processes giving rise to the selection of a given measurement. Thus as things stand the experiments may not be in a good position to provide us with a crucial experiment for whether the world is locally causal or not. But this is far from saying that they are not interesting, however! Seeing (if that is what we will see) more instances of strikingly quantum behaviour in new regimes we have not closely studied before experimentally is an important endeavour. But more than this, we can also seek to develop our understanding of various aspects of these high energy experiments, and in particular our understanding of the process of measurement in the sense of the quantum-to-classical transition in the experiments. The quantum-to-classical transition is an important topic in its own right and has been very little studied in the context of realistic high energy experiments. Careful analysis of how classical measurement results come about in this setting may well move us towards the possibility of developing stronger reasons for belief that λ -independence should be thought to hold in these experiments. We may be able to move towards non-question-begging grounds for conviction that λ -independence holds.

5. Bell inequality violation as an entanglement witness

There is a different kind of reason altogether why one might be interested in Bell inequality violation. We saw the definitions of pure and mixed, bipartite and N -party entanglement earlier. These definitions are clear enough. What may be less clear, and what in some cases is a very difficult problem, is whether some given quantum state is entangled or not. Recall—the definition is couched negatively: one's state is entangled if it is not possible to write it as a separable (or a product) state. If we are not already given a state in product or separable form in general it is a difficult (in some cases, unsolved) problem whether it can be put in that form. The device of *entanglement witnesses* was developed to help address this question [9, 53, 54].

An entanglement witness is a self-adjoint operator \mathcal{W} which has a positive expectation value for all separable states, and a negative expectation value for at least one entangled state. Thinking geometrically in the vector space of linear operators, $\text{Tr}(\rho\mathcal{W}) \geq 0$ defines a plane, normal to \mathcal{W} , on one side of which (the positive side) sit all the separable states, and on the other side of which is at least one entangled state. The set of separable states is a convex set (i.e. convex combinations of separable states gives you back a separable state—the same is not necessarily true for entangled states, we may note: entanglement is not preserved under convex combination). It was first noted in [53] that it is therefore a consequence of the Hahn-Banach theorem that for any entangled state, there will be some plane which separates it from the set of separable states, i.e. there will be some entanglement witness \mathcal{W} for it.

Various entanglement witnesses, and techniques for identifying entanglement which go by way of entanglement witnesses, have been developed [9]. The important point for our purposes is that Bell inequalities are entanglement witnesses [54]—that is, we can write down a self-adjoint operator corresponding to the inequality, and if a state gives a certain expectation value with that operator, we know the state must be entangled.

The operator corresponding to the CHSH inequality, for example, would be of the form: $A_0 \otimes B_0 + A_0 \otimes B_1 + A_1 \otimes B_0 - A_1 \otimes B_1$, with A_x, B_y dichotomous self-adjoint operators for x/y measurements on Alice and Bob's systems, respectively.

Therefore if measurements on a multi-party quantum system violate a Bell inequality, we know that the system is in an entangled state. (The converse does not in general hold: not all entangled states are such that there is some Bell inequality that they will violate.)

In various circumstances it can be important to know whether the states one is concerned with are entangled or not, and it may be an interesting question how highly entangled they are. (Various measures of degree of entanglement exist, typically guided by respecting the ordering given by the principle that amount of entanglement cannot increase under local operations and classical communication. The singlet state is a maximally entangled state for a pair of two dimensional systems, for example.) Bell inequality violation (and degree of Bell inequality violation) can certainly help us with these tasks. Importantly, assessing in detail the degree of entanglement of quantum states produced in high energy experiments can be an important test for beyond-Standard-Model particles and interactions [55, 56].

6. Conclusions

We may care about Bell inequality violation because we want to show something deep and general about the world, not just about some particular theory: that Local Causality (as mathematically formulated) does not obtain. That no satisfactory theory of the world—no theory which can make the predictions we have observed—can also obey that principle.

We may care about Bell inequality violation because, sticking firmly within quantum theory, we want to show something about some particular quantum systems we are dealing with—that they are entangled, or entangled to a certain degree. This fact might have important further consequences, including for new physics, as is the case in these high energy experiments.

In the context of high energy experiments, we have seen that given the lack of independent access to how x and y values are selected, we have difficulty in maintaining the necessary high degree of conviction that λ -independence should hold. Thus we cannot readily infer failure of Local Causality from Bell inequality violation as things stand. But further investigation, starting from a careful analysis of quantum-to-classical measurement models for high energy particle detection, may well allow us to move to a more general understanding of the measurement processes involved, which might in turn furnish lines of support for λ -independence. Either way, an increasingly detailed understanding of how these high energy experiments can approach the ideal for a Bell test for Local Causality is a highly desirable aim.

Thanks


I thank Alan Barr for my introduction to the topic of high energy Bell tests, for discussion, and for the invitation to the workshop to give the talk on which this chapter is based. I thank Harvey Brown for discussions on Bell matters going back many years now.

Author details

Christopher G. Timpson
Faculty of Philosophy, University of Oxford, UK

*Address all correspondence to: christopher.timpson@bnc.ox.ac.uk

IntechOpen

© 2023 The Author(s). Licensee IntechOpen. This chapter is distributed under the terms of the Creative Commons Attribution License (<http://creativecommons.org/licenses/by/3.0>), which permits unrestricted use, distribution, and reproduction in any medium, provided the original work is properly cited. 

References

- [1] Barr AJ. Testing Bell inequalities in Higgs boson decays. *Physics Letters B*. 2022;**825**:136866
- [2] Ashby-Pickering R, Barr AJ, Wierzychucka A. Quantum state tomography, entanglement detection and Bell violation prospects in weak decays of massive particles. *JHEP*. 2023;**05**:020
- [3] Fabbrichesi M, Floreanini R, Gabrielli E, Marzola L. Bell inequality is violated in $b^0 \rightarrow j/\psi k^*(892)^0$ decays. arXiv:hep-th 2305.04982. 2023
- [4] Hensen B, Bernien H, Dréau A, et al. Loophole-free Bell inequality violation using electron spins separated by 1.3 kilometres. *Nature*. 2015;**526**:682-686
- [5] Bell JS. On the Einstein-Podolsky-Rosen paradox. *Physics*. 1964;**1**:195-200
 Reprinted in [56]
- [6] Gao S, Bell M, editors. *Quantum Nonlocality and Reality: 50 Years of Bell's Theorem*. Cambridge: Cambridge University Press; 2016
- [7] Brunner N, Gühne O, Huber M. Special issue on fifty years of Bell's theorem. *Journal of Physics A: Mathematical and Theoretical*. 2014;**47**(42):420301
- [8] Bell JS. The theory of local beables. *Epistemological Letters*. 1976;**9**:11-24
 Reprinted in [56]
- [9] Horodecki R, Horodecki P, Horodecki M, Horodecki K. Quantum entanglement. *Reviews of Modern Physics*. 2009;**81**:865-942
- [10] Schrödinger E. Discussion of probability relations between separated systems. *Mathematical Proceedings of the Cambridge Philosophical Society*. 1935;**31**(4):555-563
- [11] Feynman R, Leighton R, Sands M. *Lectures on Physics*, volume 1, chapter 37. Reading, Mass: Addison-Wesley; 1964
- [12] Peres A. *Quantum Theory: Concepts and Methods*. Dordrecht: Kluwer; 1993
- [13] Seevinck M, Uffink J. Sufficient conditions for three-particle entanglement and their tests in recent experiments. *Physical Review A*. 2001;**65**:012107
- [14] Nielsen M, Chuang I. *Quantum Computation and Quantum Information*. Cambridge: Cambridge University Press; 2010
- [15] Bohr N. Discussion with Einstein on epistemological problems in atomic physics. In: Schilpp PA, editor. *Albert Einstein: Philosopher Scientist*. La Salle, Illinois: Open Court; 1949. pp. 199-242
- [16] Bacciagaluppi G, Valentini A. *Quantum Theory at the Crossroads: Reconsidering the 1927 Solvay Conference*. Cambridge: Cambridge University Press; 2009
- [17] Bohr N. The quantum postulate and the recent development of atomic theory. *Nature*. 1928;**121**:580-590
- [18] Fine A. *The Shaky Game: Einstein Realism and the Quantum Theory*. Chicago, Illinois: University of Chicago Press; 1988
- [19] Einstein A, Podolsky B, Rosen N. Can quantum mechanical description of physical reality be considered complete? *Physical Review*. 1935;**47**:777-780

- [20] Einstein A. Autobiographical notes. In: Schilpp PA, editor. *Albert Einstein: Philosopher-Scientist*. La Saller, Illinois: Open Court; 1949. pp. 1-95
- [21] Bohr N. Can quantum mechanical description of physical reality be considered complete? *Physical Review*. 1935;**48**:696-702
- [22] Bell JS. Bertlemann's socks. *Journal de Physique*. 1981;**42**(C2):41-61 Reprinted in [56]
- [23] Fine A. Bohr's response to EPR: Criticism and defense. *Iyyun: The Jerusalem Philosophical Quarterly*. 2007; **56**:31-56
- [24] Brown HR, Timpson CG. Bell on Bell's theorem: The changing face of nonlocality. 2016. pp. 91-123. Chapter 6 in [6]
- [25] Clauser JF, Horne MA, Shimony A, Holt RA. Proposed experiment to test local hidden-variable theories. *Physical Review Letters*. 1969;**23**:880-884
- [26] Brunner N, Cavalcanti D, Pironio S, Scarani V, Wehner S. Bell nonlocality. *Reviews of Modern Physics*. 2014;**86**: 419-478
- [27] Bell JS. La nouvelle cuisine. In: *Between Science and Technology*. Amsterdam: Elsevier; 1990 Reprinted in [56]
- [28] Aspect A, Dalibard J, Roger G. Experimental test of Bell's inequalities using time-varying analyzers. *Physical Review Letters*. 1982;**49**:1804-1807
- [29] Wallace D. *The Emergent Multiverse: Quantum Theory According to the Everett Interpretation*. Oxford: Oxford University Press; 2012
- [30] Wallace D, Timpson CG. Quantum mechanics on spacetime i: Spacetime state realism. *The British Journal for the Philosophy of Science*. 2010;**61**(4): 697-727
- [31] Henson J. Non-separability does not relieve the problem of Bell's theorem. *Foundations of Physics*. 2013;**43**: 1008-1038
- [32] Healey R. Local causality, probability and explanation. 2016. pp. 172-194. Chapter 11 in [6]
- [33] Friederich S. *Interpreting Quantum Theory: A Therapeutic Approach*. Basingstoke: Palgrave; 2015
- [34] Fuchs CA, David Mermin N, Schack R. An introduction to QBism with an application to the locality of quantum mechanics. *American Journal of Physics*. 2014;**82**(8):749-754
- [35] Clauser JF, Shimony A. Bell's theorem: Experimental tests and implications. *Reports on Progress in Physics*. 1978;**41**(12):1881
- [36] David N, Mermin. Quantum mechanics vs local realism near the classical limit: A Bell inequality for spin s . *Physical Review D*. 1980;**22**(2):356-361
- [37] Norsen T. Against 'Realism'. *Foundations of Physics*. 2007;**37**:311-340
- [38] Maudlin T. What Bell proved: A reply to Blaylock. *American Journal of Physics*. 2010;**78**:121-125
- [39] Laudisa F. How and when did locality become 'local realism'? A historical and critical analysis (1963–1978). *Studies in History and Philosophy of Science*. 2023;**97**:44-57
- [40] Popescu S, Rohrlich D. Quantum nonlocality as an axiom. *Foundations of Physics*. 1994;**24**:379-385

- [41] Brans CH. Bell's theorem does not eliminate fully causal hidden variables. *International Journal of Theoretical Physics*. 1988;**27**:219-216
- [42] Barrett J, Gisin N. How much measurement independence is needed to demonstrate nonlocality? *Physical Review Letters*. 2011;**106**:100406
- [43] Hall MJW. Local deterministic model of singlet state correlations based on relaxing measurement independence. *Physical Review Letters*. 2010;**105**:250404
- [44] Pütz G, Rosset D, Barnea TJ, Liang Y-C, Gisin N. Arbitrarily small amount of measurement independence is sufficient to manifest quantum nonlocality. *Physical Review Letters*. 2014;**113**:190402
- [45] Bell JS, Shimony A, Hall M, Clauser J. An exchange on local beables. *Dialectica*. 1985;**39**(2):85-110 Includes [46]
- [46] Bell JS. Free variables and local causality. *Epistemological Letters*. 1977; **15**:79-84 Reprinted in [56]
- [47] Price H. *Time's Arrow and Archimedes' Point*. Oxford: Oxford University Press; 1996
- [48] Evans P, Price H, Wharton K. A new slant on the EPR-Bell experiment. *The British Society for the Philosophy of Science*. 2013;**64**(2):297-324
- [49] Palmer T. Superdeterminism without conspiracy. *arxiv:quant-ph* 2308.11262. 2023
- [50] Hooft GT. *The Cellular Automaton Interpretation of Quantum Mechanics*. Berlin/Heidelberg: Springer; 2016
- [51] Afik Y, Muñoz JR, de Nova. Quantum discord and steering in top quarks at the LHC. *Physical Review Letters*. 2023;**130**(22):221801
- [52] ATLAS Collaboration. Observation of Quantum Entanglement in Top-Quark Pair Production using pp Collisions of $\sqrt{s} = 13$ tev with the ATLAS Detector. 2023. Available from: <https://atlas.web.cern.ch/Atlas/GROUPS/PHYSICS/CONFNOTES/ATLAS-CONF-2023-069/>
- [53] Horodecki M, Horodecki P, Horodecki R. Separability of mixed states: Necessary and sufficient conditions. *Physics Letters A*. 1996;**223**(1-2):1-8
- [54] Terhal BM. Bell inequalities and the separability criterion. *Physics Letters A*. 2000;**271**(5):319-326
- [55] Aoude R, Madge E, Maltoni F, Mantani L. Probing new physics through entanglement in diboson production. *arxiv:hep-ph/2307.09675*. 2023
- [56] Bell JS. *Speakable and Unspeakable in Quantum Mechanics*. 2nd ed. Cambridge: Cambridge University Press; 2004

Chapter 9

Perspective Chapter: Experiments in Entangled Time

Karin Marie Fierke

Abstract

The purpose of this chapter is to revisit the concept, ‘To See is to Break an Entanglement,’ through an exploration of insights from a three-year project (2020–2023), ‘Mapping the Empire: The Contemporary Legacy of Historical Trauma and Forced Displacement.’ The project arose from observations that have no explanation in classical physics, and sought to explore the significance of the ‘quantum effects’ that underpin the dynamics of a particular form of systems therapy and its potential adaptation to the analysis of global entanglements of past, present and future. The chapter develops insights relating to entanglement, language and consciousness that arose from an ‘experiment.’

Keywords: time, affective resonance, entanglement, language, consciousness

1. Introduction

The past few years have seen the publication of several books and special issues about the implications of quantum theory for the social sciences [1–8] many of which ask how particular socio-political phenomena look different when lifted from the assumptions of classical physics and placed in an uncertain quantum world. My co-authored contribution with Nicola Mackay, ‘To See is to Break an Entanglement’ [9], reflected on an ‘experiment’ that at the time was at a very early stage. Just after the article was published, we received funding to do exploratory research on a project titled ‘Mapping the Empire: The Contemporary Legacy of Historical Trauma and Forced Displacement’ (MtE).

The concept ‘to see is to break an entanglement’ is significant against the backdrop of the award of the 2022 Nobel Prize in Physics to John Clauser, Alain Aspect and Anton Zeilinger for experiments with entangled photons. Within quantum mechanics, nature is not locally real, that is, particles lack properties such as spin up or spin down prior to measurement, which corresponds with observation. They also communicate and respond to one another regardless of the distance. Entanglement is thus a non-local phenomenon. The prize winners were said to have ‘proved’ that the Universe is not locally real, on the one hand; on the other hand, as noted by Charles Bennett, a quantum researcher at IBM, ‘The experiments...show that this stuff isn’t just philosophical, it’s real – and like other real things, potentially useful’ [10]. The contrast suggests that quantum entanglement is real, but not in the way that ‘real’ is usually

understood. As Niels Bohr, the father of the Copenhagen School, noted, ‘The word “reality” is a word, a word which we must learn to use correctly.’ [11].

The reality/philosophy question has haunted discussions of quantum physics [12]. The quantum social theory debate has been mired in the binary either/or of whether, when applied to the social sciences, the quantum is real or mere analogy, metaphor or metaphysics ([5], p. 44). The application of insights derived from the analysis of microscopic phenomenon to macroscopic phenomena seems to pose a question of how to scale up from one level of life, that is, the subatomic, which is the pre-occupation of quantum physicists, to another, that is, human social and political life, which is the focus of social scientists. In this respect, the language of quanta, the smallest amount, contributes to the problem, as do claims that quantum effects wash out above the macroscopic level. The MtE project is unique within the social science debate in so far as it grew out of an observation that has no explanation in classical physics.

The ‘quantum effects’ in this case arose from the dynamics of a particular form of systems therapy, which has been widely used with families and organizations. The MtE experiment, which took place over a two and a half year period, sought to adapt the method to the analysis of more global phenomena. Material entanglements [1] and entanglements in language and social structure [2] have had a central place in the quantum social theory debate. The affective resonances that arose within a mapping process, discussed below, can only be explained in terms of non-local micro-scopic entanglements, although also relevant to both materiality and language. The study thus provides a potential bridge between discussions of quantum entanglement in the natural and social sciences.

The current race to develop quantum computing and artificial intelligence has included attempts to create emotional robots [13]. The potential simulation of human emotions in machines at the very least implies that similar properties of quantum entanglement can be found within human and other life, yet, until recently, there has been resistance to the study of consciousness, including emotions, in both the natural and social sciences. The question raised by ‘to see is to break an entanglement’ is whether in seeing non-local entanglements between past and present, spaces might be opened for turning toward the loss and ‘ungrieved grief’ of centuries of empire and war and whether an act of ‘seeing,’ as a measurement, breaks an entanglement between past and present.’

In what follows, section two brings a problem of seeing and not seeing to an ‘experiment,’ exploring its broad contours. Section three examines a concept of affective resonance as a diffracted experience within the experiment. Section four illustrates several different cuts into the analysis of the collapse of affective resonances into language within a process of blind mapping. Section five then turns to a discussion of consciousness. The conclusions highlight provisional insights from the exploratory research and further avenues for potential interdisciplinary and practical development.

2. The puzzle and experiment

Several years ago, I stumbled onto a form of family systems therapy, the underlying dynamics of which have no explanation in classical physics. A central principle of systems therapy more generally is that how and where people stand—whether facing each other, or turning their backs, or alone in a corner embodies a relationship between family members. The particular approach I encountered had a further

dimension. The family constellations modality, developed by a German, Bert Hellinger in the 1960s,¹ has been used widely in the treatment of transgenerational trauma in Germany, relating in particular to the experience of World War II, and has since spread globally. Rather than working with actual family members, Hellinger brought in complete strangers who knew nothing about one another or the family of the person who was the focus of any particular constellation. The task of these volunteers was to stand in or represent a place within a system [16].

Standing in or representing a place is a form of second party experience that can be distinguished from either first party (subjective) or third party (objective) experience (see [17]). ‘Representatives’ for different family members are able, through speaking and moving within a created system, to access the feelings and dynamic relationships of the client [18], who is seeking to resolve an issue.² Through a facilitated process, the problem is disentangled and family members who were previously excluded are given a place, which ‘releases’ the problem and restores balance to the system [19].

The title of Hellinger’s seminal book, *Acknowledging What Is* [20], suggests that acknowledging ‘what is,’ even when it is staring us in the face, may be less than straightforward. In this respect, the central dynamic revolves around a question of what can be seen and what is unseen. The potential that individuals could stand within a created system and experience traces of affect relating to someone they do not know and have no knowledge of, not least because they belong to an earlier generation, only begins to make sense in the context of some notion of non-locality, quantum field, and transgenerational entanglement. If family systems are entangled non-locally, the assumed ontological separateness of individuals is an illusion, and a question arises about the existence of entanglements within other domains of experience.

The MtE project sought to explore whether the modality could be adapted to the analysis of entanglements of historical experience and contemporary memory and practice of a more social and political nature, particularly as these relate to a global legacy of historical trauma and forced displacement. What is meant by entanglement as used here is discussed in the next section. Our focus was the legacy of the past in the present, and how entanglements of memory and habit impact on what we are able to look at and what we turn away from. The Covid pandemic provided an unusual opportunity to explore the problem. The pandemic saw an unfolding field of trauma that impacted on populations globally which amplified a range of historical memories, and not least that of the Spanish Flu Pandemic (1918–1920). The run-up to Brexit was haunted by memories of British empire. In May of 2020 George Floyd’s murder at the hands of a white policeman in Minneapolis gave rise to a greater ability ‘to see’ systemic racism, which is a legacy of enslavement, and to challenge it. By early 2022, Western attention shifted away from questions of racial inequality as Russia invaded Ukraine. Different memories of experience during World War II or the Cold War framed this context, which also revealed evidence of a struggle over who would lead a future post-pandemic order, magnified by memories of various historical empires. A

¹ Hellinger’s method was influenced by other family systems methods, such as that of Virginia Satir; German phenomenology; and observations he made of Zulu healing practices in South Africa where he served as a priest for 16 years before becoming a psychotherapist (see, e.g. [14]). Mackay was trained by Hellinger and has 20 years of experience with the modality, as well as writing about it as a practitioner [15].

² For an introduction to family constellations, which includes live sessions of Hellinger working with representatives, see: <https://www.youtube.com/watch?v=wZ1oYiR5VpM>.

more recent link between a history of colonialism and a future of climate change has highlighted the relationship between past, present and future.

The methodological objective of the exploratory research was to examine the potential to adapt a particular form of systems analysis from its use within family or organizational systems to the analysis of global entanglements of past, present and future. The substantive objective of the project was to explore the legacy of historical trauma and forced displacement in the present.

2.1 A quantum experiment?

The project developed two complementary methods of analysis, both of which evolved over the 3 years as we brought insights from each to the other. A method of *tracking* involved research assistants in the exploration of the relationship between contemporary trending events, including the memories expressed by political agents within them; historical experiences of trauma, particularly in the context of various empires; and the multiplicity of future potentials at work in relation to the events in question. The method evolved over the 3 years from a more linear and local application which was gradually replaced by a non-linear approach to the analysis of global entanglements of empire. The tracking looked at empirical contexts, while developing theoretical insights about how a legacy of the past impacts on events in the present and shapes probabilities for the future.³

A complementary method of non-linear *mapping*, which is the focus of this chapter, fed off of the data developed by the trackers.⁴ Constructing a map begins with an intentional question relevant to both contemporary events and the existing historical record. An advantage of the more socio-political application of the systems method, over the family application, is the easier access to accounts of the past. The obvious problem, which is increasingly recognized by historians [21], regards the extent to which historical narratives have been impacted by, for instance, dominant national stories, which in the context of empire, facilitated an inability to see the more negative consequences. So, for instance, national histories of empire, such as the British, have highlighted the positive role of Britain's past global presence.

A growing literature has argued that this positive take on empire has made it difficult to see or acknowledge the suffering imposed on colonized populations [21–26]. While existing historical narratives might not provide a complete picture, the unseen elements of a system become more evident in the process of the mapping itself. The historical experiences explored by the trackers revealed material practices of horrific violence. The affective resonances of these experiences were the subject matter of the maps. The conversation within an active map makes it possible to observe how different parts of a system stand in relation to each other, who or what is seen or unseen, the affective dynamics of the system, how the separate parts triangulate (to make certain other parts unseen), as well as obstacles that stand in the way of acknowledging the unseen and giving them a place.

What does this have to do with quantum entanglement and why call it an experiment? First, as already suggested, the initial puzzle arose from an experience of *quantum effects*. Quantum effects are said to wash out at the macroscopic level due to quantum decoherence, by which a system's behavior changes from that which

³ The Research Assistant trackers hailed from diverse global locations, including India, China, Vietnam, Egypt, South Korea, Nigeria, Germany and Scotland.

⁴ We refer to the method as *Dynamic Entangled Memory Mapping* [9].

can be explained by quantum mechanics to that which can be explained by classical mechanics. The question is whether the effects disappear altogether or are simply unobservable in daily life. The experiment provided a modality and an apparatus for observing an otherwise unobservable and non-local phenomena over a sustained period of time.⁵ The ‘quantum effects’ would seem to point to the superposition of entangled states that exist in physically separated locations, past and present, which in the process of the mapping are ‘measured’ as they collapse into language.

Second, an entangled *complementarity* is evident in several aspects of the experiment, starting with the engagement of two complementary methods, one more oriented to the observable material world, and the other to unobservable entanglements of consciousness. Further, the emphasis on presence and non-presence, seen and unseen, resonates with Bohr’s claim that complementary opposites are both mutually exclusive and intertwined, which makes it difficult to observe two parts of an entangled pair simultaneously. Presence and non-presence is an entangled relationship which means any account that deals only with the directly observable will be incomplete.

Third, the mapping process involved analysis of the affect, bodily movements and/or language of the ‘mappers,’⁶ or those who represented positions within a given map. To insure that any patterns emerging from the process could be understood to arise from a system or field rather than individual interpretation, the experiment was undertaken *blind*. Consistent with the definition of a blind experiment, information that would influence the participants in the mapping was withheld until any one session was completed.

An *experiential* method is difficult to grasp without having had the experience. Readers may be inclined to assume that the words or gestures of the mappers express their subjective consciousness as individuals, but this is *not* the case. Instead, in stepping into a created system, the mappers become temporarily entangled with a category of socio-political experience which they represent and speak from. Recognizing that most people have traumas in their family histories, arising from larger social and political phenomena, the ethical criteria emphasized the importance that the mappers had prior training, including analysis of their own family entanglements, in order to minimize the potential to be overly triggered by stepping into a more global map.⁷ In this respect, the individual, as part of a holographic world, does not disappear altogether, but the blindness of the process minimized the role of individual interpretation, thereby maximizing the potential to analyze the extent to which the collapse of affective resonance into language within the maps arose from an holographic field. During the mapping process, the individual participants knew neither the context,

⁵ The blind group mapping took place once a month over a two and a half year period. An online application of the method made it possible to continue with the group work during the pandemic. Word-for-word transcripts were made from recordings of the sessions. Due to the terms of participants consent, the data underpinning this research cannot be made publicly available.

⁶ Use of the term ‘mappers,’ rather than ‘representatives,’ as is common with family constellations, was an attempt to avoid a potential misreading through Barad’s [1] quantum critique of representation.

⁷ Prior experience with and training in the family constellation method was identified as an ethical requirement for participation in the mapping. This background also meant they had some idea of what to expect, given the palpable energy circulating through any one map. In the rare case that a mapper experienced distress, a designated therapist provided an individual post-mapping session to further separate individuals from their experience within the map.

the question, nor the category they represented, which were only introduced to the transcripts after a session was completed.

In setting up a map, the focus of family constellations on individuals within a family system was replaced by categories of memory (e.g. the Siege of Leningrad, the U.S. Civil War, World War II, the Opium Wars), of experience (e.g. forced displacement, hunger and scarcity, war, enslavement, genocide), of emotion (e.g. grief or ungrieved grief, betrayal, guilt, shame, compassion), of collective identity (e.g. particular states, present populations, children), of happenings (e.g. Brexit, climate change, invasions) or belief (e.g. profit as belief, safety, collective agreements not to know), which are derived from an intentional question, the formulation of which drew on the contemporary and historical data compiled by the trackers. At face value, there is no reason to believe that the blind engagement of what on the surface appear to be abstract categories would be anything except a chaotic jumble of words. The surprising and significant observation regards the extent to which, as illustrated in Section 4, patterns that emerged from the maps revealed the broad contours of the topic in question, as well as unseen aspects.

The emergence of patterns from a blind conversation is difficult to grasp and easily conflated with words that evoke negative connotations in Western culture, related, for instance, to parapsychology or talking to the dead. The created maps revolved around categories of experience and memories related to *socio-political phenomena*, rather than individuals, whether alive or dead, and as such express something qualitatively different, i.e. affective resonances or traces of past experience that remain alive, and are threaded through socio-political experience in the present. In this respect, as the physicist/social theorist Karen Barad notes, memory is 'written into the fabric of the world' ([27], p. 260) rather than being purely a property of individual mind. In the next section, I set the stage by thinking about the entanglement of the present with affective resonances of the past.

3. Entanglements of trauma

There is a growing literature on artificial intelligence and the potential that robots, i.e. machines, might be endowed with properties of emotion and consciousness, yet we lack sufficient understanding of how the assumptions of quantum entanglement, which makes such an endeavor conceivable, works in sentient life. Much of the research relating to the latter has focused on the human brain and subjective consciousness. A focus on machines, individuals and the brain would seem to resonate more with the assumptions of classical Newtonian physics, which has sidelined the sentient aspects of life. Quantum mechanics is said to provide a better point of departure for taking emotions seriously. In a discussion of quantum decision theory, Alexander Wendt ([2], p. 167) makes the point that emotions do not follow a classical logic; neuroscientific studies have confirmed that reason and emotion are deeply intertwined in decision making.

The compatibility is not only evident in regard to the reason/emotion relationship. Emotions are *indeterminate*, often changing as frequently as the weather in Scotland. The indeterminism of quantum mechanics highlights randomness and chance, and multiple possible outcomes and thus the importance of probability rather than singular cause. Emotions are *complementary*, often existing in oppositional pairs, which cannot simultaneously be seen and thus express a relationship of presence and non-presence. Hate can mask love. The attribution of blame can mask guilt. Grief

may be masked by anger. The manifestation of any one will be subject to a measurement by participant observers. Emotions are also both individual and *relational*—they are experienced or expressed in relation to others, and are heavily shaped by histories, language, memory and habit, particularly as one moves toward their circulation in a global space. Global relations, often forged through war and practices of mutual harm, of betrayal, humiliation, and fear are themselves entanglements, despite the apparent fragmentation. For example, the anthropologist Gregory Bateson has noted that the humiliation of Germany at Versailles (1919) set the stage for all that has happened since. His main point was to highlight that emotional patterns matter [28]. ‘Hurt’ or trauma, particularly when it is silenced and hidden away, can be radioactive in its persistence. While positive emotions of compassion or love involve ‘seeing’ an other, the ‘ungrieved grief’ that accompanies trauma often gives rise to a tendency to turn away and to not see or know, as the emotions, whether guilt, shame or grief, may be too difficult for all parties involved to sit with [29]. The silence that so often surrounds historical traumas is part of the ‘radioactivity,’ i.e. persistence over generations, of *non-local entanglements* of past and present. The purpose of this section is to briefly set the stage by exploring a notion of non-local affective entanglements with the past, which maintain a resonance in the present, i.e. the ‘quantum effects.’ The subject matter connects to diverse interdisciplinary literatures, but, as space does not allow for a comprehensive review, the objective is to make sense of the affective dynamics of the mapping process.

3.1 Time and affective resonance

‘Seeing’ and ‘not seeing’ may be a spatial relationship but may also be temporal, non-local and non-linear. Linear constructions of time draw lines between past, present and future. Past ‘events’ may be known factually, but are separated out and relegated to a bygone era where they exist in a linear relationship to the present as something that no longer is. Theoretical mathematicians, physicists and cosmologists have argued that linear notions of time as flowing forward, separated neatly into past, present and future, rest on an illusion [30]. In discussing superposition and entanglement, which she identifies with diffraction, Barad argues that ‘different times bleed through one another’ [31].

The literature on socio-political memory includes claims that contemporary populations use memory for purposes of the present (e.g. [32]) or in the realization of future projects (e.g. [33]). While not denying the importance of the observation, the mapping sought to explore non-local entanglements between historical *experiences* of trauma by segments of populations, and performances of *memory* in contemporary socio-political contexts, a distinction that emerged from the development of the tracking method. While important for analytical purposes, the distinction disguises the extent to which memory arises from an accumulation of past experience, which in its continuous performance, sediments aspects of the past, thereby thickening memory and habits relating to it. The experience/memory distinction, relates to a further distinction between *affect*, which usually refers to an experience of sentience, and the articulation of *emotion* in the political performance of memory and in language, which are often also entangled. The following unpacks these distinctions to make some sense of the ‘bleeding’ of socio-political trauma across time within the ‘experiment.’

‘To see is to break an entanglement’ rested on a claim that not only individual memories of trauma, but also social memories are entangled with both sensory

imprints of past trauma and language [9]. Commenting on a century of study of traumatic memories, the psychiatrist Bessel van der Kolk [34] argued that semantic memories may coexist with sensory imprints, which often remain stable over time, but may return when triggered by reminders. Sensory imprints of trauma appear as fragments, rather than narratives, and are expressed in images, physical sensations and intense emotions [35]. Traumatic memories are also more persistent in their recurring presence than ‘normal’ everyday memory; they intrude without welcome and often in response to triggers in the environment that resemble an earlier trauma. In cases of complex trauma, woven over extended periods of time, the intrusions become part and parcel of a relational world, structured around types of habitual experience and the use of language [36].

Bateson’s point about patterns of hurt suggests that sensory imprints are not exclusive to individuals but infuse experiences of traumatic memory that are more socio-political. Given the association between sensory imprints and the physical body, a concept of *affective resonance* is more useful for understanding a sentient experience that crosses over and through individual bodies, in which past and present bleed through each other. Within the context of the maps, the words, facial expressions or bodily movements of the participants expressed traces or fragments of traumatic historical experience, although, it should be emphasized, without re-experiencing the historical trauma itself. The affective resonance did not arise from personal experience, but rather expressed a diffracted resonance of past social experience in the present. Diffraction in its basic form is the bending of light around an obstacle. The two-slit experiment at the heart of quantum physics used a diffraction grating, to reveal the entanglement of particles and waves, and the importance of the observer and their apparatus for what is seen. Diffraction patterns highlight the presence of waves in matter, which is less about where difference appears than mapping where the effects of difference appear [37].

The 2020 article made a further claim that ‘articulations within the context of a created map express a form of wave-function collapse and a pattern of diffracted entanglement by which the attributes of a system become visible or “seen” as the vibrational frequencies surrounding a particular represented space, and the affect that arises from it, are transformed into language and thus become available for analysis’ [9]. Within the spacetime of the blind maps, the affective resonances experienced by the mappers might be said to work on the same principle as the forced-resonance tuning fork experiment, in which a vibrating tuning fork forces a stationary tuning fork into resonant vibration when placed beside it [38]. In stepping into a map, the participants come into resonance with the diffracted interference of the category of experience that they represent, where the boundaries of linear time are erased; as they speak from a position of blindness, the affective resonance is ‘measured’ in the collapse into language.

The experiment also revealed the greater complexity of multiple differently positioned mappers accessing past entangled states blindly. A cloud, which stores the memories of computer systems, might provide an analogy. The entangled mappers resonate with information stored in a cloud-like space—a sort of supercomputer in the cosmos—which is an interesting contrast to the efforts of physicists to use supercomputers to simulate the universe,⁸ a contrast that suggests the former may not be that far-fetched. The theoretical physicist David Bohm [39] refers to an implicate order, a seamless quantum field, of all that has been, with all potentials, habits and memories recorded in spacetime. Bohm contrasts the wholeness of this implicate order with the fragmentation of the macroscopic explicate order, with which it is

⁸ Examples include NASA’s Pleiades supercomputer or Japan’s ATERUI II.

entangled. The mapping provides a means to observe the relationship between the potentials within this larger quantum field and the active presence of fragmented entanglements within the world.

In so far as the diffracted affect relates to past experience, whether dispossession, famine, scarcity or enslavement, which is larger than individuals, the resonances arise from a *field* of experience which may or may not be contiguous with the 'collective memory' of a state or culture. The basic assumption of a system or field, while taking diverse forms in the literature, is that the whole coordinates the relationship between parts. In the context of the maps, patterns of affect emerge from the whole rather than the intentions or consciousness of the individuals involved. The biologist Rupert Sheldrake suggests that what he refers to as 'morphic resonance' is the past 'pressed up' against the present, which is potentially present everywhere ([40], p. 161). The resonance arises from past patterns of activity that influence the fields of subsequent and similar systems, which involves a kind of action at a distance in both space and time. Morphogenetic fields are probability structures within which the most common past types, sedimented in memory and habit, combine to increase the probability of a recurrence of that type ([40], p. 157).

At stake is a presence of the past expressed through memory and habit. Epigenetics suggests a potential that traumas from earlier generations may reappear in the bodies of successor generations, often triggered by environmental conditions that resemble an earlier trauma [41–44].⁹ Transgenerational trauma has become a widespread concern, particularly in relation to entanglements of race in the U.S. [45]; or as evidenced in a PBS documentary about Pike Island, a sacred Native American space at the meeting point of the Minnesota and Mississippi Rivers, which was transformed into a concentration camp in the aftermath of the U.S.-Dakota War of 1862 [46]. Ruth Davern, the granddaughter of a previous owner of the Island, explores the roots of her family, who fled persecution in Ireland at the hands of the British, only to participate in similar processes of exploitation by European settlers in the U.S.

It is not that work on the more social and political dimensions of transgenerational trauma is new; the problem has been a tendency to turn away from it. Gabriella Schwab discusses the engendering of silence in relation to the transgenerational trauma passed on to German children by those who perpetrated or accommodated the horrors of the Nazi regime [47]. Ngugi wa Thiong'o refers to a similar problem of transgenerational memory in post-colonial Africa, in relation to the millions of unmourned victims of a system of enslavement and colonialism [48]. How grief is processed or not has implications for how further relations unfold [49], and whether traumatic entanglements are reinforced or seen and broken.

A concept of affective resonance points to something like a sensory imprint, not in the individual body but within the world as a living organism, bristling with hurt accumulated through repeated practices of harm, also to nature, and expressed in non-local affective resonances, which can be more clearly seen within the created system of a map. The key question raised by 'to see is to break an entanglement' is whether in seeing these entanglements, a space might be opened for turning toward the loss and 'ungrieved grief' of centuries of empire and war and whether an act of 'seeing,' as a measurement, breaks an entanglement between past and present.

⁹ Epigenetics shifts attention to the influence of environment on bodies and specifically on the expression or suppression of genes. Over the past decade, the interface between environment and biology has increasingly been used to understand the intergenerational transmission of trauma.

4. Language

The analysis of affect, resonance and field in the previous section raises a difficult question about how we know what we know and why it is important to know. What happens in the collapse of the affective resonances, within the context of a given map, into language? What happens in the shift from a more classical understanding of language as representing, mirroring or corresponding to ‘things’ in the world to its role in the constitution of non-local relationships between entangled *phenomena*? To examine a phenomenon is to ask ‘what it is like’ [50, 51] to be in a state of X, in relation to other phenomena, which is to move from an exploration of essence to experience and meaning within a particular entangled moment that is unfolding between past, present and future. The question is what we can know from the process of mapping, or how to make sense of the relationship between an intentional question, as an apparatus, and the words expressed by the blind mappers in the unfolding of a particular map.

There is little agreement among physicists about the nature of ‘reality,’ and its relationship to language, including mathematical language, and, for instance, whether reality *is* a mathematical structure ([52], italics added), or the world is physical but mathematics is a way of representing it [53]; or that interpretation and storytelling are prior to mathematical formalism ([54], pp. 5, 17). Bohr’s claim that we are ‘suspended in language’ [11] suggests that every aspect of human communication involves the use of language, which in the case of physics extends to mathematical tools, but is not exclusive to them ([55], p. 2). The physicist Stig Stenholme identifies a family resemblance between Bohr’s thought on language and that of the philosopher Ludwig Wittgenstein [55]. From this perspective, the scientific apparatus, as the unit of description, functions in much the same way as everyday language, playing a role in the constitution of limited systems rather mirroring universal ones. As such, the relationship between language and reality is both/and rather than either/or. Mathematics captures something real, but, in so far as this is ‘useful’ [10] also modifies that reality, e.g. in the form of MRI’s, AI or quantum computing.

The French philosopher Michael Bitbol explores the relevance of Wittgenstein’s philosophy for physics, starting with a distinction between factual propositions and mathematical propositions [56]. He identifies the latter with the performative use of particular rules, norms or signs, the meaning of which is conferred by their relation to phenomena. Rather than mirroring isolated objects or forms, whether empirical or platonic, respectively, the mathematical language invokes a ‘system of propositions’ that is constitutive of phenomena [57]. The use of language is a measurement that brings into being a realm of possibility, which does not represent *a* reality, but rather that allows one to act or speak *as if* such a correspondence has been established ([56], p. 192). In the physics laboratory, the apparatus produces the conditions that the scientist, who is entangled with it, seeks to explore, including obstacles, which are then read through the semantic grid that is imposed by the project ([56], p. 193). A similar process, I would argue, happens within the experimental conditions of the mapping.

The intentional question of a particular map, like, the semantic grid of the scientist, positions the investigation of a phenomenon. As the apparatus, the question is entangled with the facilitator and other participants, even while the latter neither know what they represent or the context with which they engage. Nor do they control what emerges from the field or system. The dynamic captured within any one map cannot be said to represent an independent ‘reality’ (the worlds ‘as it is’) but provides the broad contours of a positional phenomenon in space and time, which reveals unseen aspects (of ‘what is’) in the world.

The following three illustrations make distinct cuts into the analysis of the non-local entanglements arising from the maps. The first explores the *replication* of an unfolding system of propositions relating to World War II memory, based on the collapse of affective resonances into language within successive maps over the period of a year in the lead up to the Russian invasion of Ukraine in 2022. The second provides a *visualization* of a non-local field expressed within a particular map, and discusses its relationship to the material context at a particular moment in time. The third illustration provides a *narrative construction* of a map from a single day, which emerged from stringing together the fragments of the blind conversation. The memory of World War II is only a single category of experience within a vast amount of data, which due to the terms of participants consent, cannot be made publicly available. The analysis provides a glimpse of the working of memory both within specific maps and as it unfolded across the maps and over time, and what this potentially says about the relationship between the physicality of the non-local affective resonances, language and materiality.

While material and physical are often conflated, a distinction can be made between the former as ‘made of matter’ and the latter as having a ‘real existence’ that can be measured and represented mathematically, an example being an electromagnetic field that is physical but not material [58]. In the present analysis, a similar distinction might be made between the present material reality of war and the physical resonances of memory, which in our case are measured through the blind mapping rather than mathematically.

Where do the textual analyses and visualizations below come from? In setting up any one map, a letter was assigned to the participants, which corresponded with the category of experience they represented. After the exercise, and prior to analysis, the letters were replaced with the categories of memory and experience within the map. Each of the transcripts was then processed, line by line, to clarify the relationship between the represented space and the words spoken by the mappers. Visual maps of each session were also created using a Miro tool. The illustrations provide three different cuts into the blind maps, which provide a glimpse of what can be known through the seeing of the otherwise unobservable relationship between the physical and non-local affective resonances and the contours of an unfolding material context.

4.1 The unfolding phenomenon of World War II memory

The following analysis, drawn from a series of maps, structured around different intentional questions at specific points in time over a year, reinforces two insights in particular. First, as suggested in the last section, in stepping into a map, the mappers become entangled with non-local affective resonances surrounding a particular category, of memory in this case, which has been assigned to them in advance, but is unknown to them while in the maps. Second, what collapses into language is less as an essence of the ‘event’ World War II, than a phenomenon, surrounded by an affective resonance, which is active in the unfolding of a context, prior to, during and in the aftermath of the invasion. Given that the context is not static, but continuously changing, replication does not take the form of seeing the same result, given that any one map is a limited system, revolving around an intentional question at a specific moment in time. The replication is evident in the expression of potentials that can be recognized as ‘what it is like’ to be World War II. For instance, in the example below, the identification of World War II memory with war (1/27/22), rather than diplomacy, or with revenge and humiliation, rather than compassion, is consistent with

knowledge of the phenomenon, which would not be the case if the contrasts appeared in reverse. The memory of World War II has a sense and a use, which is neither fixed nor arbitrary.

The table below illustrates fragments of ‘what it is like’ to be World War II memory that are replicated *across successive blind maps* in the year preceding and month following the Russian invasion of Ukraine. Each item in this brief sampling of memory fragments is preceded by the date of the map and the intentional question that was its point of departure and context (**Table 1**).

The table illustrates an unfolding system of propositions that is consistent with our knowledge of the phenomenon of World War II memory, the affective resonance

Feb25,21 (<i>What historical memories are animating the aftermath of the British withdrawal from the EU against the backdrop of pandemic?</i>): The memory of World War II is wary, particularly of emotions and what they might do. The memory holds hidden agreements [59].
Mar25,21 (<i>What needs to be acknowledged in order to take the aggression out of the relationship between the EU and the Westminster government following Brexit?</i>): A dynamic potential for the re-emergence of World War has been unleashed, with the breakdown of old agreements for peace in Europe. The grief surrounding the memory of World War II needs to be acknowledged, but it remains hard to do so. The memory of World War II animates everything in the map [60].
June24,21 (<i>How is memory shaping the structure of the post-pandemic agreements?</i>): Russia wants to play a game with the memories of World War II...The memory of World War II is full of potentials but it is not yet clear which potential the post-pandemic agreement will activate [61].
Jan27,22 (<i>What needs to be seen in order to neutralise the threat of a Russian invasion of Ukraine?</i>): The memory of World War II doesn't see the usefulness of diplomacy and wants a place for war. There is a strong threat of Russian invasion. The memory of World War II is being dressed up, but it is unclear whether it will play a role in battle or provide a framework for academic analysis of the conflict. The memory is in any case being prepared for an entrance on the stage. Bringing in World War II will start a fire. From the perspective of World War II, multiple memories and potentials inform the context...World War II memories are animated by revenge and humiliation, which are becoming stronger and more dangerous...The memory of World War II invokes a predictable recurrence of the past, which arises from a particular way of thinking in the world that is lacking in compassion [62].
Feb24,22 (<i>What would support and facilitate a shift into seeing a collective agreement for peace?</i>): War is happening in Europe again...The past and present political environment has been organized around a heavily militarised aggressive game, and, while it would be desirable to change this, there is a lack of agency and a powerlessness...Seeing a more global safety and a future for children requires looking at memories of war. Past sacrifice and memories of war are being used for political purposes rather than being acknowledged and grieved [63].
Mar24,22 (<i>Does witness to and grieving memories of WWI and WWII support a humanitarian response in Ukraine?</i>): The memory of Stalin connects to the memory of the Siege of Leningrad and the Nazi invasion, which have a solid place and resonate with the larger map. NATO is on the periphery, watching but not reacting. It is unclear how the context will unfold, but Putin is like a gamemaster, not necessarily in charge but pulling the cards and making up the story. The memory of the Siege of Leningrad is within him, making him feel very big'. The memory of the Nazi Invasion, which impacts on the sovereignty of land, provides the distorted lens through which Putin sees others. For NATO, the memory of the Nazi invasion is only a single part of a larger whole, relating to other memories of atrocity during World War II. A numbness of emotions is pervasive and everything is focused on the Nazi invasion, which seems to provide cohesion but is fragmented and experienced differently from different angles, with no common thread. Unacknowledged guilt underpins the memory of the Nazi invasion. Introducing guilt into the map connects the memory of Versailles to the memory of Nazi invasion [64].
<i>*Putin, who is from Leningrad, hadn't yet been born at the time but his brother died in the siege.</i>

Table 1.
Memories of World War II: Sampling across successive maps from February 2021 to March 2022.

surrounding it, and its working in the world. In successive maps, the ‘hidden agreements’ (1/21) reappear as the ‘breakdown of old agreements for peace in Europe’ (2/21), which, in both maps is linked to Brexit, followed later by the potentials for a new post-pandemic agreement (6/21). Over time, further entailments of World War II memory unfold. The memory ‘wants a place for war’ rather than diplomacy and is ‘being dressed up’ for entrance on the stage (1/22). Specific memories (3/22) arise from multiple positions (6/21, 1/22) but also empower Putin (3/22), who initially wants ‘to play a game with the memories’ (6/21) and after the invasion becomes ‘like a gamemaster’ (3/22). The memory is infused with emotions, from grief, which needs to be acknowledged (3/21), to revenge and humiliation, which animates the memory (1/22), to numbness (3/22), to unacknowledged guilt and a lack of compassion (3/22). The memory, which invokes a ‘predictable recurrence of the past’ (1/22), is used strategically for ‘political purposes’ (2/22) and provides cohesion while remaining fragmented at the level of experience (3/22).

The system of propositions within the maps overlap with the empirical context and as such captures the broad contours of the latter. For instance, Putin did put the memory to use in justifying the defensive nature of his ‘special military operation,’ pointing to ‘Nazi’s’ in Ukraine. NATO, consistent with its position in the early days of the war, stands at the sidelines without responding to the invasion. The clustering of memories of Stalin, the Siege of Leningrad, and Nazi invasion reflects an historical relationship. The memory of Versailles, which the French President Macron brought in at an early stage of the conflict, received little support and faded from use; as the map from 24 March 2022 (above) suggests, not seeing the memory of Versailles has implications, which I return to below.

4.2 Analysis of single maps

Two types of analysis were brought to the individual maps, as illustrated in the following examples. The first provides a *visualization* of the represented spaces and how the ‘blind’ mappers engaged within a specific map a month before the Russian invasion. The eyes on the symbols point either toward or away from other parts within the whole, which indicates what each can see or not see. As already stated, prior to the exercise, the mappers were assigned a letter that corresponded with the category of experience they represented. After the exercise, the letters were replaced with the categories presented in the illustration below. In the brief summary that follows, each of the positions is placed in quotation marks to indicate that it is a space within the map. Again, as it is so difficult to comprehend, it is worth reinforcing the point, which is relevant to all three illustrations, that the blindness of the process meant that the mappers had no knowledge of the context or the particular categories that they represented within the map (**Figure 1**).

As the map unfolded, ‘Ukraine’ was apprehensive, stating it was looking for an ally, but did not think it had one. ‘Russia in the present’ was aware of the memory of the ‘Versailles Treaty 1919,’ which suggests the potential influence of the memory on Russia. None of the other categories were looking at the memory of the ‘Versailles Treaty,’ which is consistent with the larger context of the invasion. Memories of ‘World War II’ and ‘Cold War,’ which are clustered at this stage and aware of each other, are the greater influence on the map as a whole. ‘NATO’ is aware of the ‘threat of Russian Invasion,’ which is angry, and of the ‘threat of nuclear war,’ and states that it is both in danger and dangerous. The ‘threat of nuclear war,’ which is aggravated, could see an affinity between the ‘memory of



Figure 1.
27Jan 2022: *What needs to be seen in order to neutralize the threat of a Russian invasion of Ukraine?* [65].

World War II' and the 'threat of Russian invasion,' which are both experiences of invasion. 'Diplomacy' wasn't interested in the 'threat of Western Expansion' but can see it, which is interesting in light of NATO arguments that minimized the significance of its Western expansion [66]. 'Diplomacy' describes itself as feeling '*sociopathic*' (lacking in empathy, anti-social) which is compatible with the failure of diplomacy in the run-up to the invasion.

This is just a brief snippet from an early stage of a session that continued for an hour and a half. As the mapping progressed, and further objects, representing other categories were brought in, the relationship between the different spaces further unfolded. Among these, memory of the Ukrainian famine (Holodomor, 1932–1933) and the Siege of Leningrad (1941–1944) shifted the lens bringing attention to the role of hunger and scarcity as well as profit (during the famine, wheat was Stalin’s ‘Gold’). The Siege had a solid place within the map and resonated with it. It also made Putin feel ‘big,’ which is interesting in light of his family history and the resemblance between Hitler’s tactics in Leningrad and Putin’s in Mariupol and elsewhere. Consistent with the economic sanctions against Russia and Putin’s later attempts to obstruct grain shipments from Ukraine, which raised concerns about global food supplies and famine, diplomacy played into food scarcity. The introduction of guilt formed a connection between memories of Versailles and Nazi invasion, which points to the role of punishing sanctions on Germany in paving the ways for Hitler’s rise and World War II. NATO wasn’t seeing either aspect of the context, but, based on the map, needed to. The larger trans-map analysis of World War II memory above shows a repeated inability to see an earlier legacy of memory, against the dominance of World War II memory. The pattern was repeated in a later map, on 24 March.

The analysis of the unseen memories in the last paragraph highlights several points. First, not only the memories that are directly articulated by leaders in the present were important; others memories woven into a longer past had an unseen

but active physical presence. It further highlights the positional experience of the different actors involved in the conflict. Second, further memories are diffracted through the dominant one. The memories together reveal long-standing and criss-crossing patterns of hurt and complicity. Third, the physical reality of past experience expressed in memory infuses a material context of war.

The illustration above provides a visualization of ‘seeing’ within a particular map at an early stage of its unfolding, which intersects with and replicates positional memories expressed in other maps. The third example illustrates the *narrative* construction of a map from the day Russia invaded Ukraine, a month later, which provides a more cohesive story. The full decoded transcript from that day is too long to include here; the summary answer more directly shapes the narrative to the question. It is interesting that the full decoded transcript began with ‘War is happening in Europe again.’ (Table 2).

It is hard to account for the philosophical nature of the narrative that emerged from stringing together the fragments of a particular blind conversation or where it comes from.¹⁰ Interestingly, it points to a problem that has defined the study of international relations, that is, the desirability of more global security, contrasted with the reality of state action driven by insecurity, commonly referred to as the ‘security dilemma.’ However, in contrast to more traditional accounts, the narrative highlights

Question: *What would support and facilitate a shift into seeing a shared global collective agreement for peace?*

Answer: Addressing the absence of trust, which is the heart of the problem. Trust requires turning toward ungrieved grief, with its roots in the past, but grief is presently being used as a political football. There is a need to let go of a sense of safety that arises from fragmentation (*a world divided into states*) in order to give a place to holistic (*global*) safety*. The past and present political environment has been organized around a heavily militarised aggressive game, and, while it would be desirable to change this, there is a lack of agency and a powerlessness. This environment has been a source of grief for past and present populations, and has given rise to an irreversible accumulation of unacknowledged guilt. Because the fragmentation of populations has been seen in the past as a solution, it has left them continuously responding to triggers that repeat old patterns. Seeing a more global safety and a future for children requires looking at memories of war. Unacknowledged guilt is continuously reproducing itself in new forms, and a new post-pandemic agreement is emerging from this. The media, the military-industrial complex, global institutions and scientific observers are watching what is going on but through a lens influenced by beliefs that peace comes through war. Present populations can’t yet see what is coming as a result of the Russian invasion of Ukraine. The past is in the process of being repeated and there is a need to gain insight from what has happened before, i.e. looking at the past, rather than seeing the present as unique through a lens of unacknowledged guilt. The emphasis on fragmented safety is energised through war and madness and Russia could destroy us all. This sense of fragmented safety becomes a means to mobilise present populations to escalate war as a way of doing something, but is antagonising Russia into self-destruction and destruction of the world. While Russia appears to be the agent of destruction, belief in the sanctity of fragmentation (*sovereignty*) contributes to the present chaos. Past sacrifice and memories of war are being used for political purposes rather than being acknowledged and grieved. Profit as belief goes hand in hand with the fragmentation, but will eventually bring about its own death. The threat of nuclear war is a potential that arises from the fragmentation of the political environment. The threat of environmental destruction is endangering the future of children, who want the ungrieved grief to be grieved in order to restore a balance. Creating a place for a holistic safety would contribute to seeing the situation more clearly and to compassion. While it seems too late to acknowledge the guilt (*given that it appears irreversible*), from the perspective of ungrieved grief there is a choice and it is never too late. From the perspective of a global collective agreement for peace a totally new approach is needed; the proposed mobilization of present populations won’t help the situation [63].

**Italicized points in parentheses have been added by the author for purposes of clarification.*

Table 2.
Sample question and answer from blind mapping on the day that Russia invaded Ukraine.

¹⁰ Given the huge amount of detail involved in wading through any one transcript line by line, it would be impossible from within the process of analysis to make this up.

the importance of memories of war and ungrieved grief, which is a function of the apparatus.¹¹

The various cuts into the analysis suggest that consciousness is a property of a *system*, which is entangled with the apparatus of measurement, i.e. an intentional question. The system is not static but expresses an unfolding series of propositions which resonate with ‘what it is like’ to be a particular kind of experience at a moment in time and space. The non-local affective resonances arising from the blind maps provide a window into a material reality that has been woven by political actors in memories of historical experience, which cannot be separated from the drawing of boundaries in a context of war. They further raise a question about the tendency to separate materiality from consciousness. Like the particle and wave, the two exist in a complementary relationship. The final section shifts to an exploration of preliminary insights regarding the nature of consciousness as it emerged from the ‘experiment.’

5. Consciousness

The quantum mind/consciousness debate in quantum mechanics, which has been underway for more than a century, began with a question about the role of the observer and consciousness in measurement [67]. Despite these origins, there has been a resistance within physics [68], no less than the social sciences [2], to tackling the hard problem of consciousness. While the simulation of human consciousness in artificial intelligence is a rapidly expanding field, quantum consciousness is often conflated with new age mysticism and thus discredited, although this is beginning to change.¹² Within biology, there is growing evidence of, for instance, the place of quantum effects in photosynthesis, by which plants turn sunlight into fuel (e.g. [71, 72]), or the role of the Earth’s magnetic field in providing a ‘quantum compass’ for migratory birds in navigation ([73], p. 2). The physicist Matthew Fisher [69, 70] has proposed that the nuclear spins of phosphorus atoms may act as rudimentary ‘qubits’ in the human brain that enable the brain to function like a ‘quantum computer.’

Our experiment did not set out to explain consciousness but rather to observe the ‘quantum effects’ and to identify patterns of non-local entanglement between past and present arising from a blind process over several years. Having said that, the exercise raised significant questions about the nature of consciousness. The first regards the frequent reference in the literature to consciousness as an individual subjective experience (e.g. [6], pp. 323–342; [68, 74]). The analysis above of ‘what it is like’ [50] to be a particular kind of experience, i.e. of war, does not deny the importance of subjective consciousness or the role of the brain in processing, but shifts emphasis from the mechanism of the ‘container’ to experience. ‘What it is like to be in a state’ is a problem of experience which is more than individual experience, or for that matter, human experience; it was indeed used by the philosopher Thomas Nagel in relation to bats [50] and arguably applies to any category of experience. ‘What it is like’ to be in a state is a property of field or system, which in the first instance is holographic and non-local rather than subjective.

¹¹ For an expanded analysis of the dynamics and difference between fragmented and holistic safety, and a thought experiment regarding the ‘Safety Paradox,’ see ref. [29].

¹² Critics have referred, e.g., to ‘hocus pocus’ and ‘pixie dust in the synapses’ [69, 70]. The emphasis on mysticism arguably relies on a misreading of Asian traditions such as Buddhism and Daoism [7].

The 'experiment' highlighted the positional nature of consciousness. In the illustration, the range of propositions belonging to the memory of World War II take multiple forms within an unfolding context, even while remaining a phenomenon that is recognizable as 'what it is like' to be World War II. Further, how World War II was experienced at the time, or its memory in the present, is a function of many different positions, whether as a victim or perpetrator of invasion, famine, rape, etc. where the individual experience was part of a larger social positioning, which was differentiated within and across states in Europe, but also refers to war as an experience across time and space. The maps suggest that affective resonances arise from categories of human experience, within a context of relationships. Consciousness is a product of experience which, through repetition is both shaped by and shapes memory, habit and practice, as well as the meaningful potentials that arise from them. Traces of past experience persist as affective resonances. The collapse of these resonances into language within the blind maps makes it possible to examine the positioning of particular experiences vis-à-vis multiple other experiences at specific moments in space and time.

A second question regards the apparent contradiction that the mappers were 'seeing' or witnessing within a 'blind' map. The consciousness that emerges from a given map does not express a subjective individual state but a non-local entanglement between past experience and present memory. The second party experience of consciousness reveals patterns of diffracted affect, i.e. traces of affect diffracted as the past 'presses up' against the present [40] in the material world, which are also diffracted through the maps [9]. The perplexing problem in regard to our 'experiment' regards a second party experience that is not a first party experience because of the 'blindness,' on the one hand, and in light of the holographic and positional nature of experience within the maps, on the other hand. Consciousness is not a property of separate individuals per se, although expressed in its particularity by them; it is a holographic property of memory, which can be found in life all the way up and all the way down, although specific to species [40].

The mapping is potentially useful, not as a tool of calculation, like the mathematical formulae of physics, but rather as a tool for expanding and changing consciousness. As the project evolved, the investigators noted a change in themselves and how they were viewing the subject matter, often in a more visceral manner, which gave rise to a question of how other participants were impacted by their involvement. In order to better understand the 'witness effect,' we asked both trackers and mappers to regularly reflect on their experience. During the first year, the more empirical research of the trackers was understood to be in a totally different category than the mapping. The one involved reading and writing; the other involved blind engagement within the maps. However, having monitored the 'witness effect' of both, the two experiences do not appear to be qualitatively different. The consciousness that emerges from the maps is more concentrated and a function of a particular intentional question, but is only an intensified experience of everyday consciousness. Both are manifestations of the entangled nature of mind and consciousness with the material world and with language, as distinct from a tendency to identify mind with the mechanism of the individual brain.

Does the holographic entanglement of consciousness and memory suggest that seeing in one place percolates out, expanding the potential for the larger world to see? The question was highlighted by an exploration of memories of slavery and Civil War in 2017, against the backdrop of the U.S. 'politics of hate' and the Trump presidency, several years before the funded research began. Over a series of blind maps, we saw the emergence of a pattern: The mappers could not look at the person who represented the

category of slavery, which reflected a more widespread tendency to turn away from this shameful aspect of the U.S. past. The mapping process facilitated a shift into seeing the slavery position within the maps. A month later, the events in Charlottesville, VA, unfolded and have since been referred to as a marker of a new conversation in the U.S. about this history [75]. We questioned whether the correlation was pure coincidence. Charlottesville was a manifestation of violence that has been there all along; the difficulty of facing or reconciling with this past over decades and a century since the Civil War is the core problem. To address a problem requires acknowledgement that it exists, which may be difficult when ‘collective agreements not to know’ [29] stand in the way of seeing the loss and suffering that often hides behind them. Denial and silence accompany trauma of all kinds and can carry into future generations.

As exploratory research, the MtE project sought to develop tools for analyzing the affective dynamics of seen and unseen within the maps, which expressed non-local quantum entanglements. However, measuring non-local impacts is far more problematic. In any case, neither the blind mapping process nor potential non-local impacts can be understood in classical causal terms, of a scientist manipulating variables. Indeed, given the emphasis on acknowledging ‘what is’ the point is to achieve a more complete view and, in so far as seeing breaks an entanglement, contribute to opening spaces for reflection and agency that are less burdened by traumatic entanglements with the past.

During the first year of the exploratory research, we became aware, both conceptually and experientially, of the extent to which we were part of the uncertain world surrounding us. From a quantum perspective, the scientist or analyst is a participant observer who is bound up with the apparatus of observation and what is seen is a function of the positioning of both. Those involved in the tracking and the mapping began to see the world in a different way, just as in the midst of the chaos of the pandemic, potentials for acknowledging past harm, some of which have been turned away from for centuries, began to be seen, e.g. in demands for reparations or the return of stolen artifacts to post-colonial spaces or the linkages between colonialism in the past and climate change in the future. Whether and how the two processes intersected non-locally remains an open question.

The affective resonances within the maps, and the palpable experience of them,¹³ provided evidence that something interesting was happening, even while it was impossible to say precisely what. The group mapping began with an assumption that the blind nature of the exercise would minimize individual interpretation, and indeed, given that the mappers did not know what they or others represented, it is safe to say that this was the case. In the aftermath of a session, once the question and the positions became known, there was, however, a tendency for individuals to place their own transgenerational legacies within a larger global socio-political context, thereby increasing consciousness of their relationship to land in different parts of the world, and of earlier collective experiences of dispossession, scarcity or war, among others. There was also a greater sense that things in the present are entangled, not only with something older but also with that which has been denied life or is yet to come. Looking back also made it possible to look forward, raising questions about the legacy of the past and present in the future.

A frequent theme of the anonymous survey data was one of hopefulness arising from participation in the project, although the enhanced awareness of suffering in the world was sometimes tinged with futility, particularly for the trackers. The hopefulness, I would suggest, arose in part from a feeling that the act of witnessing is itself

¹³ Specific protocols were developed for entering and leaving the maps in order to minimize the possibility that participants would carry resonances into their daily lives.

important. But the sense of empowerment was also due to experiences of seeing and feeling the world from different positions in global space, and thus a perspective that is larger than the narrow positional perspective each of us carry as individuals. The mapping experience was akin to stepping into someone else's shoes; the shoes in this case did not belong to individuals but categories of collective experience across global space and time. The experience of trackers, as already suggested, was not qualitatively different, as captured in one reflection:

At an early stage...the choices of tracking events and historical memories were heavily influenced by my own background. It was also easy to get very emotional or to be influenced by historical traumas which are more likely to have resonances with my own experiences. As the tracking unfolded, I started to shift to topics that I am not familiar with...Through the witness of other people's traumas, I found myself become less emotional both in terms of looking at historical traumas and the present situation – I don't know whether this is good or bad. But by looking at traumas from multiple perspectives and traumas of people unlike me, I have a feeling of stretching, which means I feel that my body and my memories themselves become records and carriers of various traumas through 'seeing'. But this process is quite different from the process of traumatization as I am not personally traumatized. For me, it is more like a process of biological recording as if I have become an automatic memory component of a larger social scheme [76].

Both types of experience potentially gave rise to a more visceral sense of 'seeing' particular kinds of historical and present experience, including the experience of 'what it is like' to be unseen. This 'witness effect' potentially provides a point of departure for developing pedagogical tools that might increase sensitivity among a broader population, and particularly more privileged populations, thereby minimizing a tendency, noted by one of the mappers, to blame victims for their suffering, or to fail to see our own complicity in global practices that are a source of suffering, e.g. the use of child labourers in Cobalt mining in Africa which is integral to the development of green technologies. The cumulative effect of participating in the project over an extended period of time was greater awareness of the entanglement of multiple historical empires, and of practices of appropriating land and what this has meant for occupants of the land, who were dispossessed and/or enslaved, among others. The practices are not purely a thing of the past, but bleed into the present, not least in relation to continuing practices of land appropriation, displacement, deforestation and the extraction of natural resources. As was recognized at the COP27 gathering in 2022, there is a link between colonialism and climate change, and victims of the former are suffering more directly from the latter as a result of this history. The failure to act decisively to address either as we walk blindly to the brink of environmental catastrophe itself suggests an unwillingness to 'see' the problem or the implications for future generations.

6. Conclusions

As exploratory research, the focus was less on testing or falsification than proof of concept. The analysis above suggests three preliminary insights:

- Memories and habits of past trauma are a legacy that we find it hard to look at. The mapping process provides a way to step into affective resonances of past trauma, diffracted in the present, to 'see' their continuing presence.

- The collapse of the non-local affective resonances into language within the blind maps expresses a limited system, or the positioning of phenomena in space and time. The lines of difference within the maps provide insight into what is seen and unseen and the working of memory within the world.
- Consciousness is a property of a holographic field of experience rather than individuals per se.

The conceptual focus on affective resonance, entanglement, language and consciousness would benefit from a more interdisciplinary engagement around questions raised by the experiment.

The continuing analysis of data from the MtE project may bring further insights, including the potential practical significance of the work, and whether the maps are primarily a tool of analysis or might be developed for pedagogical or 'therapeutic' use. In regard to the latter, the modality raises a question of whether 'seeing' in the context of the maps potentially provides 'release' of resonances of past trauma from present experience, making it possible to deal with the present more on its own terms. In the family constellation model, release results from giving a place to the unseen parts, thereby restoring balance to a family system, which is an important component of the therapy. A further example from the individual treatment of trauma is possibly comparable and provides a way to think about the potential importance. EMDR (Eye Movement Desensitization and Reprocessing) can very quickly desensitize and reprocess an individual's bodily experience of trauma. Through the reprocessing of memories of negative events, the individual no longer experiences high levels of distress associated with a particular memory. The reprocessing integrates the traumatic material, separating it from the present, thereby restoring a potential for agency [35]. The question is whether 'seeing' global entanglements of 'ungrieved grief' from centuries of empire, and giving it a place within the maps, similarly provides 'release' from affective resonances of past trauma, thereby reprocessing and taking some of the distress out of engaging with legacies of the past in the present.

Second, given the fragmented nature of traumatic memory, might the reconstruction of the blind conversations in narrative form itself represent a form of reprocessing, similar in intention to truth and reconciliation commissions, but without the accompanying risk of re-traumatization, and/or open spaces for ethical reflection and agency? As the geographer Karen O'Brien notes, telling a different story may be critical to enhancing individual and collective agency to generate transformative change ([77], p. 75). The problem, as suggested by the MtE project, regards the difficulty of opening spaces to 'see' differently, given a tendency to turn away from the suffering that often hides behind assumptions and 'agreements' embedded in everyday language. In so far as traumatic memory intrudes and triggers powerful and defensive reactions, it can be an obstacle to seeing the present on its own terms, which is necessary for exercising autonomy and agency.

The topic of the project is very large in scope but no more so than the magnitude of the problems we presently face as a planet. Further research might develop methods that facilitate the opening of potentials for a change of consciousness and a transition to another way of living together in the world. The experiment was not about the manipulation of variables separate from us but rather the potential to turn toward seeing the self and others, whether individual or collective, from a different angle, with a more complete view such that the unseen might be seen and given a place. Unacknowledged harm in the past remains a toxic influence not only in the present

but potentially on the future as well. To acknowledge the presence of the past is itself to break entanglements with ‘collective agreements not to know’ [29], which stand in the way of restoring balance to a dangerously imbalanced global system. Entanglement is not by definition positive or negative; both potentials exist but are different in kind. The issue is less one of being entangled or not, but rather the ability to acknowledge ‘what is,’ and the extent to which this recognition opens a space for global conversation [78] and agency in addressing the legacy of human inequality and the destruction of nature, which is blindly propelling us toward the precipice of climate emergency.

Acknowledgements

The Mapping the Empire project was funded by the U.S. Human Family Unity foundation through a donation to the University of St. Andrews. The research was undertaken with Nicola Mackay who has complementary expertise as a systems therapist with training in medical physics. The present analysis grows out of the project but the chapter was written solely by the author as a first step of the project evaluation.

Thanks

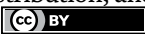
I would like to thank the Human Family Unity Foundation, Nicola Mackay and all of the mappers and trackers for their contribution to the project, including Ahmed Abozaid, Andrew Milne, Phuong Anh Nguyen, Adagbo Onoja, Joost Pietschmann, Mary Kay Reinemann, D. Lauren Ross, Aarushi Sharma, Denise Stallcup, Alison Strandberg, Lorraine Tolmie, Shambhawi Tripathi, Sayre Vickers, Kirsty Walsh, Karen Withaus, Chaeyoung Yong, and Yang Yuanfuyi, several of whom also, along with David Sylvan and Nadine Voelkner, provided insightful comments on various drafts of the chapter. Thanks also to Roberta Weber, who, during a acupuncture session in 2015 pulled me off the therapy table and into a family constellation which gave rise to my curiosity and to exploration of that curiosity in the years since.

Author details

Karin Marie Fierke
University of St. Andrews, St. Andrews, Scotland

*Address all correspondence to: kf30@st-andrews.ac.uk

IntechOpen

© 2023 The Author(s). Licensee IntechOpen. This chapter is distributed under the terms of the Creative Commons Attribution License (<http://creativecommons.org/licenses/by/3.0>), which permits unrestricted use, distribution, and reproduction in any medium, provided the original work is properly cited. 

References

- [1] Barad K. *Meeting the Universe Halfway: Quantum Physics and the Entanglement of Matter and Meaning*. Durham, NC: Duke University Press; 2007. DOI: 10.1215/9780822388128
- [2] Wendt A. *Quantum Mind and Social Science: Unifying Physical and Social Ontology*. Cambridge: Cambridge University Press; 2015. DOI: 10.1017/CBO9781316005163
- [3] Zanotti L. *Ontological Entanglements, Agency and Ethics in International Relations: Exploring the Crossroads*. London: Routledge; 2019. DOI: 10.4324/9781315227764
- [4] Kurki M. *International Relations in a Relational Universe*. Oxford: Oxford University Press; 2020. DOI: 10.1093/oso/9780198850885.001.0001
- [5] Murphy MPA. *Quantum Social Theory for Critical International Relations Theorists: Quantizing Critique*. London: Palgrave Macmillan; 2020. DOI: 10.1007/978-3-030-60111-9
- [6] DerDerian J, Wendt A. Quantizing international relations: The case for quantum approaches to international theory and security practice. *Security Dialogue*. 2020;**51**(5):399-413. DOI: 10.1177/0967010620901905
- [7] Fierke KM. *Snapshots from Home: Mind, Action and Strategy in an Uncertain World*. Bristol, UK: Bristol University Press; 2022. DOI: 10.46692/9781529222647
- [8] Voelkner N, Zanotti L. Ethics in a quantum world. *Special Issue of Global Studies Quarterly*. 2022;**3**(2):1-5. DOI: 10.1093/isagsq/ksac044
- [9] Fierke KM, Mackay N. Mint: To see is to break an entanglement: Quantum measurement, trauma and security. *Security Dialogue*. 2020;**51**(5):450-466. DOI: 10.1177/0967010620901909
- [10] Garisto D. The universe is not locally real, and the physics Nobel prize winners proved it. *Scientific American*. 6 October 2022. Available from: <https://www.scientificamerican.com/article/the-universe-is-not-locally-real-and-the-physics-nobel-prize-winners-proved-it/>
- [11] Peterson A. Mint: The philosophy of Niels Bohr. *Bulletin of Atomic Scientists*. 1963;**19**(7):8-14. DOI: 10.1080/00963402.1963.11454510
- [12] Ball P. *Beyond Weird: Why Everything you Thought you Knew about Quantum Physics Is ... Different*. London: The Bodley Head; 2018. DOI: 10.7208/chicago/9780226594989.001.0001
- [13] Stock-Homberg R. Mint: Survey of emotions in human-robot interactions: Perspectives from robotic psychology on 20 years of research. *International Journal of Social Robotics*. 2022;**14**:389-411. DOI: 10.1007/s12369-021-00778-6
- [14] Mayer C, Viviers R. Mint: Constellation work and Zulu culture: Theoretical reflections on therapeutic and cultural concepts. *Journal of Sociology and Social Anthropology*. 2016;**7**(2):101-110. DOI: 10.1080/09766634.2016.11885706
- [15] Mackay N. *Your Invisible Inheritance: Releasing the Hidden Legacy of Ancestral Trauma*. London: Rebel Magic Books; 2020
- [16] Bilger B. When Germans make peace with their dead. *The New Yorker*. 2016.

Available from: <https://www.newyorker.com/magazine/2016/09/12/familienaufstellung-germanys-group-therapy>

[17] Scott JW. Mint: The evidence of experience. *Critical Inquiry*. 1991;17(4):773-797

[18] Ulsamer B. *The Healing Power of the Past: The Systemic Therapy of Bert Hellinger*. Nevada City, NE: Underwood; 2005

[19] Cohen DB. *Systemic Family Constellations and the Use with Prisoners Serving Long-Term Sentences for Murder or Rape [Thesis]*. San Francisco, CA: Saybrook Graduate School and Research Centre; 2008

[20] Hellinger B, ten Hovel G. *Acknowledging What Is: Conversations with Bert Hellinger*. Phoenix, AZ: Zieg, Tucker and Co., Inc.; 1999

[21] Satia P. *Times Monster: History, Consciousness and Britain's Empire*. London: Allen Lane; 2020

[22] Andrews K. *The New Age of Empire*. London: Allen Lane; 2021. DOI: 10.1080/17449855.2023.2175951

[23] Gildea R. *Empires of the Mind: The Colonial Past and the Politics of the Present*. New York: Cambridge University Press; 2019

[24] Armitage D. *The Ideological Origins of British Empire*. Cambridge: Cambridge University Press; 2010. DOI: 10.1017/CBO9780511755965

[25] Bell D. *Reordering the World: Essays on Liberalism and Empire*. Princeton, NJ: Princeton University Press; 2016. DOI: 10.23943/princeton/9780691138787.001.0001

[26] Inca O. *Colonial Capitalism and the Dilemmas of Liberalism*. Oxford: Oxford University Press; 2018

[27] Barad K. Mint: Quantum entanglements and hauntological relations of inheritance: Dis/continuities, spacetime enfoldings and justice-to-come. *Derrida Today*. 2010;3(2):240-268. DOI: 10.3366/drt.2010.0206

[28] Bateson G. *Steps to an Ecology of Mind*. Chicago: University of Chicago Press; [1972]2000

[29] Fierke KM, Mackay N. Mint: The safety paradox: Unknown knowns, ungrieved grief and collective agreements not to know. *International Relations*. 2023. online first. DOI: 10.1177/04711782231187499

[30] Kuhn RL. *The illusion of time: What's real? Spaceflight*. 2022. Available from: <https://www.space.com/29859-the-illusion-of-time.html> [Accessed: August 29, 2023]

[31] Barad K. Mint: Troubling time/s and ecologies of nothingness: Re-turning, re-memembering and facing the incalculable. *New Informations*. 2017;92(5). DOI: 10.3898/NEWF

[32] Eyerman R. *Memory, Trauma, Identity*. London: Palgrave Macmillan; 2019

[33] Kratochwil F. *Praxis: On Acting and Knowing*. Cambridge: Cambridge University Press; 2018

[34] Kolk Bvd. Mint: Trauma and memory. *Psychiatry and Clinical Neurosciences*. 1998;52(S1):S52-S64. DOI:10.1046/j.1440-1819.1998.0520s5S97.x

[35] Kolk Bvd. *The Body Keeps the Score: Mind, Brain and Body in the Transformation of Trauma*. London: Penguin; 2014

- [36] Fierke KM. Bewitched by the past: Social memory, trauma and international relations. In: Bell D, editor. *Memory, Trauma and World Politics*. Basingstoke: Palgrave; 2006
- [37] Barad K. Mint: Diffracting difference: Cutting-together-apart. *Parallax*. 2014;**20**:168-187. DOI: 10.1080/13534645.2014.927623
- [38] Ooe, H., et.al. Mint: Resonance frequency-retuned quartz tuning fork as a force sensor for noncontact atomic force microscopy. *Applied Physics Letters*. 2014, 105, 043107 DOI: 10.1063/1.4891882
- [39] Bohm D. *Wholeness and the Implicate Order*. London: Routledge; [1980] 2002. DOI: 10.4324/9780203995150
- [40] Sheldrake R. *Presence of the Past: Morphic Resonance and the Habits of Nature*. London: Icon Books; 2011
- [41] Walters KL, Beltran RE, Huh D, Evans-Campbell T. Dis-placement and dis-ease: Land, place and health among American Indians and Alaska natives. In: Burton LM, Kemp SP, Leung MC, Matthews SA, Takeuchi DT, editors. *Communities, Neighborhood, and Health: Expanding the Boundaries of Place*. Philadelphia, PA: Springer Science+Business Media; 2011. pp. 163-199. DOI: 10.1007/978-1-4419-7482-2
- [42] Lehrner A, Yehuda R. Mint: Cultural trauma and epigenetic inheritance. *Development and Psychopathology*. 2018;**30**(5):1763-1177. DOI: 10.1017/s0954579418001153
- [43] Yehuda R, Lehrner A. Mint: Intergenerational transmission of trauma effects: Putative role of epigenetic mechanisms. *World Psychiatry*. 2018;**17**(3):243-257. DOI: /10.1002%2Fwps.20568
- [44] Jablonka E. Mint: Cultural epigenetics. *The Sociological Review*. 2016;**64**(1-suppl):42-60. DOI: 10.1002/2059-7932.12012
- [45] Menakem R. *My Grandmother's Hands: Racialized Trauma and the Pathway to Mending our Hearts and Bodies*. Las Vegas: Central Recovery Press; 2017
- [46] PBS. *Stories I did not Know*. 2021. Available from: <https://www.pbs.org/show/stories-i-didnt-know/> [Accessed: May 22, 2023]
- [47] Schwab G. *Haunting Legacies: Violent Histories and Transgenerational Trauma*. New York: Columbia University Press; 2010
- [48] Ngugi wa Thiong'o. *Something Torn and New: An African Renaissance*. New York: Basic Books; 2009
- [49] Hutchison E, Bleiker R. Grief and the transformation of emotions after war. In: Ahall L, Gregory T, editors. *Emotions, Politics and War*. London: Routledge; 2015. DOI: 10.4324/9781315765068
- [50] Nagel T. Mint: What is it like to be a bat? *Philosophical Review*. 1974;**83**(4):435-450
- [51] Block N. Mint: On the confusion about a state of consciousness. *Brain and Behavioral Sciences*. 1995;**18**:227-247. DOI: 10.1017/s0140525x00038188
- [52] Tegmark M. *Our Mathematical Universe: My Quest for the Ultimate Nature of Reality*. London: Allen Lane; 2014
- [53] Carroll, S. S02E01 Is Consciousness Emergent? *Mind Chat*. You Tube
- [54] Fuchs C. *My Struggles with the Block Universe: Selected Correspondence, January 2001–May 2011; 2014–2015*.

Available from: <https://arxiv.org/pdf/1405.2390.pdf> [Accessed: July 10, 2023]

[55] Stenholm S. The Quest for Reality: Bohr and Wittgenstein, Two Complementary Views. Oxford: Oxford University Press; 2011. DOI: 10.1093/acprof:oso/9780199603589.001.0001

[56] Bitbol M. Mint: Mathematical demonstration and experimental activity: A Wittgensteinian philosophy of physics. *Philosophical Investigations*. 2018;**41**(2):188-203. DOI: 10.1111/phin.12187

[57] Wittgenstein L. On Certainty. Wiley-Blackwell; 1975

[58] Ron Davis, physicist. Available from: <https://www.quora.com/Is-there-a-difference-in-the-meaning-of-physical-and-material> [Accessed: July 13, 2023]

[59] Based on unpublished preliminary data analysis of transcripts from the Mapping the Empire Project: 7GT240421

[60] Based on unpublished preliminary data analysis of transcripts from the Mapping the Empire Project: 8GT250321

[61] Based on unpublished preliminary data analysis of transcripts from the Mapping the Empire Project: 10GT240621

[62] Based on unpublished preliminary data analysis of transcripts from the Mapping the Empire Project: 14GT270122

[63] Based on unpublished preliminary data analysis of transcripts from the Mapping the Empire Project: 15GT240222

[64] Based on unpublished preliminary data analysis of transcripts from

the Mapping the Empire Project: 16GT240322

[65] Based on unpublished preliminary data analysis from the Mapping the Empire Project: 14GM270122

[66] NATO. NATO-Russia Relations: the facts. 2023. Available from: https://www.nato.int/cps/en/natohq/topics_111767.htm [Accessed: July 10, 2023]

[67] Tarlaçı S, Pregolato M. Mint: Quantum neurophysics: From non-living matter to quantum neurobiology and psychopathology. *International Journal of Psychophysiology*. 2016;**103**:161-173. DOI: 10.1016/j.ijpsycho.2015.02.016

[68] Tegmark M. Why Consciousness is one of the most Divisive Issues in Physics Today, 2022. Available from: <https://www.youtube.com/watch?v=Lul6M13F-ao> [Accessed: July 14, 2023]

[69] Fisher M. Mint: Are we quantum computers, or merely clever robots? *International Journal of Modern Physics B*. 2017;**31**. DOI: 10.1142/S021797921743700019

[70] Fisher M. Mint: Quantum cognition: The possibility of processing with nuclear spins in the brain. *Ann. Physics*. 2015;**362**:593-602. DOI: 10.1016/j.aop.2015.08.020

[71] Arndt M, Juffmann T, Vedral V. Mint: Quantum physics meets biology. *HFSP Journal*. 2009;**3**(6):386-400. DOI: 10.2976/1.3244985

[72] Lloyd S. Mint: Quantum coherence in biological systems. *Journal of Physics: Conference series*. 2011:302. DOI: 10.1088/1742-6596/302/1/012037

[73] Ouellet, J. A New Spin on the Quantum Brain. *Quanta Magazine*.

2016. Available from: <https://www.quantamagazine.org/20161102-quantum-n> [Accessed: May 22, 2023]

[74] Bitbol M. Mint: La Conscience a-t-elle une origine? Des neuroscience a' la pleine conscience: une nouvelle approche de l'esprit. Paris: Flammarion; 2014

[75] PBS. A Year Ago Charlottesville Shined a Light on White Supremacists and Sparked Overdue Conversations. 2018. Available from: <https://www.pbs.org/newshour/show/a-year-ago-the-charlottesville-rally-shined-a-light-on-white-supremacists-and-sparked-overdue-conversations> [Accessed: May 11, 2023]

[76] Based on unpublished preliminary data analysis from the Mapping the Empire Project: YY/19/07/22

[77] O'Brien K. You Matter More than you Think: Quantum Social Change for a Thriving World. Oslo, Norway: cChange Press; 2021

[78] Fierke KM, Jabri VM. Global conversations: Relationality, embodiment and power in the move toward global IR. *Global Constitutionalism*. 2019;8(3):506-535. DOI: 10.1017/S2045381719000121

Entanglement in High-Energy Physics: An Overview

Mohammed Nadir

Abstract

This abstract explores the entwined realms of quantum field theory, holography, and the AdS/CFT correspondence, converging upon the enigmatic phenomenon of entanglement within high-energy physics (HEP). At the core of this narrative lies the concept of entanglement entropy—a profound measure of quantum entanglement that threads the connections between quantum information, correlations, and the very architecture of spacetime. As the journey unfolds, the AdS/CFT correspondence illuminates entanglement’s holographic nature, decoding its role in deciphering the enigmas of HEP. Bell’s inequality emerges as a lighthouse, probing the non-local essence of entanglement and challenging the classical boundaries of reality. Quantum cryptography emerges as a practical extension, harnessing the unique attributes of entanglement for secure communication. The tensor product formalism weaves together the quantum tapestry, while gravity—nature’s sculptor of spacetime—molds the dynamics of entanglement within HEP. This abstract paves the path for a chapter that traverses based on original findings, unraveling the secrets of entanglement’s significance within the intricate fabric of high-energy physics. The Nobel Prize in Physics 2022, awarded to Alain Aspect, John F. Clauser, and Anton Zeilinger, enriches this narrative. Their experiments solidify entanglement’s non-locality, bridging the realms of quantum mechanics and HEP. This abstract encapsulates the entangled narrative and its dialog with gravity.

Keywords: quantum field theory, holography, AdS/CFT (anti-de sitter/conformal field theory) correspondence, entanglement entropy, quantum information, quantum correlations, spacetime, Bell’s inequality, quantum cryptography, tensor product, gravity

1. Introduction

Entanglement, a quintessential phenomenon of quantum mechanics, has transcended its role as a conceptual enigma to become a pivotal player in the narrative of high-energy physics (HEP). This chapter embarks on a journey to unravel the deep-seated connections between entanglement and the fundamental aspects of our universe. The principle of superposition, where particles can exist in multiple states simultaneously, and entanglement, where particles become inherently connected across vast distances, are at the core of this mysterious quantum world [1].

1.1 Quantum field theory: Foundations and Frontiers

Quantum field theory (QFT) is the bedrock of modern theoretical physics, providing a framework for describing the interactions of particles and fields. At the heart of QFT lies the peculiar phenomenon of entanglement, where particles become inexorably intertwined, their fates interlinked in a manner that defies classical intuition [1]. This interconnection transcends spatial separation, manifesting non-local correlations that have confounded physicists and spurred debates on the very nature of reality [2].

Quantum field theory intersects with the fabric of spacetime, giving rise to the intricate interplay between entanglement and gravity. The holographic principle, symbolized by the AdS/CFT correspondence, presents a radical perspective that links a gravitational theory in anti-de Sitter space to a quantum field theory (AdS/CFT) on its boundary [3]. This duality evokes profound implications for understanding the emergence of spacetime and the role of entanglement in the underpinnings of gravity [4].

The quest for unraveling entanglement secrets has led to the notion of entanglement entropy, a measure of the quantum entanglement inherent in complex systems [5]. This quantity, intertwined with the fabric of quantum information theory, has offered fresh insights into the architecture of quantum states, phase transitions, and the fabric of spacetime [6].

1.2 Beyond Bell's inequality

Bell's inequality and its experimental violations mark a turning point in the exploration of entanglement. Experiments have confirmed the non-local nature of entanglement, challenging classical notions of causality and realism [7, 8]. The ramifications of these violations span from the foundations of quantum theory to the realm of quantum cryptography, promising secure communication protocols that hinge on the inseparability of entangled particles [9].

1.3 Navigating the quantum terrain

The quantum landscape brims with uncharted territories, offering tantalizing prospects for revolutionizing computation, cryptography, and our understanding of the universe. Quantum computing and quantum cryptography leverage entanglement's unique properties to potentially outperform classical counterparts and ensure communication security in the quantum realm [10]. The tensor product formalism, a powerful mathematical tool, lies at the heart of these endeavors, allowing for the description of composite quantum systems and their interactions [11].

2. Motivation for studying entanglement in high-energy physics

Motivating research in high-energy physics concerning entanglement is essential due to its potential to provide deeper insights into fundamental physical phenomena and their significance in various theoretical frameworks. Here are some key motivations, along with relevant references:

1. *Understanding Quantum Complexity*: High-energy physics deals with complex quantum systems, and entanglement serves as a fundamental tool to understand

and quantify their intricate quantum correlations. Entanglement entropy, in particular, has been extensively studied to characterize the entanglement structure in quantum field theories and many-body systems [5].

2. *Quantum Gravity and Holography*: Investigating the role of entanglement in the holographic AdS/CFT correspondence provides crucial insights into the connection between quantum field theories and gravity in higher-dimensional spacetime. Entanglement entropy in the boundary theory is related to the area of minimal surfaces in the bulk AdS spacetime, offering tantalizing clues about the quantum nature of spacetime [12].
3. *Quantum Computing and Information*: Entanglement plays a central role in quantum information theory and quantum computing. Understanding the role of entanglement in quantum algorithms and quantum communication is crucial for developing efficient computational tools and communication protocols [11].
4. *Quantum Field Theories and Phase Transitions*: The study of entanglement entropy has led to significant advances in understanding phase transitions and critical phenomena in quantum field theories. Entanglement measures have proven to be powerful tools in characterizing quantum phase transitions [13–15].
5. *Black Hole Physics and Information Paradox*: Investigating the entanglement properties of black holes can provide insights into the nature of black hole entropy and the resolution of the information paradox. Entanglement entropy in black hole systems is a fascinating topic in the study of quantum gravity [3].
6. *Quantum Foundations*: Entanglement is at the heart of quantum non-locality and the Einstein-Podolsky-Rosen (EPR) paradox [16]. Understanding the foundational aspects of entanglement and its implications for quantum mechanics can deepen our understanding of quantum reality [1, 14].
7. *Quantum Information in Collider Physics*: In collider experiments, the efficient handling of enormous data sets and the optimization of event selections are critical. Quantum computing and quantum machine learning, harnessing entanglement and quantum correlations, promise to revolutionize data analysis in HEP [17]. It enables us to probe entanglement in extreme conditions. These experiments can provide empirical evidence for the quantum nature of particle interactions [18, 19].
8. *Fundamental Tests of Quantum Mechanics*: HEP provides a unique testing ground for fundamental principles of quantum mechanics. Future experiments may explore aspects like entanglement, non-locality, and quantum correlations to probe the boundaries of our current understanding [1, 20]. These research areas represent just a glimpse of the exciting possibilities that entanglement holds in the realm of High-Energy Physics. As technology advances and our knowledge deepens, these investigations are likely to shape our understanding of the fundamental forces of the universe.
9. *Beyond the Standard Model*: HEP is dedicated to probing the fundamental forces and particles of the universe. Entanglement can be a powerful tool for discover-

ing deviations from the Standard Model of particle physics, including the search for dark matter and understanding neutrino properties [21, 22].

10. *Quantum Gravity and Entanglement*: The search for a theory of quantum gravity remains a fundamental challenge. Entanglement is expected to play a significant role in reconciling quantum mechanics with general relativity. Research in this area aims to uncover the quantum nature of spacetime itself [23, 24].
11. *Quantum Cryptography and Secure Communication*: While not exclusive to HEP, quantum cryptography harnesses entanglement to enable secure communication. Its applications extend to safeguarding sensitive data in HEP experiments, ensuring the integrity of results [25–28].
12. *Quantum Chromodynamics (QCD) and Quark-Gluon Plasma (QGP)*: HEP experiments often involve extreme conditions, such as the quark-gluon plasma (QGP) created in heavy-ion collisions. Understanding the entanglement properties of QGP can shed light on its quantum behavior and phase transitions, which are of great interest for studying the early universe and fundamental interactions. Investigating the entanglement properties of particles in the early universe, specifically in the Quark-Gluon Plasma phase, remains a critical area of research. This includes understanding the role of entanglement in QCD and its implications for the early universe [29–31].

In conclusion, entanglement is a versatile and indispensable concept in high-energy physics, offering avenues for understanding fundamental physics, quantum gravity, quantum information, and technological advancements. Research in this area can lead to breakthroughs with wide-ranging implications for our understanding of the universe and our ability to harness quantum phenomena for practical applications.

3. Explanation of the significance of the chosen keywords

The following explanation underscores the significance of the chosen keywords, showcasing how they interconnect to shape the landscape of high-energy physics and our understanding of entanglement's role in fundamental particles, quantum gravity, quantum technologies, and more.

1. *Quantum Field Theory*: Quantum field theory (QFT) serves as the mathematical framework for describing fundamental particles and their interactions. It unifies quantum mechanics with special relativity and provides a foundation for understanding the behavior of particles in high-energy processes [32]. QFT elucidates how entanglement operates in particle interactions, paving the way for unraveling the intricate quantum dynamics that govern these phenomena.
2. *Holography (AdS/CFT Correspondence)*: Holography, specifically the AdS/CFT correspondence, establishes a profound connection between quantum field theories and gravity in higher-dimensional spacetimes [2]. This duality suggests that entanglement patterns in a quantum field theory correspond to geometric features in its gravitational counterpart. The AdS/CFT correspondence hints at a deeper unity between these seemingly disparate realms, ushering in novel insights into entanglement's role in both contexts.

3. *Entanglement Entropy*: Entanglement entropy quantifies the amount of entanglement between different components of a quantum system [4]. It provides a powerful tool for probing the entanglement structure within complex systems, such as those found in high-energy physics. Entanglement entropy unveils critical information about the behavior of particles, phase transitions, and emergent phenomena, enriching our understanding of quantum systems.
4. *Quantum Information*: Quantum information theory explores how information is processed and manipulated in the quantum realm [11]. In the context of high-energy physics, understanding how entanglement and quantum correlations can be harnessed for quantum information processing is crucial for the development of quantum technologies such as quantum computing and cryptography. These technologies hold transformative potential for solving complex problems that are beyond the reach of classical computers.
5. *Quantum Correlations*: Quantum correlations extend beyond classical correlations, giving rise to phenomena like entanglement. These correlations defy classical intuitions and hold the key to harnessing the power of quantum mechanics for information processing and fundamental research [33]. Investigating quantum correlations in various platforms, from photons to qubits, is essential for understanding the entanglement landscape in different physical systems.
6. *Quantum Simulation*: Quantum simulation involves using quantum systems to simulate and study complex quantum processes that are challenging to simulate on classical computers [34]. By utilizing entangled states, quantum simulation enables researchers to explore high-energy processes, study particle interactions, and uncover insights into the behavior of particles in extreme conditions.
7. *Gravity and Spacetime*: Gravity, as described by general relativity, governs the curvature of spacetime and the behavior of massive objects [35]. Entanglement's connection to gravity through concepts like the holographic principle highlights its potential role in revealing the underlying nature of spacetime. Exploring entanglement in the context of gravity and spacetime can provide insights into the fundamental fabric of the universe.
8. *Quantum Computing and Quantum Cryptography*: Quantum computing leverages entanglement to perform computations with a quantum advantage [10]. Quantum cryptography exploits the non-local nature of entanglement to establish secure communication protocols [36]. These emerging technologies hold promise for revolutionizing various aspects of high-energy physics, from simulating complex systems to securing communication channels. A more recent entanglement-based secure quantum cryptography has been reported by Yin, Juan et al. [27].
9. *Tensor Products*: The tensor product formalism, a powerful mathematical tool, lies at the heart of the Quantum Field Theory, allowing the representation of composite quantum systems and interactions which are central to the simulation of complex HEP systems [11].

4. Quantum field theory and entanglement

4.1 Entanglement in quantum field theory

In the realm of high-energy physics (HEP), quantum field theory (QFT) takes on a paramount role in modeling the fundamental forces and particles that govern the universe. Entanglement, a quintessential feature of quantum mechanics, plays a pivotal role in this context. As particles are described by quantum fields, their interactions and correlations are inherently entangled [32]. The entanglement entropy, which quantifies the degree of entanglement in a quantum system, has found profound applications in unveiling the complex nature of QFTs, shedding light on quantum phase transitions and critical phenomena [5].

4.2 Entanglement as quantum correlations

Entanglement serves as a manifestation of quantum correlations beyond classical limits, defying our classical intuitions about the separability of particles. In HEP, this non-local interdependence of particles is crucial for understanding phenomena like confinement, where quarks and gluons remain entangled within hadrons [37]. Entanglement entropy not only characterizes the entanglement but also provides a window into the structure of the underlying quantum states, revealing connections between particles and their collective behavior [29].

4.2.1 Furthermore

For example, “von Neumann entropy” quantifies the amount of entanglement between two subsystems in a quantum system. Mathematically, it is described as follows:

$$S(\rho_A) = -\text{Tr}(\rho_A \log(\rho_A)) \quad (1)$$

Where:

- $S(\rho_A)$ is the von Neumann entropy of subsystem A.
- ρ_A is the reduced density operator for subsystem A, obtained by taking the partial trace over subsystem B.

To be more explicit, let us express ρ_A and its components:

$$\rho_A = \text{Tr}_B(\rho) \quad (2)$$

Here, $\text{Tr}_B(\rho)$ represents taking the partial trace over subsystem B, which mathematically means summing over all degrees of freedom in subsystem B. This operation leaves you with a reduced density operator that only contains information about subsystem A.

So, in a more detailed form, the von Neumann entropy for subsystem A is:

$$S(\rho_A) = -\text{Tr}(\rho_A \log(\rho_A)) = -\text{Tr}(\text{Tr}_B(\rho) \log(\text{Tr}_B(\rho))) \quad (3)$$

Some recent references related to von Neumann entropy are cited in [38–42], while the original work is in Von Neumann [43].

4.3 Quantum field theory and Bell's inequality (Nobel prize 2022)

The study of Bell's inequality in HEP explores the boundaries of classical correlations and sets the stage for exploring the non-locality inherent in entanglement. In experiments involving entangled particles, such as those in the domain of HEP, violations of Bell's inequality affirm the predictions of quantum mechanics over classical theories [1, 8]. These violations underscore the profound implications of entanglement for our understanding of particle interactions and the non-local nature of reality [16]. The Nobel Prize in Physics 2022, awarded to Alain Aspect, John F. Clauser, and Anton Zeilinger, enriches this narrative [6, 44]. Their experiments solidify entanglement's non-locality, bridging the realms of quantum mechanics and HEP. The entangled narrative encapsulates entanglement's centrality in HEP, its weaving into quantum simulations, and its dialog with gravity.

4.4 Quantum information and HEP

Quantum information theory finds synergy with HEP, particularly in the context of quantum computing and cryptography. Quantum field theory allows for the representation of complex systems using tensor product formalism [11], a crucial tool in quantum information processing. Quantum computers, leveraging entanglement, hold the potential to revolutionize simulations of quantum systems relevant to HEP [10]. Moreover, quantum cryptography exploits the principles of entanglement to establish secure communication protocols, offering insights into particle interactions and information transfer in HEP [45].

5. Holography and the AdS/CFT correspondence

5.1 The holographic principle and emergent gravity

In the pursuit of understanding the elusive connection between quantum mechanics and gravity, the holographic principle emerges as a revolutionary concept. It posits that the information contained in a region of space can be encoded on its boundary, suggesting a deep connection between quantum systems and their gravitational descriptions [46]. The holographic principle not only challenges our traditional understanding of spacetime but also offers insights into the nature of entanglement.

5.2 The AdS/CFT correspondence: Quantum fields and gravity

At the forefront of this intersection lies the AdS/CFT correspondence, a groundbreaking duality that relates certain quantum field theories in “anti-de Sitter” (AdS) spacetime to theories of gravity in one higher dimension [2]. This correspondence provides a remarkable tool to study the interplay between entanglement and gravity. In HEP, the AdS/CFT correspondence allows researchers to explore strongly coupled quantum field theories by mapping them to weakly coupled gravitational theories, enabling investigations into complex phenomena that were previously inaccessible.

Quantum entanglement in the context of gravity is an area of ongoing research that poses significant challenges due to the complex interplay between quantum mechanics and general relativity. While there is ongoing progress in developing rigorous mathematical frameworks, a complete and universally accepted mathematical description of quantum entanglement in gravity is still an active area of investigation. However, several approaches have been proposed that aim to provide more rigorous mathematical tools and derivations in this field:

1. **AdS/CFT Correspondence:** The Anti-de Sitter/Conformal Field Theory (AdS/CFT) correspondence, a concept derived from string theory, relates certain gravitational theories in anti-de Sitter space (AdS) to conformal field theories (CFTs) in lower dimensions. This duality has been extensively studied and provides a powerful framework to explore the connection between gravity and quantum entanglement. Mathematical techniques from both AdS and CFT sides are employed to understand the entanglement properties of the dual theories.
2. **Holography and Entanglement Entropy:** Holography, a principle stemming from the AdS/CFT correspondence, suggests that the information within a gravitational system can be encoded on its boundary. In this framework, the entanglement entropy of a quantum field theory living on the boundary is related to the gravitational properties of the corresponding bulk theory. Mathematical tools such as the Ryu-Takayanagi formula and the Hubeny-Rangamani-Takayanagi formula [12] have been derived to calculate the entanglement entropy in holographic setups.

5.3 Entanglement and geometry: Insights from holography

The AdS/CFT correspondence unveils the holographic nature of entanglement, where the entanglement structure of a quantum field theory is mirrored in the geometry of its gravitational counterpart [3]. The “holographic entanglement entropy” captures this relationship, showing that the entanglement entropy of a boundary region corresponds to the area of a minimal surface in the bulk spacetime. This deep connection between entanglement and geometry enriches our understanding of both quantum mechanics and gravity.

5.4 Spacetime as an emergent phenomenon

Emergence lies at the heart of the AdS/CFT correspondence, where gravity and spacetime emerge from the collective behavior of quantum fields. This hints at a deeper understanding of gravity as a consequence of entanglement and quantum correlations at a more fundamental level [3]. This perspective has profound implications for black hole physics, information theory, and the nature of spacetime itself.

The exploration of holography and the AdS/CFT correspondence uncovers the intricate connection between quantum field theories, entanglement, and the emergence of gravity, reshaping our understanding of the fabric of the universe.

6. Entanglement entropy: unveiling quantum information

6.1 Entanglement entropy in quantum field theories

In the realm of high-energy physics (HEP), the concept of entanglement entropy serves as a powerful tool to probe the intricate nature of quantum field theories. Entanglement entropy quantifies the amount of quantum entanglement between different regions of a quantum system, revealing crucial insights into its underlying structure [5]. In HEP, it provides a means to explore the fundamental nature of particle interactions and their entangled correlations.

6.2 Renormalization and scale dependence

The study of entanglement entropy within HEP has led to a deep connection between the behavior of entanglement and the renormalization group flow of quantum field theories [47]. The entanglement entropy exhibits intriguing scale dependence, reflecting the way that quantum fluctuations and particle interactions manifest at different energy scales. This perspective sheds light on the behavior of particles as they undergo energy changes, providing an intricate understanding of quantum field dynamics.

6.3 Holographic insights into entanglement entropy

The AdS/CFT correspondence also plays a pivotal role in understanding entanglement entropy in HEP. The holographic entanglement entropy prescription relates the entanglement structure of a boundary theory to the geometry of its corresponding bulk spacetime [12]. This deepens our comprehension of how quantum correlations and entanglement are intertwined with the geometry of the universe. Moreover, it offers a novel perspective on the emergence of spacetime itself from the entanglement of underlying degrees of freedom.

6.4 Applications in critical phenomena

Entanglement entropy finds significant applications in the study of critical phenomena, where phase transitions occur in quantum systems. In HEP, this concept provides a unique lens to explore the behavior of quantum fields as they undergo dramatic changes. By characterizing the scaling properties of entanglement entropy near critical points, researchers gain valuable insights into the underlying quantum phase transitions [4]. This has the potential to illuminate the behavior of particles in extreme conditions, such as the early universe.

Exploring entanglement entropy within HEP provides a unique lens to probe the fundamental interactions of particles, revealing insights into renormalization, holography, and critical phenomena, and unveiling the deep connections between quantum mechanics and spacetime.

7. Quantum correlations and spacetime

7.1 Quantum correlations in high-energy physics

In the realm of high-energy physics (HEP), the exploration of quantum correlations takes the central stage. Quantum correlations, often manifested as entanglement, play a fundamental role in describing the behavior of particles and their interactions. These correlations go beyond classical correlations, enabling particles to exhibit non-local connections that challenge our intuition about the nature of reality [1].

7.2 Entanglement and spacetime

One of the most intriguing aspects of quantum correlations in HEP is their connection to spacetime geometry. The AdS/CFT correspondence illuminates how entanglement in a boundary quantum field theory corresponds to geometric features in the dual higher-dimensional spacetime [2]. This suggests that the fabric of spacetime itself might emerge from the intricate web of quantum correlations. Such a perspective provides a new paradigm for understanding gravity as an emergent phenomenon arising from quantum entanglement [3].

7.3 Quantum correlations in extreme conditions

In HEP, the study of quantum correlations becomes particularly fascinating in the context of extreme conditions, such as those found in the early universe or near black holes. Quantum entanglement may play a crucial role in unraveling the mysteries of cosmic inflation, the Big Bang, and the behavior of matter in ultra-high-energy collisions [48]. By harnessing the power of quantum correlations, researchers aim to gain deeper insights into the fundamental nature of particles and their interactions.

7.4 Spacetime as an entanglement structure

Recent research within HEP has unveiled tantalizing connections between the structure of spacetime and the entanglement of quantum degrees of freedom. Entanglement wedges and causal wedges, emerging from the AdS/CFT correspondence, provide new insights into how spacetime is intricately woven from quantum correlations [49]. This suggests that spacetime may be an emergent consequence of quantum entanglement, raising profound questions about the nature of reality at the smallest scales.

Exploring the quantum correlations within HEP offers insights into the nature of spacetime, its connection to entanglement, and the role of quantum correlations in extreme conditions, ultimately leading to a deeper understanding of the fundamental interactions of particles.

8. Bell's inequality and quantum cryptography

8.1 Bell's inequality: Testing the limits of classical correlations

In the realm of high-energy physics (HEP), the violation of Bell's inequality stands as a crucial experiment that challenges classical notions of correlations [16].

Bell's theorem demonstrates that no local realistic theory can reproduce the quantum mechanical predictions of entangled systems, thereby highlighting the non-classical nature of quantum correlations [1].

8.2 Experimental verification and violation of Bell's inequality

Experiments involving entangled particles, such as photons or ions, have validated the violation of Bell's inequality and confirmed the fundamentally non-local nature of entanglement [20]. These experiments not only provide compelling evidence against classical realism but also open avenues for harnessing quantum entanglement for practical applications.

8.3 Quantum cryptography: Leveraging quantum correlations for security

The violation of Bell's inequality has paved the way for revolutionary advancements in quantum cryptography. Quantum key distribution protocols, such as the famous BB84 protocol, utilize entanglement to enable secure communication channels that are inherently immune to eavesdropping [36]. This has immense implications for secure communication, with the potential to revolutionize data encryption and transmission. However, entanglement-based secure quantum cryptography over 1120 kilometers has been reported by Yin, Juan et al. [27].

The exploration of Bell's inequality and its violation not only challenges classical theories but also finds applications in quantum cryptography, offering a secure foundation for quantum communication protocols.

9. Quantum information processing and tensor product

9.1 Harnessing quantum information for simulation

In the context of high-energy physics (HEP), quantum information processing has gained significant traction due to its potential to simulate complex quantum systems that are computationally intractable with classical methods [34]. Quantum simulators, often implemented using platforms like trapped ions or superconducting qubits, can mimic the behavior of fundamental particles and interactions, offering insights into the behavior of HEP phenomena [10].

9.2 Tensor product formalism: Enhancing computational power

The tensor product, a mathematical construct representing the combined state of multiple quantum systems, plays a pivotal role in quantum information processing. By encoding the entanglement structure between particles, the tensor product enables the manipulation of composite quantum systems, which is central to the simulation of complex HEP systems [11].

9.3 Quantum parallelism and exponential speedup

Quantum computers leverage the inherent parallelism of quantum states to perform certain calculations exponentially faster than classical counterparts. This

capability has the potential to revolutionize fields like lattice gauge theory, aiding in the understanding of strong interactions in HEP [50].

Quantum information processing, guided by the tensor product formalism, holds immense promise in simulating complex HEP systems and unlocking unprecedented computational power for addressing fundamental interactions.

10. Entanglement in gravity

10.1 Quantum Entanglement's role in gravity

Entanglement, a cornerstone of quantum mechanics, has intriguing implications for gravity in the context of HEP. Quantum entanglement's role in gravitational theories can offer insights into the nature of spacetime itself and the unification of fundamental forces [51]. Entanglement entropy, a measure of quantum entanglement, has revealed a deep connection between gravity and quantum information. The AdS/CFT correspondence suggests that the entanglement entropy of a boundary quantum field theory is related to the area of a bulk black hole horizon, indicating a profound link between quantum information and spacetime geometry [12].

10.2 Entanglement entropy and black holes

In the study of black holes, entanglement entropy has emerged as a crucial concept. The famous “holographic principle” suggests that the information content of a black hole is encoded in its event horizon's surface area, highlighting the deep connection between entanglement entropy and the geometry of spacetime [52]. Quantum entanglement seems to imply that information is never truly lost, posing a challenge to classical notions of black hole evaporation [52]. The study of entanglement entropy in the context of black holes has opened new avenues for understanding the quantum nature of spacetime [53].

10.3 Emergent spacetime from entanglement

The idea that spacetime may emerge from entanglement has gained traction through the AdS/CFT correspondence. This concept implies that gravity itself could be a consequence of entanglement, reshaping our understanding of the fundamental nature of spacetime in the realm of HEP [3].

The interplay between entanglement and gravity in HEP opens the door to novel perspectives on spacetime's nature and the fundamental forces governing the universe.

11. Breakthroughs and their awaited applications

Breakthroughs in entanglement within High-Energy Physics (HEP) are eagerly awaited and could have profound implications for our understanding of the fundamental forces of the universe. It could provide new insights into how spacetime emerges from entangled quantum states, potentially leading to a theory of quantum gravity as exploring *entanglement's implications* for quantum gravity could reveal

deeper insights into the fabric of spacetime Susskind [54]. The potential entanglement structure of the quantum vacuum remains a tantalizing enigma, with implications for phenomena like vacuum energy and the cosmological constant.

1. *Entanglement and the Quantum Nature of Spacetime*: Understanding how entanglement is related to the fundamental structure of spacetime is a key goal. Breakthroughs in this area might involve new insights into the nature of spacetime itself and how it emerges from entangled quantum states [2].
2. *Quantum Gravity Unification*: One of the most significant open questions lies in reconciling General Relativity with Quantum Mechanics, giving rise to a theory of quantum gravity. Entanglement's role here is pivotal. The holographic principle, stemming from the AdS/CFT correspondence, suggests that the universe's fabric is encoded in lower-dimensional entanglement patterns [2, 54]. Bridging this principle with real-world observations could unlock the elusive theory of everything.
3. *Quantum Computing for HEP Simulations*: Leveraging entanglement for quantum simulations of high-energy physics processes may lead to breakthroughs in our ability to understand complex particle interactions more efficiently than classical computers [10, 55].
4. *Quantum Simulations Revolutionized*: Harnessing entanglement for quantum simulations stands at the forefront. Simulating complex quantum systems, inaccessible through classical computation, could revolutionize material science, drug discovery, and even cosmology. In HEP, simulating quantum chromodynamics to understand confinement and strong interactions is a compelling avenue. Entanglement-based quantum simulations Preskill [10], Cirac & Zoller [55] have the potential to revolutionize our understanding of fundamental interactions. Quantum computers, exploiting entanglement, could efficiently simulate quantum field theories, yielding insights into phenomena that are computationally intractable using classical methods [11].
5. *Fundamental Symmetries Under Scrutiny*: Entanglement provides a unique lens for probing fundamental symmetries in particle interactions. Research into the violation of Bell's inequality Aspect [1] and entangled neutrino oscillations Bilenky et al. [56] could uncover new facets of the Standard Model and point the way to physics beyond it.
6. *Testing Bell's Inequality Violation in HEP*: Further experimental tests of Bell's inequality violation in particle physics could provide insights into the non-local nature of entanglement and quantum correlations [1, 8].
7. *Black Hole Information Paradox*: The information paradox, which arises when quantum information seems to be lost in black holes, is a major challenge surrounding black holes and continues to baffle physicists. Discoveries related to entanglement could help resolve this paradox by shedding light on how information is encoded and preserved in black holes [57, 58]. Discovering how entanglement properties of particles near black holes contribute to this paradox could lead to a breakthrough, resolving the information paradox [59].

8. *Quantum Gravity and Black Holes*: Entanglement plays a role in addressing the black hole information paradox. The ER = EPR conjecture [60] suggests that entangled particles might be connected by a wormhole, shedding light on the connection between quantum entanglement and gravity [61].
9. *Entanglement and Black Hole Information Paradox*: Resolving the information paradox, which arises when quantum information seems to be lost in black holes, is a major challenge. Discovering how entanglement properties of particles near black holes contribute to this paradox could lead to a breakthrough [58].
10. *Entanglement in Particle Collisions*: In HEP experiments like those at the Large Hadron Collider (LHC), understanding how entanglement plays a role in particle collisions could lead to new discoveries about the fundamental forces and particles of the universe [18].
11. *Entanglement and Quantum Field Theory*: Advancements in our understanding of how entanglement is described within the framework of quantum field theory can lead to deeper insights into the behavior of particles and fields [5].
12. *Quantum Information Protocols in HEP*: Developing practical quantum information protocols, such as quantum cryptography, tailored to the needs of high-energy physics experiments, could enhance data security and communication [62].
13. *Entanglement Entropy in Quantum Field Theory (QFT)*: In condensed matter physics, entanglement entropy has been used to study topological phases of matter. It helps classify and understand different quantum states [5].
14. *AdS/CFT Correspondence*: The AdS/CFT correspondence has transformative significance in high-energy physics. It provides a remarkable bridge between two distinct theoretical frameworks—gravity and quantum field theory—enabling researchers to address complex problems in a simpler setting [63, 64]. It has facilitated the study of strongly coupled systems, such as quark-gluon plasmas (QGP) produced in heavy-ion collision [45, 65].
15. *Dark Matter and Dark Energy*: These systems are notoriously difficult to analyze using traditional methods. Researchers have explored quantum correlations and entanglement to understand the nature of dark matter and dark energy, critical components of the universe [45, 66].

Breakthroughs in these areas have the potential to revolutionize our understanding of the universe, the behavior of particles, and the nature of spacetime, and they may also have practical applications in quantum technologies.

12. Conclusion

In this chapter, we have delved into the intricate interplay between entanglement and high-energy physics (HEP), showcasing how this fundamental quantum phenomenon has profound implications for our understanding of the universe. From the vantage point of quantum field theory (QFT), entanglement emerges as a key player

in elucidating the behavior of particles and their interactions [67]. The holographic nature of entanglement, illuminated by the AdS/CFT correspondence, demonstrates its potential as a bridge between quantum field theories and gravitational theories [2].

Entanglement entropy serves as a powerful tool to quantify and explore the intricate connections within HEP systems. Its applications in deciphering critical phenomena have led to a deeper comprehension of quantum phase transitions [14, 15]. Moreover, its role in black hole physics through the holographic principle hints at the profound relationship between information, spacetime, and gravity [54].

We have also explored how entanglement plays a pivotal role in testing the foundations of quantum mechanics, as exemplified by Bell's inequality and its implications for quantum correlations [1]. Furthermore, the deployment of entanglement for quantum simulations promises to revolutionize computational capabilities for HEP [34]. The potential of entangled states in quantum cryptography underscores its importance in securing sensitive information [26].

As we look to the future, the prospects for harnessing entanglement to unlock the mysteries of gravity, advance quantum computing, and deepen our understanding of quantum information remain tantalizingly promising. Yet, open questions persist, beckoning researchers to explore uncharted territories at the nexus of entanglement and HEP. How can we leverage entanglement to enhance our computational and communicative capacities? These questions and more constitute the frontier of entanglement in HEP, inviting future explorations that promise to reshape our understanding of the fundamental fabric of the cosmos [68]. The Nobel Prize in Physics for 2022 highlights the fundamental role of quantum entanglement nexus and HEP [44]. Can entanglement guide us toward a unified theory encompassing quantum and Bell violations in our understanding of quantum mechanics and its relevance to HEP? These experiments have opened new avenues for exploring the quantum behavior of particles, testing fundamental theories, and shedding light on the mysteries of the universe. In the context of HEP, these developments have significance for understanding the behavior of particles and forces in the universe, especially under extreme conditions.

In conclusion, the entanglement in HEP serves as a guiding thread, weaving through the intricate fabric of the cosmos, offering glimpses into the deepest mysteries of nature, and paving the way for new frontiers in research and understanding.

Acknowledgements


The author thanks the publisher IntechOpen and Tampere University.

Author details

Mohammed Nadir
Tampere University, Finland

*Address all correspondence to: mohammed.nadir.fi@ieee.org

IntechOpen

© 2023 The Author(s). Licensee IntechOpen. This chapter is distributed under the terms of the Creative Commons Attribution License (<http://creativecommons.org/licenses/by/3.0>), which permits unrestricted use, distribution, and reproduction in any medium, provided the original work is properly cited. 

References

- [1] Aspect A, Dalibard J, Roger G. Experimental test of Bell's inequalities, using time-varying analyzers (time-resolved photon counting). *Physical Review Letters*. 1982;**49**(25):1804-1807. DOI: 10.1103/PhysRevLett.49.1804
- [2] Maldacena JM. The large N limit of superconformal field theories and supergravity. *Advances in Theoretical and Mathematical Physics*. 1999;**2**(2):231-252
- [3] Van Raamsdonk M. Building up spacetime with quantum entanglement. *General Relativity and Gravitation*. 2010;**42**(10):2323-2329. DOI: 10.1007/s10714-010-1034-0
- [4] Amico L, Fazio R, Osterloh A, Vedral V. Entanglement in many-body systems. *Review of Modern Physics*. 2008;**80**(2):517-576
- [5] Calabrese P, Cardy J. Entanglement entropy and quantum field theory. *Journal Statistical Mechanics: Theory and Experiment*. 2004;**2004**(06):P06002. DOI: 10.1088/17425468/2004/06/P06002
- [6] Clauser JF, Horne MA, Shimony A, Holt RA. Proposed experiment to test local hidden-variable theories. *Physical Review Letters*. 1970;**24**:549. DOI: 10.1103/PhysRevLett.24.549
- [7] Fox R, Rosner B. Proposed experiment to test local hidden-variable theories. *Physical Review D*. 1971;**4**(4):1243-1244
- [8] Hensen B et al. Loophole-free Bell inequality violation using electron spin separated by 1.3 kilometres. *Nature*. 21 Oct 2015;**526**:682-686. DOI: 10.1038/nature15759
- [9] Ekert AK. Quantum cryptography is based on Bell's theorem. *Physical Review Letters*. 1991;**67**:661-663
- [10] Preskill J. Quantum computing in the Noisy intermediate-scale quantum (NISQ) era and beyond. *Quantum*. 2018;**2**:79. DOI: 10.22331/q-2018-08-06-79.ni
- [11] Nielsen MA, Chuang IL. *Quantum Computation and Quantum Information*. UK: Cambridge University Press; 2010 (One of the most cited books in physics of all time - Google)
- [12] Ryu S, Takayanagi T. Holographic derivation of entanglement entropy from AdS/CFT. *Physical Review Letters*. 2006;**96**(18):181602. DOI: 10.1103/PhysRevLett.96.181602
- [13] Vidal G, Latorre JI, Rico E, Kitaev A. Entanglement in quantum critical phenomena. *Physical Review Letters*. 2003;**90**(22):227902. DOI: 10.1103/PhysRevLett.90.227902
- [14] Aspect A, Grangier P, Roger G. Experimental tests of realistic local theories via Bell's theorem. *Physical Review Letters*. 1982;**47**(7):460-463. DOI: 10.1103/Phys
- [15] Shi X, Chen L. An extension of entanglement measures for pure states. *Annalen der Physik*. 26 Jul 2020;**533**(4):2000452. Available from: <https://api.semanticscholar.org/CorpusID:220794033>. DOI: 10.1002/andp.202000462. Available from: arXiv:2007.13164v1 [quant-ph]
- [16] Bell JS. On the Einstein Podolsky Rosen paradox. *Physics*. 1964;**1**(3):195-200
- [17] Benedetti M, Faccin M. Quantum-enhanced machine learning. *Physical Review X*. 2019;**9**(4):041011
- [18] Chatrchyan S et al. Observation of a new boson at a mass of 125 GeV with

the CMS experiment at the LHC. *Physics Letters B*. 2012;**716**(1):30-61

[19] The ATLAS Collaboration. Observation of a new particle in the search for the standard model Higgs boson with the ATLAS detector at the LHC. *Physics Letters B*. 2012;**716**(1):1-29

[20] Aspect A. Bell's theorem: The naïve view of an experimentalist. Text of a Talk in Memory of John Bell. 2004. DOI: 10.48550/arXiv.quant-ph/0402001

[21] Bertone G et al. *Physics Reports*. 2005;**405**(5-6):279-390

[22] Giunti C, Kim CW. *Fundamentals of Neutrino Physics and Astrophysics*. New York, US: Oxford University Press; 2007

[23] Almheiri A et al. *Journal of High Energy Physics*. 2013;**2013**(2):82

[24] Harlow D. *Reviews of Modern Physics*. 2016;**88**(1):015002

[25] Wilde MM. *Quantum Information Theory*. Cambridge: Cambridge University Press; 2013

[26] Gisin N, Thew R. Quantum communication. *Nature Photonics*. 2007;**1**(3):165-171. DOI: 10.1038/nphoton.2007.22

[27] Yin J et al. Entanglement-based secure quantum cryptography over 1,120 kilometres, *Nature*. 20 Jun 2020;**582**. DOI: 10.1038/s41586-020-2401-y

[28] Gisin N, Ribordy G, Tittel W, Zbinden H. Quantum cryptography. *Reviews of Modern Physics*. 2002;**74**(1):145

[29] Casini H, Huerta M. Entanglement entropy in free quantum field theory. *Journal of Physics A*. 2009;**42**(50):504007. p. 41. arXiv:0905.2562arXiv:0905.2562. DOI: 10.1088/1751-8113/42/50/504007

[30] Shuryak EV. What RHIC experiments and theory tell us about properties of quark-gluon plasma? *Nuclear Physics A*. 2004;**750**(1-2):64-83. arXiv:hep-ph/0405066 (hep-ph)

[31] Abdallah J et al. Simplified models for dark matter and missing energy searches at the LHC. *Physics of the Dark Universe*, Elsevier. Sep-Dec 2015;**(9-10)**:8-23. Available from: arXiv:1808.10036 arXiv:1808.10036. DOI: 10.1016/j.dark.2015.08.001

[32] Peskin ME, Schroeder DV. *An Introduction to Quantum Field Theory*. US: CRC Press; 2018

[33] Horodecki R, Horodecki P, Horodecki M, Horodecki K. Quantum entanglement. *Reviews of Modern Physics*. 2009;**81**(2):865-942

[34] Georgescu IM, Ashhab S, Nori F. Quantum simulation. *Reviews of Modern Physics*. 2014;**86**(1):153-185

[35] Carroll SM. *Spacetime and Geometry: An Introduction to General Relativity*. UK: Cambridge University Press; 2019

[36] Bennett CH, Brassard G. Quantum cryptography: Public key distribution and coin tossing. In: *Proceedings of IEEE International Conference on Computers, Systems and Signal Processing*. Bangalore, India. 10-12 Dec 1984. pp. 175-177. arXiv:2003.06557 [quant-ph]

[37] Wilczek F. *Quantum Chromodynamics. The Modern Theory of the Strong Interaction*. US AIP; 1982;**32**:177-209

[38] Rajibu I. Entanglement entropy in quantum many-body systems. *Nature*. 2020;**528**:77-83. DOI: 10.1038/nature15750

[39] Nishioka T, Takayanagi T. Entanglement entropy: Holography

- and renormalization group. Reviews of Modern Physics. Jul-Sep 2018;**90**:035007-1. DOI: 10.1103/RevModPhys.90.03500
- [40] Laflorencie N. Quantum entanglement in condensed matter systems. Physics Reports. Elsevier; 2016;**646**:1-59
- [41] Casini H, Huerta M, Myers RC. Towards a derivation of holographic entanglement entropy. Journal of High Energy Physics. 2011;**036**:1105 DOI: 10.1007/JHEP05%282011%29036
- [42] Eisert J, Cramer M, Plenio MB. Area laws for the entanglement entropy – A review. Reviews of Modern Physics. 2010. DOI: 10.48550/arXiv.0808.3773
- [43] Von Neumann J. Mathematical Foundations of Quantum Mechanics. US, London, UK: Princeton University Press, Geoffrey Cumberlege, Oxford University Press; 1995
- [44] Nobel Prize. Awarded to Alain Aspect, Clauser and Anton Zeilinger that entanglement is real as described on webpages. 2022. Available from: <https://www.nobelprize.org/uploads/2022/10/popular-physicsprize2022.pdf>, <https://www.nobelprize.org/educational-nobel-prize-lessons-physics-2022>
- [45] Casallerrey-Solana J, Mateos D. Gauge/string duality, hot QCD and heavy ion collisions. Journal of Physics A: Mathematical and Theoretical. 2014;**47**(25):253001. DOI: 10.1017/CBO9781139136747
- [46] 't Hooft G. Dimensional reduction in quantum gravity. 1993. arXiv preprint gr-qc/9310026
- [47] Swingle B. Entanglement renormalization and holography. Physical Review D. 2012;**86**:065007 DOI: 10.1103/PhysRevD.86.065007
- [48] Hirvonen H, Eskola KJ, Niemi H. Deep learning for flow observables in ultrarelativistic heavy-ion collisions. 8 Mar 2023. arXiv:2303.04517v1 [hep-ph]. DOI: 10.48550/arXiv.2303.04517
- [49] Geoffrey P. Entanglement wedge reconstruction and the information paradox. Aug 2020:1-75. arXiv:1905.08255 [hep-th] DOI: 10.48550/arXiv.1905.08255
- [50] Jordan SP, Lee KSM, Preskill J. Quantum algorithms for quantum field theories. Science. 2012. DOI: 10.48550/arXiv.1111.3633
- [51] Maldacena SJ, Alexey MSYK wormhole formation in real-time, Published for SISSA by Springer, JHEP04 2021:258. DOI: 10.1007/JHEP04(2021)258
- [52] Bekenstein JD. Information holographic universe. Scientific American. Aug 2003:45-52
- [53] Harlow D. Quantum gravity at a distance. Journal of High Energy Physics. 2014;**2014**(11):1-39
- [54] Susskind L. The world as a hologram. Journal of Mathematical Physics. Nov 1995;**36**(11). DOI: 10.1063/1.531249
- [55] Cirac JI, Zoller P. Goals and opportunities in quantum simulation. Nature Physics. 2012;**8**(4):264-266
- [56] Bilenky SM, Giunti C, Grimus W. Phenomenology of neutrino oscillations. Progress in Particle and Nuclear Physics. 1999;**43**:1-86.
- [57] Hawking SW. Particle creation by black holes. Communications in Mathematical Physics. 1975;**43**(3):199-220
- [58] Stefano A et al. The black hole information paradox. 2018. Available from: https://www.cs.umd.edu/class/fall2018/cmsc657/projects/group_2.pdf

- [59] Hawking SW. Breakdown of predictability in gravitational collapse. *Physical Review D*. 1976;**14**:2460
- [60] Baez JC, Vicary J. Wormholes and Entanglement. 4 Feb, 2014. arXiv:1401.3416v2 [gr-qc] 3 Feb 2014. Available from: <https://arxiv.org/abs/1401.3416>
- [61] Baez JC, Vicary J. Wormholes and entanglement. *Classical and Quantum Gravity*. 2014;**31**(21):214007
- [62] Scarani V et al. The security of practical quantum key distribution. *Reviews of Modern Physics*. 29 Sep 2009;**81**:1301
- [63] Sadeghi D et al. Application of AdS/CFT in quark-gluon plasma, (HEP_theory). 2013. DOI: 10.1155/2013/759804
- [64] Swingle B. Entanglement renormalization and holography. 2012. arXiv:1209.3304v1 [hep-th] [Accessed: Sep 14, 2012]
- [65] Casalderrey-Solana J, Liu H, Mateos D, Rajagopal K, Wiedemann UA. Gauge/string duality, hot QCD and heavy ion collisions. CUP. 2014. arXiv:1101.0618 (HEP-TH)
- [66] Verlinde EP. Emergent Gravity and the Dark Universe. 2016. arXiv:1611.02269 [hep-th]. DOI: 10.21468/SciPostPhys.2.3
- [67] Weinberg S. The Quantum Theory of Fields. Vol. 1. UK: Cambridge University Press; 1995
- [68] Arkani-Hamed N et al. The universe as a hologram. *Journal of High Energy Physics*. 2001;**2001**, JHEP08. DOI: 10.1088/1126-6708/2001/08/017

Section 4

Experiments

Translational Symmetry of Intermediate Nodes and Antinodes of Entangled Particles

Kisalaya Chakrabarti

Abstract

In a 1935 publication, Albert Einstein, Boris Podolsky, and Nathan Rosen present a thought experiment meant to demonstrate the apparent absurdity of quantum entanglement, which appeared to be in direct opposition to a fundamental law of the world. It was obvious to the men who created quantum mechanics in the decade of 1920, that quantum entanglement is unsettling because of the fact that quantum superposition is a real phenomenon. Thomas Vidick, a professor of physics, says it may be alluring to believe that the particles are somehow interacting with each other across such vast distances. A key resource for quantum networks is entanglement, a fundamental aspect of quantum theory that enables the sharing of unbreakable quantum connections between distant participants. Distributing entanglement across distant items that can act as quantum memory is very important. This has been accomplished in the past employing systems like warm and cold atomic vapours, single atoms and ions, and flaws in solid-state system

Keywords: K-state, entangled pair, standing waves, distributed locality, POVM

1. Introduction

Einstein splendidly criticised the phenomenon of quantum physics, particularly quantum entanglement, which shows how particles can share a combined state while separated arbitrarily far apart. Struggling with the oddity of this phenomenon, he referred to it as “spooky action at a distance” [1, 2]. This uncertainty has recently become more pronounced in various non-locality forms. The truth of this phenomenon has recently been confirmed by scientists over ever-greater distances, even from Earth to an orbiting spacecraft. Many times, it defies the special theory of relativity’s fundamental tenet that nothing can move faster than the speed of light, which has baffled scientists for years. In this study, the author suggests a potential quantum entanglement mechanism that upholds the special theory’s basic premise. It is important to note that the spin directions of the entangled particles such as vector bosons in Higgs boson decays are comparable to the corresponding phases of the standing wave’s intermediate field particles. Furthermore, a crucial phenomenon known as “phase transitions” can be observed in one-dimensional overlaid mixed wave functions. A crucial finding is that the application of a magnetic field to any entangled

particle, no matter how minute, results in the same spin orientations in the intermediate antinodes regardless of temperature changes.

By effectively splitting a system into two parts, where the sum of the portions is known, entangled particles are produced. For instance, it is possible to divide a particle with spin zero into two particles whose spins will inevitably be opposite one another, resulting in a sum of zero.

David Bohm is credited with coming up with a condensed version of this thought experiment that takes the decay of the pi meson into account. The electron and positron that are created when this particle decays have opposite spins and are traveling away from one another. So, if the measured spin of the electron is up, the measured spin of the positron can only be down, and the opposite is true. Even if the particles are billions of miles distant, this is still true.

If the measured positron spin were always down and the measured electron spin were always up, everything would be OK. Each particle's spin, however, has both an up and a down component until it is detected due to quantum physics. The quantum state of the spin does not "collapse" into either up or down until the measurement takes place, at which point the other particle instantly assumes the opposite spin. This appears to indicate that the particles are in communication with one another via a method that is moving faster than light. However, nothing can move more quickly than the speed of light, according to the laws of physics. Undoubtedly, it is impossible to instantly predict the state of one particle from its measured condition.

A formula created by Bell is now known as Bell's inequality, and it is only and always true for hidden variable theories—never for quantum mechanics. This means that local hidden variable theories cannot account for quantum entanglement if Bell's equation is proven to be unsatisfied in a real-world experiment. The idea that entangled particles are communicating with one another faster than the speed of light contradicts Einstein's special theory of relativity, and is a popular fallacy about entanglement. This is not the case, and quantum physics cannot be employed to deliver messages that travel at a faster-than-light rate. The origin of the entanglement phenomena, which at first glance appears strange, is still a topic of controversy among scientists, but they are aware that the theory behind it holds up to repeated testing. Despite the fact that Einstein famously called entanglement "spooky action at a distance," modern quantum scientists assert that it is not spooky in any way. According to Schrödinger, with a certain probability, a particle in another location could be guided into one of a set of states by an entangled state. In reality, the 'remote guiding' potential is considerably more spectacular than Schrödinger's experiment. Assuming, two experimenter Bob and Alice both possess a pair of entangled photons that are in an entangled pure state similar to those Bell considered, with Alice possessing one of the entangled photons and Bob is holding the other. Assume that Alice also receives an additional photon with unknown polarisation $|a\rangle$ where " $|\rangle$ " represents a quantum state. If Alice performs an operation on the two photons in her possession, Bob's photon may change into one of the four states. The four possible (random) outcomes of Alice's operation are either the state $|a\rangle$ or a state that is clearly related to $|a\rangle$. The two photons Alice is holding become entangled as a result of Alice's operation, which also manages to separate Bob's photon and direct it into a state of $|a^*\rangle$. Bob is either aware that $|a^*\rangle = |a\rangle$ or understands how to do a local operation to change $|a^*\rangle$ to $|a\rangle$ after Alice tells him the results of her operation. Quantum teleportation is the term used to describe this phenomenon. Both Alice and Bob are unable to determine the state $|a\rangle$ following the teleportation technique [3, 4]. Two conventional bits of information can be used to specify Alice's operation's result, which has four potential outcomes and an equal probability of 0.25. Surprisingly, Bob can recreate the state $|a\rangle$ from just two bits of

classical information that Alice has communicated. It appears that Bob did this by using the entangled state as a quantum communication channel. The noteworthy aspect of these phenomena is that Alice and Bob were able to use their shared entangled state as a quantum communication channel to alter the state $|a\rangle$ of a photon in Alice's part of the universe and reproduce it in Bob's portion of the universe.

In 1989, Daniel Greenberger, Michael Horne, and Anton Zeilinger conducted the initial research on it. A Greenberger-Horne-Zeilinger state (GHZ state) is a specific kind of entangled quantum state in the field of quantum information theory that involves three subsystems (particle states, qubits, or qudits). In advancement of this aforesaid theory on the year 2020, Kosalaya Chakrabarti proposed an entangled quantum state in the field of quantum information theory that involves four subsystems called Kosalaya state (K state) [4].

In this regard, it is worth mentioning, a ground-breaking workshop that was held at the Brookhaven National Laboratory in 2018, from onwards the ideas of using quantum information methods and tools in high-energy physics is gaining more and more attention. We know that, the density matrix of the hadrons – the bound states of quarks and gluons, must be averaged over the phase with the associated Haar integration measure because it is impossible to detect the phase of the wave function in high energy interactions. This results in the density matrix of the Parton model, which is a mixed state density matrix that is diagonal in Parton number. With the help of this method, one can better grasp the limits of the Parton model, such as how it cannot accurately describe spin-dependent processes [5].

2. Probability transfer matrix of an entangled particle at a distance

Mixed state states are possible for quantum mechanical systems. The term “pure state” refers to the states that wave functions describe. In this case, the probability states are superimposed. Starting from the Pauli's matrix of quantum physics, which accounts for the interaction between a particle's spin and an external electromagnetic field and additionally they depict the interaction states of two polarisation filters for 45° right or left, circular or horizontal or vertical polarisation, given by:

$$\sigma_x = \begin{bmatrix} 0 & 1 \\ 1 & 0 \end{bmatrix}, \sigma_y = \begin{bmatrix} 0 & -i \\ i & 0 \end{bmatrix} \text{ and } \sigma_z = \begin{bmatrix} 1 & 0 \\ 0 & -1 \end{bmatrix}$$

Now, taking the tensor products of two parallel operations at superimposed similar states given as follows;

$$\sigma_x \otimes \sigma_x = [A] = \begin{bmatrix} 0 & 1 \\ 1 & 0 \end{bmatrix} \begin{bmatrix} 0 & 1 \\ 1 & 0 \end{bmatrix} = \begin{bmatrix} 0 & 0 & 0 & 1 \\ 0 & 0 & 1 & 0 \\ 0 & 1 & 0 & 0 \\ 1 & 0 & 0 & 0 \end{bmatrix} = \begin{bmatrix} \rho_i & \rho_i & \rho_i & 1 - \rho_i \\ \rho_i & \rho_i & 1 - \rho_i & \rho_i \\ \rho_i & 1 - \rho_i & \rho_i & \rho_i \\ 1 - \rho_i & \rho_i & \rho_i & \rho_i \end{bmatrix} \quad (1)$$

Instead of using wave functions in this situation, we must employ the idea of a probability transfer matrix. A mixed state can be represented as an incoherent summation of Orthonormal bases $|\psi_i\rangle$'s as $\rho = \sum_i \rho_i |\psi_i\rangle \langle \psi_i|$ where ρ_i is the probability P

for the system in the state of ψ_i , and ψ_i 's are the diagonal basis for ρ . ρ_i are referred to as the density matrix's Eigen values ρ .

Similarly,

$$\begin{aligned}\sigma_y \otimes \sigma_y = [B] &= \begin{bmatrix} 0 & -i \\ i & 0 \end{bmatrix} \begin{bmatrix} 0 & -i \\ i & 0 \end{bmatrix} = \begin{bmatrix} 0 & 0 & 0 & -1 \\ 0 & 0 & +1 & 0 \\ 0 & +1 & 0 & 0 \\ -1 & 0 & 0 & 0 \end{bmatrix} \\ &= \begin{bmatrix} \rho_i & \rho_i & \rho_i & |\rho_i - 1| \\ \rho_i & \rho_i & 1 - \rho_i & \rho_i \\ \rho_i & 1 - \rho_i & \rho_i & \rho_i \\ |\rho_i - 1| & \rho_i & \rho_i & \rho_i \end{bmatrix}\end{aligned}\quad (2)$$

and

$$\begin{aligned}\sigma_z \otimes \sigma_z = [C] &= \begin{bmatrix} 1 & 0 \\ 0 & -1 \end{bmatrix} \begin{bmatrix} 1 & 0 \\ 0 & -1 \end{bmatrix} = \begin{bmatrix} 1 & 0 & 0 & 0 \\ 0 & -1 & 0 & 0 \\ 0 & 0 & -1 & 0 \\ 0 & 0 & 0 & 1 \end{bmatrix} \\ &= \begin{bmatrix} 1 - \rho_i & \rho_i & \rho_i & \rho_i \\ \rho_i & |\rho_i - 1| & \rho_i & \rho_i \\ \rho_i & \rho_i & |\rho_i - 1| & \rho_i \\ \rho_i & \rho_i & \rho_i & 1 - \rho_i \end{bmatrix}\end{aligned}\quad (3)$$

Tensor Products or Tensor Matrices A, B and C are a set of three 4×4 complex matrices which are Hermitian, involutory and unitary. Here worth mentioning that, if and only if; $M^2 = I$, where I is the 4×4 identity matrix, then multiplying by the matrix M results in an involution. Each and every involutory matrix is the square root of the identity matrix. This is merely a result of the fact that the identity is obtained by multiplying any non-singular matrix by its inverse.

It is an important observation that none of the Tensor matrices (Tensor products) A, B and C have elements consisting of imaginary quantity. The two Eigen values of the three Hermitian Tensor products are +1 and -1.

In the same fashion one can achieve:

$$\begin{aligned}\sigma_x \otimes \sigma_y = [D] &= \begin{bmatrix} 0 & 1 \\ 1 & 0 \end{bmatrix} \begin{bmatrix} 0 & -i \\ i & 0 \end{bmatrix} = \begin{bmatrix} 0 & 0 & 0 & -i \\ 0 & 0 & i & 0 \\ 0 & -i & 0 & 0 \\ i & 0 & 0 & 0 \end{bmatrix} \\ &= i \begin{bmatrix} \rho_i & \rho_i & \rho_i & |\rho_i - 1| \\ \rho_i & \rho_i & 1 - \rho_i & \rho_i \\ \rho_i & |\rho_i - 1| & \rho_i & \rho_i \\ 1 - \rho_i & \rho_i & \rho_i & \rho_i \end{bmatrix}\end{aligned}\quad (4)$$

$$\begin{aligned}\sigma_y \otimes \sigma_z = [E] &= \begin{bmatrix} 0 & -i \\ i & 0 \end{bmatrix} \begin{bmatrix} 1 & 0 \\ 0 & -1 \end{bmatrix} = \begin{bmatrix} 0 & 0 & -i & 0 \\ 0 & 0 & 0 & i \\ i & 0 & 0 & 0 \\ 0 & -i & 0 & 0 \end{bmatrix} \\ &= i \begin{bmatrix} \rho_i & \rho_i & |\rho_i - 1| & \rho_i \\ \rho_i & \rho_i & \rho_i & 1 - \rho_i \\ 1 - \rho_i & \rho_i & \rho_i & \rho_i \\ \rho_i & |\rho_i - 1| & \rho_i & \rho_i \end{bmatrix}\end{aligned}\quad (5)$$

$$\begin{aligned}\sigma_z \otimes \sigma_x = [F] &= \begin{bmatrix} 1 & 0 \\ 0 & -1 \end{bmatrix} \begin{bmatrix} 0 & 1 \\ 1 & 0 \end{bmatrix} = \begin{bmatrix} 0 & 1 & 0 & 0 \\ 1 & 0 & 0 & 0 \\ 0 & 0 & 0 & -1 \\ 0 & 0 & -1 & 0 \end{bmatrix} = \begin{bmatrix} \rho_i & 1 - \rho_i & \rho_i & \rho_i \\ 1 - \rho_i & \rho_i & \rho_i & \rho_i \\ \rho_i & \rho_i & \rho_i & |\rho_i - 1| \\ \rho_i & \rho_i & |\rho_i - 1| & \rho_i \end{bmatrix}\end{aligned}\quad (6)$$

In the reverse order the Tensor products are given as follows:

$$\begin{aligned}\sigma_y \otimes \sigma_x = [G] &= \begin{bmatrix} 0 & -i \\ i & 0 \end{bmatrix} \begin{bmatrix} 0 & 1 \\ 1 & 0 \end{bmatrix} = \begin{bmatrix} 0 & 0 & 0 & -i \\ 0 & 0 & -i & 0 \\ 0 & i & 0 & 0 \\ i & 0 & 0 & 0 \end{bmatrix} \\ &= i \begin{bmatrix} \rho_i & \rho_i & \rho_i & |\rho_i - 1| \\ \rho_i & \rho_i & |\rho_i - 1| & \rho_i \\ \rho_i & 1 - \rho_i & \rho_i & \rho_i \\ 1 - \rho_i & \rho_i & \rho_i & \rho_i \end{bmatrix}\end{aligned}\quad (7)$$

$$\begin{aligned}\sigma_x \otimes \sigma_z = [H] &= \begin{bmatrix} 0 & 1 \\ 1 & 0 \end{bmatrix} \begin{bmatrix} 1 & 0 \\ 0 & -1 \end{bmatrix} = \begin{bmatrix} 0 & 0 & 1 & 0 \\ 0 & 0 & 0 & -1 \\ 1 & 0 & 0 & 0 \\ 0 & -1 & 0 & 0 \end{bmatrix} = \begin{bmatrix} \rho_i & \rho_i & 1 - \rho_i & \rho_i \\ \rho_i & \rho_i & \rho_i & |\rho_i - 1| \\ 1 - \rho_i & \rho_i & \rho_i & \rho_i \\ \rho_i & |\rho_i - 1| & \rho_i & \rho_i \end{bmatrix}\end{aligned}\quad (8)$$

$$\begin{aligned}\sigma_z \otimes \sigma_y = [I] &= \begin{bmatrix} 1 & 0 \\ 0 & -1 \end{bmatrix} \begin{bmatrix} 0 & -i \\ i & 0 \end{bmatrix} = \begin{bmatrix} 0 & -i & 0 & 0 \\ i & 0 & 0 & 0 \\ 0 & 0 & 0 & i \\ 0 & 0 & -i & 0 \end{bmatrix} \\ &= i \begin{bmatrix} \rho_i & |\rho_i - 1| & \rho_i & \rho_i \\ 1 - \rho_i & \rho_i & \rho_i & \rho_i \\ \rho_i & \rho_i & \rho_i & 1 - \rho_i \\ \rho_i & \rho_i & |\rho_i - 1| & \rho_i \end{bmatrix}\end{aligned}\quad (9)$$

Measurements of this type are referred to as Positive operator valued measure (POVM). The most general type of POVM in which sums are substituted by integrals; so they are termed measures, which has a continuous family of outcomes. In this case there are a finite number of potential outcomes, over a finite dimensional quantum space. Hermitian matrices having finite dimensional positive operators are used here as the elements. We use these measures implicitly when we measure some qubits of a quantum computer while leaving other qubits unaffected, described in a proper mathematical definition given below:

$$\prod_i \prod_j = 0 \quad \text{if } i \neq j \text{ and } \sum_{i=1}^k = 1 \quad (10)$$

Considering the case when we have a collection of projectors onto the orthogonal subspaces $\Pi_1, \Pi_2, \dots, \Pi_k$ which implies that the tensor products to be $[D] = [E] = [F] = [G] = [H] = [I] = 0$, from Ortho-normality condition depicted in Eq. (10) where the projective measurement in these subspaces that evolves a quantum state $|\psi\rangle$ in the state given by

$$|\psi'\rangle = \frac{\prod_{i \neq j \neq k} |\psi\rangle}{\langle \psi | \prod_{i \neq j \neq k} |\psi\rangle^{1/2}} \quad \text{where Probability } P = \langle \psi | \prod_{i \neq j \neq k} |\psi\rangle \quad (11)$$

A minimum rate of unresolved events or error probability P_e , is imposed by the state's impossible to differentiate detection and is given by the following equation:

$$P_e = 1 - \mu \quad \text{where, } \mu = \langle \psi_i | \psi_j \rangle \quad (12)$$

From Eq. (12) it is clearly seen that when $i \neq j$, $P_e = 1$.

Therefore, the equations of importance are (1), (2) and (3) only corresponds to [A], [B] and [C] tensor product matrices where

$$\prod_i \prod_i = \prod_j \prod_j = \prod_k \prod_k = 1 \quad (13)$$

Solving for Eigenvalues and Eigenvectors for [A], we find that the Eigenvalues $\lambda = \pm 1$ and the Eigenvectors are as follows:

$$\text{for } \lambda = 1 \quad \text{Eigenvectors } X = \begin{pmatrix} \psi_1 \\ \psi_2 \\ \psi_2 \\ \psi_1 \end{pmatrix} \quad (14)$$

Eq. (14) can be written as:

$$X = \psi_1 \begin{pmatrix} 1 \\ 0 \\ 0 \\ 1 \end{pmatrix} + \psi_2 \begin{pmatrix} 0 \\ 1 \\ 1 \\ 0 \end{pmatrix} \quad (15)$$

and

$$\text{for } \lambda = -1 \quad \text{Eigenvectors } X = \begin{pmatrix} \psi_1 \\ \psi_2 \\ -\psi_2 \\ -\psi_1 \end{pmatrix} \quad (16)$$

Eq. (16) can be written as:

$$X = \psi_1 \begin{pmatrix} 1 \\ 0 \\ 0 \\ -1 \end{pmatrix} + \psi_2 \begin{pmatrix} 0 \\ 1 \\ -1 \\ 0 \end{pmatrix} \quad (17)$$

In the same fashion Eigenvalues and Eigenvectors for [B] are as follows:

$$\text{for } \lambda = 1 \quad \text{Eigenvectors } X = \begin{pmatrix} \psi_1 \\ \psi_2 \\ \psi_2 \\ -\psi_1 \end{pmatrix} \quad (18)$$

Eq. (18) can be written as:

$$X = \psi_1 \begin{pmatrix} 1 \\ 0 \\ 0 \\ -1 \end{pmatrix} + \psi_2 \begin{pmatrix} 0 \\ 1 \\ 1 \\ 0 \end{pmatrix} \quad (19)$$

and;

$$\text{for } \lambda = -1 \quad \text{Eigenvectors } X = \begin{pmatrix} \psi_1 \\ \psi_2 \\ -\psi_2 \\ \psi_1 \end{pmatrix} \quad (20)$$

Eq. (20) can be written as:

$$X = \psi_1 \begin{pmatrix} 1 \\ 0 \\ 0 \\ 1 \end{pmatrix} + \psi_2 \begin{pmatrix} 0 \\ 1 \\ -1 \\ 0 \end{pmatrix} \quad (21)$$

Similarly, Eigenvalues and Eigenvectors for [C] are as follows:

$$\text{for } \lambda = 1 \quad \text{Eigenvectors } X = \begin{pmatrix} \psi_1 \\ 0 \\ 0 \\ \psi_4 \end{pmatrix} \quad (22)$$

Eq. (22) can be written as:

$$X = \psi_1 \begin{pmatrix} 1 \\ 0 \\ 0 \\ 0 \end{pmatrix} + \psi_4 \begin{pmatrix} 0 \\ 0 \\ 0 \\ 1 \end{pmatrix} \quad (23)$$

and;

$$\text{for } \lambda = -1 \quad \text{Eigenvectors } X = \begin{pmatrix} 0 \\ \psi_2 \\ \psi_3 \\ 0 \end{pmatrix} \quad (24)$$

Eq. (24) can be written as:

$$X = \psi_2 \begin{pmatrix} 0 \\ 1 \\ 0 \\ 0 \end{pmatrix} + \psi_3 \begin{pmatrix} 0 \\ 0 \\ 1 \\ 0 \end{pmatrix} \quad (25)$$

Now, from the set of two Eqs. (15) and (17); and (19) and (21) it is noticeable that only two vector states $|\psi_1\rangle, |\psi_2\rangle$ with two different orientations $|+, -\rangle$ are originated from the interference of forward and reverse moving waves at the antinodes sections resulting in Standing waves, whereas Eqs. (21) and (23) describe that presence of all the four states $|\psi_1\rangle, |\psi_2\rangle, |\psi_3\rangle, |\psi_4\rangle$ have been noticed with a single orientation $|+\rangle$. As there are only two Eigen vector states $|\psi_1\rangle, |\psi_2\rangle$ in three dimensional vector space and with two different orientations $|+, -\rangle$, it is obvious that $|\psi_4\rangle = -|\psi_1\rangle$ and $|\psi_3\rangle = -|\psi_2\rangle$.

So we can modify Eq. (23) as follows:

$$\text{for } \lambda = 1 \quad X = \psi_1 \begin{pmatrix} 1 \\ 0 \\ 0 \\ -1 \end{pmatrix} \quad (26)$$

Similarly, Eq. (25) as follows and

$$\text{for } \lambda = -1 \quad X = \psi_2 \begin{pmatrix} 0 \\ 1 \\ -1 \\ 0 \end{pmatrix} \quad (27)$$

From Eqs. (15) and (17); (19) and (21) and (26) and (27) we find that only two pure states or the combination of two states are manifested with two different orientations $|\psi_{1\pm}\rangle, |\psi_{2\pm}\rangle$ at the antinodes positions due to interference of two waves originated from two entangled particles lying far apart. It is important and observed from

(26) and (27) that only two pure states $|\psi_{1\pm}\rangle, |\psi_{2\pm}\rangle$ exist at antinodes at the standing wave perpendicular to the direction of propagations.

3. Entanglement theory with stationary phase approximation

Consider two entangled particles with superimposed states between them at positions “A” and “B” separated by an arbitrarily large distance “d” and having superimposed states between them ψ_s . Since there is no net energy transfers in either the forward or backward direction because the two particles are entangled, this composite wavefunction ψ_s is composed of two ψ states, ψ_1 and ψ_2 , where, ψ_1 denotes the wave moving forward from “A” to “B” and a backward travelling wave ψ_2 moving from “B” to “A”. The propagation of forward or backward travelling waves does not yet take the spin directions of either particle into consideration; therefore we can express the superimposed wavefunction in the context of the Schrodinger equation [4],

$$\psi_s = \psi_1 + \psi_2 = \left(\psi_{01} e^{\frac{ip_x}{\hbar}} + \psi_{02} e^{-\frac{ip_x}{\hbar}} \right) \quad (28)$$

Without taking spin effect on directions into account, Eq. (28) can be written as

$$\psi_s = \left(\psi_{01} e^{\frac{ip_x}{\hbar}} - \psi_{01} e^{-\frac{ip_x}{\hbar}} \right) \quad (29)$$

Now, taking into account the spin direction of the particle at location “A” during the forward wave propagation ψ_1 and we must select an axis to line up with the measuring device’s axis in order to measure the spin direction. Finally, we denote this observed spin of the particle at “A” by unit vector by moving the axis of the measurement device located at point “A” in the direction of the forward travelling wave ψ_1 in the forward “+x” direction and we will denote this observed spin of the particle at point “A” by unit vector \hat{x} , and bringing in this factor to “ ψ_1 ” we obtained the modified wavefunction expressed as:

$$\psi_1 = \psi_{01} e^{\frac{ip_x}{\hbar} \hat{x}} \quad (30)$$

Taking into account the time evolution of the combined wavefunction, Eq. (29) is customised and can be written as follows:

$$\psi_s(t) = \text{Re} (\psi_s e^{i\omega t}) = 2\psi_{01} \cos\left(\frac{P_x}{\hbar}\right) \cos(\omega t) \hat{x} \quad (31)$$

where, ω is the angular velocity of $\psi_s(t)$, given by E/\hbar .

It is now necessary to comprehend the stationary phase approximation of the combined wavefunction of all entangled particles, which is given by combined wave function $\psi_s(t)$, as shown in equation, in order to comprehend how quantum entanglement changes with time (31).

$$J = \lim_{\Omega \rightarrow 0} \int_{-\infty}^{\infty} e^{i\psi_s(t)/\Omega} dt \quad (32)$$

Eq. (32) can be stretched out as follows:

$$J \approx \sum_n \int_{-\infty}^{\infty} e^{i \left\{ \frac{\psi_S(t_0)}{\Omega} + \frac{d\psi_S(t_0)}{dt} \frac{(t-t_0)}{\Omega} + \frac{d^2\psi_S(t_0)}{dt^2} \frac{(t-t_0)^2}{2\Omega} \right\}} dt \approx e^{i \frac{\psi_S(t_0)}{\Omega}} \sqrt{\frac{2\Omega\pi}{i \frac{d^2\psi_S(t_0)}{dt^2}}} \quad (33)$$

In order to formally follow the convention of Gaussian integration, one should replace “i” to “-i” inside the square root portion of Eq. (33). The imaginary unit “i” is assumed to be a true positive constant even though the integral mathematically speaking does not exist. We obtain nonzero contributions precisely where, just like in the Path Integral case;

$$\delta S[\psi_S(t), p(t), t] = 0 \quad (34)$$

which is the prerequisite for the functional of the classical trajectory “S” and is expressed in units of \hbar ; $p(t)$ is the momentum of the entangled system; as a result, in any physical domain where “S” is much larger than, even the slightest deviation from the classical trajectory causes $\psi_S(t)$ to wiggle out so quickly that it has no impact on the value of “J”. The conventional boundary is $\frac{S}{\hbar} \gg 1$.

As is evident, that $J = \psi_S(t)$, therefore squaring and comparing Eq. (31) with Eq. (33) and allowing for the real part, we obtain

$$\frac{\Omega\pi \sin\left(\frac{2\psi_S(t_0)}{\Omega}\right)}{2\psi_{01}^2 \cos^2(\omega t)} = \frac{d^2\psi_S(t_0)}{dt^2} \cos^2\left(\frac{Px}{\hbar}\right) \quad (35)$$

Putting the average value of $\cos^2\left(\frac{Px}{\hbar}\right) = \frac{1}{2}$ at x direction, Eq. (35) can be written as

$$\frac{\Omega\pi \sin\left(\frac{2\psi_S(t_0)}{\Omega}\right)}{\psi_{01}^2 \cos^2(\omega t)} = \frac{d^2\psi_S(t_0)}{dt^2} \quad (36)$$

Now, Eq. (36) can be rewritten as;

$$\frac{d^2\psi_S(t_0)}{dt^2} = \kappa \frac{\sin(\psi_S(t_0))}{\cos^2(\omega t)} \quad (37)$$

where, $\kappa = \frac{\Omega\pi}{\psi_{01}^2}$ = constant and equating it to “1” with book-keeping constant “ Ω ” for the sake of arithmetical straightforwardness which serves only as a scaling factor.

Now solving the differential Eq. (37) with angular frequency $\omega = 1$, we can derive the solution of $\psi_S(t_0)$ by double integration at any point of time t_0 , is in the form:

$$\psi_S(t_0) = \ln(|\tan(t_0) + \sec(t_0)|) + C \quad (38)$$

Now, assuming any value of Constant “C = 7” and plotting the graph we get **Figure 1**.

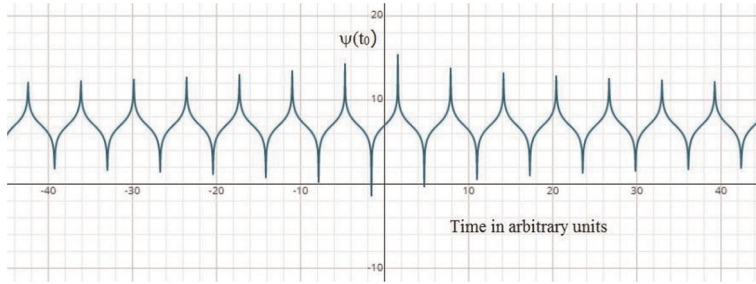


Figure 1.
 Superimposed wave function $\psi_s(t_0)$ field distribution with time.

4. Results and discussions

An interesting fact is observed from the **Figure 1** that the Standing wave pattern formed and has a Translational symmetry. This pattern is periodic and is repeated after a time interval “T”. This phenomenon is called “Distributed locality” which implies the same pattern is repeated throughout the space after regular time interval. Therefore once such pattern is formed, the information of spin is translated immediately between two entangled particles kept in far apart [2]. This forms a “String”. For an “N” dimensional observations there are “N” number of such strings which are superimposed to each other in different phases and amplitudes. Now, when we measure the spin at any end of the entangled pair particle at any particular direction or orientation, immediately the string correlated with the other directions or orientations collapses. This is called String lowering Operation.

When the measurement has taken place to calculate the Spin Orientation of an entangled particle for any particular direction; supposedly in the \hat{x} direction, we get:

$$|\psi\rangle = \frac{1}{\sqrt{2}}(|\psi_1\rangle + |\psi_2\rangle) \quad (39)$$

$$\text{where, } \hat{x} = \sqrt{\frac{\hbar}{2m\omega}}(a + a^\dagger)$$

Now,

$$\begin{aligned} \langle\psi|\hat{x}|\psi\rangle &= \frac{1}{2} \langle(\langle\psi_1| + \langle\psi_2|)|\sqrt{\frac{\hbar}{2m\omega}}(a + a^\dagger)|(|\psi_1\rangle + |\psi_2\rangle)\rangle \\ &= \frac{1}{2} \sqrt{\frac{\hbar}{2m\omega}} \langle(\langle\psi_1| + \langle\psi_2|)|(|\psi_1\rangle + |\psi_2\rangle + \sqrt{2})|\psi_3\rangle\rangle \\ &= \frac{1}{2} \sqrt{\frac{\hbar}{2m\omega}}(1 + 1) = \sqrt{\frac{\hbar}{2m\omega}} \end{aligned} \quad (40)$$

We find a finite expectation value in the \hat{x} direction which is quite obvious and all the others strings are immediately readjusted to “0” as follows:

We know, due to Ortho-normality conditions, $|\psi\rangle = \frac{1}{\sqrt{2}}(|\psi_1\rangle + i|\psi_2\rangle) = 0$.

Therefore,

$$\begin{aligned}\langle\psi|\hat{x}|\psi\rangle &= \frac{1}{2}\langle(\langle\psi_1| + i\langle\psi_2|)|\sqrt{\frac{\hbar}{2m\omega}}(a + a^\dagger)(|\psi_1\rangle + i|\psi_2\rangle)\rangle \\ &= \frac{1}{2}\sqrt{\frac{\hbar}{2m\omega}}(1 - 1) = 0\end{aligned}\tag{41}$$

This Operation is “String Lowering Operation”.

5. Conclusion

A particle with spin zero can be split into two particles whose spins are invariably opposite one another, giving rise to a sum of zero. Until the measurement is made, the quantum state of the spin does not “collapse” into either up or down; nevertheless, when the measurement is made, the other particle immediately assumes the opposing spin.


Author details

Kisalaya Chakrabarti

Department of Electronics and Communication Engineering, Haldia Institute of Technology, Haldia, W.B, India

*Address all correspondence to: kisalayac@gmail.com

IntechOpen

© 2023 The Author(s). Licensee IntechOpen. This chapter is distributed under the terms of the Creative Commons Attribution License (<http://creativecommons.org/licenses/by/3.0>), which permits unrestricted use, distribution, and reproduction in any medium, provided the original work is properly cited. 

References

- [1] Einstein A et al. Can quantum-mechanical description of physical reality be considered complete? *Physical Review*. 1935;**47**:777-780
- [2] Chakrabarti K. Is there any spooky action at a distance? In: Maji AK, Saha G, Das S, Basu S, Tavares JMRS, editors. *Proceedings of the International Conference on Computing and Communication Systems. Lecture Notes in Networks and Systems*. Vol. 170. Singapore: Springer; 2021. DOI: 10.1007/978-981-33-4084-8_65
- [3] Bennett C, Brassard G, Crepeau C, Jozsa R, Peres A, Wootters W. Teleporting an unknown quantum state via dual classical and Einstein-Podolsky-Rosen channels. *Physical Review Letters*. 1993;**70**:1895-1899
- [4] Chakrabarti K. Realization of original quantum entanglement state from mixing of four entangled quantum states. In: Castillo O, Jana D, Giri D, Ahmed A, editors. *Recent Advances in Intelligent Information Systems and Applied Mathematics: ICITAM 2019. Studies in Computational Intelligence*. Vol. 863. Cham: Springer; 2020. DOI: 10.1007/978-3-030-34152-7_12
- [5] Kharzeev DE. Quantum information approach to high energy interactions. *Philosophical Transactions on Royal Society A*. 2022;**380**:20210063. DOI: 10.1098/rsta.2021.0063

Perspective Chapter: EPR Paradox – Experimental and Quantum Field Theoretical Status of Light Meson Resonances

Alexander Machavariani

Abstract

The inclusive reaction of the V -meson resonance production is studied in order to check consistency of the field-theoretical approach with formulation based on the Einstein-Podolsky-Rosen (EPR) concepts. For this aim we have constructed the relativistic field-theoretical amplitudes of the V -meson resonance decay $1 + 2 \leftarrow V$ with structureless (pointlike) and composite (non-pointlike) resonance. Nonlocal composite states of a resonance are obtained using quark-gluon degrees of freedom in accordance with quantum chromodynamics (QCD). Particle 1 and 2 have opposite momenta $\mathbf{p}_1 = -\mathbf{p}_2$ and strongly correlated spin states in the rest frame of V -meson decay. Moreover, for electron-positron decay of the V -meson resonance, electron and positron have the opposite helicity if the electron mass is neglected. Therefore, the decay of V -meson into two particles can be considered as the formation of the EPR-pair according to EPR gedanken experiment. In addition, the color quark-gluon states can be interpreted as hidden (non-observed) states within EPR formulation. As an example of such an approaches, we have considered papers with high-energy experimental data where for description of observable was used quark-antiquark states and concepts of EPR pairs and entanglement.

Keywords: paradox, entanglement, quantum, field, theory, meson, resonance

1. Introduction

Paradox of Einstein, Podolsky and Rosen [1] has motivated numerous experimental and theoretical investigations of basic concepts in quantum mechanics. In particular, in review papers [1–7] were studied the highly correlated so called EPR-pairs of particles with following possibility of determination of the location of one of these particles through the location of another particle. Schrödinger [8] showed that the EPR paradox lies in the possibility of separabilization of the two-particle wave function $|\psi_{A+B}\rangle$ as product of the single-particle wave functions $|\psi_{A+B}\rangle \Leftrightarrow |\psi_A\rangle |\psi_B\rangle$. The next principal result was obtained by Bell [9], where it is proved that EPR paradox in quantum mechanics should be supplemented by

additional local hidden variables which enables to restore causality and locality. Subsequently, particles which satisfy the conditions of Schrödinger and Bell were called EPR pairs and interaction (correlation) of these particles in final states are defined as entanglement [2]. The notable exception of the Bell theory are given in [5] using nonlocal hidden variables and in [10–12] using the concept of superdeterminism. Superdeterministic hidden-variable theories can be local Superdetermine yet be compatible with observations. Theoretical and experimental evidences for the violation of Bell's inequalities for n -particle systems of with spin are considered in [13].

On the other hand, Bell's inequalities and modified Bell's inequalities are based on simple, model-independent mathematical proofs [14]. Therefore, the mechanism and mathematical the justification for the violation of Bell's inequalities is of particular interest.

At present, interest in the study of the EPR paradox and EPR pairs has grown due to the possibility of their practical application in different technologies and in the quantum computing. Review papers in this direction [2–7] are constantly updated with new investigations (see e.g. [15, 16]).

Comprehensive study of the EPR paradox and its modifications involves analysis of locations of particles from EPR-pair in coordinate space. Measurements of cross sections and other characteristics of particle interactions in the high-energy region are usually carried out in momentum space since the time and radius of interaction of hadrons are very small and are not available for the direct measurement. The nonrelativistic quantum mechanical measurement of trajectory of particle is also strongly restricted via Heisenberg's uncertainty principle. An alternative point of view on the theoretical possibility of measuring the trajectory of quantum particles is discussed in the review article [17] using formulations of Einstein, De Broglie and Bohm. In relativistic quantum mechanics and relativistic quantum field theory interaction (entanglement) of particles and their trajectories are restricted also by strong interconnection between the temporal and spatial components of coordinate of each particle. This interconnection follows from the principles of relativity and causality. However, entanglement between two hadrons in coordinate space can be established on the basis of a theoretical model, which allows one to unambiguously determine the dependence of the observed characteristics from a two-hadron system. For example, entanglement of two atoms at a stand of 1 cm was found in [18] using one-photon exchange. Similarly, one can establish entanglement between two hadrons at microscopic distance using the theoretical model dependence of measurements of the two-hadron production.

Another aspect of the EPR paradox is problem of hidden variables to determine particle states and particle interactions. The color-charged quark-gluon states one can consider as hidden degrees of freedom because they can not be observed or isolated due to confinement in quantum chromodynamics (QCD). Hadronic and nuclear states are formed from colorless states. Confinement was analytically reproduced using two-dimensional Schwinger model or Abelian gauge theories in 2 and 3 space-time dimensions. Moreover QCD as well as confinement obtained in the framework of the multi-dimensional String theory which is not yet justified experimentally. Note that the introduction of unobservable generalizations of particle states for convenient description of their interactions or reproduction of experimental data, is long-known and effective method in theoretical physic. For example, in the review article [19] are analyzed the five-dimensional theoretical models of many outstanding physicists from 1922 to 1991 years, where the fifth dimension has an auxiliary, mathematical meaning.

The above considerations can be applied to the analysis of high-energy experimental data using quark interaction models and with the emergence of the EPR-pairs.

The production of the EPR pair of the neutral B^0 -mesons mesons at the $\Upsilon(4S)$ -resonance was measured in [20] in order to study the non-local entanglement between B^0 and \bar{B}^0 mesons. For this aim was measured the time-dependent asymmetry between two B^0 states with different flavor, which is compared with prediction of quantum mechanical model and predictions of two realistic models. The flavor asymmetry of quarks for weak interacted particles as well as the mass difference and mixing (oscillating) of B^0 and \bar{B}^0 was predicted by standard model and was supported by many experiments (see e.g. [21]).

Another application of the concept of entanglement between quark states in the high energy particle scattering experiments is done in [22, 23] using LHC CERN data set collected by ATLAS detector for $\sqrt{s} = 13$ TeV between 2013 and 2018 years. From this data were extracted differential cross section of the reaction $e^+ + e^- \leftarrow t + \bar{t}$ with top diquark masses $m_{t\bar{t}} = 350\text{GeV}$ and $m_{t\bar{t}} \geq 1\text{TeV}$. It was shown that the separability of finite states e^+ and e^- are violated due to interaction in the reaction $e^+ + e^- \leftarrow t + \bar{t}$, which significantly depends on the scattering angle in this sub-process. Besides in these papers is considered application of suggested entanglement in quantum information theory and quantum technologies. Thus the entanglement of the electron-positron pair in [22, 23] is determined by inelastic scattering of a quark-antiquark pair $e^+ + e^- \leftarrow t + \bar{t}$.

Most detailed and complete measurements of the exclusive ρ^0 -meson resonance with the polarized virtual photons were fulfilled in numerous experiments during many years at CERN (see ref. [24] and papers quoted there), where the applications of various kinematic, quark-parton models were implemented.

The purpose of this paper is to consider the the implementation of the EPR-criteria for resonances in the framework of the relativistic quantum field theory. In particular, it will be considered the spin 1 meson (V -meson) resonance decay into hadronic or leptonic pairs in the high-energy experiments, where the measurement results are analyzed using concepts of EPR-pair and entanglement of particles in this pair.

Measuring the mass and width of the resonance M_V and Γ_V is usually performed using selection of the resonating pair of particles 1 and 2 by their four momentums $p_1 = \sqrt{m_1^2 + \mathbf{p}_1^2}, \mathbf{p}_1$) and $p_2 = \sqrt{m_2^2 + \mathbf{p}_2^2}, \mathbf{p}_2$) which are located in the resonant region $(M_V - \frac{\Gamma_V}{2})^2 \leq (p_1 + p_2)^2 \leq (M_V + \frac{\Gamma_V}{2})^2$. This condition determines the relationship or entanglement of particles 1 and 2 after the decay of the resonance. In the rest frame of the V -meson resonance, \mathbf{p}_1 and \mathbf{p}_2 have opposite direction and $\mathbf{p}_1 = -\mathbf{p}_2$. Moreover, spin of these particles is strongly correlated. For instance, neglecting mass of electrons in vector meson decay one obtains that helicity of the electron and positron are also opposite. Therefore the V -meson resonance decay particle 1 and 2 form the EPR pair-type system.

For the relativistic description of the resonances we will use the field-theoretical formulation of Huang and Weldon [25–28], where hadrons are bound states of quarks. In this formulation quarks and gluons are the point-like (structureless) particle which are described by local field operator. The field operators of quarks and gluons satisfy the QCD equation of motion and causality condition. Hadron states are constructed via colorless time-ordered product of the quark fields. In this approach is constructed also the asymptotic one hadron creation or annihilation operator and corresponding S -matrix of the hadron-hadron interaction, which satisfies unitarity condition in hadronic sector. Therefore propagation of quarks in the intermediate states does not destroy the unitarity of the hadron-hadron S -matrix. Therefore one can obtain the equation of motion for amplitudes of the hadron-hadron and hadron-nuclear interaction, where color states appear only between colorless hadronic or nuclear states.

This enables to avoid problems with confinement in this approach. The 3D field-theoretical equations for the scattering amplitude as an alternate approach for the 4D Bethe-Salpeter equations is considered in Appendix A.

In contrast to the non-relativistic formulation, relativistic quantum mechanics requires strong connection between the temporal and spatial components of coordinates according to invariance under Lorentz transformation. Besides in the relativistic approach arise additional mechanisms of entanglement which are caused by off-energy and off mass shell effects and contributions from creation and annihilation of particles in intermediate states.

The organization of this papers is as follows. In Section 1 the general properties of the relativistic field-theoretical S -matrix of reactions $1 + 2 + X \leftarrow V + X \leftarrow A + B$ and corresponding construction of the resonance decay amplitude $1 + 2 \leftarrow V$ are outlined. Section 2 is devoted to the V -meson resonance decay amplitude with intermediate quark-gluon degrees of freedom. In Section 3 angular distribution of the reaction $1 + 2 + X \leftarrow V + X \leftarrow A + B$ is given in terms of the decay angles of the V -meson resonance and is considered the alignment of the particles 1 and 2 in this reaction. The last fourth part of the article provides a brief formulation of the results and examines the formation of an EPR pair and their entanglement based on relativistic field-theoretical description of the resonance. In particular are compared amplitudes with the local point-like resonance and with the nonlocal resonance consisting of quarks.

2. Amplitude of the structureless (point-like) resonance

In relativistic quantum field theory [29–31] S -matrix of inclusive collision of two particles A and B which generated particles 1, 2 and subsystem X is

$$\begin{aligned} S_{1+2+X \leftarrow A+B} &\equiv \langle out; \mathbf{p}_1, \mathbf{p}_2, X | S | \mathbf{p}_A, \mathbf{p}_B; in \rangle \\ &= \langle 0 | a_{\mathbf{p}_1}(out) a_{\mathbf{p}_2}(out), b_{\mathbf{p}_1}(out), \dots, b_{\mathbf{p}_X}(out) a_{\mathbf{p}_A}^+(in), a_{\mathbf{p}_B}^+(in) | 0 \rangle \end{aligned} \quad (1)$$

where $a_{\mathbf{p}_1}(out)$, $a_{\mathbf{p}_2}(out)$ and $a_{\mathbf{p}_A}^+(in)$ and $a_{\mathbf{p}_B}^+(in)$ denotes corresponding particle creation operators in *out* and *in* states with momentum \mathbf{p}_1 , \mathbf{p}_2 , \mathbf{p}_A , \mathbf{p}_B correspondingly. $b_{\mathbf{p}_1}(out), \dots, b_{\mathbf{p}_X}(out)$ stands for particle from subsystem X . We shall suppose that particles 1 and 2 compose intermediate vector meson V with spin 1 and we shall consider V -meson decay into electron-positron e^-e^+ and two pion $\pi^+\pi^-$ pairs. Therefore in the V -resonance energy region one gets following chain of subreactions $A + B \rightarrow V + X \rightarrow 1 + 2 + X$. It is convenient to express S -matrix (1) via corresponding amplitude

$$S_{1+2+X \leftarrow A+B} = i(2\pi)^4 \delta^4(p_A + p_B - p_1 - p_2 - P_X) \mathcal{A}_{1+2+X \leftarrow A+B} \quad (2)$$

where p_A, p_B, p_1, p_2 and P_X are four momentums of on shell asymptotic particles $p_{A,B} = (\sqrt{m_{A,B}^2 + \mathbf{p}_{A,B}^2}, \mathbf{p}_{A,B})$, $p_{1,2} = (\sqrt{m_{1,2}^2 + \mathbf{p}_{1,2}^2}, \mathbf{p}_{1,2})$ with masses $m_{A,B}$, $m_{1,2}$ and three momentums $\mathbf{p}_{A,B}$, $\mathbf{p}_{1,2}$. Besides we shall use four-vector of V -meson resonance $P_V \equiv (P_V^0, \mathbf{P}_V) = (\sqrt{M_V^2 + \mathbf{P}_V^2}, \mathbf{P}_V)$.

Spin of relativistic particle or resonance is defined in the rest frame of this particle or resonance. Therefore we shall consider the rest frame of system of particles 1 and 2, where .

Resonance in quantum mechanics is defined as pole of the amplitude in the complex momentum plane at $\sqrt{s_{12}} \equiv \sqrt{(p_1 + p_2)^2} \rightarrow M_V - i\Gamma_V/2$, where M_V and Γ_V denote the pole position and the V -resonance decay width in the particle system 1 + 2. Therefore $\mathcal{A}_{1+2+X \leftarrow A+B}$ must have the following form

$$\lim_{s_{1,2} \rightarrow M_{12} - i\Gamma_{12}/2} (\sqrt{s_{1,2}} - M_{12} + i\Gamma_{12}/2) \mathcal{A}_{1+2+X \leftarrow A+B} = \mathcal{A}_{1+2 \leftarrow V} \mathcal{A}_{V+X \leftarrow A+B} \quad (3)$$

or

$$\mathcal{A}_{1+2+X \leftarrow A+B} = \mathcal{A}_{1+2 \leftarrow V} \frac{1}{\sqrt{s_{1,2}} - M_V + i\frac{\Gamma_V}{2}} \mathcal{A}_{V+X \leftarrow A+B} + \text{nonresonant part} \quad (4)$$

where the pole part of the amplitude is represented by the V -meson exchange term. It is convenient to express $\mathcal{A}_{1+2 \leftarrow V}$ via the product of the wave function $|\Psi_V\rangle$ and two-body potential $\langle 1, 2|V|1', 2'\rangle$

$$\mathcal{A}_{1+2 \leftarrow V}(\sqrt{s_{1,2}}) = \langle 1, 2|V\Psi_V\rangle \quad (5)$$

where $|\Psi_V\rangle$ satisfies the equation

$$\langle 1, 2|\Psi_V\rangle = \frac{1}{\sqrt{s_{1,2}} - M_V + i\frac{\Gamma_V}{2}} \langle 1, 2|V\Psi_V\rangle. \quad (6)$$

Unlike to the bound state, $\langle 1, 2|\Psi_V\rangle$ is not the eigen-function of the Hamiltonian of the system $1 + 2 - 1' + 2'$.

Eqs. (4) and (6) enables to describe the resonant and non-resonant parts of $\mathcal{A}_{1+2+X \leftarrow A+B}$ using the same Lagrangian and same phenomenological potential for all partial waves of 1 + 2 subsystem. In this approach were reproduced low energy $\pi N - \pi N$, $NN - NN$ and $\gamma N - \pi N$ reactions [26, 32, 33]. In particular, description of low-energy πN scattering amplitude in the Δ -resonance region was performed within the Born approximation in [30] (see eq. (10.67) and (10.79)).

In other relativistic approach resonance is treated as particle-type degrees of freedom with imaginary mass $M_V - i\Gamma_V/2$, spin s_V and with corresponding Lagrangian. Corresponding S,P,D,F pion-nucleon S,P,D,F phase shifts are calculated within third order chiral effective field theory in [34].

Cross section of the reaction $1 + 2 + X \leftarrow A + B$ according to (4) is [31].

$$\frac{d\sigma_{1+2+X \leftarrow A+B}}{d\Omega_{1+2+X \leftarrow A+B}} = \sum_{MM'} \frac{d\sigma_{1+2 \leftarrow V}^{MM'}}{d\Omega_{1+2 \leftarrow V}} \frac{1}{(m_V - \sqrt{s_{12}})^2 + \Gamma_V^2/4} \frac{d\sigma_{V+X \leftarrow A+B}^{MM'}}{d\Omega_{V+X \leftarrow A+B}} \quad (7)$$

where M, M' are magnetic quantum number of V resonance

$$\frac{d\sigma_{V+X \leftarrow A+B}^{MM'}}{d\Omega_{V+X \leftarrow A+B}} = \mathcal{N}_{A+B} \prod_i^X \mathcal{A}_{V+X \leftarrow A+B}^M (\mathcal{A}_{V+X \leftarrow A+B}^*)^{M'} \quad (8)$$

$$d\Omega_{V+X \leftarrow A+B} = (2\pi)^3 \frac{d\mathbf{P}_{12}}{(2\pi)^3} \prod_{i=1}^X d\tilde{\mathbf{p}}_i (2\pi)^4 \delta^3(\mathbf{P}_A + \mathbf{P}_B - \mathbf{P}_{12} - \mathbf{P}_X) \delta(P_A^o + P_B^o - P_{12}^o - P_X^o)$$

where $\mathbf{P}_{12} = \mathbf{p}_1 + \mathbf{p}_2$ and $P_{12}^o = p_1^o + p_2^o$,

$$\frac{d\tilde{\sigma}_{1+2 \leftarrow V}^{MM'}}{d\Omega_{1+2 \leftarrow V}} = \mathcal{A}_{1+2 \leftarrow V}^M (\mathcal{A}_{1+2 \leftarrow V}^*)^{M'} \quad (9)$$

$$d\Omega_{1+2 \leftarrow V} = d\tilde{\mathbf{p}}_1 d\tilde{\mathbf{p}}_2 \delta^3(\mathbf{p}_1^* + \mathbf{p}_2^*)$$

where $N_A = 1/(2p_A^o)$ for bosons and $N_A = m_A/p_A^o$ for fermions

$$\mathcal{N}_{A+B} = \frac{1}{(2S_A + 1)(2S_B + 1)} \frac{N_A N_B}{\sqrt{(P_A P_B)^2 - m_A^2 m_B^2}}; \quad d\tilde{\mathbf{p}}_a = N_a \frac{d\mathbf{p}_a}{(2\pi)^3} \quad (10)$$

$d\tilde{\sigma}_{1+2 \leftarrow V}^{MM'}/d\Omega_{1+2 \leftarrow V}$ does not contain $\delta(P_V^o - p_1^o - p_2^o)$ and $\mathcal{A}_{1+2 \leftarrow V}^M$ depends on the decay width Γ_V of resonance according to (5) and (6). That's why amplitude $\mathcal{A}_{1+2 \leftarrow V}^M$ is nonlocal and off shell even for the point-like, structureless resonance. General field theoretical construction of the nonlocal V -resonance with quark degrees of freedom is given in next section.

According to the vector meson dominance model the main contribution into vector meson decay is made by diagram of the V -meson transformation into off shell photon $\gamma^* \leftarrow V$. Therefore in phenomenological $\mathcal{A}_{1+2 \leftarrow V}^M$ is used the form factor of electromagnetic-type (see e.g. [29] ch. 10.6), where current operator of the V -meson resonance is replaced by the current operator of the elementary particle with the mass M_V , spin 1 and the coupling constant g_V . Then $\mathcal{A}_{1+2 \leftarrow V}^M$ for the leptonic decay takes the form

$$\mathcal{A}_{\ell^+ \ell^- \leftarrow V}^M = g_{\ell^+ \ell^- \leftarrow V} \xi_\mu^* (\mathbf{P}_V, M) \bar{u}(\mathbf{p}_\ell) \gamma_\mu v(\mathbf{p}_{\bar{\ell}}) \quad (11)$$

where $\xi_\mu^* (\mathbf{P}_V, M)$ is the polarization vector of the spin 1 particle and coupling constant $g_V \equiv g_{\ell^+ \ell^- \leftarrow V}$ is defined according to vector meson dominance model.

In this approximation the hadronic decay amplitude is

$$\mathcal{A}_{h+\bar{h} \leftarrow V}^M = g_{h+\bar{h} \leftarrow V} \left((p_h + p_{\bar{h}})^2 \right) (\xi_\mu^* (\mathbf{P}_V, M) p_h^{*\mu}) \quad (12)$$

where for simplicity only spineless hadrons are considered. $g_{h+\bar{h} \leftarrow V} \left((p_h + p_{\bar{h}})^2 \right)$ is form factor of $h + \bar{h} \leftarrow V$.

3. V -meson decay amplitude with the quark-gluon degrees of freedom

Amplitude $\mathcal{A}_{1+2 \leftarrow V}$ (5) can be constructed with intermediate quark-antiquark-gluon degrees of freedom $q - \bar{q} -$ using the field-theoretical approach of the composite particle states [25, 26]. In this formulation the Heisenberg field operator of the composite particle is defined via the Bethe-Salpeter wave functions (see [31] ch. 10.2.1)

$$\chi_{m_V, \mathbf{P}_V}(Y, y_{1,2}) = \langle 0 | T(\psi_1(y_1) \psi_2(y_2)) | m_V, \mathbf{P}_V, M; in \rangle, \quad (13)$$

where

$$Y = y_1 + y_2, \quad y_{1,2} = \eta_2 y_1 - \eta_1 y_2; \quad \eta_1 + \eta_2 = 1 \quad (14)$$

are Jacobi coordinates. For the sake of simplicity in (1) we have introduced the complex mass $m_V = M - V - i\Gamma_V/2$ for the resonance state. In alternate formulation the dependence on Γ_V of wave function implicitly through solution of the Bethe-Salpeter equation. In alternate formulation the dependence on Γ_V of wave function occurs implicitly through solution of Bethe-Salpeter equation.

One can introduce nonlocal operator of the resonance in analogy with bound-state field

$$\mathcal{B}_{m_V, \mathbf{P}_V}(Y_o) = i \int d^3\mathbf{Y} d^4y_{12} \exp(iP_V Y) \left[\frac{\partial}{\partial Y_o} - iP_V^o \right] \chi_{m_V, \mathbf{P}_V}(Y, y_{12}) T(\psi_1^+(x_1) \psi_2^+(x_2)). \quad (15)$$

which transforms into single composite particle creation or annihilation operator in asymptotic regions $\pm\infty \Leftarrow Y_o$

$$\langle \Psi | \mathcal{B}_{m_V, \mathbf{P}_V}(out(in)) | \Phi \rangle = \lim_{\pm\infty \Leftarrow Y_o} \langle \Psi | \mathcal{B}_{m_V, \mathbf{P}_V}(Y_o) | \Phi \rangle, \quad (16)$$

where $|\Phi\rangle$ and $|\Psi\rangle$ denote an arbitrary wave functions.

The asymptotic operators satisfy the same commutation relation as elementary (point-like) particle

$$\begin{aligned} [\mathcal{B}_{m_V, \mathbf{P}_V}^+(out(in)), \mathcal{B}_{m_V, \mathbf{P}_V}(out(in))] &= (2\pi)^3 2P_V^o \delta(\mathbf{P}'_V - \mathbf{P}_V); \\ [\mathcal{B}_{m_V, \mathbf{P}_V}(out(in)), \mathcal{B}_{m_V, \mathbf{P}_V}(out(in))] &= 0; \end{aligned} \quad (17)$$

But unlike elementary (point-like, structureless) particle, the same commutation relations for $\mathcal{B}_{m_V, \mathbf{P}_V}(Y_o)$ (15) are violated

$$\begin{aligned} [\mathcal{B}_{m_V, \mathbf{P}_V}^+(Y_o), \mathcal{B}_{m_V, \mathbf{P}_V}(Y_o)] &\neq (2\pi)^3 2P_V^o \delta(\mathbf{P}'_V - \mathbf{P}_V); \\ [\mathcal{B}_{m_V, \mathbf{P}_V}(Y_o), \mathcal{B}_{m_V, \mathbf{P}_V}(Y_o)] &\neq 0. \end{aligned} \quad (18)$$

Inequalities (18) are caused by nonlocality of $\mathcal{B}_{m_V, \mathbf{P}_V}(Y_o)$ (15) which depends exactly on interacted fields $\psi_1(y_1)$, $\psi_2(y_2)$. and on the resonance decay width $\Gamma_V/2$.

Using $\mathcal{B}_{m_V, \mathbf{P}_V}(Y_o)$ (15) one can built the V meson field $\Upsilon_{m_V, \mathbf{P}_V}(Y)$ and corresponding source operator $\mathcal{J}_{m_V, \mathbf{P}_V}(Y)$

$$\Upsilon_{m_V, \mathbf{P}_V}(Y) = \int \frac{d^3\mathbf{P}_V}{(2\pi)^3 2P_V^o} \left[e^{-iP_V Y} \mathcal{B}_{m_V, \mathbf{P}_V}(Y_o) + e^{iP_V Y} \mathcal{B}_{m_V, \mathbf{P}_V}^*(Y_o) \right], \quad (19)$$

$$\mathcal{J}_{m_V, \mathbf{P}_V}(Y) = (W_Y + M_V^2) \Upsilon_{m_V, \mathbf{P}_V}(Y) \quad (20)$$

which enables to obtain the general expression for amplitude of V meson resonance

$$\mathcal{A}_{1+2 \leftarrow V}(\text{nonlocal}) = \langle \text{out}; 1, 2 | \mathcal{J}_{m_V \mathbf{p}_V}(0) | 0 \rangle \quad (21)$$

where $m_V = M_V - i\Gamma_V/2$.

4. Spin density matrix and alignment for reaction $1 + 2 + X \leftarrow V + X \leftarrow A + B$

The cross sections (7), (8) and (9) make it possible to obtain a convenient formula for the expansion of the angular distribution $W_{1+2+X \leftarrow A+B}$ in terms of the sum spin density matrices (see e.g. ch. 8 [35]) $\rho_{V+X \leftarrow A+B}^{MM'}$ and $\rho_{1+2 \leftarrow V}^{MM'}$.

$$W_{1+2+X \leftarrow A+B} = \sum_{M, M'} \rho_{1+2 \leftarrow V}^{MM'} \rho_{V+X \leftarrow A+B}^{MM'}, \quad (22)$$

where

$$\rho_{V+X \leftarrow A+B}^{MM'} = \frac{d\sigma_{V+X \leftarrow A+B}^{MM'} / d\Omega_{V+X \leftarrow A+B}^*}{\int d\Omega_{V+X \leftarrow A+B}^* \sum_M d\sigma_{V+X \leftarrow A+B}^{MM} / d\Omega_{V+X \leftarrow A+B}^*}; \quad (23)$$

where

$$\rho_{1+2 \leftarrow V}^{MM'} = \frac{d\tilde{\sigma}_{1+2 \leftarrow V}^{MM'} / d\Omega_{1+2 \leftarrow V}}{\int d\Omega_{1+2 \leftarrow V}^* \sum_M d\tilde{\sigma}_{1+2 \leftarrow V}^{MM} / d\Omega_{1+2 \leftarrow V}^*} \quad (24)$$

Upper index $*$ in (22)-(24) indicate the rest frame of V -meson, where $\mathbf{p}^* \equiv \mathbf{p}_1^* = -\mathbf{p}_2^*$ and decay angles θ^*, ϕ^* are defined by momentum of the final particle

$$\mathbf{p}^* \equiv \mathbf{p}_1^* = |\mathbf{p}^*|(\sin \theta^* \cos \phi^*, \sin \theta^* \sin \phi^*, \cos \theta^*), \quad (25)$$

$d\Omega_{V+X \leftarrow A+B}^*$ and $d\Omega_{1+2 \leftarrow V}$ stands for Lorentz invariant phase space elements

$$d\Omega_{V+X \leftarrow A+B}^* = \frac{d^3 \mathbf{p}_V^*}{(2\pi)^3} \prod_{i=1}^X N_i \frac{d^3 \mathbf{p}_i^*}{(2\pi)^3} \quad (26)$$

$$d\Omega_{1+2 \leftarrow V} = N_1 N_2 \frac{d^3 \mathbf{p}^*}{(2\pi)^3} \quad (27)$$

Cross sections (7) and decomposition of the corresponding angular distribution (22) through products of spin density matrices are often used to describe experimental data of exclusive and inclusive reactions using the helicity basis. Polarization effects in the corresponding generalizations of the cross sections (7) and corresponding spin density matrices are taking into account in [36, 37]. Beam polarization effects, decomposition of the spin density matrix by the transverse and longitudinal components of the virtual photon are considered in [24] for the exclusive reactions $\mu' + p' + \rho^0 \leftarrow \mu + p$ and $p' + \rho^0 \leftarrow \gamma^* + p$.

Using vertex functions (11) and (12) and relationship between $\xi^\mu(0, M)$ and Wigner D -matrices $D_{mn}^1(\theta^*, \phi^*)$

$$\left(\xi^\mu(0, M) p_\mu^* \right) = |\mathbf{p}^*| D_{M0}^1(\theta^*, \phi^*) \quad (28)$$

we obtain

$$W_{1+2+X \leftarrow A+B} = C + \sum_{MM'} D_{M0}^{*1}(\theta^*, \phi^*) \rho_{V+X \leftarrow A+B}^{MM'} D_{M'0}^1(\theta^*, \phi^*) \quad (29)$$

where $C = 0$ if 1, 2 are pions and $C = 1$ if 1, 2 are electron-positron pair.

Angular distributions $W_{1+2+X \leftarrow A+B}$ (29) describe decay of the point-like (structureless) resonance V on two particles 1 and 2, where dependence of $W_{1+2+X \leftarrow A+B}$ on the resonance decay angles is contained in $D_{M'0}^1(\theta^*, \phi^*)$. Therefore anisotropy regarding angles θ^*, ϕ^* in $W_{1+2+X \leftarrow A+B}$ (29) appear due to spin density matrix $\rho_{V+X \leftarrow A+B}^{MM'}$ of the sub-reaction $V + X \leftarrow A + B$. This anisotropy is called alignment of the decay particles. In particular, if $\rho_{V+X \leftarrow A+B}^{M=M'} \simeq 1/3$ and $\rho_{V+X \leftarrow A+B}^{M \neq M'} \simeq 0$, then V -meson decay is isotropic. In this case the decay particles 1 and 2 move independently from the interactions in the initial sub-reaction $V + X \leftarrow A + B$. Thus for isotropic decay entanglement between particles 1 and 2 caused only by location of effective mass of subsystem 1 + 2 in resonance region

$$\left(M_V - \frac{\Gamma_V}{2} \right)^2 \leq (p_1 + p_2)^2 \leq \left(M_V + \frac{\Gamma_V}{2} \right)^2. \quad (30)$$

Vertex (21) for composite V -meson resonances can be presented as

$$\begin{aligned} \mathcal{A}_{1+2 \leftarrow V} &= \langle out; \mathbf{p}^*, S_1^* M_1^*; -\mathbf{p}^*, S_2^* M_2^* | \mathcal{J}_{m_V \mathbf{0}_V}^{*1M}(0) | 0 \rangle = \\ &= \delta_{J^*, 1} \sum_{L^*, S^*} \mathcal{Y}_{L^*, S^*}^{JM}(\hat{\mathbf{p}}^*) F_{S^* L^*}^{J^*}(\sqrt{s_{12}}), \end{aligned} \quad (31)$$

where $\mathcal{Y}_{L^*, S^*}^{JM}(\hat{\mathbf{p}}^*)$ and $Y_{L^* M}^*(\hat{\mathbf{p}}^*)$ are tensor spherical harmonics and spherical harmonics

$$\mathcal{Y}_{L^*, S^*}^{JM}(\hat{\mathbf{p}}^*) = \sum_{M_L^*} \langle L^* M_L^* S^* M_S^* | 1M \rangle Y_{L^* M}^*(\hat{\mathbf{p}}^*) \chi_{S^* M_S^*}(S_1^* M_1^*, S_2^* M_2^*), \quad (32)$$

and

$$\begin{aligned} F_{S^* L^*}^{J^*}(\sqrt{s_{12}}) &= (\xi_\mu(0, M) \mathbf{p}^{*\mu}) \int d^3 \mathbf{q}^* F_{S^* L^*}^{(1)}(\mathbf{p}^*, \mathbf{q}^*, \sqrt{s_{12}}) \\ &+ \int d^3 \mathbf{q}^* (\xi_\mu(0, M) \mathbf{q}^{*\mu}) F_{S^* L^*}^{(2)}(\mathbf{p}^*, \mathbf{q}^*, \sqrt{s_{12}}) \end{aligned} \quad (33)$$

is the radial part of $\mathcal{A}_{1+2 \leftarrow V}$ with spin S^* , orbital momentum L^* and their projections M_S^* and M_L^* .

Using (31)–(33) one can represent the cross section of reaction $1 + 2 + X \leftarrow A + B$ in the form

$$\frac{d\sigma_{1+2+X \leftarrow A+B}}{d\Omega_{1+2+X \leftarrow A+B}^*} = \sum_{MM'} \left(\sum_{L^* S^*} \left[\mathcal{Y}_{JM}^{L^* S^*}(\hat{\mathbf{p}}_{12}^*) F_{S^* L^*}^1(\sqrt{s_{12}}) \right]^+ \frac{d\sigma_{A+B \Rightarrow V+}^{MM'}}{d\Omega_{A+B \Rightarrow V+}^*} \frac{\sum_{L'S'} \left[\mathcal{Y}_{JM'}^{L'S'}(\mathbf{p}_{12}^*) F_{S'L'}^1(\sqrt{s_{12}}) \right]}{(M_V^2 - s_{12})^2 + M_V^2 \Gamma_V^2} \right), \quad (34)$$

Thus cross sections (34) and (7) with the amplitude of the composite and structureless V -meson resonance decay (31), (11) and (12) have different angular momentum dependence and different meson decay form factors.

5. Conclusion and outlook

In this paper we have discussed the entanglement of two hadrons and two leptons, which occur in high energy collision $1 + 2 + X \leftarrow V + X \leftarrow A + B$ after V meson resonance decay $1 + 2 \leftarrow V$. For the most general reproduction of entanglement mechanisms, we used a field-theoretic construction of the resonance decay amplitude with and without quark-gluon degrees of freedom.

In the both cases the two-body decay of any resonance automatically forms EPR-pair-type system in their rest frame, where these particles have opposite momentums and the strongly correlating spin states.

Big difference in the leptonic and hadronic resonance decay of V -meson produce corresponding difference between form factors (11) and (12). In particular, the hadronic and leptonic decay of the point-like (structureless) V -meson contains form factors $g_{h\bar{h}-V} \left((p_h + p_{\bar{h}})^2 \right)$ (12) and $g_{\ell\bar{\ell}-V} \simeq \text{const}$ (11). There are even more differences between the hadron decay form factors (33) and (12) with and without quark-gluon degrees of freedom for the non-point-like (non-local) and point-like (local) resonances correspondingly. Even more difference appear between the hadronic decay form factors (12) and (33) point-like (local) and non-point-like (nonlocal) resonances.

If decay of the V -meson resonance is approximately isotropic $\rho_{11} = \rho_{00} = \rho_{-1-1} \simeq 1/3$, then decay of it is identical with the decay of the isolated resonance. In this case decay of the V -meson is independent on the influence of the initial subprocess $V + X \leftarrow A + B$. After that, decay $1 + 2 \leftarrow V$ can be considered as the decay of a quasi-free V -meson resonance and the entanglement between particles 1 and 2 can be determined only by the resonant decay mechanism.

Nonlocality of hadrons or nucleons in quantum field theory is a consequence of the composite (nonlocal) structure of hadrons or nuclei. The composite hadrons are built through the interactions of local (point-like) fields of quarks and gluons, and the composite (nonlocal) structure of nuclei in nuclear physics is determined through the interaction of local (point-like) nucleons. The equal-time commutators of the composite field operators composite particles (15) or (19) and (20) are not equal to zero even in a space-like region.

Cross sections (7) are valid for both local and non-local resonant decay of the V -meson $\tilde{N}\tilde{Z}$. One can rewrite this expression as

$$\frac{d\tilde{\sigma}_{1+2 \leftarrow V}^{MM'}}{d\Omega_{1+2 \leftarrow V}} = \mathcal{A}_{1+2 \leftarrow V}^M (\mathcal{A}_{1+2 \leftarrow V}^*)^{M'} \quad (35)$$

Representation of (35) in the form of a product of cross sections of the reactions $1 + 2 \leftarrow V$ and $V + X \leftarrow A + B$ is a consequence of the separability of scattering

amplitudes with a single-particle s -channel exchange in quantum field theory or in nonrelativistic scattering theory [38].

Thus the nonlocality of the hadrons in quantum field theory [25] differs from Bell nonlocality (see [5] eq. (3)), where nonlocality arises due to integration over a certain variables λ , “having a joint causal influence on both outcomes, and which fully account for the dependence between” 1 and 2.

This discrepancy with Bell nonlocality is a consequence of the two reasons. First, nonlocality in quantum field theory and nonrelativistic nuclear and collision theories is introduced via construction of the composite particle states through degrees of freedom of local, structureless particles. And Bell’s nonlocality is determined through integration over λ of the local probability in the Bell formulation.

Secondly, EPR thought experiments and similar subsequent formulations imply independent measurements of the location of a single particle from an EPR pair in coordinate space based on the uncertainty principle Heisenberg. But in real experiments in elementary particle physics and nuclear physics, the momentum of particles and the states of these particles in the momentum space are measured. Determining the position of particles in coordinate space requires not only a relativistic generalization of the Heisenberg uncertainty principle, but also model-independent calculations of the trajectory of quantum particles and other tasks beyond the scope of this article.

Appendix A: relativistic 4D and 3D field-theoretical equations

Field-theoretical Bethe-Salpeter equations for 4D amplitude

$$\mathcal{A}^{4D} \equiv \mathcal{A}^{4D}(p_A^o \mathbf{p}_A, p_B^o \mathbf{p}_B; p_C^o \mathbf{p}_C, p_D^o \mathbf{p}_D) \quad (36)$$

and relativistic Lippmann-Schwinger-type equations for 3D amplitude

$$\mathcal{A}^{3D} \equiv \mathcal{A}^{3D}(\mathbf{p}_A, \mathbf{p}_B; \mathbf{p}_C, \mathbf{p}_D) \quad (37)$$

describe reactions $C + D \leftarrow A + B$ in framework of the relativistic field theory taking into account the absorption and appearance of particles. In (A1) \mathcal{A}^{4D} depends on the off shell four-momentum of each particle, p_B, p_C and p_D . In (A2) \mathcal{A}^{3D} is

function of on mass shell momentums $p_A^{on} = (\sqrt{m_A^2 + \mathbf{p}_A^2}, \mathbf{p}_A)$,

$$p_B^{on} = (\sqrt{m_B^2 + \mathbf{p}_B^2}, \mathbf{p}_B), p_C^{on} = (\sqrt{m_C^2 + \mathbf{p}_C^2}, \mathbf{p}_C) \text{ and } p_D^{on} = (\sqrt{m_D^2 + \mathbf{p}_D^2}, \mathbf{p}_D).$$

Observed particles of the reaction $C + D \leftarrow A + B$ are on shell, where $p_k = p_k^{on}$ ($k = A, B, C, D$) and $p_C^{on} + p_D^{on} = p_A^{on} + p_B^{on}$. On shell 4D and 3D amplitudes coincide

$$\mathcal{A}_{on}^{4D} = \mathcal{A}_{on}^{3D} \quad (38)$$

In case of spin less particles Bethe-Salpeter equation for \mathcal{A}^{4D} (A1) in coordinate space have the form (see e.g. [31] ch. 10)

$$\begin{aligned} \mathcal{A}^{4D}(x_C x_D; x_A x_B) &= \mathcal{V}^{4D}(x_C x_D; x_A x_B) \\ &+ \int d^4 x_\alpha d^4 x_\beta \mathcal{V}^{4D}(x_C x_D; x_\alpha x_\beta) (W_{x_\alpha} + m_\alpha^2 + i\epsilon)^{-1} (W_{x_\beta} + m_\beta^2 + i\epsilon)^{-1} \mathcal{A}^{4D}(x_\alpha x_\beta; x_A, x_B), \end{aligned} \quad (39)$$

where $\mathcal{V}^{4D}(x_C x_D; x_A x_B)$ consist of sum of all Feynman diagrams with all possible intermediate states excluding asymptotic two-body states $\alpha + \beta \equiv C + D, A + B$.

General form of Bethe-Salpeter equations are derived in framework of the method of functional integrals [31] and graphical summation method for Feynman diagrams [39, 40]. These equations depend on non-physical relative time variables $x_A^o - x_B^o$, $x_C^o - x_D^o$ which greatly complicates their application and requires additional approximations. Therefore, were proposed so called 3D quasi-potential reductions of Bethe-Salpeter equations, where they are replaced by a set of four-dimensional equations for the relation between the 4D and 3D potentials and 3D reduced equation for the sought amplitude, 3D potential (so called quasipotential of Bethe-Salpeter equation) and the 3D Green's functions [41–43]. However, there are an infinite number of three-dimensional reductions of same Bethe-Salpeter equation which produce different 3D equations with different potentials, different 3D off shell amplitudes and different Green function. Another version of the 3D reduction of the Bethe-Salpeter equations is given in [44].

From the beginning 3D field-theoretical equations \mathcal{A}^{3D} (A2) are derived within modified “old perturbation theory” [45–47] where all particles are being on shell. In this formulation arose the additional quasi-particle degrees of freedom, which enables to take into account off-shellness of the intermediate states.

Another type of initially three-dimensional field-theoretic equations [26, 33, 48] was obtained within the S -matrix reduction method [29–31]. In this case

$$\mathcal{A}^{3D} = \langle out; \mathbf{p}_A | j_B(0) | \mathbf{p}_C \mathbf{p}_D; in \rangle \quad (40)$$

where $j_B(x) = (W_x + m_B^2)\phi_B(x)$ is the source operator of particle B . In this approach final equations have the form of the relativistic Lippmann Schwinger-type equations

$$\begin{aligned} T^{3D}(\mathbf{p}', \mathbf{p}; P_o) &= \mathcal{U}^{3D}(\mathbf{p}', \mathbf{p}; P_o) \\ &+ \int \mathcal{U}^{3D}(\mathbf{p}', \mathbf{p}''; P_o) \frac{d^3 \mathbf{p}_1'' d^3 \mathbf{p}_2'' \delta(\mathbf{P} - \mathbf{P}'')}{2E_{\mathbf{p}_1''} 2E_{\mathbf{p}_2''} (P_o - E_{\mathbf{p}_1''} - E_{\mathbf{p}_2''} + i\epsilon)} T^{3D}(\mathbf{p}'', \mathbf{p}; P_o), \end{aligned} \quad (41)$$

where $P_o = E_{\mathbf{p}_1} + E_{\mathbf{p}_2}$, $\mathbf{P} = \mathbf{p}_1 + \mathbf{p}_2$ denote total energy and total momentum of the system 1 + 2, $E_{\mathbf{p}_{1,2}} = \sqrt{\mathbf{p}_{1,2}^2 + m_{1,2}^2}$, and $\mathbf{p} = 1/2(\mathbf{p}_1 - \mathbf{p}_2)$ are the relative momentum of particles 1, 2 in the rest frame $\mathbf{P} = \mathbf{p}_1 + \mathbf{p}_2 = 0$.

Potential $\mathcal{U}^{3D}(\mathbf{p}', \mathbf{p}; P_o)$ of (A6) consists of all three-dimensional time ordered diagrams with on mass shell particle exchanges in u , \bar{u} and \bar{s} . Besides \mathcal{U}^{3D} contains so called seagull term which produces off mass shell one-particle exchange term and overlapping (contact) terms.

On shell \mathcal{T}_{on}^{3D} and \mathcal{A}_{on}^{3D} coincides.

Unlike the Bethe-Salpeter equations and their 3D reductions, the potential of three-dimensional field-theoretic Eq. (A6) is determined by vertex functions and amplitudes $\langle out; n | j_a(0) | m; in \rangle$, which contain only one particle a with off shell source operator $j_a(0)$. Therefore, in these three-dimensional equations, it is not required to make approximations which simplify off shell behavior of the vertex functions and amplitudes.


Note that taking into account the quark-gluon degrees of freedom does not change the form of the Eq. (41) for the amplitudes of hadron interactions.

Author details

Alexander Machavariani
High Energy Physics Institute of Tbilisi State University, Tbilisi, Georgia

*Address all correspondence to: aimachavariani@gmail.com

IntechOpen

© 2023 The Author(s). Licensee IntechOpen. This chapter is distributed under the terms of the Creative Commons Attribution License (<http://creativecommons.org/licenses/by/3.0>), which permits unrestricted use, distribution, and reproduction in any medium, provided the original work is properly cited. 

References

- [1] Einstein A, Podolsky B, Rosen N. Can quantum-mechanical description of physical reality be considered complete? *Physics Review*. 1935;**47**:777
- [2] Reid MD et al. Colloquium: The Einstein-Podolsky-Rosen paradox: From concepts to applications. *Reviews of Modern Physics*. 2009;**81**:1727. arXiv: 0806.0270v2[quant-ph] 08Dec 2008
- [3] Cavalcanti D, Skrzypczyk P. Quantum steering: A. *Reports on Progress in Physics*. 2017;**80**:024001
- [4] Peise J et al. Satisfying Einstein-Podolsky-Rosen criterion with massive particle. *Nature Communications*. 2015. Available from: www.nature.com/naturecommunications
- [5] Brunner N et al. Bell nonlocality. *Reviews of Modern Physics*. 2014;**86**: 419. arXiv:1303.2849v3 [quant-ph] 10 Apr 2014
- [6] Fine A, Ryckman TA. In: Zalta EN, editor. *The Einstein-Podolsky-Rosen Argument in Quantum Theory*. Stanford, USA: The Stanford Encyclopedia of Philosophy; 2020. Available from: <https://plato.stanford.edu/archives/sum2020/entries/qt-epr>
- [7] Klyshko DN. A simple method of preparing pure states of an optical field, of implementing the Einstein-Podolsky-Rosen experiment and of demonstrating the complementarity principle. *Soviet Physics Uspekhi*. 1988;**31**:74. Available from: <http://iopscience.iop.org/0038-5670/31/1/A05>
- [8] Schrödinger E. Discussion of probability relations between separated systems. *Proceedings-Cambridge Philosophical Society*. 1935;**31**:555 and
- Probability relations between separated systems. *Proceedings-Cambridge Philosophical Society*. 1936;**32**:446
- [9] Bell JS. On Einstein Podolsky Rosen paradox. *Physics*. 1964;**1**:195
- [10] G. 't Hooft. The cellular automaton interpretation of quantum mechanics. In: *Fundamental Theories of Physics*. Vol. 185. Heidelberg, New York, Dordrecht, London: SpringerOpen; 2016. Open Access: <https://library.oapen.org/bitstream/id/470b7d7e-768c-4b5f-936e-d9cb5fb6fa13/1002003.pdf>
- [11] Andreoletti G, Vervoort L. Superdeterminism: A reappraisal. *Synthese*. 2022;**200**:361. Available from: <https://philarchive.org/rec/ANDSAR-9>
- [12] Hossenfelder S, Palmer T. Rethinking superdeterminism. 2020;**8**:1. Available from: <https://www.frontiersin.org/articles/10.3389/fphy.2020.00139/full>
- [13] Cabello A. Bell's inequality for n spin- s particles. *Physical Review A*. 2002;**65**:062105
- [14] Maccone L. A simple proof of Bell's inequality. *American Journal of Physics*. 2013;**81**:854
- [15] Colgiachi P et al. Einstein-Podolsky-Rosen experiment with two Bose-Einstein condensates. *Physical Review X*. 2023;**13**:021031
- [16] Schnabel R. The solution to the "Einstein-Podolsky-Rosen" paradox. arXiv: 2208.13831v4 [quant-ph] 2023
- [17] Aristarhov S. Heisenberg's uncertainty principle and particle trajectories. *Foundations of Physics*. 2023;**53**:7

- [18] Hagley E et al. Generation of Einstein-Podolski-Rosen pairs of atoms. *Physical Review Letters*. 1997;**79**:1
- [19] Fanchi JR. Review of invariant time formulations of relativistic quantum theories. *Foundations of Physics*. 1992; **23**:487
- [20] Go A, Bay A. Measurement of EPR-type flavor entanglement in $\Upsilon(4S) \rightarrow B^0 \bar{B}^0$ decays. *Physical Review Letters*. 2007;**99**
- [21] Nestle U. Three lectures on meson mixing and CKM phenomenology. Karlsruhe. 2009. Available from: <https://www.ttp.kit.edu/media/preprints/2009/ttp09-07.pdf>
- [22] Afik Y, de Nova JRM. Entanglement and quantum tomography with top quarks at the LHC. *European Physical Journal - Plus*. 2021;**136**:907; Quantum discord and steering in top quarks at the LHC. *Physical Review Letters*. 2023;**130**: 221801
- [23] Xinari T. Quantum Entanglement with Top Quarks at the LHC. CERN-Students-Students-Note-2022-062. CERN 2022
- [24] Alexeev GD et al. Spin Density Matrix Elements in Exclusive ρ Meson Muon-production CERN-EP-2022-23 and 1arXiv: 2210.16932v2 [hep-ex] 2023. COMPASS Collaboration. To be publ [Preprint]
- [25] Huang K, Weldon HA. Bound state wave functions and bound state scattering in relativistic field theory. *Physical Review D*. 1975;**11**:257
- [26] Machavariani A. Three-dimensional field-theoretical equations for a two-particle system and the problem of πN , NN and $q\bar{q}$ scattering. *Physics of Particles and Nuclei*. 1993;**24**:317. American Institute of Physics
- [27] Machavariani AI, Faessler A. Current conservation and analytic determination of the magnetic moment of the Δ resonance in the πN bremsstrahlung: II. Formulation with quark degrees of freedom. III. Magnetic moment of the Δ^0 and Δ^- resonances. *Journal of Physics G: Nuclear and Particle Physics*. 2011;**38**: 035002
- [28] Machavariani A. TMD PDF model of the ρ^0 -meson production in the inclusive proton-proton collision. Available from: <https://arxiv.org/pdf/1712.06395.pdf>
- [29] Weinberg S. *The Quantum Theory of Fields – Volume I: Foundations*. Cambridge: Cambridge University Press; 1995
- [30] Bjorken JD, Drell SD. *Relativistic Quantum Fields*. New York, USA: McGraw Hill Book Company; 1965
- [31] Itzykson C, Zuber C. *Quantum Field Theory*. New York: McGraw-Hill; 1980
- [32] Banerjee MK, Cammarata JB. Theory of low-energy pion-nucleon interaction. *Physical Review C*. 1978;**17**: 11251
- [33] Machavariani AI, Rusetsky AG. On the field-theoretical formulation of the low-energy pion-nucleon scattering problem. *Nuclear Physics A*. 1990;**515**: 671
- [34] Yao D-L et al. Pion-nucleon scattering in covariant baryon chiral perturbation theory with explicit Delta resonances. *Journal of High Energy Physics*. 2016;**38**:05. ArXiv: 1603.03638
- [35] Pilkuhn HM. *Relativistic Quantum Mechanics*. Berlin Heidelberg: Springer-Verlag; 2003
- [36] Abdulameer NJ et al. Improving constraints on gluon spin-momentum

correlations in transversely polarized protons via midrapidity open-heavy-flavor electrons in $p \uparrow + p$ collisions at $\sqrt{s} = 200 \text{ GeV}$; (PHENIX collaboration). Physical Review D. 2023;**107**:052012

[37] S. Adhikari et al. Measurement of spin-density matrix elements in $\rho(770)$ production with a linearly polarized photon beam at $E_\gamma = 8.2 \cdot 8.8 \text{ GeV}$. ArXiv: 2305.09047v1 [nucl-exp] 2023. GLUOX collaboration.

[38] Goldberger MI, Watson M. Collision Theory. New York-London-Sydney: Wiley; 1965

[39] Taylor JG. Graphical methods for Bethe-Salpeter equations. Supplimento of Nuovo Cimento. 1963;**1**:13

[40] Nakanishi N. A general survey of the theory of the Bethe-Salpeter equation. Progress of Theoretical Physics Supplement. 1969;**43**:1

[41] Logunov AA, Tavkhelidze AN. Quasi-optical potential in quantum field theory. Nuovo Cimento. 1963;**29**:380

[42] Blankenbecler R, Sugar R. Linear integral equations for relativistic multichannel scattering. Physics Review. 1966;**142**:1051

[43] Gross F. Three dimensional covariant integral equations for low energy systems. Physics Review. 1969; **186**:1448

[44] Yamasaki T et al. Relation between scattering amplitude and Bethe-Salpeter wave functions in quantum field theory. UTHEP-704 UTTCS-P104. ArXiv: 1709.09779v2 [hep-lat] 2017

[45] Kadyshevsky VG. Quasipotential type equation for the relativistic scattering amplitude. Nuclear Physics B. 1968;**6**:125

[46] Kadyshevsky VG. Three dimensional formulation of the relativistic two-body problem. Fizika Elementarnikh Chastits at Yadra. 1972;**2**: 635. Soviet Journal of Nuclear Physics 1972;**2**:69

[47] Carbonell J et al. Explicitly covariant light-front dynamics and relativistic few-body systems. Physics Reports. 1998;**300**:215

[48] Machavariani AI, Dj Chelidze A. On the field-theoretical approach to nucleon-nucleon scattering problem in the low energy region. Journal of Physics G. 1993;**24**:317

Perspective Chapter: Squeezing and Entanglement of Two-Modes Quantum X Waves

*Ali Saif M. Hassan, Waleed S.A. Hasan and
Mohamed A. Shukri*

Abstract

Quantum theory of generalized X waves with orbital angular momentum in dispersive media, and the interaction of quantized X waves in quadratic nonlinear media were studied in (J. opt,20,065201 (2018)). We present a kind of phase matching, which is called velocity phase matching, and this phase matching can be used for determining the length of the nonlinear crystal or the interaction time in the experiment setup, to produce X waves with particular velocity v . Moreover, we introduce more analysis for the dependence of squeezing of X waves on its spectral order, and for spectral orders $j > 0$, we predict the existence of a characteristic axicon aperture for maximal squeezing. Then, we find the quantum squeezed state of the down-converted state generated by the χ^2 -nonlinear process. Finally, we detect their entanglement using a criterion of separability.

Keywords: entanglement, X waves, squeezed state, nonlinear quantum optics, phase matching, scalar field

1. Introduction

Based on the work of Tesla, German physicist Konstantin Meyl created a new unified field and particle theory. In Meyl's theory [1], vortices are used to explain quantum and classical physics, mass, gravitation, the constant speed of light, neutrinos, waves, and particles. With the help of this model, the properties of subatomic particles may be precisely estimated. The unified equation can also be used to derive well-known equations. He offers resources for carrying out an experiment by Tesla that proves the existence of scalar waves. Simple energy vortices in the form of particles are what scalar waves are. The electromagnetic, eddy current, potential vortex, and special distributions are all covered by the unified field theory. According to Meyl, the field—which creates particles through decay or conversion—always comes first. Energy particles (i.e., potential vortices) were not included in the theory because they are not recognized by classical physics. Quantum physics attempted to explain everything in terms of vortices which is why it is incomplete. Gravitation is

from the speed of light difference caused by proximity that, proportional to field strength, decreases the distance of everything for the field strength [2]. The spatially localized vortex structures include pseudo-nondiffracting (P-N) vortex beams and their superpositions and provide additional effects interesting for theoretical research, experiments, and applications [3]. As we see, this kind of vortex in its quantum form can connect to Meyl's vortex to explain unified field and particle theory of Meyl. Also, it can connect to the localizability of Busch [4] and others for elementary particle physics to solve the theory of measurement in relativistic quantum mechanics problems as stated in Ref. [5]. Vortex solutions produced in some particle physics models like extended Abelian Higgs model [6], Galaxies and their dark-matter halos [7].

The primary characteristic that unifies numerous advancements in quantum physics is entanglement [8]. Entanglement is required, as a prime example, to distinguish between classical and quantum physics using Bell inequalities [9, 10]. Another way to think of entanglement is as the tool that permits real quantum protocols like teleportation [11] and Bell inequalities-based cryptography [12]. When a quantum method, like Shor's algorithm, yields a meaningful performance advantage over a classical computer, large entanglement is anticipated to be present in quantum registers [13]. It is obvious that entanglement is essential to comprehending and using quantum physics. Therefore, it makes sense to examine the creation of entanglement at its most fundamental source, which are the particle physics theories of fundamental interactions. A Bell inequality would never be violated in nature if the quantum theory of electromagnetic, or QED, never produced electron entanglement. This suggests that at a fundamental level, quantum unitary development must produce entanglement. The gauge principle, which states that the physical laws are invariant despite internal local rotations for particular symmetry groups, has become widely accepted as a way to explain the fundamental interactions seen in nature. With regard to electroweak and strong interactions, the Standard Model uses a Lagrangian that is essentially constrained by gauge symmetry requirements, except from quantum gravity. It is only logical to continue looking for a principle that is even more basic. Previous research has looked at entanglement's function in particle physics. Orthopositronium has been demonstrated in Ref. [14] to decay into 3-photon states that can be used in Bell-like experiments that reject classical physics more quickly than the conventional 2-particle Bell inequality. Bell inequalities have also been considered in regard to neutrino oscillations [15], kaon physics [16, 17], and their relationship with the characterization of T-symmetry violation [18]. The S-matrix formalism has been used to examine how entanglement varies in an elastic scattering process in Ref. [19]. A recent study on entanglement in deep elastic scattering is also worth mentioning [20]. Bell inequalities have also been discussed in regard to quantum correlations in CMB radiation [21].

Squeezed states, and two-mode-squeezed states, are foundational for describing the basis nature of quantum mechanical phenomena. Their quantum entanglement plays a central role in quantum physics, experiments of quantum optics, and quantum information science [22–27]. Nonlinear quantum optics, in particular, parametric down-conversion (PDC), gives us ways to study issues in the foundations of quantum mechanics that are not readily available using other technologies [27, 28]. The quantum communication encode information into the polarization degrees of freedom of photons [12] or the orbital angular momentum (OAM) [29–35]. The important problem related to multi-modes quantum communications is the diffraction and dispersion of the electromagnetic waves [30]. Electromagnetic waves packet is usually subjected to diffraction and dispersion. Diffraction create a broadening in space during propagation of the wave and dispersion create a broadening in the time during the propagation. Ultimately, these effects are

connected with the bounded nature of the wave spectrum and, therefore, to its finite energy content [36]. A great effort has been done in studying the effect of atmosphere turbulence in free-space communication [31, 37–40]. Maxwell's equations admit diffraction-free and dispersion-free solutions, the so-called localized waves [3]. In particular, such solutions in the monochromatic domain are the Bessel beams [41], and in the pulsed domain, the most renowned localized waves are the X waves, first introduced in acoustics in 1992 by Lu and Greenleaf [42]. Despite the great work in the literature concerning X waves, the investigations of their quantum properties are very few [43, 44]. Generalization of the traditional X waves to the case of OAM-carrying X wave and the coupling between angular momentum and the temporal degrees of freedom of ultrashort pulses have been investigated [45]. Very recently, quantum and squeezing of X waves with OAM in nonlinear dispersive media have been proposed [46, 47], and they can open a new direction for free-space quantum communication and different areas of physics. In this work, we state the propagation of a scalar electromagnetic field in a linear dispersive medium. We present a kind of phase matching called velocity phase matching and introduce a relation between the interaction time and the velocity of X wave as well as a relation between the length of the $\chi^{(2)}$ -nonlinear crystal and the velocity of X wave generated by the spontaneous parametric down-conversion (SPDC) process in Section 2. We study the SPDC process in a quadratic medium, in particular the dependence of squeezing of the down-converted state generated by the $\chi^{(2)}$ -nonlinear crystal on the spectral order of quantum X waves in Section 3. We introduce the quantum squeezed form of the state generated by the SPDC process and its entanglement in Section 4. Finally, the results are summarized in Section 5.

2. Propagation of a generalized X wave in dispersive media and its quantization

We consider the propagation of a scalar electromagnetic field in a linear dispersive medium with refractive index $n = n(\omega)$. Applying the paraxial and slowly varying envelope approximation to the envelope function $A(\mathbf{r}, t)$ of an electric field

$$E(\mathbf{r}, t) = \sqrt{\frac{2}{\epsilon_0 n^2}} A(\mathbf{r}, t) e^{i(kz - \omega t)}, \quad (1)$$

where $A(\mathbf{r}, t)$ varies slowly with z and $k = n(\omega)\omega/c$, which are the propagation coordinate and the wave number, respectively.

The field envelope $A(\mathbf{r}, t)$ satisfies the following eq. [48],

$$i \frac{\partial A}{\partial t} + i\omega' \frac{\partial A}{\partial z} - \frac{\omega''}{2} \frac{\partial^2 A}{\partial z^2} + \frac{\omega'}{2k} \Delta_{\perp}^2 A = 0, \quad (2)$$

where $\omega' = c^2 dk/d\omega$ and $\omega'' = c^2 d^2 k/d\omega^2$ are the first and the second order dispersion, respectively.

The solution of Eq. (2) can be written as a superposition of the generalized X waves as follows [47]:

$$A(\mathbf{r}, t) = \sum_{m,p} \int dv C_{mp}(v) e^{-i\frac{v^2}{2\omega'} t} \psi_{m,p}^{(v)}(R, \zeta), \quad (3)$$

where $\psi_{m,p}^{(v)}(R, \zeta)$ is the generalized X wave of OAM number m , spectral order p and velocity v defined as,

$$\psi_{m,p}^{(v)}(R, \zeta) = \int_0^\infty d\alpha f_p(\alpha) J_m\left(\sqrt{\omega' k / \omega' \alpha R}\right) e^{i(\alpha - v/\omega')\zeta} e^{im\theta}, \quad (4)$$

with $R = \sqrt{x^2 + y^2}$, $\zeta = z - (\omega' + v)t$ which is the co-moving reference frame associated to the X waves, and $f_p(\alpha) = \sqrt{k/\pi^2\omega'(1+p)}(\Delta\alpha)L_p^{(1)}(2\alpha\Delta)e^{-\alpha\Delta}$ which is the spectrum function, where $L_p^{(1)}(x)$ is the generalized Laguerre polynomials of the first kind of order p [48], and Δ is the reference length related to the spatial extension of the spectrum [47]. The quantized field of Eq. (3) can be written as [47],

$$\hat{A}(\mathbf{r}, t) = \sum_{m,p} \int dv e^{\frac{i}{\hbar}(\frac{Mv^2}{2})t} \sqrt{\hbar\omega_{m,p}(v)} \psi_{m,p}^{(v)}(R, \zeta) \hat{a}_{m,p}(v) + h.c., \quad (5)$$

where $h.c.$ denotes to the Hermitian conjugate, $\omega_{m,p}(v) = v^2/(2\omega')$ and $M = \hbar/\omega'$ is the mass of X wave. The Hamiltonian operator can be written as follows [47]:

$$\hat{H} = \sum_{m,p} \int dv \hbar\omega_{m,p}(v) \left(\hat{a}_{m,p}^\dagger(v) \hat{a}_{m,p}(v) + \frac{1}{2} \right), \quad (6)$$

with the following usual bosonic commutation relations of creation and annihilation operators of the field,

$$\begin{aligned} [\hat{a}_{m,p}(v), \hat{a}_{n,q}^\dagger(u)] &= \delta_{m,n} \delta_{p,q} \delta(u - v), \\ [\hat{a}_{m,p}(v), \hat{a}_{n,q}(u)] &= 0 = [\hat{a}_{m,p}^\dagger(v), \hat{a}_{n,q}^\dagger(u)]. \end{aligned} \quad (7)$$

Now, we turn our attention to the quadratic nonlinear process involving X waves, particularly to the spontaneous parametric down-conversion (SPDC) [28]. The interaction Hamiltonian of this process, with a practical case $\rho = \sqrt{k_1\omega'_2/k_2\omega'_1} \simeq 1$, can be written in two different forms [47]:

The first form is for the time-dependent interaction Hamiltonian which can be written as follows [47]:

$$\mathcal{H}_I = \chi \langle A_1 | A_2^* \rangle + \chi^* \langle A_2 | A_1^* \rangle, \quad (8)$$

$$\chi \langle A_1 | A_2^* \rangle = \chi \int d^3r \hat{A}_1^\dagger(\mathbf{r}, t) \hat{A}_2^\dagger(\mathbf{r}, t) \quad (9)$$

$$\begin{aligned} \chi \langle A_1 | A_2^* \rangle &= \chi \sum_{m,p,n,q} \int du dv e^{\frac{i(u^2+v^2)t}{2\omega'}} \sqrt{\hbar^2\omega_{m,p}(u)\omega_{n,q}(v)} \\ &\times \int d^3r \psi_{m,p}^{(u)*}(R, \zeta_1) \psi_{n,q}^{(v)*}(R, \zeta_2) \hat{a}_{m,p}^\dagger(u) \hat{b}_{n,q}^\dagger(v), \end{aligned} \quad (10)$$

$$\hat{H}_I(t) = \hbar \sum_{m,p,q} \int du dv \chi_{m,p,q}(u+v) \sqrt{\omega_{m,p}(u)\omega_{-m,p}(v)} e^{iF(u,v)t} \hat{a}_{m,p}^\dagger(u) \hat{b}_{-m,q}^\dagger(v) + h.c., \quad (11)$$

with

$$F(u, v) = \frac{1}{2\omega'} [2uv + (v - u)(\omega'_1 - \omega'_2)], \quad (12)$$

and the interaction function is

$$\chi_{m,p,q}(u + v) = \frac{(-1)^m \chi \Delta^2}{\omega'^2 \sqrt{(1+p)(1+q)}} (u + v) L_p^{(1)} \left(\frac{(u + v)\Delta}{2\omega'} \right) L_q^{(1)} \left(\frac{(u + v)\Delta}{2\omega'} \right) e^{\frac{-(u+v)\Delta}{2\omega'}} \theta(u + v), \quad (13)$$

where $\theta(u + v)$, is the Heaviside step function [48]. The second form is for the finite length interaction Hamiltonian which can be given by Ref. [47]

$$\hat{H}_I(z) = \int dt [\chi \langle A_1 | A_2^* \rangle + \chi^* \langle A_2 | A_1^* \rangle]. \quad (14)$$

The final form of $\hat{H}_I(z)$ can be written as follows:

$$\hat{H}(z) = \hbar \sum_{m,p,q} \int du dv \Xi_{m,p,q}(u, v) \sqrt{\omega_{m,p}(u) \omega_{-m,q}(v)} e^{i\Lambda(u,v)z} \hat{a}_{m,p}^\dagger(u) \hat{b}_{-m,q}^\dagger(v) + h.c., \quad (15)$$

where $\Lambda(u, v) = 2uv/\omega'(u + v)$, and $\Xi_{m,p,q}(u, v)$, which is the modified vertex function can be given by Ref. [47],

$$\Xi(u, v) = \frac{(-1)^m 2 \chi \Delta^2}{\omega'^2 \sqrt{(1+p)(1+q)}} \frac{u^2 + v^2}{u + v} L_p^{(1)} \left(\frac{(u^2 + v^2)\Delta}{(u + v)\omega'} \right) L_q^{(1)} \left(\frac{(u^2 + v^2)\Delta}{(u + v)\omega'} \right) e^{\frac{-(u^2+v^2)\Delta}{(u+v)\omega'}}. \quad (16)$$

To calculate the state of the system after the interaction, we apply Schwing-Dyson expansion of the propagator $\exp[-i\hat{H}_I(t)/\hbar]$, and consider only the first term of the expansion [49]. For the time-dependent form of the interaction Hamiltonian stated in Eq. (11), the final state after the $\chi^{(2)}$ -nonlinear interaction can be expressed as follows [47]:

$$|\psi^{(1)}(t)\rangle = \frac{-i}{\hbar} \int_0^t d\tau \hat{H}_I(\tau) |0\rangle. \quad (17)$$

Substituting Eq. (11) into the above equation and after some calculations, the final state can be written in the following form:

$$|\psi^{(1)}(t)\rangle = \sum_{m,p,q} \int du dv \mathcal{G}_{m,p,q}(u, v) \mathcal{F}(u, v, t) |m, p, u; -m, q, v\rangle, \quad (18)$$

where $|m, p, u; -m, q, v\rangle \equiv \hat{a}_{m,p}^\dagger(u) \hat{b}_{-m,q}^\dagger(v) |0, 0\rangle$, the amplitude $\mathcal{G}_{m,p,q}(u, v)$ is defined as

$$\mathcal{G}_{m,p,q}(u, v) = -i \sqrt{\omega_{m,p}(u) \omega_{-m,q}(v)} \frac{\chi_{m,p,q}(u + v)}{F(u, v)}, \quad (19)$$

and $\mathcal{F}(u, v, t) = [e^{iF(u,v)t} - 1]$. The above state represents the superposition of two particles corresponding to the modes ω_1 and ω_2 (generated by the nonlinear interaction) traveling with velocities u and v , respectively. For the second form of the interaction Hamiltonian stated in Eq. (15), the final state of the system can be written as

$$|\psi^{(1)}(L)\rangle = \frac{-i}{\hbar} \int_0^L dz \hat{H}_I(z) |0\rangle. \quad (20)$$

Substituting Eq. (15) into the above equation, the state of the field at the output face of the crystal can be written as follows:

$$|\psi^{(1)}(L)\rangle = \sum_{m,p,q} \int du dv \mathcal{L}_{m,p,q}(u, v) \mathcal{F}(u, v, L) |m, p, u; -m, q, v\rangle, \quad (21)$$

where $\mathcal{F}(u, v, L) = [e^{i\Lambda(u,v)L} - 1]$, and

$$\mathcal{L}_{m,p,q}(u, v) = \frac{-i}{2} \sqrt{\omega_{m,p}(u) \omega_{-m,q}(v)} \left[\frac{\omega''(u+v)}{uv} \right] \Xi_{m,p,q}(u, v). \quad (22)$$

The transition probability for the field to be in such a state after the time-dependent interaction with the $\chi^{(2)}$ -nonlinear crystal is proportional with $|\mathcal{F}(u, v, t)|^2$ as follows:

$$P(t) \propto |\mathcal{F}(u, v, t)|^2, \quad (23)$$

similarly, the transition probability for the finite length interaction of the $\chi^{(2)}$ -nonlinear crystal is proportional with $|\mathcal{F}(u, v, L)|^2$ as follows [47]:

$$P(L) \propto |\mathcal{F}(u, v, L)|^2. \quad (24)$$

Explicitly, $|\mathcal{F}(u, v, t)|^2$ can be expressed as follows:

$$|\mathcal{F}(u, v, t)|^2 = 2[1 - \cos(F(u, v)t)]. \quad (25)$$

From the above equation, we notice that the transition probability reaches its maximum, when $|\mathcal{F}(u, v, t)|^2$ reaches its maximum, and that occurs when the condition $F(u, v)t = (2m + 1)\pi$, with $m = 0, 1, 2, 3, \dots$, is achieved. The above condition is considered as a new phase matching condition, called velocity matching condition over the velocities of the two-modes X waves generated from SPDC process. This condition requires that

$$u = \frac{2k'_m + v \Delta\omega'}{2v + \Delta\omega'}, \quad (26)$$

where $\Delta\omega' = \omega'_1 - \omega'_2$, and $k'_m = (2m + 1)\pi\omega'/t$. For the case, when $\Delta\omega' = 0$, we get $uv = k'_m = (2m + 1)\pi\omega'/t$, and the interaction time can be given by $t = (2m + 1)\pi\omega'/uv$. When $u = v$, regardless of that $\Delta\omega' = 0$, we get $v^2 = k'_m = (2m + 1)\pi\omega'/t$.

Thus, the interaction time can be written in terms of the velocity of X waves modes as follows:

$$t = \frac{(2m+1)\pi\omega''}{v^2}. \quad (27)$$

For the finite length of the nonlinear crystal, the velocity matching condition is given by Ref. [47],

$$u = \frac{k_n v}{v - k_n}, \quad (28)$$

where $k_n = (n + \frac{1}{2})\pi\omega''/L$, with $n = 0, 1, 2, \dots$. Therefore, the velocity matching condition fixes either the length of the crystal L or the relative velocity of the two modes X wave involved in the SPDC process as, $uv/(u+v) = k_n = (n + 1/2)\pi\omega''/L$, and the length of the crystal L can be given by,

$$L = \frac{(n + \frac{1}{2})\pi\omega'' (u+v)}{uv}. \quad (29)$$

For $u = v$, the above equation becomes

$$L = \frac{(2n+1)\pi\omega''}{v}. \quad (30)$$

From Eqs. (27) and (30), we note that the ordinary relation between the length and the time is achieved ($L = vt$). This result can be used for determining the length of the nonlinear crystal in the experimental setup, to produce X waves with velocity v . This is the first result of our work.

3. Squeezing of quantum X waves

Now, we can study the general case of the squeezing effect in the SPDC process, in particular, the dependence of squeezing of the down-converted state, generated by $\chi^{(2)}$ -nonlinear media, on the spectral orders of quantum X waves, for the case, when the velocities of the two-modes X waves are equal $u = v$, and their spectral orders are equal as well $p = q = j$. The interaction time Hamiltonian in Eq. (11) becomes

$$\hat{H}_I(t) = \hbar \sum_{mj} \int dv \chi_{mj}(2v) \omega(v) \hat{a}_{mj}^\dagger(v, t) \hat{b}_{-mj}^\dagger(v, t) + h.c., \quad (31)$$

where $\hat{a}_{mj}^\dagger(v, t) = e^{iF(v)t/2} \hat{a}_{mj}^\dagger(v)$, and $\hat{b}_{-mj}^\dagger(v, t) = e^{iF(v)t/2} \hat{b}_{-mj}^\dagger(v)$. Also, the interaction function in Eq. (13) becomes

$$\chi_{mj}(2v) = \frac{2(-1)^m \chi \Delta^2 v}{\omega'^2(1+j)} L_j^{(1)}\left(\frac{v\Delta}{\omega'}\right) L_j^{(1)}\left(\frac{v\Delta}{\omega'}\right) e^{\frac{-v\Delta}{\omega'}}. \quad (32)$$

And the modified vertex function in Eq. (16) can be rewritten as follows:

$$\Xi_{mj}(v) = \frac{2(-1)^m \chi \Delta^2 v}{\omega'^2(1+j)} L_j^{(1)}\left(\frac{v\Delta}{\omega'}\right) L_j^{(1)}\left(\frac{v\Delta}{\omega'}\right) e^{\frac{-v\Delta}{\omega'}}. \quad (33)$$

From Eqs. (32) and (33) we notice that the interaction function and the modified vertex function have the same form. In the interaction picture, we consider the time evolution controlled by $\hat{H}_I(t)$. Thus, the equations of motion for $\hat{a}_{mj}(v, t)$ and $\hat{b}_{-mj}(v, t)$ are:

$$\frac{d\hat{a}_{mj}(v, t)}{dt} = \frac{1}{i\hbar} [\hat{a}_{mj}(v, t), \hat{H}_I(t)], \quad (34)$$

$$\frac{d\hat{b}_{-mj}(v, t)}{dt} = \frac{1}{i\hbar} [\hat{b}_{-mj}(v, t), \hat{H}_I(t)]. \quad (35)$$

Substituting Eq. (31) into the above equations, we obtain

$$\frac{d\hat{a}_{mj}(v, t)}{dt} = -2i \omega(v) \chi_{mj}(2v) \hat{b}_{-mj}^\dagger(v, t), \quad (36)$$

$$\frac{d\hat{b}_{-mj}(v, t)}{dt} = -2i \omega(v) \chi_{mj}(2v) \hat{a}_{mj}^\dagger(v, t). \quad (37)$$

The general solutions of these equations are [50],

$$\hat{a}_{mj}(v, t) = \cosh(\beta_{mj}(v) t) \hat{a}_{mj}(v) + \sinh(\beta_{mj}(v) t) \frac{\alpha_{mj}}{\beta_{mj}(v)} \hat{b}_{-mj}^\dagger(v), \quad (38)$$

$$\hat{b}_{-mj}(v, t) = \cosh(\beta_{mj}(v) t) \hat{b}_{-mj}(v) + \sinh(\beta_{mj}(v) t) \frac{\alpha_{mj}}{\beta_{mj}(v)} \hat{a}_{mj}^\dagger(v). \quad (39)$$

Here, we consider the expression $\alpha_{mj} = -2i \omega(v) \chi_{mj}(2v)$, with $\omega(v) = v^2/2\omega'$. To find the squeezing parameter $\xi_{mj}(v) = \beta_{mj}(v)t$, we use the relation $\beta_{mj}(v) = \sqrt{\alpha_{mj}\alpha_{mj}^*}$, then we can write the squeezing parameter as follows:

$$\xi_{mj}(v) = \frac{2(-1)^m \chi t}{(1+j)\Delta} \frac{\tilde{v}^3}{\omega'^3} \left(L_j^{(1)}\left(\frac{\tilde{v}}{\omega'}\right) \right)^2 e^{-\frac{\tilde{v}}{\omega'}}, \quad (40)$$

with $\tilde{v} = v\Delta$. The above equation represents the squeezing parameter which depends on the OAM number m , the spectral order j , and the velocity of the two-modes X waves v . Now, we can show the normalized squeezing parameter modulus $|\xi_{mj}| = \frac{\Delta|\xi_{mj}|}{4\chi t}$ as a function of the normalized velocity $\frac{\tilde{v}}{\omega'}$ for different values of j , ($j = 0, 1, 2, 3, 4, 5$), and fixing the time t so that $\frac{4\chi t}{\Delta} = 1$, when $m = 0$, as shown in **Figure 1**.

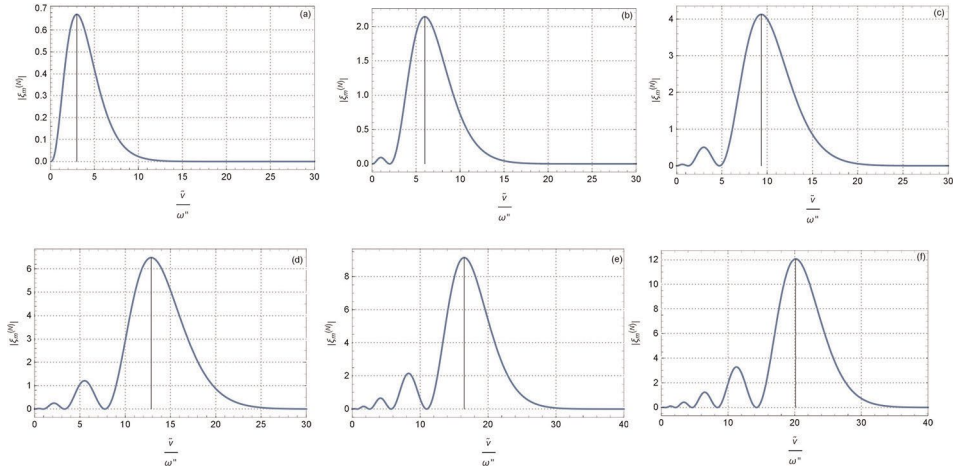


Figure 1.

Plot of the normalized squeezing parameter modulus $|\xi_{mj}| = \frac{\Delta|\xi_{mj}|}{\chi}$ in function of the normalized velocity $\frac{\tilde{v}}{\omega''}$, for different values of the spectral order j where, (a) for $j = 0$, (b) for $j = 1$, (c) for $j = 2$, (d) for $j = 3$, (e) for $j = 4$, (f) for $j = 5$, with fixing the time t , so that $\frac{4\chi t}{\Delta} = 1$, and $m = 0$.

Figure 1 shows the dependence of the squeezing on the spectral order j of X waves. This dependence can be explained in the following points:

1. The maximum value of the squeezing parameter $|\xi_{mj}|$ and the corresponding normalized velocity $\frac{\tilde{v}}{\omega''}$ increases as the spectral order j increases.
2. The number of the peak values of squeezing depends on the spectral order j and this number can be given by $j + 1$, where the smallest peak is the first and the biggest one is the last.
3. The squeezing parameter depends on the velocity of X wave as shown in Eq. (40) where the amount of squeezing parameter produced by SPDC process will be maximized at an optimal velocity for every value of the spectral order j , and this velocity can be given by $v_{opt} = n_j \omega'' / \Delta$, where $n_0 = 3, n_1 = 6, n_2 = 9.36, n_3 = 12.88, n_4 = 16.49, n_5 = 20.156$ for $j = 0, 1, 2, 3, 4, 5$, respectively as shown in **Figure 1**. **Figure 1(a)** shows that for $j = 0$ as in Ref. [46], and the corresponding optimal axicon angles for different values of j can be given by $\cos \theta_j^{opt} = \Delta / n_j \lambda$. For example, given a nondiffracting pulse with a duration of $\Delta t = 8$ fs, a carrier wavelength of $\lambda = 850$ nm and assuming that $\chi^2 \simeq 10^{-12}$ m/V, the optimal axicon angles θ_j^{opt} that maximize the squeezing for $j = 0, 1, 2, 3, 4, 5$ will take the following values respectively, $\theta_0^{opt} \simeq 20^\circ, \theta_1^{opt} \simeq 62^\circ, \theta_2^{opt} \simeq 72^\circ, \theta_3^{opt} \simeq 77^\circ, \theta_4^{opt} \simeq 80^\circ, \theta_5^{opt} \simeq 82^\circ$. Then, we can evaluate the corresponded maximal squeezing parameters to get the following values respectively, $(\xi_m^{(0)} \simeq 100s^{-1}, \xi_m^{(1)} \simeq 280s^{-1}, \xi_m^{(2)} \simeq 520s^{-1}, \xi_m^{(3)} \simeq 820s^{-1}, \xi_m^{(4)} \simeq 1160s^{-1}, \xi_m^{(5)} \simeq 1550s^{-1})$.

To illustrate the effect of the OAM on the squeezing more, we can introduce the quadrature operators $\hat{X}_{mj}(v, t) = \hat{a}_{mj}(v, t) + \hat{a}_{mj}^\dagger(v, t)$, and $\hat{Y}_{mj}(v, t) =$

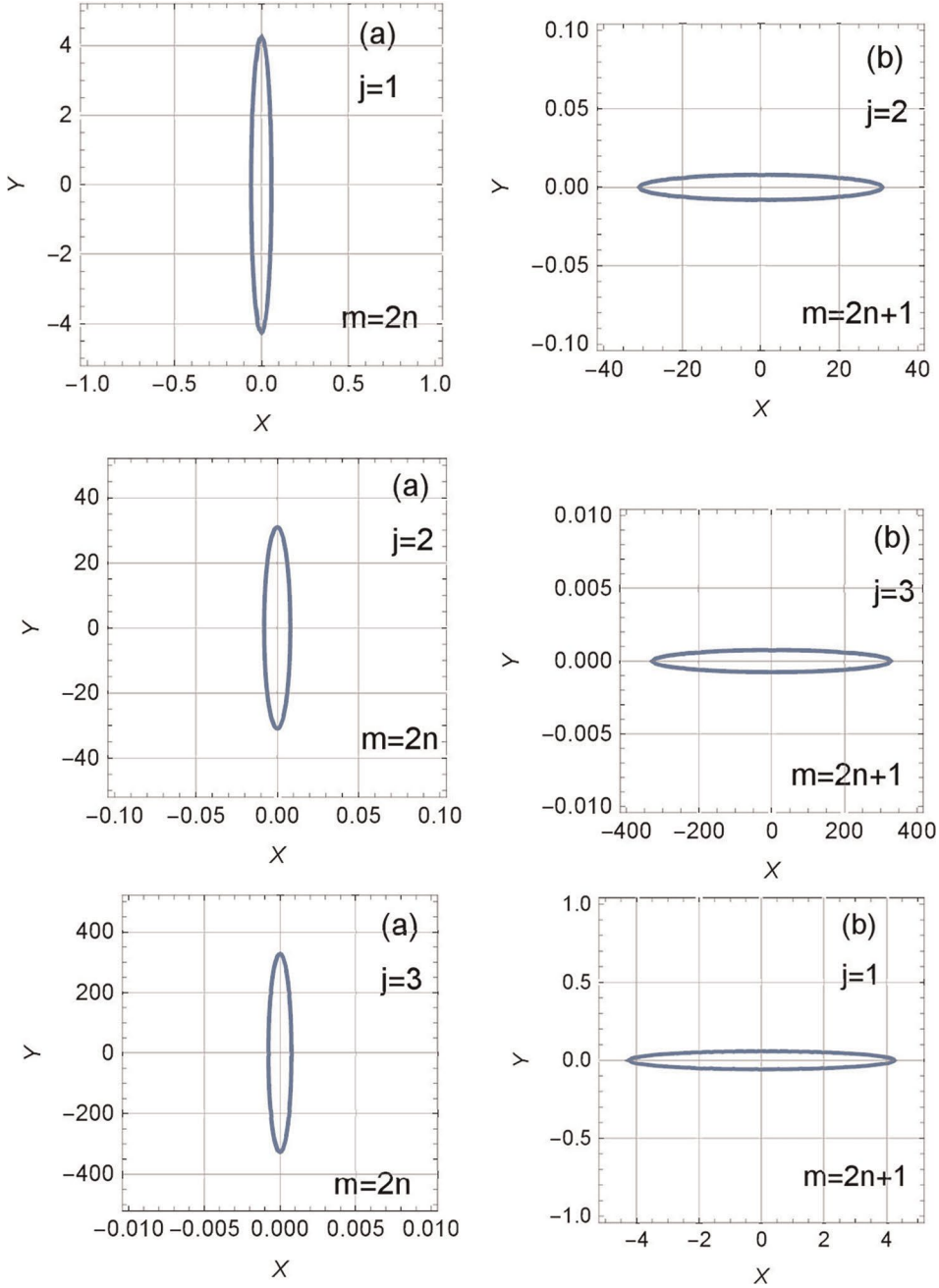


Figure 2. Quadrature space representation of the squeezed down-converted state in the case of even [panel (a)] and odd [panel (b)] values of the OAM number m with a normalized velocity $\frac{v}{\omega} = 6, 9, 36, 12.88$ for a spectral order $j = 1, 2, 3$, respectively.

$i \left[\hat{a}_{mj}^\dagger(v, t) - \hat{a}_{mj}(v, t) \right]$. For $e^{i\phi} = \alpha_{mj}/\beta_{mj} = 1$ or $\phi = 0$, we get $\hat{X}_{mj}(v, t) = e^{\xi_{mj}(v)} \hat{X}_{mj}(v, 0)$, and $\hat{Y}_{mj}(v, t) = e^{-\xi_{mj}(v)} \hat{Y}_{mj}(v, 0)$, and the variance of them is given by $\Delta \hat{X}_{mj}(v, t) = e^{\xi_{mj}(v)} \hat{Y}_{mj}(v, 0)$. This shows that the SPDC interaction Hamiltonian for the

generalized X waves acts as a two-modes squeeze operator which will be illustrated more in the next section. Noticeably, the effect of the OAM number m changes only the sign of the squeezing parameter $\xi_{mj}(v)$, that is, the squeezed quadrature changes depending on the parity of the orbital angular momentum number m . In particular, if m is even number, $\xi_{mj}(v) > 0$, the squeezing accrues on the Y quadrature. On the other hand, if m is an odd number, $\xi_{mj}(v) < 0$ and the squeezing occurs on X quadrature as in Ref. [46] for $j = 0$, and for $j = 1, 2, 3$. this effect can be shown as in **Figure 2**.

4. The two-modes squeezed state of X wave and its entanglement

In analogy to traditional case [51, 52], we look for the eigenvalues of Hamiltonian operator, represented by Eq. (6). Let us introduce the N -particle states $|m, j, v; N\rangle$ as states with N field excitation with velocity v in the traveling mode (i.e., the X wave) $\psi_{m,p}^{(v)}(\mathbf{r}, t)$ with energy $Mv^2/2$ [47]. The eigenstates $|m, p, v, N\rangle$ of the photon (particle) number operator $\hat{N}(v) = \hat{a}_{mp}^\dagger(v) \hat{a}_{mp}(v)$ are called Fock states, where $\hat{a}_{mp}(v)$ is the annihilation operator of the single mode in Eq. (7). These states are orthogonal

$$\langle n, q, u, N | m, p, v, N \rangle \equiv \delta_{nm} \delta_{pq} \delta(u - v), \quad (41)$$

and complete. The number state $|m, p, v, N\rangle$ can be generated from the vacuum state (i.e., the eigenstate of $\hat{N}(v)$ with the eigenvalue equal to zero) as

$$|m, p, v, N\rangle = \frac{[\hat{a}_{mp}^\dagger(v)]^N}{\sqrt{N!}} |0\rangle. \quad (42)$$

The expectation value of the electric field operator is zero on the particle number operator eigenstates [47],

$$\langle m, p, v, N | \hat{A}(r, t) | m, p, v, N \rangle = 0. \quad (43)$$

However, the Fock states $|m, p, v, N\rangle$ are not normalizable [47], since their representation in configuration state $\langle \mathbf{r}, t | m, p, v, N \rangle = \psi_{mp}^{(v)}(r, t)$ carries infinite energy. The particle number states of the two modes (A, B) with particle numbers (N_A, N_B) are defined as

$$|m, j, v; N_A\rangle_A = \frac{[\hat{a}_{mj}^\dagger(v)]^{N_A} |0\rangle_A}{\sqrt{N_A!}}, \quad (44)$$

and

$$|-m, j, v, N_B\rangle_B = \frac{[\hat{b}_{-mj}^\dagger(v)]^{N_B} |0\rangle_B}{\sqrt{N_B!}} \quad (45)$$

Together with the conditions for the vacuums, $\hat{a}_{mj}(v)|0\rangle_A = 0$ and $\hat{b}_{-mj}(v)|0\rangle_B = 0$.

The operators $\hat{a}_{mj}(v)$ and $\hat{b}_{-mj}(v)$ obey the bosonic commutation relations in Eq. (7). Now, we can define the two-mode squeeze operator, which is a unitary operator, using the normalized squeezing parameter $\bar{\xi}_{mj}(v) = \frac{(-1)^m}{2(1+j)} \frac{\bar{v}^3}{\omega'^3} \left(L_j^{(1)} \left(\frac{\bar{v}}{\omega'} \right) \right)^2 e^{-\frac{\bar{v}}{\omega'}}$, as

$$V_{\bar{\xi}_{mj}} = \exp \left(e^{-i\phi} \bar{\xi}_{mj} \hat{a}_{mj}(v) \hat{b}_{-mj}(v) - e^{i\phi} \bar{\xi}_{mj} \hat{a}_{mj}^\dagger(v) \hat{b}_{-mj}^\dagger(v) \right). \quad (46)$$

The two-mode squeezed vacuum TMSV state can be obtained from the vacuum state as [52],

$$|0, 0, \bar{\xi}_{mj}\rangle_{AB} = V_{\bar{\xi}_{mj}} |0, 0\rangle = \left[\cosh(\bar{\xi}_{mj}) \right]^{-1} \sum_{N=0}^{\infty} \left(e^{i\phi} \tanh(\bar{\xi}_{mj}) \right)^N |m, j, v, N; -m, j, v, N\rangle. \quad (47)$$

Also, we can define the annihilation operators crossing over the separation of part A and part B as [53],

$$\begin{aligned} \hat{A}_{\bar{\xi}_{mj}} &= V_{\bar{\xi}_{mj}} \hat{a}_{mj}(v) V_{\bar{\xi}_{mj}}^\dagger = \cosh(\bar{\xi}_{mj}) \left[\hat{a}_{mj}(v) + e^{i\phi} \tanh(\bar{\xi}_{mj}) \hat{b}_{-mj}^\dagger(v) \right] \\ \hat{B}_{\bar{\xi}_{mj}} &= V_{\bar{\xi}_{mj}} \hat{b}_{-mj}(v) V_{\bar{\xi}_{mj}}^\dagger = \cosh(\bar{\xi}_{mj}) \left[\hat{b}_{-mj}(v) + e^{i\phi} \tanh(\bar{\xi}_{mj}) \hat{a}_{mj}^\dagger(v) \right]. \end{aligned} \quad (48)$$

The new field operators satisfy the bosonic commutation relations in Eq. (7)

$$\left[\hat{A}_{\bar{\xi}_{mj}}, \hat{A}_{\bar{\xi}_{m'j'}}^\dagger \right] = \left[\hat{B}_{\bar{\xi}_{mj}}, \hat{B}_{\bar{\xi}_{m'j'}}^\dagger \right] = \delta_{m,m'} \delta_{j,j'} \delta(v - v'), \quad (49)$$

and

$$\left[\hat{A}_{\bar{\xi}_{mj}}, \hat{B}_{\bar{\xi}_{m'j'}} \right] = \left[\hat{A}_{\bar{\xi}_{mj}}, \hat{B}_{\bar{\xi}_{m'j'}}^\dagger \right] = 0. \quad (50)$$

The TMSV state corresponds to the vacuum of the new field operators, as we have used $\hat{a}_{mj}(v)|0\rangle = 0$, $\hat{b}_{-mj}(v)|0\rangle = 0$, Eq. (47), Eq. (48), and the unitary property of the squeeze operator, we get $\hat{A}_{\bar{\xi}_{mj}}|0, 0, \bar{\xi}_{mj}\rangle = 0$, and $\hat{B}_{\bar{\xi}_{mj}}|0, 0, \bar{\xi}_{mj}\rangle = 0$.

The two-mode number state is defined by the number state of nonlocal modes as [53],

$$|N_A, N_B, \bar{\xi}_{mj}\rangle = \frac{\left[\hat{A}_{\bar{\xi}_{mj}}^\dagger \right]^{N_A} \left[\hat{B}_{\bar{\xi}_{mj}}^\dagger \right]^{N_B}}{\sqrt{N_A!} \sqrt{N_B!}} |0, 0, \bar{\xi}_{mj}\rangle. \quad (51)$$

In our case, we have $N_A = N_B = 1$, so we obtain

$$|1, 1, \bar{\xi}_{mj}\rangle = \hat{A}_{\bar{\xi}_{mj}}^\dagger \hat{B}_{\bar{\xi}_{mj}}^\dagger |0, 0, \bar{\xi}_{mj}\rangle. \quad (52)$$

The state in the above equation represents a two-particles squeezed state of the two modes X wave. The superposition of the two particles corresponding to the two modes ω_1 and ω_2 see Eq. (18) (when $u = v$) can be written as

$$|\psi^{(1)}(t)\rangle = \sum_{mj} \int dv \mathcal{G}_{mj}(v) \mathcal{F}(v, t) \hat{a}_{mj}^\dagger(v) \hat{b}_{-mj}^\dagger(v) |0, 0\rangle, \quad (53)$$

where $\mathcal{F}(v, t) = [e^{iF(v)t} - 1]$, and $\mathcal{G}_{mj}(v) = -i \omega(v) \chi_{mj}(2v)/F(v)$, with $\chi_{mj}(2v)$ as in Eq. (32). The superposition of the two particles squeezed state corresponds to the state in Eq. (53) is

$$|\psi_{\xi_{mj}}^{(1)}(t)\rangle = V_{\xi_{mj}} |\psi^{(1)}(t)\rangle = \sum_{mj} \int dv \mathcal{G}_{mj}(v) \mathcal{F}(v, t) V_{\xi_{mj}} \hat{a}_{mj}^{\dagger}(v) \hat{b}_{-mj}^{\dagger}(v) |0, 0\rangle. \quad (54)$$

Using Eq. (48), the above state can be written in the form

$$|\psi_{\xi_{mj}}^{(1)}(t)\rangle = \sum_{mj} \int dv \mathcal{G}_{mj}(v) \mathcal{F}(v, t) \hat{A}_{\xi_{mj}}^{\dagger} \hat{B}_{\xi_{mj}}^{\dagger} |0, 0, \bar{\xi}_{mj}\rangle, \quad (55)$$

which is a superposition of the squeezed states $|1, 1, \bar{\xi}_{mj}\rangle$ in Eq. (52).

Now, for calculating the entanglement of the state in Eq. (55), we consider the separable conditions based on the operators that form $SU(2)$ algebra and $SU(1, 1)$ algebra [53]. The measurements of quadrature moments of the fourth order are sufficient to verify the entanglement of this state. Let us define the operators,

$$\begin{aligned} J_z &= \frac{1}{2}(N_A - N_B), \\ K_x &= \frac{1}{2}(\hat{a}_{mj}^{\dagger}(v) \hat{b}_{-mj}^{\dagger}(v) + \hat{a}_{mj}(v) \hat{b}_{-mj}(v)), \\ K_y &= \frac{1}{2i}(\hat{a}_{mj}^{\dagger}(v) \hat{b}_{-mj}^{\dagger}(v) - \hat{a}_{mj}(v) \hat{b}_{-mj}(v)) \end{aligned} \quad (56)$$

where $\hat{N}_A = \hat{a}_{mj}^{\dagger}(v) \hat{a}_{mj}(v)$ and $\hat{N}_B = \hat{b}_{-mj}^{\dagger}(v) \hat{b}_{-mj}(v)$ are number operators of the local modes.

The relations of the annihilation and creation operators $\hat{a}_{mj}(v)$, $\hat{a}_{mj}^{\dagger}(v)$, $\hat{b}_{-mj}(v)$, and $\hat{b}_{-mj}^{\dagger}(v)$ with the new field operators in Eq. (48) can be represented by

$$\begin{aligned} \hat{a}_{mj}(v) &= \cosh(\bar{\xi}_{mj}) \left(\hat{A}_{\xi_{mj}} - e^{i\phi} \tanh(\bar{\xi}_{mj}) \hat{B}_{\xi_{mj}}^{\dagger} \right) \\ \hat{a}_{mj}^{\dagger}(v) &= \cosh(\bar{\xi}_{mj}) \left(\hat{A}_{\xi_{mj}}^{\dagger} - e^{-i\phi} \tanh(\bar{\xi}_{mj}) \hat{B}_{\xi_{mj}} \right) \\ \hat{b}_{-mj}(v) &= \cosh(\bar{\xi}_{mj}) \left(\hat{B}_{\xi_{mj}} - e^{i\phi} \tanh(\bar{\xi}_{mj}) \hat{A}_{\xi_{mj}}^{\dagger} \right) \\ \hat{b}_{-mj}^{\dagger}(v) &= \cosh(\bar{\xi}_{mj}) \left(\hat{B}_{\xi_{mj}}^{\dagger} - e^{-i\phi} \tanh(\bar{\xi}_{mj}) \hat{A}_{\xi_{mj}} \right) \end{aligned} \quad (57)$$

The separable condition is [53],

$$\left[\langle \Delta^2 K_y \rangle - \frac{1}{4} \right] \langle \Delta^2 J_z \rangle \geq \frac{1}{4} |\langle K_x \rangle|^2 \quad (58)$$

where $\langle \hat{O} \rangle = \text{tr}(\hat{O}\rho)$ denotes the expectation value of the observable \hat{O} with respect to state ρ , $\Delta \hat{O} = \hat{O} - \langle \hat{O} \rangle$, and $\langle \Delta^2 \hat{O} \rangle = \langle \hat{O}^2 \rangle - \langle \hat{O} \rangle^2$. The state we use in Eq. (58) is the superposition of simultaneous eigenstates of the number operators $\hat{A}_{\xi_{mj}}^{\dagger} \hat{A}_{\xi_{mj}}$ and $\hat{B}_{\xi_{mj}}^{\dagger} \hat{B}_{\xi_{mj}}$. From the definition of J_z in Eq. (56), we have

$$\hat{A}_{\xi_{mj}}^{\dagger} \hat{A}_{\bar{\xi}_{mj}} - \hat{B}_{\xi_{mj}}^{\dagger} \hat{B}_{\bar{\xi}_{mj}} = N_A - N_B = 2J_z \quad (59)$$

This implies that the two-mode squeezed (TMS) number states are eigenstates of J_z and $\langle \Delta^2 J_z \rangle = 0$.

Also, we can write

$$K_x = \frac{1}{2} \cosh^2(\bar{\xi}_{mj}) \left[\left(\hat{A}_{\xi_{mj}}^{\dagger} - \eta^* \hat{B}_{\xi_{mj}} \right) \left(\hat{B}_{\xi_{mj}}^{\dagger} - \eta^* \hat{A}_{\xi_{mj}} \right) + \left(\hat{A}_{\bar{\xi}_{mj}} - \eta \hat{B}_{\bar{\xi}_{mj}}^{\dagger} \right) \left(\hat{B}_{\bar{\xi}_{mj}} - \eta \hat{A}_{\bar{\xi}_{mj}}^{\dagger} \right) \right], \quad (60)$$

with $\eta = e^{i\phi} \tanh(\bar{\xi}_{mj})$.

Then, the expectation value of K_x for the TMS number state of Eq. (55) can be given by

$$\langle K_x \rangle = - \sum_{mj} \int \frac{dv}{2} \cosh^2(\bar{\xi}_{mj}) |\mathcal{G}_{mj}(v)|^2 |\mathcal{F}(v, t)|^2 (\eta^* + \eta) \langle \hat{A}_{\xi_{mj}}^{\dagger} \hat{A}_{\bar{\xi}_{mj}} + \hat{B}_{\xi_{mj}}^{\dagger} \hat{B}_{\bar{\xi}_{mj}} + 1 \rangle \quad (61)$$

with $\langle \hat{A}_{\xi_{mj}}^{\dagger} \hat{A}_{\bar{\xi}_{mj}} + \hat{B}_{\xi_{mj}}^{\dagger} \hat{B}_{\bar{\xi}_{mj}} + 1 \rangle = 3$. From Eq. (25) we get the maximum value $|\mathcal{F}(v, t)|^2 = 4$, thus

$$\langle K_x \rangle = -6 \sum_{mj} \int dv \cosh^2(\bar{\xi}_{mj}) |\mathcal{G}_{mj}(v)|^2 (\eta^* + \eta) \quad (62)$$

where, $(\eta^* + \eta) = 2 \cos(\phi) \tanh(\bar{\xi}_{mj})$, which implies that $\langle K_x \rangle = 0$, if $\phi = \frac{\pi}{2}$, this problem can be avoided by applying a local phase shift [53], we obtain

$$\begin{aligned} \langle K_x \rangle &= -12 \cos(\phi) \sum_{mj} \int dv |\mathcal{G}_{mj}(v)|^2 \cosh(\bar{\xi}_{mj}) \sinh(\bar{\xi}_{mj}) \\ &= -6 \cos(\phi) \sum_{mj} \int dv |\mathcal{G}_{mj}(v)|^2 \sinh(2\bar{\xi}_{mj}). \end{aligned} \quad (63)$$

If we take $\phi = (2n + 1)\pi$, $n = 0, 1, 2, 3, \dots$, then $\langle K_x \rangle$ will be maximized. This implies that $|\langle K_x \rangle| > 0$, for $\phi = n\pi$, $n = 0, 1, 2, 3, \dots$. Therefore, for the state in Eq. (55), the L.H.S. of Eq. (58) is equal to zero and its R.H.S. is positive. Hence, we can confirm the inseparability of the state in Eq. (55) from the violation of the condition in Eq. (58), means that we can take it as an indicator of quantifying the amount of the entanglement of squeezed states which can be detected by increasing $|\langle K_x \rangle|$. In other words, we have found that $|\langle K_x \rangle|$ increases as the spectral order j increases, which indicates that the amount of entanglement of the state in Eq. (55) increases.

5. Summary and comments

To summarize, we obtain the velocity phase matching, which can be used for determining the length of nonlinear crystal in the experiment setup to produce X a

wave with velocity v . We have introduced the relation between the squeezing parameter and the spectral order of X waves which shows that the maximal squeezing increases as the spectral order increases, and there exists an optimal velocity (i.e., axicon angle) that maximizes the amount of squeezing generated for each value of the spectral order. Moreover, we have constructed the squeeze operator of the two modes X wave, then we act by it on the two-particle state generated by SPDC process to obtain the squeezed form of it. Finally, we have used the criterion of the quadrature moment of the fourth order to verify the entanglement of the two modes squeezed state of X wave. We have observed that the entanglement of the state increases as the spectral order increases.

Author details


Ali Saif M. Hassan^{1*}, Waleed S.A. Hasan^{1,2} and Mohamed A. Shukri²

1 Department of Physics, University of Amran, Amran, Yemen

2 Department of Physics, University of Sana'a, Sana'a, Yemen

*Address all correspondence to: alisaif@amu.edu.ye; alisaif73@gmail.com

IntechOpen

© 2023 The Author(s). Licensee IntechOpen. This chapter is distributed under the terms of the Creative Commons Attribution License (<http://creativecommons.org/licenses/by/3.0>), which permits unrestricted use, distribution, and reproduction in any medium, provided the original work is properly cited. 

References

- [1] Ing Konstantin Meyl, *Scalar Waves, Theory and Experiments*. Available from: http://www.k-meyl.de/go/Primae_rliteratur/Scalar-Waves.pdf
- [2] Zohuri B. *Scalar Wave Driven Energy Applications*. Cham, Switzerland: Springer Nature Switzerland AG; 2019
- [3] Hernandez-Figueroa HE, Zamboni-Rached M, Recami E. *Localized Waves*. New York: Wiley; 2008
- [4] Busch P. *Journal of Physics A: Mathematical and General*. 1999;**32**: 6535-6546
- [5] Jaeger G. *Journal of Physics: Conference Series*. 2020;**1638**:012010
- [6] Adhikari P, Choi J. *Acta Physica Polonica B*. 2017;**48**:145-161
- [7] Noah Glennon, Anthony E. Mirasola, Nathan Musoke, Mark C. Neyrinck, Chanda Prescod-Weinstein 2023, arXiv: 2301.13220v1
- [8] Schrödinger E. Discussion of probability relations between separated systems. *Mathematical Proceedings of the Cambridge Philosophical Society*. 1935;**31**:555
- [9] Bell JS. On the Einstein-Podolsky-Rosen paradox. *Physics*. 1964;195-200
- [10] Aspect A, Grangier P, Roger G. Experimental tests of realistic local theories via Bell's theorem. *Physical Review Letters*. 1981;**47**:460-463
- [11] Bennett CH, Brassard G, Crépeau C, Jozsa R, Peres A, Wootters WK. Teleporting an unknown quantum state via dual classical and Einstein-Podolsky-Rosen channels. *Physical Review Letters*. 1993;**70**:1895
- [12] Ekert AK. Quantum cryptography based on Bell's theorem. *Physical Review Letters*. 1991;**67**:661
- [13] Shor PW. Polynomial-time algorithms for prime factorization and discrete logarithms on a quantum computer. *SIAM Journal on Computing*. 1997;**26**:1484
- [14] Acín A, Latorre JI, Pascual P. Three-party entanglement from positronium. *Physical Review A*. 2001;**63**:042107
- [15] Banerjee S, Kumar Alok A, Srikanth R, Hiesmayr BC. A quantum-information theoretic analysis of three-flavor neutrino oscillations. *European Physical Journal C: Particles and Fields*. 2015;**75**:487
- [16] Bertlmann RA, Hiesmayr BC. Kaonic qubits. *Quantum Information Processing*. 2006;**5**:421
- [17] Hiesmayr BC. Limits of quantum information In weak interaction processes of hyperons. *Scientific Reports*. 2015;**5**:11591
- [18] Bernabeu J. T and CPT symmetries in entangled neutral meson systems. *Journal of Physics: Conference Series*. 2011;**335**:012011
- [19] Peschanski R, Seki S. Entanglement entropy of scattering particles. *Physics Letters B*. 2016;**758**:89
- [20] Kharzeev DE, Levin EM. Deep inelastic scattering as a probe of entanglement. *Physical Review D*. 2017; **95**:114008
- [21] Maldacena J. A model with cosmological Bell inequalities. *Fortschritte der Physik*. 2015;**64**:10-23

- [22] Nielsen MA, Chuang IL. Quantum Computation and Quantum Information. Cambridge: Cambridge University Press; 2000
- [23] Bennett CH, DiVincenzo DP. Nature (London). 2000;**404**:247
- [24] Cerf NJ, Leuchs G, Polzik ES, editors. Quantum Information with Continuous Variables of Atoms and Light. London: Imperial College Press; 2007
- [25] Braunstein SL, van Loock P. Reviews of Modern Physics. 2005;**77**:513
- [26] Adesso G, Illuminati F. Journal of Physics A: Mathematical and Theoretical. 2007;**40**:7821
- [27] Reid MD et al. Reviews of Modern Physics. 2009;**81**:1727
- [28] Drummond P, Hilary M. The Quantum Theory of Nonlinear Optics. New York, USA: Cambridge University Press; 2014
- [29] Boyd RW, Jha A, Malik M, O'Sullivan C, Rodenburg B, Gauthier DJ. Proceedings of SPIE. 2011;**7948**: 79480L
- [30] Mirhosseini M, Magaña-Loaiza OS, O'Sullivan MN, Rodenburg B, Malik M, Lavery MPJ, et al. New Journal of Physics. 2015;**17**:033033
- [31] Mirhosseini M, Rodenburg B, Malik M, Boyd R. Journal of Modern Optics. 2013;**61**:43
- [32] Hamadou Ibrahim A, Roux FS, McLaren M, Konrad T, Forbes A. Physical Review A. 2013;**88**:012312
- [33] Gröblacher S, Jennewein T, Vaziri A, Weihs G, Zeilinger A. New Journal of Physics. 2006;**8**:75
- [34] Marrucci L, Karimi E, Slussarenko S, Piccirillo B, Santamato E, Nagali E, et al. Journal of Optics. 2011;**13**:064001
- [35] Cardano F, Massa F, Qassim H, Karimi E, Slussarenko S, Paparo D, et al. Science Advances. 2015;**1**:1500087
- [36] Jackson JD. Classical Electrodynamics. 3rd ed. New York: Wiley; 1998
- [37] Gopaul C, Andrews R. New Journal of Physics. 2007;**9**:94
- [38] Tyler GA, Boyd RW. Optics Letters. 2009;**34**:142
- [39] Anguita JA, Neifeld MA, Vasic BV. Applied Optics. 2008;**47**:2414
- [40] Krenn M, Fickler R, Fink M, Handsteiner J, Malik M, Scheidl T, et al. New Journal of Physics. 2014;**16**:113028
- [41] Durnin J, Miceli JJ, Eberly JH. Physical Review Letters. 1987;**58**:1499
- [42] Lu J, Greenleaf JF. IEEE Transactions on Ultrasonics, Ferroelectrics, and Frequency Control. 1992;**39**:19
- [43] Conti C. Generation of entangled 3D localized quantum wave-packets via optical parametric amplification. 2004. arXiv:quant-ph/0309069
- [44] Ciattoni A, Conti C. Journal of the Optical Society of America B: Optical Physics. 2007;**24**:2195
- [45] Ornigotti M, Conti C, Szameit A. Physical Review Letters. 2015;**115**: 100401
- [46] Ornigotti M, Di Mauro Villari L, Szameit A, Conti C. Physical Review A. 2017;**95**:011802(R)

- [47] Ornigotti M, Conti C, Szameit A.
Journal of Optics. 2018;**20**:065201
- [48] Olver FWJ, Lozier DW, Boisvert RF,
Clark CW. NIST Handbook of
Mathematical Functions. Cambridge:
Cambridge University Press; 2010
- [49] Messiah A. Quantum Mechanics.
New York: Dover; 2014
- [50] Mandel L, Wolf E. Optical
Coherence and Quantum Optics.
Cambridge, UK: Cambridge University
Press; 1995
- [51] Loudon R. The Quantum Theory of
Light. 3rd ed. Oxford: Oxford University
Press; 1997
- [52] Gerry C, Knight P. Introductory
Quantum Optics. Cambridge, UK:
Cambridge University Press; 2005
- [53] Namiki R. Physical Review A. 2012;
85:062307

Universality of Koba-Nielsen-Olesen Scaling in QCD at High Energy and Entanglement

Yizhuang Liu, Maciej A. Nowak and Ismail Zahed

Abstract

Using Mueller's dipole formalism for deep inelastic scattering in Quantum Chromodynamics (QCD), we formulate and solve the evolution for the generating function for the multiplicities of the produced particles in hadronic processes at high energy. The solution for the multiplicities satisfies Koba-Nielsen-Olesen (KNO) scaling, with good agreement with the recently re-analyzed data from the H1 experiment at HERA (DESY) and the old ALEPH detector data for hadronic Z decay at LEP (CERN). The same scaling function with KNO scaling carries to the hadronic multiplicities from jets in electron-positron annihilation. This agreement is *a priori* puzzling, since in Mueller's dipole evolution, one accounts for virtual dipoles in a wave function, whereas in electron-positron annihilation, one describes cross-sections of real particles. We explain the origin of this similarity, pointing at a particular duality between the two processes. Finally, we interpret our results from the point of view of quantum entanglement between slow and fast degrees of freedom in QCD and derive the entanglement entropy pertinent to electron-positron annihilation into hadronic jets.

Keywords: QCD, DIS, entanglement, multiplicity, KNO scaling, perturbation theory

1. Introduction

Using Mueller's dipole formalism for deep inelastic scattering in QCD, we formulate and solve the evolution for the generating function for the multiplicities of the produced particles in hadronic processes at high energy. The solution for the multiplicities satisfies Koba-Nielsen-Olesen (KNO) scaling, with good agreement with the recently re-analyzed data from the H1 experiment at HERA (DESY) and the old ALEPH data for hadronic Z decay at LEP (CERN). The same scaling function with KNO scaling carries to the hadronic multiplicities from jets in electron-positron annihilation. This agreement is *a priori* puzzling, since in Mueller's dipole evolution, one accounts for virtual dipoles in a wave function, whereas in electron-positron annihilation, one describes cross-sections of real particles. We explain the origin of this similarity, pointing at a particular duality between the two processes. Finally, we interpret our results from the point of view of quantum entanglement between slow

and fast degrees of freedom in QCD and derive the entanglement entropy pertinent to electron-positron annihilation into hadronic jets.

Universality is a powerful concept permeating several branches of physics, whereby different physical systems can exhibit similar behavior. This is usually captured by universal exponents, given general assumptions. Perhaps, the best example is the universality of the critical exponents in scaling laws in the vicinity of phase changes. Scaling laws, *per se*, form an important theoretical corpus in physics. In general, they describe the functional relationship between two physical quantities, that scale with each other over a significant interval.

In the context of high-energy particle physics, the so-called Koba-Nielsen-Olesen scaling (named KNO scaling hereafter), formulated half a century ago, is of paramount importance in the empirical analysis of many high-energy hadronic multiplicities. Yet, it is usually challenging to derive from the first principles in QCD. Historically, KNO scaling was first formulated in two independent theoretical works [1, 2], which suggested that at high energies with large Mandelstam s (squared invariant mass), the probability distribution of producing n particles in a specific collision process, scales as

$$\bar{n}(s)p_n(s) = f(z), \quad (1)$$

where $\bar{n}(s)$ is the average multiplicity at large s , and $z \equiv \frac{n}{\bar{n}(s)}$ is the argument of the scaling function $f(z)$. Remarkably, the KNO scaling hypothesis precedes the emergence of Quantum Chromodynamics (QCD) and the advent of high energy and luminosity data currently available at colliders.

This contribution is motivated by the recent work in [3], where the deep inelastic scattering (DIS) data from the H1 experiment at DESY were re-analyzed, with interest in an assessment of the quantum entanglement in high energy particle physics. Clearly, the data analyzed, especially for the highest energy range, shows KNO scaling (see **Figure 1**). Also, the Shannon entropy of the multiplicities presented bears some similarity to the entanglement entropy. However, the explicit form of the scaling

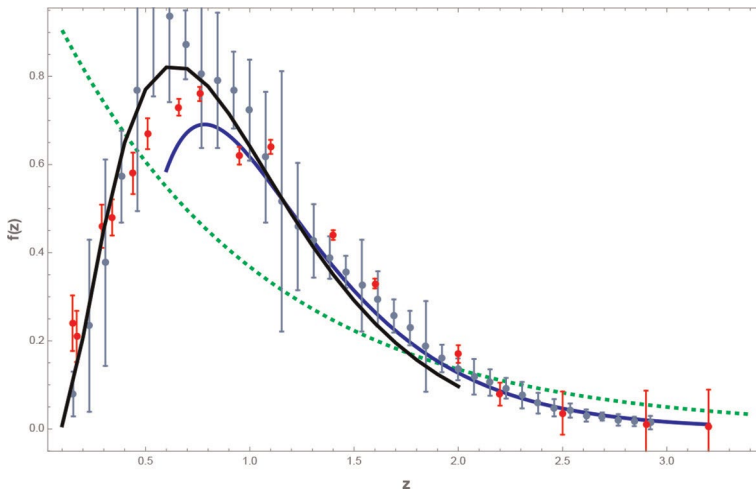


Figure 1. The numerical (black-solid curve) up to $z = 2.0$ and asymptotic (blue-solid curve) scaling of the KNO particle multiplicity $f(z)$ based on **Table 2**, compared to the recent data for DIS [3] (red) and the Z-decay data at $\sqrt{s} = M_Z$ by ALEPH [4] (gray).

function was unknown, and the QCD understanding of the hypothetical entanglement was not specified.

In the first part of this chapter, we discuss the unexpected *a priori* fact, that identical differential equations, such as the ones we derived recently in [5], yield a scaling function that applies to different settings at high energy, e.g., deep inelastic scattering (DIS) and jets in electron-positron or e^+e^- annihilation. Exploiting the duality [6, 7] between the Banfi-Marchesini-Smye (BMS) construction [8] and the Mueller's dipole [9] in the conformal limit, we show that the pertinent generating functions for the multiplicity probabilities in the case of DIS and jets, respectively, are mathematically *identical*. Furthermore, in the double-logarithm approximation (DLA), the duality holds beyond conformal limit by introducing one-loop running in the “minimal” way. Given these, we arrive at the final differential equation for the KNO function, which we then solve using methods based on analyticity. The resulting, parameter-free curve, does not only agree well with DIS data from the H1 experiment at DESY, and the Z-decay data from ALEPH at CERN, but also represents a valuable prediction for future DIS experiments, alike electron-ion collider (EIC) or electron-ion-collider in China (EicC).

In sum, this paper consists of three new results: (1) the derivation of the KNO scaling function in QCD for both DIS and jets in the DLA; (2) the use of the KNO scaling function in the DLA, to show the universality of the hadronic multiplicities from current colliders, for both DIS and jets; (3) the explicit derivation of the entanglement entropy for e^+e^- annihilation into hadronic jets, to be measured at collider energies.

2. The BMS equation for infrared (IR) logarithms in $e^+e^- \rightarrow$ multi-gluon cross-section

The BMS equation [8, 10, 11], describes the “nonglobal” logarithms in the e^+e^- annihilation process, and is based on the universal features of the soft divergences in the n -gluon contribution to the total cross-section σ_n . To leading logarithm accuracy, the “most singular” part of σ_n , can be effectively generated through a Markov process. Defining the directions of the quark-antiquark pair as p and n , soft gluons (k) are emitted from harder ones (p) through a universal eikonal current $\frac{gp^\mu}{p \cdot k}$, and the emissions are strongly ordered in time and energy. As a result, the emission depends only on the color charges that are already present in the final state but not on the history of how they are emitted. In the large number of colors N_c , the generating functional for σ_n ,

$$Z\left(\frac{E}{E_0}; n, p; \lambda\right) = \sum_{n=0}^{\infty} \lambda^n \sigma_n, \quad (2)$$

satisfies a closed integral equation (4)

$$\begin{aligned} Z\left(\frac{E}{E_0}; n, p; \lambda\right) &= S\left(\frac{E}{E_0}; \hat{p}, \hat{n}\right) \\ &+ \bar{\alpha}_s \lambda \int_{E_0}^E \frac{d\omega}{\omega} S\left(\frac{E}{E_0}; \hat{p}, \hat{n}\right) \int d\Omega_k K(\hat{k}; \hat{p}, \hat{n}) Z\left(\frac{\omega}{E_0}; n, \hat{k}; \lambda\right) Z\left(\frac{\omega}{E_0}; p, \hat{k}; \lambda\right), \end{aligned} \quad (3)$$

with the eikonalized gluonic emission kernel $K(\hat{k}; \hat{p}, \hat{n}) = \frac{1}{4\pi} \frac{p \cdot n}{k \cdot p k \cdot n}$ and $\bar{\alpha}_s = N_c \alpha_s / \pi$. The Sudakov factor reads

$$S\left(\frac{E}{E_0}; \hat{p}, \hat{n}\right) = e^{-\bar{\alpha}_s \ln \frac{E}{E_0} \int d\Omega_k K(\hat{k}; \hat{p}, \hat{n})}. \quad (4)$$

More precisely, the first term is the Sudakov contribution, where all the soft gluons are virtual, and the second term is the contribution where at least one soft gluon is real (3) is the integral form of the BMS equation, which can brought to the standard form discussed in [8, 10, 11], by taking a derivative with respect to $\ln \frac{E}{E_0}$ and some re-arrangements.

3. The Mueller's dipole for small- x logarithms and the BMS-Balitskii-Kovchegov (BK) correspondence

Mueller [9] has shown that the small- x evolution equations such as Balitskii-Fadin-Kuraev-Lipatov (BFKL) [12–14], and BK [15, 16], are also based on a very similar branching process, where small- x virtual gluons are released into the light-front wave functions (LFWFs). The same reasoning yields an evolution equation, this time for the generating function for the distribution of the virtual dipoles or $Z(b, \frac{x}{x_{\min}}, \lambda)$, which is exactly of the form (3), with the substitution $\int d\Omega_k \rightarrow \int d^2 b_2$:

$$\begin{aligned} Z\left(b_{10}, \frac{x_0}{x_{\min}}, \lambda\right) &= S\left(b_{10}, \frac{x_0}{x_{\min}}\right) \\ &+ \lambda \frac{\alpha_s N_c}{2\pi^2} \int_{x_{\min}}^{x_0} \frac{dx_1}{x_1} S\left(b_{10}, \frac{x_0}{x_1}\right) \int db_2^2 \frac{b_{10}^2}{b_{12}^2 b_{20}^2} Z\left(b_{12}, \frac{x_1}{x_{\min}}, \lambda\right) Z\left(b_{20}, \frac{x_1}{x_{\min}}, \lambda\right). \end{aligned} \quad (5)$$

Here, the corresponding Sudakov or “soft-factor” for “virtual” emissions is

$$S\left(b_{10}, \frac{x_0}{x_1}\right) = \exp\left[-\frac{\alpha_s N_c}{\pi} \ln b_{10}^2 \mu^2 \ln \frac{x_0}{x_1}\right]. \quad (6)$$

In fact, one can show that in the leading order, the BMS and BK equations map onto each through a pertinent conformal transformation [6, 7, 17–19], where the asymptotic real soft gluons at $t = \infty$, map onto the virtual gluons present at $x^+ = 0$ [5]. In this sense, the mapping is a “virtual-real” duality, in addition to the standard

	Dipole	Cusp
Distribution in	Virtual gluon	Real gluon
Large N_c	Yes	Yes
Kernel	$\frac{b_{10}^2}{b_{12}^2 b_{20}^2}$	$\frac{n \cdot p}{k \cdot n k \cdot p}$
Virtual part	TMD soft-factor	Sudakov form factor

	Dipole	Cusp
Distribution in	Virtual gluon	Real gluon
Time ordering	In LF time	In center of mass (CM) time
Momentum ordering	Decreasing k^+	Decreasing energy ω
Virtuality ordering	Increasing	Decreasing
Markov process	Yes	Yes
DLA	$b_{10} \gg b_{12} \gg \dots$	$\theta_{01} \gg \theta_{12} \gg \dots$

Table 1.
 Mueller hierarchy and BMS hierarchy.

interpretation that it maps rapidity divergence to ultraviolet (UV) divergence [6].¹ In **Table 1**, we have highlighted this duality through a parallel between the two constructions.

4. The DLA limit and the universal DLA KNO scaling function

The BK (BMS) equation resums *single* logarithms in rapidity (energy). However, in both cases, there are two types of divergences instead of one: in the Mueller's dipole construction for the LFWFs [9], there are UV divergences when k_\perp becomes large, while in the BMS construction with Wilson-line cusps, there are rapidity-divergences when the emissions become collinear to the Wilson-lines. It is natural to resum the double logarithms for both. One can then show that the double-logarithm approximation (DLA) for BK (BMS) is generated from the same branching process, with one more strong ordering in dipole sizes (emitting angles) (see **Table 1**). The strong ordering in virtuality is preserved by the DLA limit. Clearly, the two DLA and the underlying size (angle) orderings, simply map onto each other under a conformal transformation. The similarity of the branching process follows from the non-Abelian three-gluon coupling and large N_c in QCD, giving rise to a binary tree branching.

A unique feature of the DLA is that the distribution of dipoles (soft gluons) has a nontrivial KNO scaling function $f(z)$, which coincides with that suggested many years ago for jets in [20–22]. This is due to the same strong ordering in emitting angles in both cases, with **Table 1** making this plausible.

In the DLA, the equation for the generating function (3) simplifies

$$Z(\rho) = e^{-\rho} + \rho \int_0^1 dx \int_0^1 dy e^{-\rho(1-y)} Z(\rho xy) Z(\rho y), \quad (7)$$

where

$$\rho = \frac{2C_F}{\pi\beta_0} y \ln \ln \frac{Q^2}{M^2}. \quad (8)$$

¹ In nonconformal theory, the exact mapping breaks at two-loop already. But for the virtual part, it can be generalized to all orders.

with $2C_F \sim N_c$ and $\beta_0 = \frac{11N_c}{12\pi}$ for large N_c . Note that we have switched from fixed α_s in (3) to one-loop running in (9), with the scale fixed by the emitted small dipoles, hence the emergence of the beta function β_0 . A more thorough discussion of the choice of α_s at low- x can be found for example in [23], which reduces to the size of the smallest dipole in the presence of strong ordering. In case of e^+e^- , the same DLA limit holds when the running was introduced through the energy of the soft gluons. Defining $Z = \exp W$, and introducing $u = 2\sqrt{\rho}$, we arrive at the final equation $\Delta_2 W = e^W - 1$, where Δ_2 is a radial part of the 2-dimensional Laplacian. This equation is reminiscent of the Poisson-Boltzmann equation, if Δ_2 was the full Laplacian. For large energies, it reduces to

$$\frac{d^2 W}{du^2} = e^W - 1. \quad (9)$$

The solution of this equation, encodes the shape of the KNO scaling function $f(z)$, through a Fourier-Laplace transform

$$Z(t = -e^u) = \int_0^\infty dz e^{-tz} f(z). \quad (10)$$

A detailed investigation of the above equations can be found in our recent analysis [5]. With the help of complex-analytic method, we are able to unravel the scaling function $f(z)$ both in the asymptotic region analytically, and throughout numerically. For $z < 0.1$, the scaling function can be made explicit

$$f(z) \sim \frac{\alpha}{z^2} \ln \frac{\alpha}{z} \exp\left(-\frac{1}{2} \ln^2 \frac{\alpha}{z} \ln \frac{\alpha}{z} + \mathcal{O}(1)\right), \quad (11)$$

where $\alpha = 1.50972$. For $z > 2.0$, the scaling function behaves asymptotically as

$$f(z) = 2r \left(rz - 1 + \mathcal{O}\left(\frac{\ln z}{z}\right) \right) e^{-rz}, \quad z \rightarrow \infty, \quad (12)$$

where $r = 2.55297$. The explicit expression for r can be found in [20–22], and that for α in [5].

5. Scaling function vs. data

Since this scaling function represents a parameter-free QCD prediction for future experiments, including the EIC and EicC, we record our numerical solution in **Table 2**,

z	0.1	0.2	0.3	0.4	0.5	0.6	0.7	0.8	0.9	1.0
$f(z)$	0.01	0.21	0.45	0.65	0.77	0.82	0.82	0.78	0.72	0.64
z	1.1	1.2	1.3	1.4	1.5	1.6	1.7	1.8	1.9	2.0
$f(z)$	0.56	0.49	0.42	0.35	0.29	0.24	0.20	0.15	0.12	0.1

Table 2.
Table of the scaling function $f(z)$.

following our analysis in [5]. For completeness, we note that a moment reconstruction of $f(z)$ using different arguments was used in the context of jets in [21, 22, 24].

In **Figure 1**, we compare our results recorded in **Table 2** (black-solid curve) with the H1 data for DIS [3] (red data) and the old ALEPH data for Z decay [4] (gray data). The agreement is very good for both data sets, supporting the universality of our results. For comparison, we also show the exact asymptotic (11) (blue-solid curve), and the KNO particle multiplicity e^{-z} [9], following from the dimensional reduction (diffusive approximation) of Mueller's dipole wave function evolution (dashed-green curve).

6. KNO scaling and entanglement

The knowledge of the effective reduced density matrix for the virtual dipoles in the LFWF [25], and the shape of the KNO function, allow for the evaluation of the entanglement entropy between fast and slow degrees of freedom [25–28]. Remarkably, the reduced density matrix for large rapidities is diagonal [25]

$$\rho = \sum_n p_n \rho_n, \quad (13)$$

with p_n the probability for the emission of n dipoles (gluons), and ρ_n an effective reduced density matrix with n soft dipoles in-out. Hence, the entanglement entropy

$$S = -\sum_n p_n \ln p_n + \sum_n p_n s_n, \quad (14)$$

with $s_n = -\text{tr} \rho_n \ln \rho_n$. Since the wave function peaks at $n = \bar{n}$ for large n , we assume the same to hold for s_n , with the scaling $s(\frac{n}{\bar{n}})$, so that

$$S = \ln \bar{n} + \int dz f(z) (-\ln f(z) + s(z)). \quad (15)$$

For DIS in the DLA with KNO scaling, the result is [5]

$$S_{DIS}(y, Q^2) \rightarrow \ln \bar{n} \equiv 2 \left(\frac{2C_F}{\pi\beta_0} y \ln \ln \frac{Q^2}{M^2} \right)^{\frac{1}{2}}. \quad (16)$$

a measure of the Sudakov contribution (17) is measurable in the Dokshitzer-Gribov-Lipatov-Altarelli-Parisi (DGLAP) regime of DIS. We note that the KNO scaling function in the diffusive (BFKL) regime with $f(z) = e^{-z}$ [9], leads to maximal decoherence in the entanglement entropy $S_{BFKL} \sim y$ [25–28]. In contrast, the unimodal character of the scaling function in the DLA leads to a smaller entanglement entropy $S_{DIS} \sim \sqrt{y}$.

Using the BMS-BK duality, we can readily formulate the entanglement entropy between soft and hard degrees of freedom in the final state of e^+e^- annihilation into hadronic jets

$$S_{e^+e^-}(Q^2) \equiv 2 \left(\frac{C_F}{\pi\beta_0} \ln \frac{Q^2}{M^2} \ln \ln \frac{Q^2}{M^2} \right)^{\frac{1}{2}}, \quad (17)$$

also a measure of the Sudakov contribution (with no extra 2 in the bracket). The rapidity gap between the quark-antiquark pair $y \rightarrow \ln \frac{Q^2}{M^2}$, produces *another logarithm*

in Q^2 . Note that for e^+e^- , this contribution dominates the single logarithm resummation in the BFKL contribution at large Q^2 , which is

$$\ln \bar{n}_{\text{BFKL}} \sim \frac{2C_F \ln 2}{\pi\beta_0} \ln \ln \frac{Q^2}{M^2}. \quad (18)$$

The prediction (17) is amenable to experimental verification in high-energy hadronic jet physics.

7. Conclusion

To summarize, in this chapter, we presented the universal KNO scaling function underlying the DLA limit for two different systems: the $e^+e^- \rightarrow$ multi-gluon process and the Mueller's dipole wave function. In both systems, the multiplicity generating function satisfies nonlinear BK type evolution equation with respect to primary evolution variables: energy for the $e^+e^- \rightarrow$ multi-gluon process and rapidity for the Mueller's dipole. They map to each other through the BMS-BK correspondence.

On the other hand, in both systems there also exists another large logarithm: in rapidity for $e^+e^- \rightarrow$ multi-gluon process and in energy for the Mueller's dipole. The second logarithm appears naturally in the multiplicity distribution. When projected to the double-logarithm limit (DLA limit), which resumes both of the two large-logarithms, the evolution equation simplifies considerably, and the corresponding multiplicity distribution exhibits a nontrivial universal KNO scaling function. This scaling function compares well with the measured hadronic multiplicities in DIS and e^+e^- annihilation, especially in the exponential tail. Moreover, the KNO scaling also constraints, in a universal way, in the DLA limit, the asymptotic behavior of the rapidity space or energy-space entanglement entropies of the underlying process.

Acknowledgements

We are grateful to Jacek Wosiek for bringing [20] to our attention and to Yoshitaka Hatta for informing us about [19]. This work is supported by the Office of Science, U.S. Department of Energy under Contract No. DE-FG-88ER40388, and by the Priority Research Areas SciMat and DigiWorld under the program Excellence Initiative—Research University at the Jagiellonian University.

Author details

Yizhuang Liu¹, Maciej A. Nowak^{1,2*} and Ismail Zahed³


1 Institute of Theoretical Physics, Jagiellonian University, Kraków, Poland

2 Mark Kac Center for Complex Systems Research, Jagiellonian University, Kraków, Poland

3 Center for Nuclear Theory, Department of Physics and Astronomy, Stony Brook University, Stony Brook, New York, USA

*Address all correspondence to: maciej.a.nowak@uj.edu.pl

IntechOpen

© 2023 The Author(s). Licensee IntechOpen. This chapter is distributed under the terms of the Creative Commons Attribution License (<http://creativecommons.org/licenses/by/3.0>), which permits unrestricted use, distribution, and reproduction in any medium, provided the original work is properly cited. 

References

- [1] Polyakov AM. Zhurnal Éksperimental'noĭ i Teoreticheskoi Fiziki. 1970;**59**:542-552
- [2] Koba Z, Nielsen HB, Olesen P. Nuclear Physics B. 1972;**40**:317-334. DOI: 10.1016/0550-3213(72)90551-2
- [3] Andreev V et al. European Physical Journal. 2021;**81**(3):212. DOI: 10.1140/epjc/s10052-021-08896-1
- [4] Buskalic D et al. Zeitschrift für Physik. 1995;**69**:15-26. DOI: 10.1007/BF02907382
- [5] Liu Y, Nowak MA, Zahed I. Physics Review D. 2023;**2023**
- [6] Vladimirov AA. Physical Review Letters. 2017;**118**(6):062001. DOI: 10.1103/PhysRevLett.118.062001
- [7] Hatta Y, Iancu E, Mueller AH, Triantafyllopoulos DN. JHEP. 2018;**02**:075. DOI: 10.1007/JHEP02(2018)075
- [8] Banfi A, Marchesini G, Smye G. JHEP. 2002;**08**:006. DOI: 10.1088/1126-6708/2002/08/006
- [9] Mueller AH. Nuclear Physics B. 1994;**415**:373-385. DOI: 10.1016/0550-3213(94)90116-3
- [10] Caron-Huot S. JHEP. 2018;**03**:036. DOI: 10.1007/JHEP03(2018)036
- [11] Marchesini G, Mueller AH. Physics Letters B. 2003;**575**:37-44. DOI: 10.1016/j.physletb.2003.09.041
- [12] Fadin VS, Kuraev EA, Lipatov LN. Physics Letters B. 1975;**60**:50-52. DOI: 10.1016/0370-2693(75)90524-9
- [13] Kuraev EA, Lipatov LN, Fadin VS. Soviet Physics JETP. 1976;**44**:443-450
- [14] Kuraev EA, Lipatov LN, Fadin VS. Soviet Physics. JETP. 1977;**45**:199-204
- [15] Balitsky I. Nuclear Physics B. 1996;**463**:99-160. DOI: 10.1016/0550-3213(95)00638-9
- [16] Kovchegov YV. Physical Review D. 2000;**61**:074018. DOI: 10.1103/PhysRevD.61.074018
- [17] Weigert H. Nuclear Physics B. 2004;**685**:321-350. DOI: 10.1016/j.nuclphysb.2004.03.002
- [18] Cornalba L. Eikonal Methods in AdS/CFT: Regge Theory and Multi-Reggeon Exchange. arXiv. 2008. DOI: 10.48550/arXiv.0710.5480
- [19] Hatta Y, Ueda T. Nuclear Physics B. 2013;**874**:808-820. DOI: 10.1016/j.nuclphysb.2013.06.021
- [20] Dokshitzer YL, Fadin VS, Khoze VA. Z Physics C. 1983;**18**:37. DOI: 10.1007/BF01571703
- [21] Dokshitzer YL, Fadin VS, Khoze VA. Z Physics C. 1982;**15**:325. DOI: 10.1007/BF01614423
- [22] Bassetto A, Ciafaloni M, Marchesini G. Physical Report. 1983;**100**:201-272. DOI: 10.1016/0370-1573(83)90083-2
- [23] Kovchegov YV, Weigert H. Nuclear Physics A. 2007;**784**:188-226. DOI: 10.1016/j.nuclphysa.2006.10.075
- [24] Bassetto A. Nuclear Physics B. 1988;**303**:703-712. DOI: 10.1016/0550-3213(88)90426-9

[25] Liu Y, Nowak MA, Zahed I. Physical Review D. 2022;**105**(11):114028.
DOI: 10.1103/PhysRevD.105.114028

[26] Stoffers A, Zahed I. Physical Review D. 2013;**88**(2):025038.
DOI: 10.1103/PhysRevD.88.025038

[27] Kharzeev DE, Levin E. Physical Review D. 2021;**104**(3):L031503.
DOI: 10.1103/PhysRevD.104.L031503

[28] Kharzeev DE, Levin EM. Physical Review D. 2017;**95**(11):114008.
DOI: 10.1103/PhysRevD.95.114008



Edited by Oliver K. Baker

This book is devoted to research topics in quantum entanglement at the energy frontier of particle and nuclear physics, and important interdisciplinary collaborations with colleagues from fields outside of physics. A non-exhaustive list of examples of the latter can include mathematics, computer science, social sciences, philosophy, and how physics can interact with them in a way that supports successful outcomes. These are exciting times in the field of quantum information science, with new research results and their applications in society exhibiting themselves rather frequently. But what is even more exciting is that the frequency of these new results and their applications increases with a rapidity that will motivate new methods, new theories, new experiments, and new collaborations outside of the field that future researchers will find quite challenging.

Published in London, UK

© 2024 IntechOpen

© bestdesigns / iStock

IntechOpen

